



HAL
open science

Stimuli responsive cyclodextrin-based supramolecular polymers

Wenting Hu

► **To cite this version:**

Wenting Hu. Stimuli responsive cyclodextrin-based supramolecular polymers. Organic chemistry. Sorbonne Université, 2019. English. NNT : 2019SORUS133 . tel-02946763

HAL Id: tel-02946763

<https://theses.hal.science/tel-02946763v1>

Submitted on 23 Sep 2020

HAL is a multi-disciplinary open access archive for the deposit and dissemination of scientific research documents, whether they are published or not. The documents may come from teaching and research institutions in France or abroad, or from public or private research centers.

L'archive ouverte pluridisciplinaire **HAL**, est destinée au dépôt et à la diffusion de documents scientifiques de niveau recherche, publiés ou non, émanant des établissements d'enseignement et de recherche français ou étrangers, des laboratoires publics ou privés.



THÈSE

présentée à **SORBONNE UNIVERSITÉ**

Ecole doctorale de Chimie moléculaire de Paris-Centre-ED 406

Institut Parisien de Chimie Moléculaire-Équipe GOBS

Par **Mme Wenting HU**

Pour obtenir le grade de

Docteur de Sorbonne Université

Spécialité : **Chimie Organique**

Stimuli Responsive Cyclodextrin-Based Supramolecular Polymers

Dirigée par le Professeur Matthieu SOLLOGOUB

Soutenance prévue le 07 November 2019

Devant un jury composé de :

Monsieur	Frédéric HAPIOT	Professeur des universités	Rapporteur
Madame	Véronique BONNET	Maître de conférences (HDR)	Rapporteur
Monsieur	Laurent BOUTEILLER	Directeur de recherche	Examineur
Monsieur	Yongmin ZHANG	Directeur de recherche	Invité
Monsieur	Matthieu SOLLOGOUB	Professeur des universités	Directeur de thèse

“Everything will be okay in the end. If it's not okay, it's not the end.”

—John Lennon

CONTENTS

ACKNOWLEDGEMENTS	- 9 -
ABBREVIATIONS	- 11 -
ABSTRACT	- 13 -
RÉSUMÉ	- 15 -
CHAPTER 1	- 17 -
FROM SUPRAMOLECULAR CHEMISTRY TO SUPRAMOLECULAR POLYMERS	- 17 -
1. Supramolecular Chemistry	- 19 -
1.1. Introduction	- 19 -
1.2. The origins of supramolecular chemistry	- 19 -
1.3. From molecular to supramolecular chemistry	- 21 -
1.4. Nature of supramolecular interactions	- 22 -
1.4.1. Ionic-dipolar interactions	- 23 -
1.4.2. Van der Waals interactions	- 24 -
1.4.3. π -Interactions	- 24 -
1.4.4. Hydrogen bonding	- 24 -
1.4.5. Hydrophobic effects	- 25 -
2. Supramolecular Polymer	- 27 -
2.1. Definition.....	- 27 -
2.2. Mechanisms of association of supramolecular polymers.....	- 28 -
2.3. Properties of supramolecular polymers	- 29 -
2.3.1. Optoelectronic properties.....	- 30 -
2.3.2. Mechanical properties.....	- 31 -
2.3.3. Biological properties.....	- 33 -
2.4. Driving forces for supramolecular polymers	- 34 -
2.4.1. Multiple hydrogen bonds	- 35 -
2.4.2. Metal coordination bonds.....	- 35 -
2.4.3. Host-guest interaction.....	- 36 -
2.5. Characterizations of supramolecular polymers	- 40 -
2.5.1. NMR spectroscopy	- 40 -

2.5.1.1. $^1\text{H-NMR}$	- 40 -
2.5.1.2. NMR-Rotating-frame nuclear Overhauser Effect Spectroscopy.....	- 41 -
2.5.1.3. NMR-Diffusion Ordered Spectroscopy (NMR-DOSY)	- 43 -
2.5.2. Isothermal Calorimetric Titration (ITC).....	- 45 -
2.5.3. Dynamic Light Scattering (DLS)	- 46 -
2.5.4. Viscometry	- 47 -
2.5.5. Small-Angle Neutron Scattering (SANS).....	- 48 -
3. Cyclodextrins Based Supramolecular Polymers	- 48 -
3.1. Cyclodextrin (CD).....	- 48 -
3.1.1. Structure and properties of cyclodextrin.....	- 48 -
3.1.2. Properties of cyclodextrin cavity	- 50 -
3.1.2.1. Inclusion complex of cyclodextrins	- 50 -
3.1.2.2. Guest of inclusion complex of cyclodextrins.....	- 51 -
3.1.3. Reactivity of cyclodextrins.....	- 52 -
3.2. Supramolecular polymers based on cyclodextrin in solution.....	- 53 -
3.2.1. Supramolecular polymers of A_nB_m type	- 53 -
3.2.2. Supramolecular polymers of AB type.....	- 57 -
4. Conclusion	- 59 -
CHAPTER 2	- 61 -
DESIGN STRATEGY AND SYNTHESIS OF SUPRAMOLECULAR POLYMERS BASED ON BETA-CYCLODEXTRIN-ADAMANTANE IN AQUEOUS SOLUTION	- 61 -
1. Selective Functionalization of Cyclodextrins Debenzylation	- 63 -
1.1. Synthesis of cyclodextrin diol with diisobutylaluminum hydride	- 63 -
1.2. Mechanism of DIBAL-H mediated debenylation.....	- 64 -
1.3. Selectivity rationalization for α - and β -cyclodextrins debenylation.....	- 65 -
2. Our Previous Work: Supramolecular Polymerization Based on β-Cyclodextrin-Adamantane in Aqueous Solution	- 66 -
2.1. Initial considerations and preliminary experiences.....	- 66 -
2.2. Further experiences with new strategies	- 67 -
3. System Design.....	- 71 -
4. Synthesis of Functionalized CD/Adamantane Monomers	- 73 -
4.1. General retrosynthesis.....	- 73 -
4.2. Synthesis of the common precursor: bi-azide cyclodextrin	- 73 -

4.3. Synthesis of bridged neutral cyclodextrin/adamantane monomer	- 74 -
4.4. Synthesis of bridged cationic cyclodextrin/adamantane monomer	- 76 -
4.5. Synthesis of difunctionalized bridged β -cyclodextrin-adamantane monomer: functionalized 1-deoxynojirimycin derivative	- 77 -
4.6. Conclusion of synthesized cyclodextrin/adamantane monomers.....	- 79 -
5. Conclusion	- 80 -
CHAPTER 3	- 81 -
STUDY OF SUPRAMOLECULAR ASSEMBLIES BASED ON BETA-CYCLODEXTRIN- ADAMANTANE IN AQUEOUS SOLUTION	- 81 -
1. Characterization of the Supramolecular Assembly	- 83 -
1.1. Characterization of supramolecular assembly by $^1\text{H-NMR}$	- 83 -
1.2. Characterization of supramolecular assembly by NMR-ROESY.....	- 87 -
1.3. Characterization of supramolecular assembly by NMR-DOSY	- 90 -
1.4. Characterization of supramolecular assembly by ITC	- 95 -
1.5. Characterization of supramolecular assembly by viscosity	- 96 -
1.6. Characterization of supramolecular assembly by DLS	- 97 -
2. Study Influence Factors on Polymerization of Supramolecular Polymer	- 97 -
3. Conclusion	- 105 -
CHAPTER 4	- 107 -
GENERAL CONCLUSION AND PERSPECTIVE.....	- 107 -
1. General Conclusion.....	- 109 -
2. Perspectives.....	- 110 -
APPENDIX.....	- 111 -
EXPERIMENTAL PART	- 119 -
1. General Procedures.....	- 121 -
2. Nomenclature for Protons:.....	- 123 -
3. Synthesis	- 124 -
BIBLIOGRAPHY	- 195 -

ACKNOWLEDGEMENTS

Firstly, I would like to thank Prof. Frédéric Hapiot and Dr. Véronique Bonnet for having accepted to read and review my thesis, and also give sincere thanks to Dr. Laurent Bouteiller for taking part in my defense and giving insight comments.

I also thank Gaële Pembouong for her help in the characterization of my supramolecular systems.

These four years within the GOBS group have been very rich both scientifically and personally. First and foremost, I would like to thank my supervisor Prof. Matthieu Sollogoub. He allows me the opportunity to study here, presents me with such a fascinating topic, and gives his continuous support for my study. His enthusiasm and immense knowledge allow me to see a real scientist. It was a pleasure to work with him.

My sincere thanks also go to Dr. Mickaël Mérand for guiding my work and giving powerful advice, I will always be grateful. And I am deeply indebted to Dr. Yongmin Zhang for his help of my study and life in Paris.

Thanks to the GOBS group for making these rich four years with unforgettable moments: Dr. Guillaume Vives, Prof. Bernold Hasenknopf, Dr. Sylvain Roland, and Dr. Olivia Bistri for their kindness and the rich discussions.

Dr. Pinglu Zhang, Dr. Dmitri Colesnic, Dr. Xiaolei Zhu, Dr. Sha Zhu, Dr. Julien Rossignol, Dr. Pierre Evenou, Dr. Jiang Liu, Dr. Changping Zheng, Martin Warlop, Sawsen Cherraben, Leonid Lavnevich, Guangcan Xu, Zhihao Li, Lorien Benda, Kajetan Bijouard, Floriane Heis, Zhonghang Wen, Hugo Vervoitte, Haipeng Liu, Fang Liu, for helping me with my project and supporting me in many ways.

I gratefully acknowledge China Scholarship Council for a Ph.D. fellowship.

ABBREVIATIONS

ACN	acetonitrile
Ada	adamantane
Bn	benzyl
C	concentration
CD	cyclodextrin
COSY	correlation spectroscopy
Cy	cyclohexane
DCM	dichloromethane
DEPT	distortionless enhancement by polarization transfer
DIBAL-H	diisobutylaluminium hydride
DIPEA	N,N-Diisopropylethylamine
DLS	dynamic light scattering
DMF	dimethylformamide
DMSO	dimethyl sulfoxide
eq	equivalent
ESI-TOF	electrospray ionization time-of-flight
EtOAc	ethyl acetate
HMBC	heteronuclear multiple bond correlation
HPLC	high-performance liquid chromatography
HRMS	high-resolution mass spectrometry
HSQC	heteronuclear single quantum coherence
ITC	isothermal titration calorimetry
IR	infrared
LAH	lithium aluminium hydride
Ms	methanesulfonyl
NOESY	nuclear overhauser spectroscopy
Pd/C	palladium on carbon
Ph	phenyl
PTSA	<i>p</i> -toluenesulfonic acid
ROESY	rotating-frame nuclear overhauser effect spectroscopy
r. t.	room temperature
SANS	small angle neutron scattering

TBTA	tris(benzyltriazolylmethyl)amine
TEMPO	(2,2,6,6-tetramethylpiperidin-1-yl)oxidanyl
TFA	trifluoroacetic acid
THF	tetrahydrofuran
TLC	thin layer chromatography
TOCSY	total correlation spectroscopy
T-ROESY	transverse rotating-frame overhauser enhancement spectroscopy
UV	ultraviolet

ABSTRACT

Previous work developed bridged β -cyclodextrin derivative which are capable of formation supramolecular polymer, avoiding the head to head dimerization and self-inclusion. Significantly, it showed a good performance in DNA compaction and cooperative interaction with siRNA, allowing its transfection. All these properties were related to the construction of supramolecular polymers via host-guest interaction. Obtaining higher degree of polymerization of supramolecular polymer, allowing further capability in the gene condensation and gene delivery field, is the subject of thesis work.

To achieve this target, using polyfunctionalisation of cyclodextrins developed in the laboratory and the previous strategy to avoid the self-inclusion phenomenon, the β -cyclodextrin/adamantane system is designed: (1) to introduce an adamantyl group located in the center of the cavity to trigger a higher level of the assembly; (2) to introduce cationic groups carrying several positive charge for the interaction with the gene in aqueous solution. In addition, small sugar molecule is also employed to construct supramolecular dynamic system, which is expected to endow more complex functions to mimic biological macromolecules. These three β -cyclodextrin derivatives overcome the problem of the formation of self-inclusion in aqueous solution. The self-assembly of these compounds have been characterized by $^1\text{H-NMR}$, NMR-ROESY, NMR-DOSY, ITC, viscosity and DLS. Moreover, one of these compounds is able to form a liner species up to 22 repeat units. We now have to operate the transfection study to confirm the ability of our designed molecules to act as transfecting agents.

Surprisingly, the self-inclusion compound is still obtained even with bridging. A series of experiments: time effect, concentration effect, temperature effect, and pH effect were studied by $^1\text{H-NMR}$, in order to examine the influence of these factors on self-inclusion and aggregation versus supramolecular polymer formation. Apart from the observed depolymerization caused by competitive guest mentioned in the literature, we also observed depolymerization at low concentrations of monomer solution. The addition of base accelerated the transformation process and vice versa. In addition, this process is almost irreversible, attributed to the very high stability of self-included compound.

Keywords: cyclodextrins, functionalization, host-guest, supramolecular polymers.

RÉSUMÉ

Les travaux précédents du laboratoire ont mis au point un dérivé ponté de β -cyclodextrine capable de former un polymère supramoléculaire, en évitant la dimérisation en tête à tête et l'auto-inclusion. De manière significative, il a été montré que le système possédait de bonnes performances en compaction de l'ADN et pour la transfection de siARN. Toutes ces propriétés liées à la formation de polymères supramoléculaires par interaction hôte-invité. L'obtention d'un degré de polymérisation plus élevé du polymère supramoléculaire, qui permettra une plus grande capacité dans le domaine de la condensation et de la délivrance de gènes, est le sujet de ce travail.

Pour atteindre cet objectif, sur la base de la méthode de polyfonctionnalisation des cyclodextrines mise au point au laboratoire et de la stratégie visant à éviter le phénomène d'auto-inclusion, un système β -cyclodextrine/adamantane est conçu: (1) l'introduction du groupe adamantyle situé au centre de la cavité pour inclusion un meilleur assemblage; (2) l'introduction d'un groupement cationique portant plusieurs charges positives pour l'interaction avec les acides nucléiques en solution aqueuse. En outre, une molécule de sucre est également utilisée pour la construction d'un système supramoléculaire, qui devrait lui conférer des fonctions plus complexes pour imiter les macromolécules biologiques. Ces trois dérivés de β -cyclodextrine résolvent le problème de l'auto-inclusion en solution aqueuse. Les comportements d'autoassemblage des trois composés ont été caractérisés par RMN- ^1H , RMN-ROESY, RMN-DOSY, ITC, viscosité et DLS. En outre, l'un de ces composés est capable de former des assemblages jusqu'à 22 unités répétées. Nous devons maintenant mener une étude de transfection pour confirmer la capacité de notre molécule à agir en tant qu'agent de transfection.

De façon surprenante l'auto-inclusion est toujours obtenue malgré le pontage. Une série d'expériences sur l'effet du temps, de la concentration, de la température et du pH sont effectuées par RMN- ^1H afin d'examiner les facteurs influant l'auto-inclusion et l'agrégation par rapport à la formation de polymères supramoléculaires. Outre l'observation de la dépolymérisation provoquée par un invité compétitif mentionné dans la littérature, nous avons observé que le processus de dépolymérisation était lié à la concentration et au pH processus. De plus, ce processus est presque irréversible, en raison de la constante

d'association élevée entre la cyclodextrine et l'adamantane et du faible moment dipolaire de la cyclodextrine.

Mots-clés: cyclodextrines, fonctionnalisation, hôte-invité, polymères supramoléculaires.

CHAPTER 1

FROM SUPRAMOLECULAR CHEMISTRY TO SUPRAMOLECULAR POLYMERS

1. Supramolecular Chemistry

1.1. Introduction

The definition of supramolecular chemistry proposed by Lehn ^[1] is the chemistry based on intermolecular non-covalent assemblies and bonds. An informal expression of this definition may be ‘chemistry beyond the molecule’. Figure 1 describes the differences in functions and structures between molecular and supramolecular chemistry ^[2].

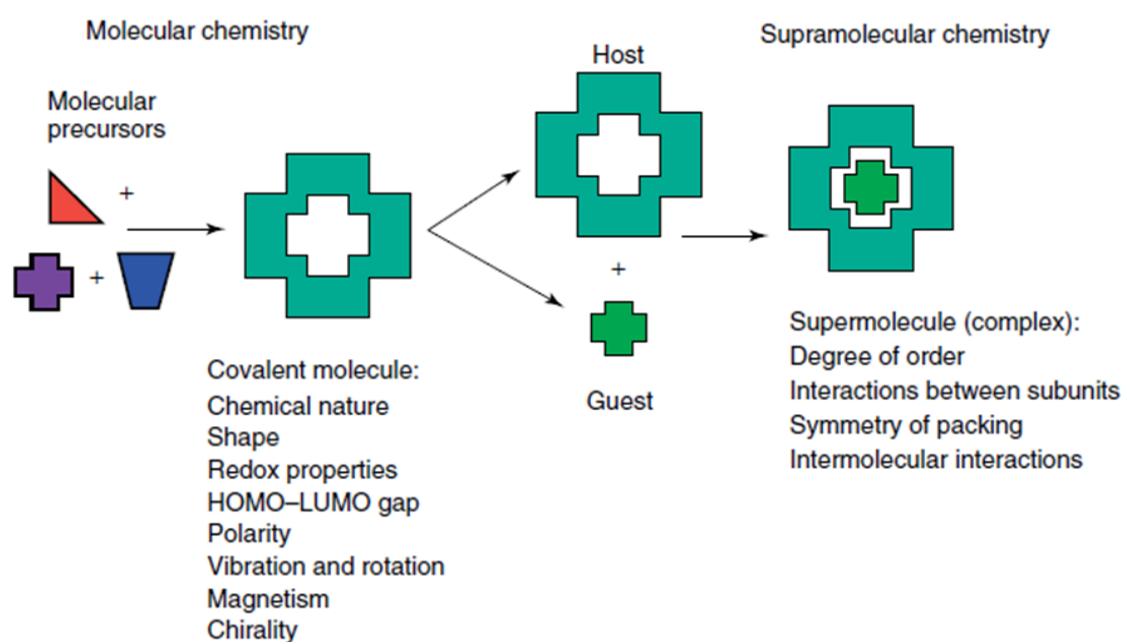


Figure 1: Difference between molecular chemistry and supramolecular chemistry according to Lehn ^[3].

1.2. The origins of supramolecular chemistry

Supramolecular chemistry is an emerging discipline that dates back to the late 1960s and early 1970s. However the concepts and roots of many supramolecular chemical systems can be almost traced back to the origins of modern chemistry. An illustrative chronology is given in Figure 2 ^[2].

The nature of intermolecular forces has been discovered, very early in the history of chemistry, such as van der Waals by Johannes Diderik in 1873, electrostatic interactions and hydrogen bonding by Latimer and Rodebush in 1920. The concept of the ‘lock and key principle’ proposed in 1894 could be seen as the root of supramolecular chemistry. This principle

developed from Nobel laureate Hermann Emil Fischer's work, in which he depicted the enzyme and substrate as the lock and key.

Scientists take advantage of the understanding of molecular interactions and complementarity to begin to understand the nature of biological structures and processes. One of the most significant is the double helix structure of DNA. It was only possible to obtain this correct structural representation when it was recognized that the hydrogen bonds of complementary nucleotide induced two strands of DNA to hold together a helical structure. Perhaps more importantly, non-covalent bond-hydrogen bond was essential to the replication of DNA because they allow the strands to be separated and act as template to produce new one.

In 1967 an important breakthrough came with the discovery of crown ethers as the first artificial host molecule with molecular recognition ability by Charles J. Pedersen. And led to the exploration of non-covalent bonds by other researchers, Donald J. Cram, Jean-Marie Lehn and Fritz Vogtle became devoted to synthesize ion- and shape-selective interlocked molecular architectures and a new field of chemistry was established. Supramolecular chemistry was born in the 1980s and grew rapidly by developing this concept into a broad range of molecular systems.

Supramolecular chemistry was recognized through the Nobel Prize for chemistry in 1987, which was awarded jointly to Donald J. Cram, Jean-Marie Lehn and Charles J. Pedersen "for their development and use of molecules with specific structure and highly selective interactions" ^[4].

The research in the fields of inorganic chemistry, analytical chemistry, physical organic chemistry, organic chemistry, and biochemistry had been greatly affected by the discovery of spherands, cryptophanes, and crown ethers. The unremitting efforts of different researchers had achieved great development of this field. In the field of supramolecular chemistry, the second Nobel Prize was awarded in 2016 to Sir J. Fraser Stoddart, Jean-Pierre Sauvage, and Bernard L. Feringa, who made great contributions to the development of the molecular machine field ^[5].

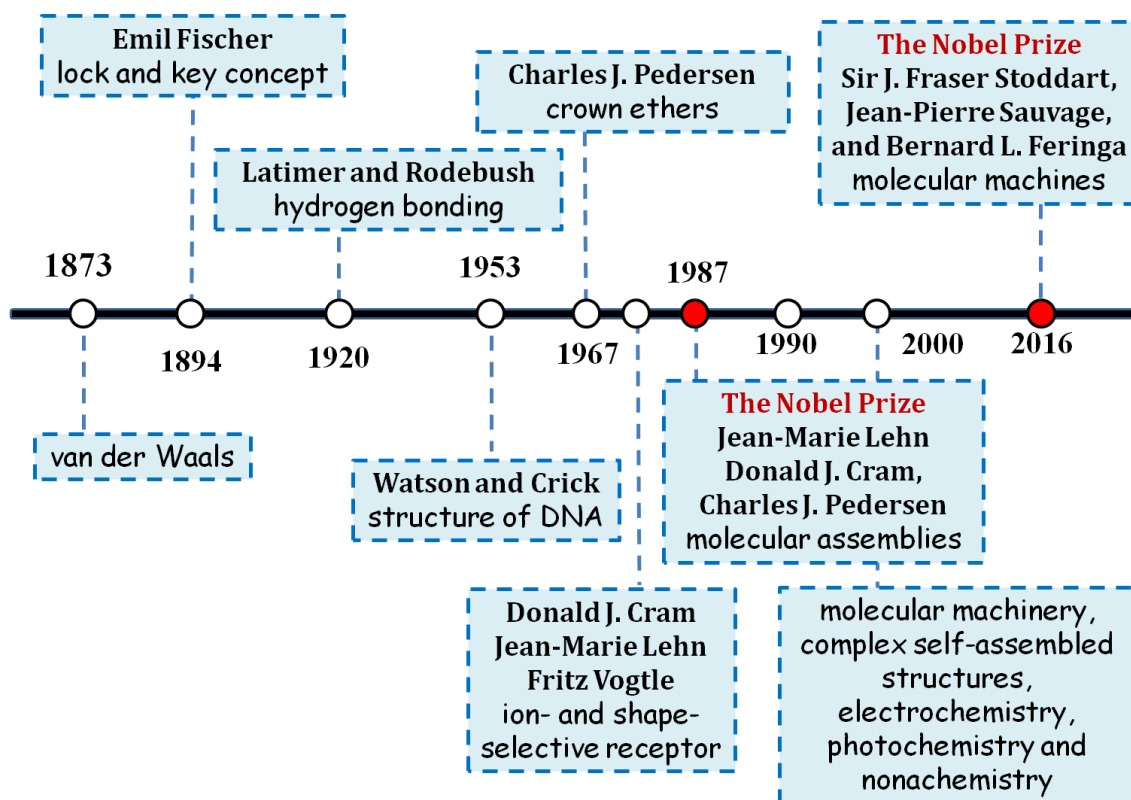


Figure 2: Timeline of supramolecular chemistry.

1.3. From molecular to supramolecular chemistry

Supramolecular chemistry can be split into two fields, ‘supramolecules’ and ‘molecular assemblies’^[6]. A supramolecule, an organized and complex system, that is formed by two or more entities held together via non-covalent interactions. The structures of supramolecules are the result of weak interactions, the nature of which differs from the properties of each individual component. Under a given set of conditions, molecular assemblies are produced by spontaneous self-assembly of multiple components^[7]. The design of the individual molecules is therefore essential and is alone in the field of molecular chemistry. The process from molecular chemistry to supramolecular chemistry is presented in Figure 3^[8].

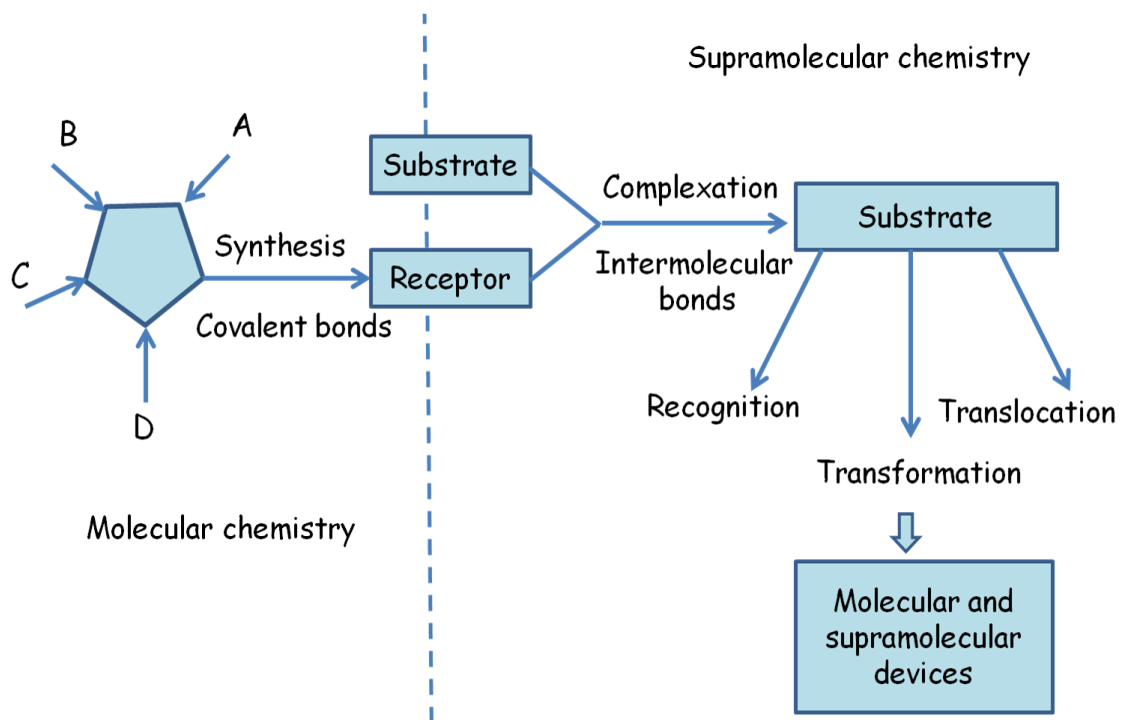


Figure 3: From molecules, to supramolecules, molecular and supramolecular devices ^[8].

1.4. Nature of supramolecular interactions

Non-covalent interactions contribute to hold the supramolecular species together. They are weaker fairly than the covalent interaction that can range between 150 to 450 kJ mol⁻¹ for single bond (Figure 4). Nevertheless, the whole range of non-covalent interactions (e.g., hydrogen bonding, van der Waals forces, hydrophobic interaction, etc) strongly affects the structures and properties of supramolecular systems. Using these weak forces will allow the supramolecular system to be stabilized, which can result in the formation of a stable architecture or a stable host-guest complex after addition small stabilizations of other interactions ^[6]. The main non-covalent interactions are shown in Figure 4 ^[6] ^[9].

Interaction	Type	Strength (KJ·mol ⁻¹)	Distances (Å)
Covalent interactions			
Covalent bond	C-O bond	340	1.43
	C-C bond	360	1.53
	C-H bond	430	1.11
	C=C bond	600	1.33
	C=O bond	690	1.21
Non-covalent interactions			
Ionic and dipolar	Ion-ion	200-300	Tetrabutylammonium chloride
	Ion-dipole	50-200	[Ru(bpy) ₃] ²⁺
	Dipole-dipole	5-50	Acetone
π-Interactions	Cation-π	5-80	Potassium ions with benzene
	Anion-π	20-50	CO ₃ ²⁻ -C ₆ F ₆
	π-π	0-50	Benzene and graphite
	CH-π	5-80	Protein
Hydrogen bonding	(see figure 5)	4-120	(see figure 5)
Van de Waals	Dipole-dipole		Ethane & fluromethane
	Dipole-induced dipole	5-50	Acetone & n-hexane
	London dispersion force		n-octane & n-hexane
Hydrophobic	-	Related to Interaction solvent-solvent interaction energy	Cyclodextrin inclusion complexes

Figure 4: Comparison between the scope of covalent interactions and non-covalent interactions ^{[6] [9]}.

1.4.1. Ionic-dipolar interactions

There are three main types of ionic-dipolar interactions that can be found in supramolecular systems: (a) ion-ion; (b) ion-dipole; (c) dipole-dipole. Strength of ionic bonding is comparable to covalent bonding, which is the strongest of these interactions and in some cases even is stronger than covalent bonds. Ion-ion interaction as a non-directional force can be an attractive or a repulsive force, which highly depends on the dielectric constant of the medium, whereas ion-dipole and dipole-dipole interaction are the relatively rigid directional interaction ^[6]. These interactions, longest-range biological relevant interactions, play a very important role in many biological processes, such as recognition process between substrates

and enzymes. The most common example is amino acids (Asp^- , Glu^- , Lys^+ , Arg^+ , His^+), phosphates in DNA backbone, lipids, etc.

1.4.2. Van der Waals interactions

This is a general term for the favorable interactions that occur between uncharged atoms, which can be split into three categories: (a) force from dipole-dipole (Keesom force); (b) force from dipole-induced dipole (Debye force); (c) force from induced dipole-induced dipole (London dispersion force) ^[10] ^[11]. These interactions, as short-range forces, are caused by the electron distribution fluctuations between nearest species, instead of all the particles. The strength of these interactions is dependent on the molecule's polarisability, not temperature except for dipole-dipole interactions. All have energies that depend on $1/\text{distance}^6$. Van der Waals interactions play an important role in the formation of inclusion compounds, in which small organic molecules have been encapsulated into permanent molecular cavities or are incorporated into a crystalline lattice ^[6].

1.4.3. π -Interactions

π - interactions can be broken down into numerous categories, including: (a) cation- π ; (b) π - π ; (c) anion- π ; (d) CH- π . These π -interactions where a region of π -rich electron system can interact with a cation (Na^+ , K^+), another π system, an anion and another molecule ^[12] are the prominent players in many key chemical selectivity and molecular recognition processes, biological processes and supramolecular structure (e.g., proteins, DNA's double helix, and G-quadruplex).

1.4.4. Hydrogen bonding

Hydrogen bonding as electrostatic interaction is formed between a donor and an acceptor. This interaction represents between a proton donor group (D-H) that involves a bonding between a hydrogen atom and an electronegative atom (O, N), and a proton acceptor group (A) with non-binding doublet, the D-H...A interaction being called as a hydrogen bond. This bonding can occur between molecules (inter-molecularly), or within different parts of a single molecule (intra-molecularly). The strength of hydrogen bonds depends on the type of electronegative atom to which the hydrogen atom is bonded and the geometry of the hydrogen bond adoption in the structure.

In general, strength of hydrogen bonds can range between 1 to 161.5 kJ mol⁻¹ [13] in different systems. Hydrogen bonding is most often associated with the functional groups summarized in Figure 5 [14] [15].

Element	Donors	Donors strength	Acceptors	Acceptors strength
fluorine	F-H	very strong	F-, F-H	very strong strong
oxygen	O-H (in an acid)	strong	⁻ O-P, ⁻ O-S ⁻ , ⁻ O-C	strong strong
oxygen	O-H (in water, or alcohols)	medium	O=P, O=S, O=C, H ₂ O, H-O-C, C-O-C	medium-strong medium
nitrogen	N ⁺ -H	strong	C=N-C	medium
nitrogen	N-H	medium	N(R) ₃	medium
sulfur	S-H	weak	S=C	medium-weak
carbon	C-H	weak	π-electrons	weak

Figure 5: Functional groups that can form hydrogen bonds, arranged by element [14] [15].

Hydrogen bonding has great potential application in the areas of material science, crystal engineering, supramolecular chemistry, and biological recognition, this being explained by their strength and their high degree of directionality. Significantly, the hydrogen bonding interaction plays an important role in stabilizing supramolecular aggregates and in determining the stability of the three-dimensional structure adopted by macromolecules like proteins and nucleic acids. Perhaps the best well-known example of hydrogen bonding is DNA for which the double helix structure is governed by many hydrogen bonds between base pairs.

1.4.5. Hydrophobic effects

Water molecules tend to exclude non-polar molecules that preferentially interact with themselves or with other more polar groups in order to limit the area between the hydrophobic molecules and the water molecules. This phenomenon is called the hydrophobic effect. In many systems related to biology, including: formation of vesicles and cell membranes, association of protein-small molecule, combination of antigen–antibody, folding

of proteins, hydrophobic effects play significant roles. Hence it is essential to life.

A hydrophobic substrate in solution breaks the hydrogen bonding network of water, creating a highly ordered layer of water molecules (hydrated clathrate) on the surface of the water ^[16]. It is the result of a thermodynamically favorable thermodynamic equilibrium and consists of two factors: the entropy factor and the enthalpy factor. When a non-polar molecule is solubilized in water, the surrounding water molecules couldn't be favorable to form hydrogen bonds with low degrees of freedom. When a non-polar cavity comes closer to it, a number of water molecules will then be released by inclusion. The ejected water molecules reformed themselves in the solvent thus lowering their energy and decreasing the enthalpy of the system ($\Delta H < 0$). On the other hand, because the water molecules pass from an organized state inside the cavity to a disorganized state in the solvent, this process is associated with an increase in entropy ($\Delta S > 0$). And the inclusion complex is also formed with heat release, while the entropic term decrease ($-T\Delta S < 0$). Further, the resulting free energy of accompanying hydrophobic interaction is negative ($\Delta G < 0$) making the binding process fast. And the result explains the preferential interaction of the non-polar molecules in water ^[17] ^[18].

$$\Delta G = \Delta H - T\Delta S$$

This hydrophobic effect participates in the formation of inclusion complexes involving cyclodextrins (Figure 6).

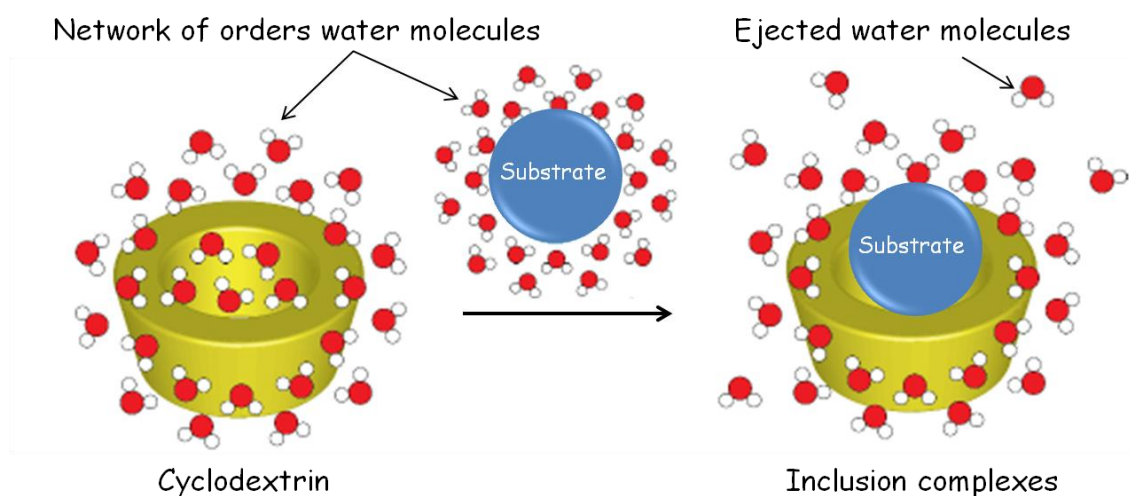


Figure 6: The hydrophobic effects involving cyclodextrins based inclusion complexes formation.

2. Supramolecular Polymer

2.1. Definition

The concept of supramolecular polymers, combination of polymer science and supramolecular chemistry, is first introduced in 1990 by Jean-Marie Lehn ^[19]. Broadly defined, supramolecular polymers can be defined as any type of assembly ^[20], on one hand by the nature of the molecular components and on the other hand by the type of interactions which link the monomers through non-covalent interactions. Subsequently, in 2001, Egbert Willem Meijer proposed a limited definition regarding supramolecular polymers: ^[21] *“polymeric arrays of monomeric units that are brought together by reversible and highly directional secondary interactions, resulting in polymeric properties in dilute and concentrated solution as well as in the bulk. The directionality and strength of the supramolecular bonding are important features of systems that can be regarded as polymers and that behave according to well-established theories of polymer physics.”* A variety of non-covalent interactions (multiple hydrogen bonds, metal coordination bonds, aromatic donor-acceptor interactions and host-guest interactions) have been employed as driving forces to form supramolecular polymers.

Unlike conventional polymers, the bond between monomeric units of supramolecular polymers is non-covalent, which indicates that it is the consequence of thermodynamic equilibrium in the assembly process. As a result, the shape and the size of polymers will directly derive from monomer concentrations, the strength of non-covalent interactions, pressure, pH, and temperature. The nature of these reversible non-covalent interactions endows the supramolecular polymers the dynamic ability, allowing modification of their constitution by incorporating, recombining, and exchanging components. They may present a variety of novel functions and properties.

Monomers for construction of supramolecular polymers can be classified into three main categories (Figure 7) ^[22]:

a) AA type



b) AB type

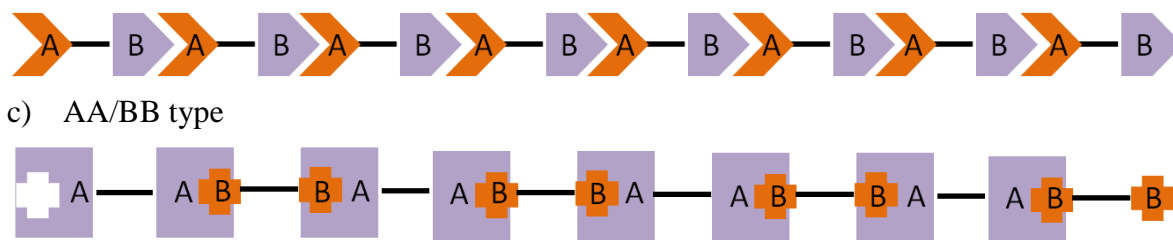
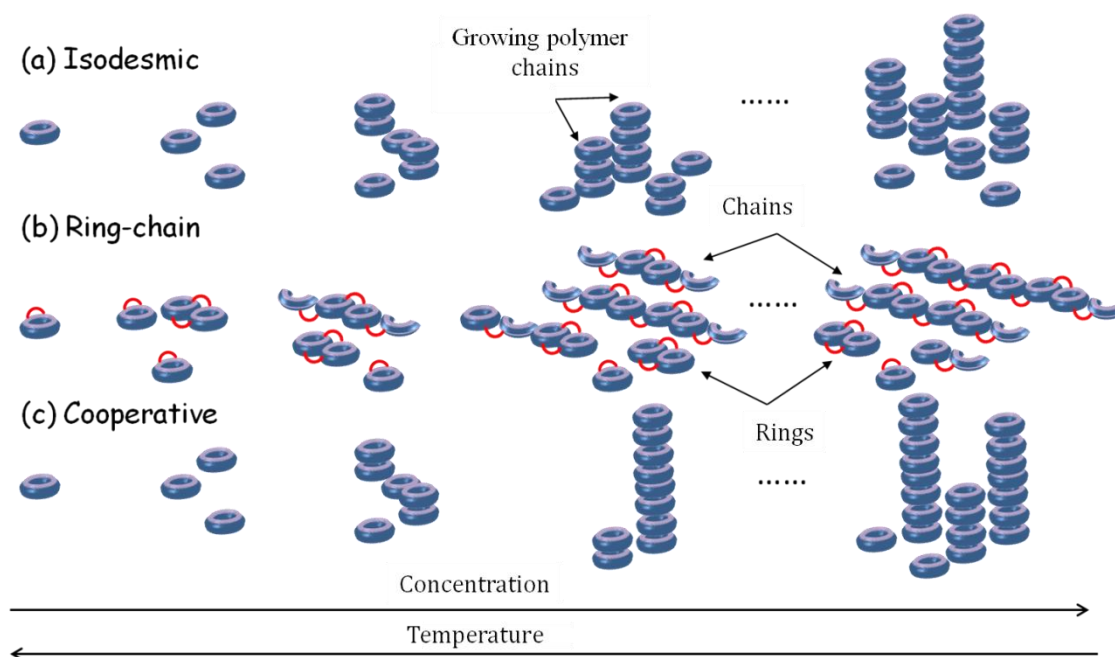


Figure 7: Supramolecular Polymer: a) AA type; b) AB type; c) AABB type.

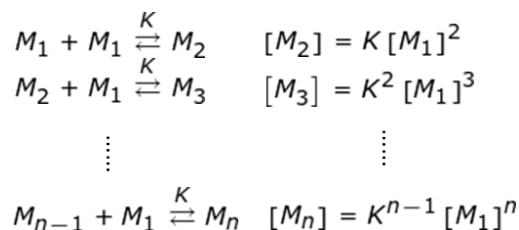
2.2. Mechanisms of association of supramolecular polymers

The mechanisms of association of supramolecular polymers are strongly dependent on the non-covalent interactions that participate in the self-assembly. In supramolecular polymerization process, there are three main growth mechanisms: isodesmic model, ring-chain model, and intermolecular cooperative model (Figure 8) ^{[23] [24]}.

Figure 8: Mechanisms of association of supramolecular polymers ^[23].

The isodesmic model (Figure 8-a) of polymerization is similar to step growth polymerization in conventional polymers, the strength of growing polymer chains is unaffected by the length of the chain. The energy of assembly is equivalent at each step, thus each step of decrease of the corresponding free enthalpy is the same. This is reflected in a single association constant for the whole polymerization process, as shown below. M_1 represents the monomer, whose molar equilibrium constant is K . Assuming no ring formation in the process, the degree of

polymerization (DP) only depends on the association constant K_a and the total concentration of monomer $[M]$, which will be approximately proportional to $(K_a [M])^{1/2}$ [25]. Furthermore, no critical concentration or temperature is required for polymerization process [26] [27] [28].



The ring-chain model of polymerization (Figure 8-b) occurs when ring oligomers could be formed by ditopic monomers. In this case, it is characterized by equilibrium between the rings (closed assemblies) and chains (open assemblies), and the concentration at which the rings and chains are equal is called the critical concentration. As a result, beyond the critical concentration, the chain polymers formation becomes more favourable, meanwhile the concentration of rings remains relatively the same. Sudden change of the degree of polymerization will be observed. The critical polymerization concentration largely depends on the rigidity and length of the monomers [24] [29] [30].

The intermolecular cooperative model (Figure 8-c) is governed by additional interactions for the growth of ordered supramolecular polymers [28]. Two phases of self-assembly are involved from the thermodynamic point of view: the nucleation phase and elongation phase. The beginning of first step follows the isodesmic model with association constant of nucleation phase (K_n) for the addition of each monomer. Until a certain size nucleus formed, the growth of polymer accelerates under the addition of new monomers, and this polymerization process continues with association constant of elongation phase (K_e). Meanwhile the association constant of nucleation phase (K_n) is lower than the association constant of elongation phase (K_e). Thus a transition is observed from a state only including the monomers to a state long polymers formed [23] [24].

2.3. Properties of supramolecular polymers

By comparison with conventional bonded polymers, a variety of non-covalent interactions play their part in supramolecular polymers, which can lead to multiple structures and formation models (Figure 9).

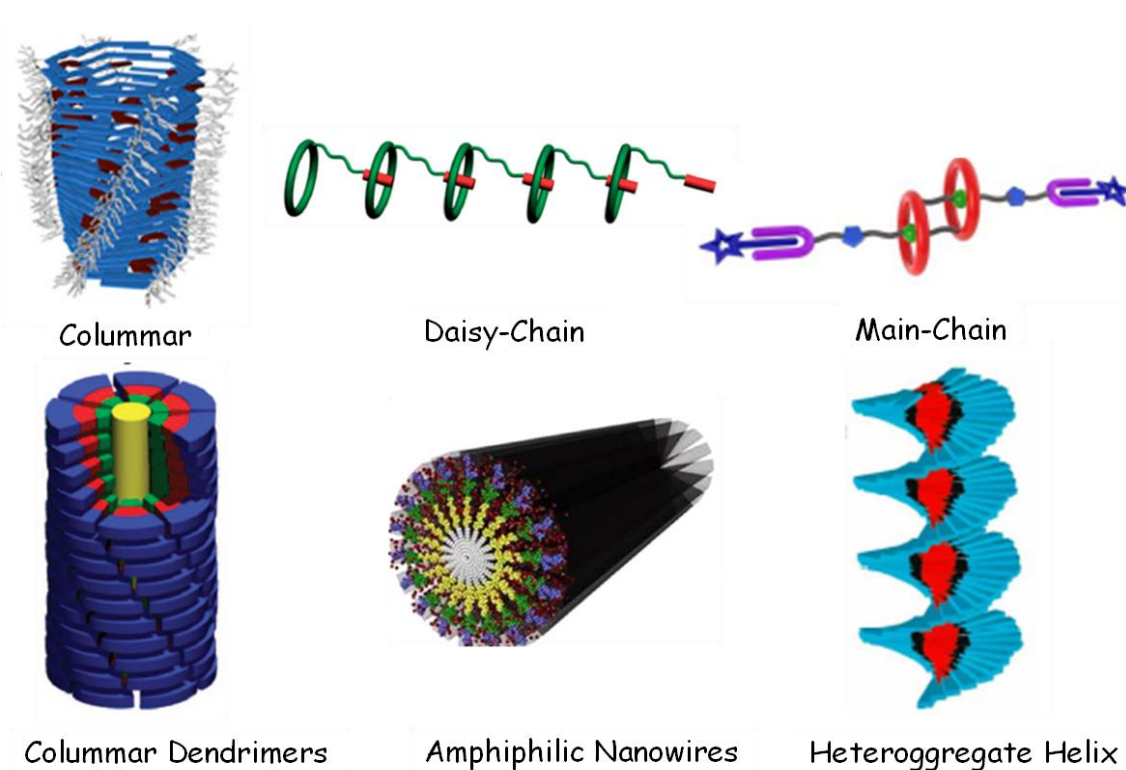


Figure 9: Supramolecular polymer consist of monomers which assemble together by non-covalent bonds, which can be split into three categories: columnar (a) ^[31]; daisy-chain (b) ^[32]; main chain (c) ^[33]; columnar dendrimers (d) ^[34]; amphiphilic nanowires (e) ^[35] and heteroaggregate helices (f) ^[36].

While supramolecular polymers can't compete with covalent polymers in terms of mechanical strength or the elasticity of plastics, their dynamic and reversible nature endow them new properties in the biological field, electronic field, and mechanical field ^[21] ^[37] ^[38] ^[39].

Covalent polymers	Supramolecular polymers
Strong, rigidity	Modular (solids, liquids, gels)
Non-dynamic nature	Dynamic and reversible nature
Stable (temperature, light, pH, electric, chemistry)	Susceptible under exposure to external stimuli (temperature, concentration, light, pH, electric, ionic strength, radiation, the addition of other molecules, or their combination)
	Biocompatible

2.3.1. Optoelectronic properties

Natural photosynthesis process proved as source of inspiration for researchers to develop optoelectronic materials to achieve the light-to-charge conversion for a wide range of applications such as electronic devices and smart windows. Simple organic molecules display elaborately designed amphiphilic interactions, quadrupole interactions, and hydrogen bonding. These supramolecular polymers show excellent properties in switching speeds, optical contrast and power conversion efficiency which are important factors for optoelectronic devices. For example, Nakayama et al. prepared a barbiturate oligo-butylthiophene based supramolecular polymer, which bore hydrogen bonds to precisely govern self-organization in the nano-level. The tapelike supramolecular array was directly observed by STM at a liquid–solid interface and further formed into helical nano-fibers in solution and bulk states by TEM, AFM and XRD (Figure 10). They gave powerful proofs that showed a high conversion efficiency of 4.5% ^[40].

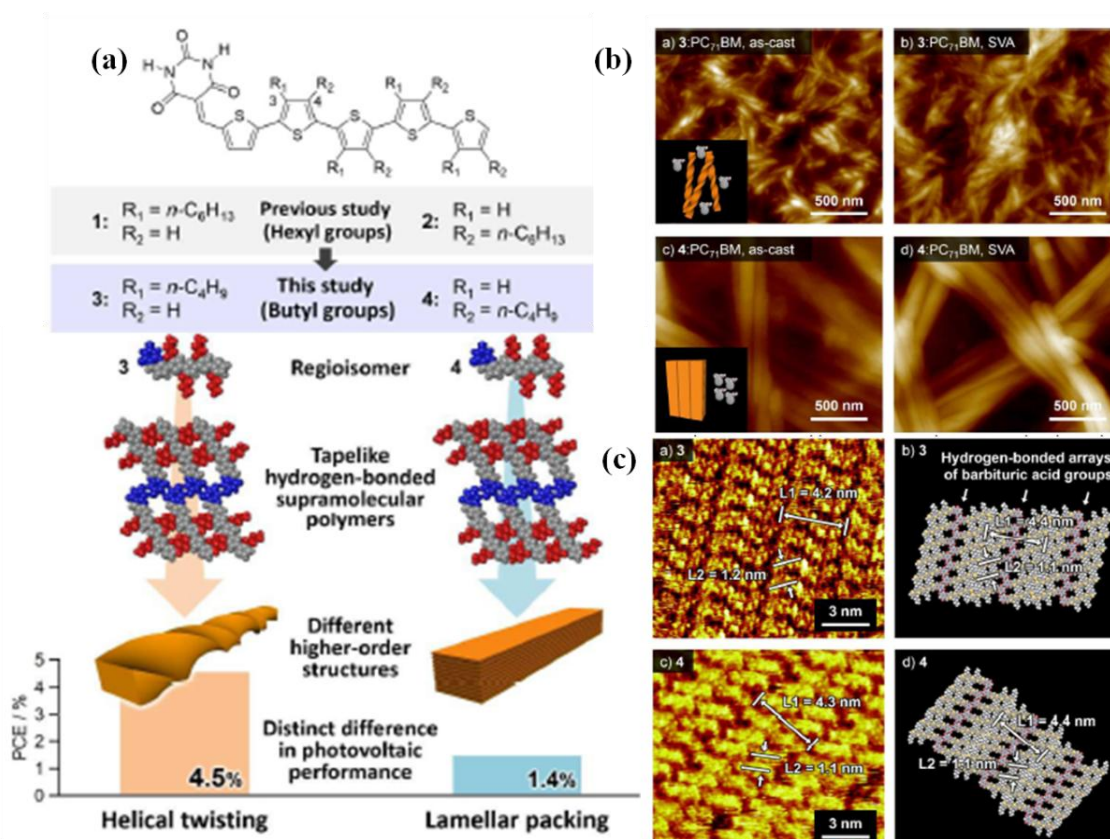


Figure 10: (a) Structures of the tapelike hydrogen-bonded supramolecular array based on barbiturated oligo(butylthiophene) molecules and nanostructures with the a power conversion efficiency; (b) AFM images; (c) STM images ^[40].

2.3.2. Mechanical properties

Highly directional forces dominate the secondary interaction between adjacent molecules. It is possible to form long chain or network polymers (plastics, hydrogels) with many mechanical properties that lead to polymer-like behaviors. Nevertheless, supramolecular polymers present feature of ‘living’ polymers due to the reversible inter-chain bonds and intra-chains bonds, which are capable of growing or shortening, of exchanging components and of rearranging their interaction patterns. Thus, it is described that supramolecular polymers respond to external stimuli (such as pH, temperature, light, chemicals, concentration or electrochemical redox).

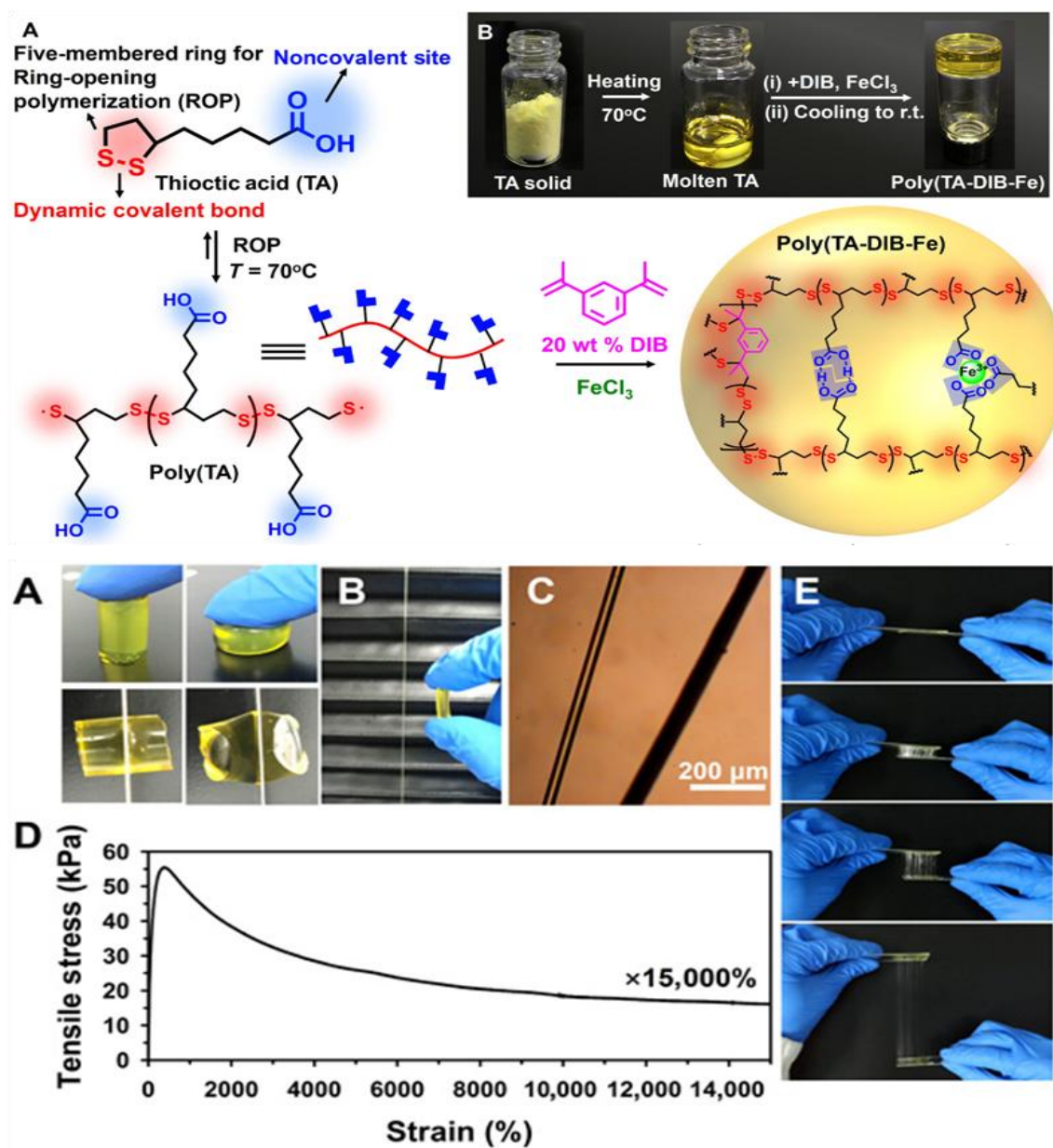


Figure 11: Schematic representation of the synthesis route of the supramolecular polymer network (above, A);

Photographs of TA powder, TA liquid, and supramolecular polymer solid at room temperature (above, B); Mechanical properties of supramolecular polymer (below) ^[41].

The Tian et al. adopted a simple and effective synthesis route toward a naturally existing small molecule, thioctic acid that assembles into a high-performance supramolecular polymer. This thermodynamically stable supramolecular polymer network consists of thioctic acid, 1, 3-diisopropenylbenzene as a quencher of the terminal diradicals of thioctic acid and ferric chloride which acted as a strong complex center with carboxylic groups to replace weak hydrogen bonds (Figure 11). The supramolecular polymer network exhibits high stretchability, low-temperature process ability, rapid self-heal ability, and reusable adhesivity ^[41].

2.3.3. Biological properties

Supramolecular polymers self-assemble by means of the combination of non-covalent interactions, which are highly vulnerable to depolymerization under external stimulus, so they are good candidates as the bioactive materials to accomplish high control over both stability and dynamics. Biological applications based on supramolecular polymers mainly involve the fields of drug delivery, bioimaging, protein/gene delivery, gene transfection, and tissue engineering.

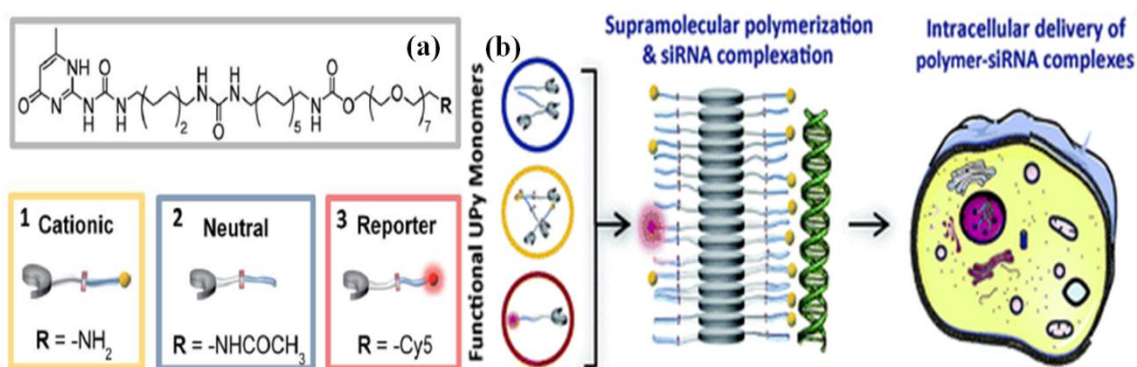


Figure 12: (a) Chemical structure of three components of supramolecular polymer: (1) cationic monomer (2) neutral monomer (3) fluorescent monomer; (b) Schematic of supramolecular polymerization-siRNA complexation and gene delivery ^[42].

Dankers et al reported the design of ureidopyrimidinone-based multicomponent supramolecular polymers in aqueous solution. They synthesized different classes of monomers through linking the ureidopyrimidinone (UPy) unit to oligo ethylene glycol (OEG) chains by three ways: amine group as end-functionalized group to obtain the cationic

monomer; acetamide as end-functionalized group to obtain the neutral monomer; Cy-5 as end-functionalized group to obtain the fluorescently labeled monomer (Figure 12). They demonstrated the ability of their system for intracellular siRNA delivery and provided a potential platform for bioimaging and biosensing ^[42].

2.4. Driving forces for supramolecular polymers

Supramolecular polymers are constructed from small molecules as building blocks, which interact through the same reversible non-covalent interactions defined previously for supramolecular chemistry in general (Figure 13). This section will discuss different bonding motifs that are employed for supramolecular polymerization: hydrogen bonds ^{[43] [44] [45]}, coordination bonds with a metal ligand and host-guest interactions ^{[46] [20]}.

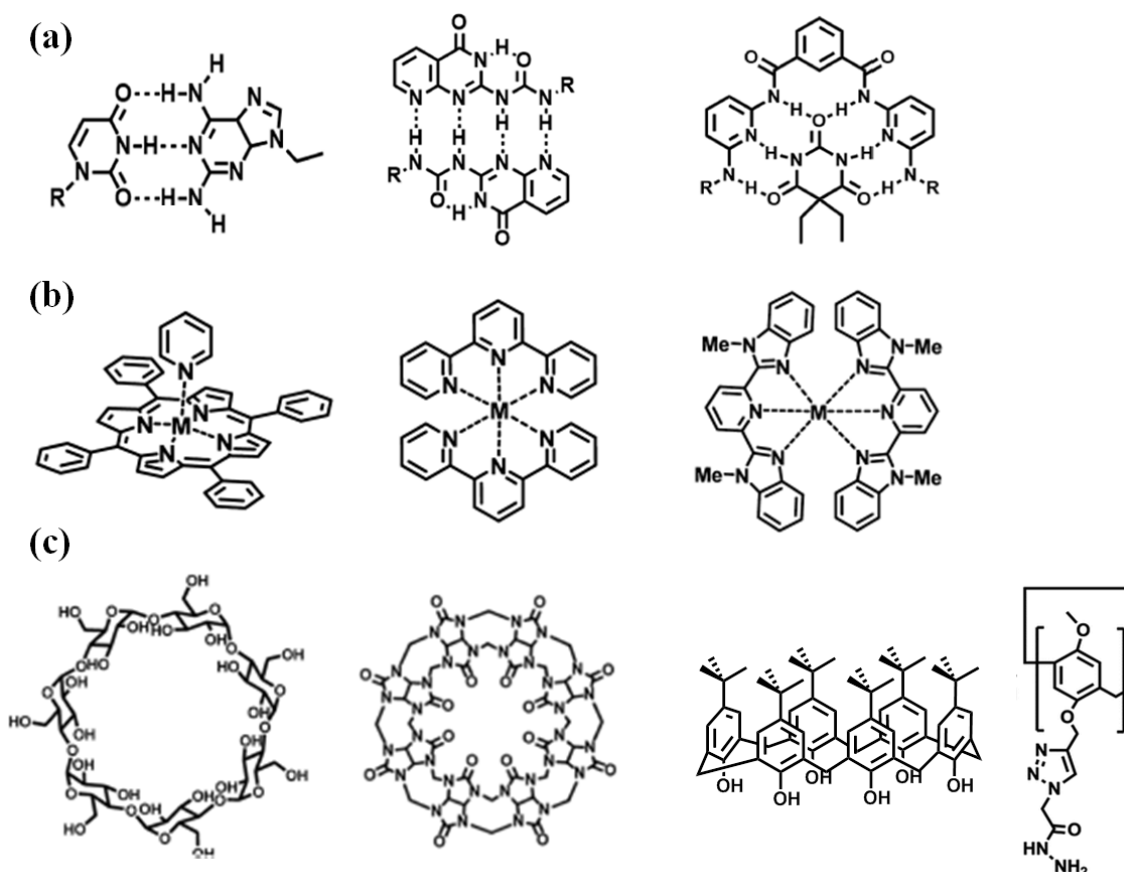


Figure 13: Supramolecular polymers are assembled by employing different type of non-covalent interaction: (a) triple-, quadruple-, and sextuple-hydrogen bonding; (b) metal coordination; (c) host guest systems: cyclodextrin, cucurbit[8]uril, calix[6]arene, and pillar[5]arene ^[20].

2.4.1. Multiple hydrogen bonds

Multiple hydrogen bonds, the first type of non-covalent bonds, were adopted to assemble supramolecular polymers. Supramolecular polymer based on hydrogen bonds was reported by Jean-Marie Lehn for the first time in 1990. The polymer synthesized via a triple hydrogen bonds show very good performance in liquid crystal ^{[47] [48]}. In 1997, Meijer et al. prepared a linear supramolecular polymer formed via quadruple-hydrogen-bonding arrays ^[49]. The polymer presented a higher association constant and degree of polymerization in CHCl₃ solution. Since the discovery of construction of supramolecular polymers employing hydrogen bonding units, the researchers have developed numerous other examples. Now multiple hydrogen bonds, a valuable type of “intermolecular glue,” are one of the most widely applied non-covalent interactions.

2.4.2. Metal coordination bonds

The organization of metal coordination bonds into metallosupra of molecular polymers through non-covalent interaction has been extensively studied. Because of the mixed of properties from organic polymers and those of metal properties (ions, magnetic, optical, electronic or catalytic), metal coordination polymers have been a flourishing interdisciplinary research topic ^{[20] [50] [51]}.

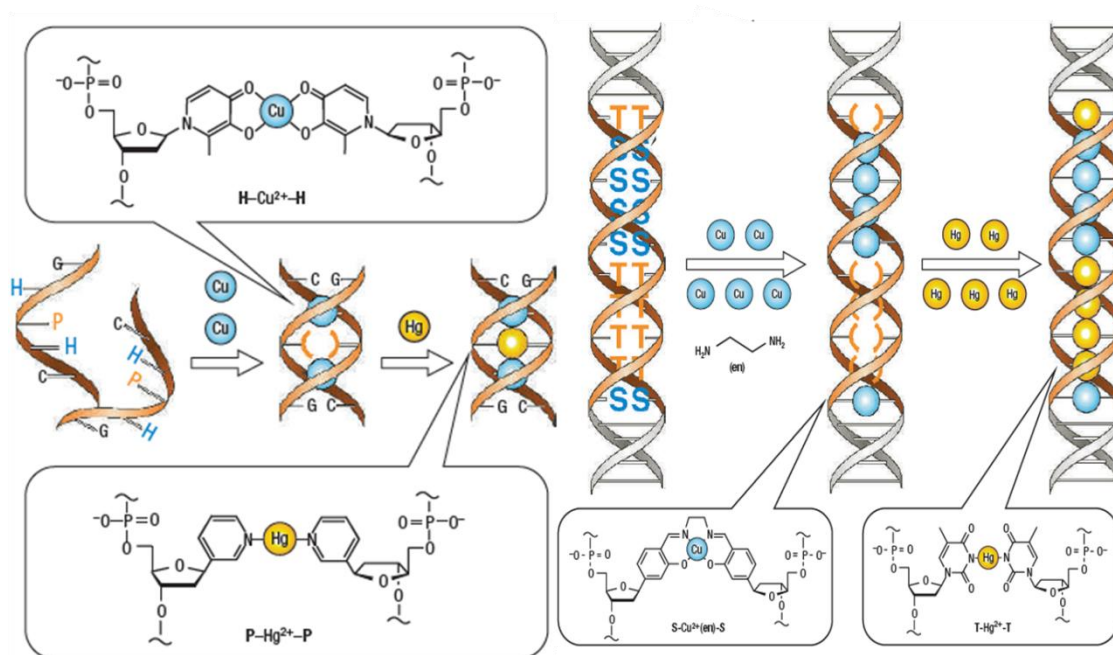


Figure 14: Schematic representation of metal ion mediated assembled artificial DNA skeleton through two metal mediated base pairs in addition to natural base pairs of DNA, in which hydroxypyridone nucleobases (H), pyridine nucleobase (P), salicylic aldehyde nucleobase (S) and thymine nucleobase (T) are included in place of natural nucleobases ^[52].

The incorporation of metal coordination bonds into metallosupramolecular polymers (MSPs) is ubiquitous in nature. And MSPs participate in many important life processes, such as oxidations and reductions, oxygen transport and gene activation ^{[51] [53] [54]}. Thomas's group reported a supramolecular polymer efficiently combining metal ions and DNA to mimic DNA, which is capable of self-assembling into complex networks (Figure 14). Two artificial single-stranded DNA contained Cu^{2+} and Hg^{2+} mediated metal base pairs (hydroxypyridone nucleobases (H), pyridine nucleobase (P), salicylic aldehyde nucleobases (S) and thymine nucleobases (T)). The artificial DNA resulted in a duplex where it was possible to control the number and position of the metal ions by altering the number and sequence of the various metal base pairs. This novel molecular architectures preparation strategy exhibited promising properties, including conducting catalysis or nanomagnetism ^[52].

2.4.3. Host-guest interaction

The well-known host molecules for construction supramolecular polymers involve cyclodextrins, cucurbit[n]urils, crown ethers, calix[n]arenes, and pillar[n]arenes. The properties of these typical host molecules are summarized in Figure 15 ^{[20] [55] [56]}. Host-guest complexes show great potential for application in the pharmaceutical, biochemical, and environmental fields.

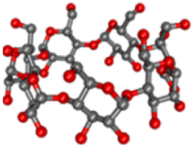
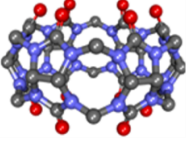
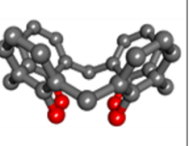
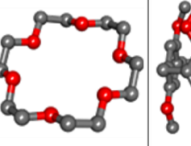
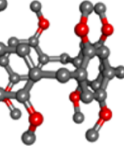
Structure					
Properties					
Name	Cyclodextrin	Cucurbituril	Calixarene	Crown ether	Pillararene
Shape	Bucket	Pumpkin	Calix	Crown	Pillar
Homologs	α , β , γ -CD	5-8	4-8	12-24	5,6
Synthesis	+	++	+++	+++	+
Solubility (Aqueous)	+++	+	+	+++	+
Solubility (Organic)	+	+++	+++	+++	+++
Functionally	+	++	+++	++	+
Host-guest (Aqueous)	+++	+	+++	++	+++
Host-guest (Organic)	++	-	+++	+++	+++
Flexibility	Rigid	Rigid	Flexible	Flexible	Flexible
Symmetry	-	+++	-	-	+++

Figure 15: The structure and properties of well-known host molecules ^[56].

In this part, we will see some selected examples of host-guest supramolecular polymers. Benefitting from π rich cavities and three-dimensional structures, supramolecular polymers based on calixarenes/pillararene are widely used. One water-soluble supramolecular polymer based on pillararene was reported by Huang's group. The pillar[10]arene and paraquat derivative formed a 1:2 [3]pseudorotaxane. The cooperation of this complexation was proved by a Scatchard plot. Moreover, this complex constructed the first pillararene-based gemini-type macromolecule in water, which self-assembled into polymeric vesicles with a wall thickness of 18 nm and an average size of 142 nm (above the LCST of paraquat-bearing homopolymer). Because of thermo-responsivenesses of pillar[10]arene and paraquat-bearing homopolymer, as well as their different LCST behaviors, a unique dual-thermo-responsive polymeric vesicle was prepared and showed great potential for application in the controlled release of hydrophobic doxorubicin and water-soluble dyes (Figure 16-a) ^[57].

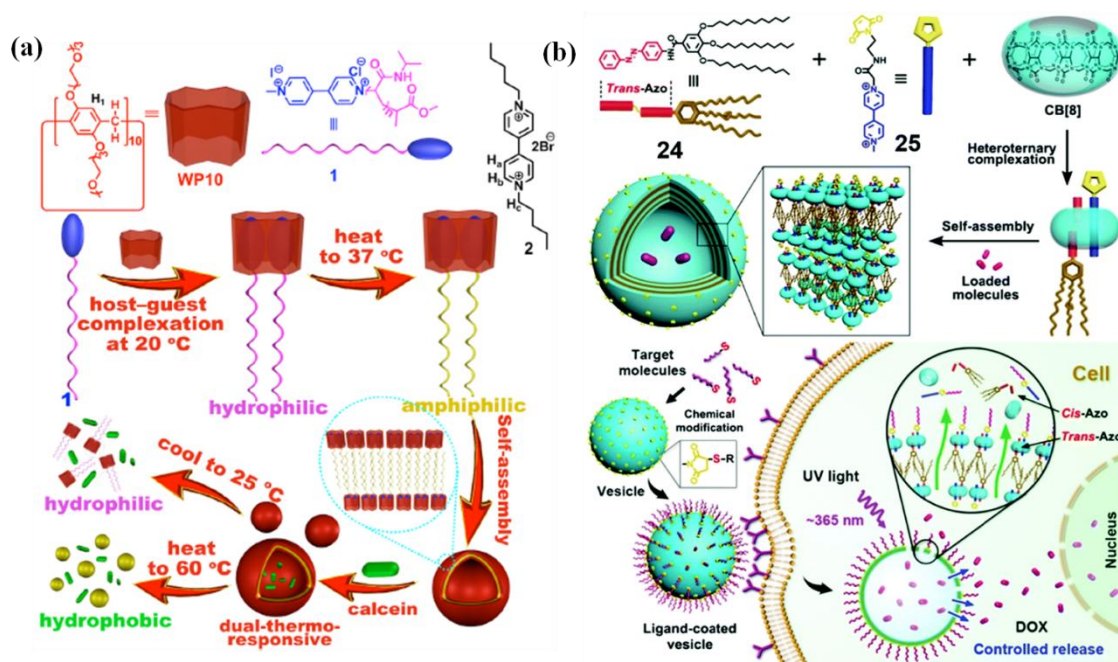


Figure 16: (a) Schematic representation of pillar[10]arene-based supramolecular assembly and its thermo-controlled release ^[57]; (b) Schematic representation of the self-assembled vesicle by the CB[8]/azobenzene/methylviologen derivatives and its light-controlled release ^[58].

Cucurbiturils (CBs) are an important type of host. Notably, two molecules together can rapidly slide into the large cavity of CBs, employing hydrophobic interaction and ion-dipole interactions to form a 1:1:1 complex, which is often regarded as a linker to construct supra-amphiphiles ^[59] ^[60]. Liu et al. developed a system containing CB[8], azobenzene and methylviologen derivatives (Figure 16-b). CB[8] could encapsulate methylviologen and azobenzene to form a 1:1:1 complex, which self-assembled into larger than 800 nm stable supra-vesicles. The trans/cis azobenzene isomers can be reversibly switched under UV/visible light and the cis-azobenzene unit could force out from the cavity ^[61]. Based on this phenomenon, photo-responsive vesicles and drug release devices were designed. Besides, the maleimide groups on the surfaces could be functionalized with hyaluronic acid, which enhanced endocytosis efficiency and the specificity for tumor cells. This work not only broadened the application in the photo-responsive field but also offered a visual drug release strategy ^[58].

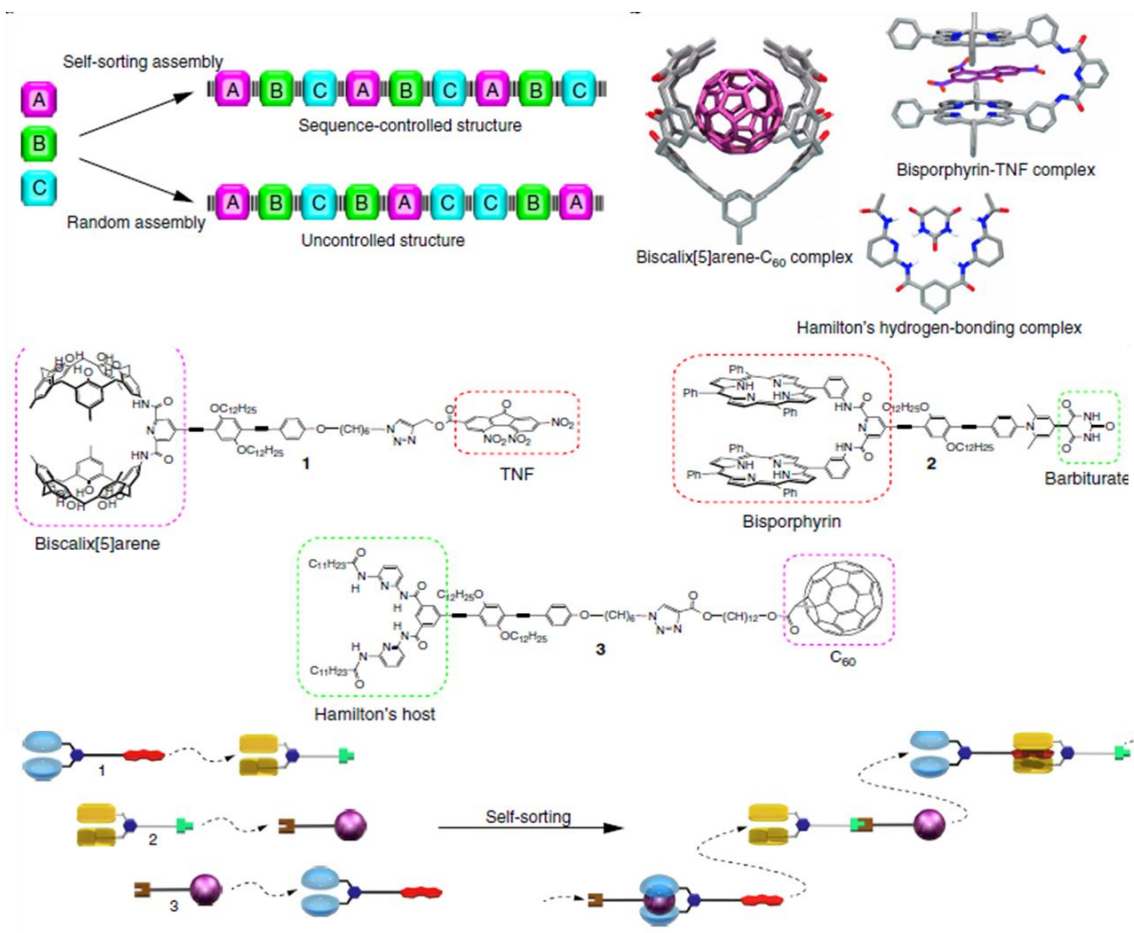


Figure 17: Schematic representation of sequence-controlled terpolymer via multiple non-covalent interactions of three monomers and the head-to-tail terpolymerization complex $[1-2-3]_n$ in sequence ^[62].

As mentioned above, supramolecular polymers are almost all fabricated containing one type of non-covalent interactions. But supramolecular polymers in nature are constructed by a combination of multiple non-covalent interactions. Chemists were inspired by complicated biological systems, attempting to assemble supramolecular polymers via multiple interaction ^{[63] [64] [65] [66] [67] [68] [69] [70]}. Haino et al. represented a sequence-controlled supramolecular terpolymer whose sequence was driven by the donor-acceptor, ball-and-socket, and multiple hydrogen bonding interactions that separately appear in the process of TNF-bisporphyrin, barbiturate-Hamilton's host and biscalix[5]arene- C_{60} , respectively (Figure 17). These three monomers were combined in a 1:1:1 complex, which highly precisely self-sorted into the head-to-tail terpolymerization complex in sequence. This strategy may be broadly applied to the manufacture of tailor-made polymer sequences with complex and diverse structures. Furthermore, sequence-controlled supramolecular polymers via self-sorting are promising to achieve controlling advanced functions related to polymer in sequences, such as stimuli

responsiveness, shape memory, and self-healing^[62].

2.5. Characterizations of supramolecular polymers

Supramolecular polymers are quite different from traditional polymers because of the dynamic and reversible natures, so many well-established characterization techniques for traditional polymers may not work well. Therefore, chemists have obtained information by combining various characterization techniques, assisted by a proper theoretical estimation.

Characterization steps	Characterization techniques
Inclusion	¹ H-NMR, ROESY
Equilibrium constant (K)	¹ H-NMR, ITC
Degree of polymerization (DP)	NMR-DOSY, MS, SANS
Size	NMR-DOSY, DLS, VPO, SANS
Shape	TEM, Cryo-TEM, AFM, SANS

Figure 18: General analysis methods of supramolecular polymers are summarized.

General analytical methods of supramolecular polymers are summarized in Figure 18. Taking cyclodextrin as an example, the first step, it is very important to confirm the spatial state of the guest within the cyclodextrin cavity. The second step, it is necessary to estimate the degree of polymerization (DP) by identification the equilibrium constant (K) of the guest for the cavity of the cyclodextrin. The third step, the size and the shape of the supramolecular polymers are observed by microscopy.

2.5.1. NMR spectroscopy

2.5.1.1. ¹H-NMR

¹H-NMR study is one way to confirm the formation of supramolecular polymers. Since the degree of supramolecular polymerization depends on the initial concentration of monomer when the process is the absence of self-inclusion, different concentrations reflect difference states of species distributions in the environment. Taking the cyclodextrins as an example, two changes can be observed: (1) it is possible to observe a variation in the chemical shifts of the protons of the monomer. In particular, the chemical shifts of protons of the guest will

show significant change, due to the surrounding from the hydrophilic environment into the hydrophobic cavity; (2) it is possible to observe broadening chemical shifts after the supramolecular polymers self-assembly in solution. Both of two changes are caused by differences in nuclear spin relaxation between the monomer/oligomer and the supramolecular polymer, which in turn leads to the magnetization of these particles of different size to be inhomogeneous in solution.

Furthermore, the analysis results of $^1\text{H-NMR}$ spectra of supramolecular complexes at variable concentration could also allow estimating thermodynamic information of the complexation process. It is possible to acquire a certain affinity constant of supramolecular polymers by $^1\text{H-NMR}$ studies: (1) the degree of the polymer (DP) can be simply estimated to be $1/(1-p)^{[71]}$, where p is defined $\Delta\delta/\Delta\delta_c$, which are respectively assumed to a chemical shift change caused by complete complexation ($\Delta\delta$) and at a given concentration of monomer ($\Delta\delta_c$); (2) the thermodynamic constant can be easily calculated as $DP \approx (KC)^{1/2}$, where K is the affinity constant and C is total monomer concentration $^{[21]}$, assuming the isodesmic model applies.

2.5.1.2. NMR-Rotating-frame nuclear Overhauser Effect Spectroscopy (NMR-ROESY)

In NMR spectroscopy, the Nuclear Overhauser Effect (NOE effect) provides accurate information on the relative orientation of a molecule in a supramolecular polymer, such as a protein or other large biological molecule with a three-dimensional structure. The NOE effect is based on spin relaxation from two atoms interaction. And it is only related to the proximity of two atoms in the space rather than through bond J couplings. In other words, this effect is almost determined by the inter-nuclear distance (distance limited to 6\AA) $^{[72] [73]}$.

The two experiments, called NMR-NOESY and NMR-ROESY, have the same principle and are performed in two dimensions, which can detect this effect by visually measuring the integration of the coupled atoms. The frequency of the spectrometer (ω) and molecules rotational correlation time (τ_c) are two important parameters for the NOE intensity. And the rotational correlation time (τ_c) directly depended on solvent viscosity and the molecular weight. Higher viscosity and larger molecular weight correspond to longer relaxation time. For small sized molecules ($MW < 600$), the NOE is positive; for medium sized molecules (MW between 700-1200), NOE is zero; for large sized molecules ($MW > 1200$), NOE is negative (Figure 19). Hence for molecules with a molecular weight between 700-1200

g mol^{-1} , the NMR-ROESY is used to measure the NOE effect rather than the NMR-NOESY [72] [74].

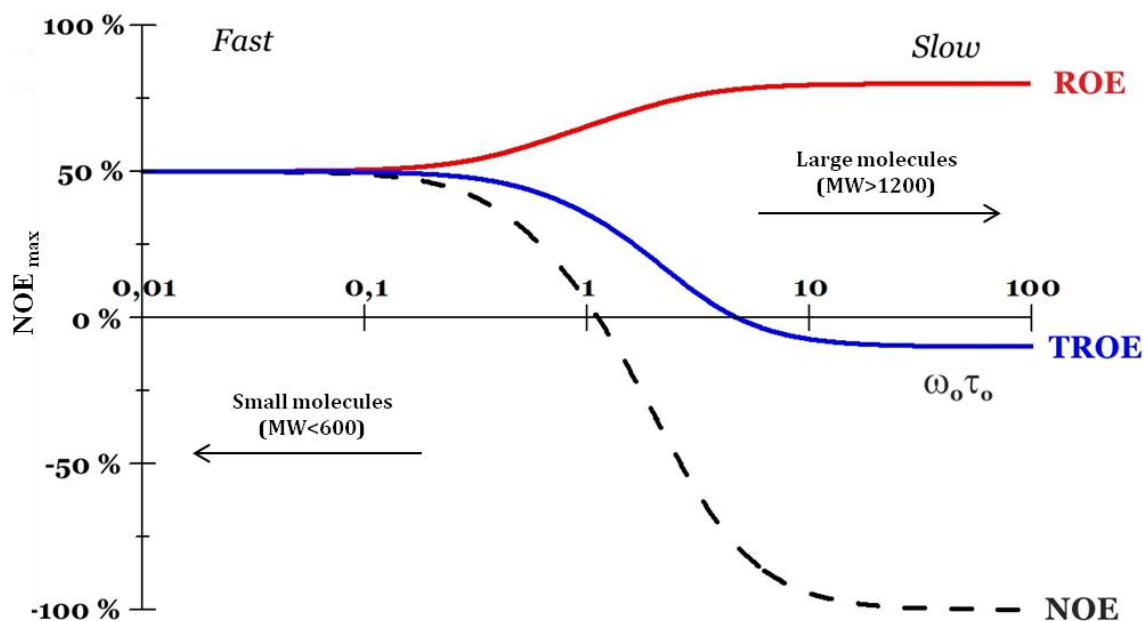


Figure 19: Maximum NOE or ROE effect as a function of rotational correlation time [75].

In the case of cyclodextrins, owing to NMR-ROESY study, we can confirm the direction of the inclusion of the guest in the cavity according to the cross-correlations observed between the protons of the guest and those of the cavity. More precisely, the H-3 protons and H-5 protons of the cyclodextrin are situated inside the cavity. The interactions with the protons of the guest help us verify the inclusion of the hydrophobic guest, allowing discrimination of the self-included species and the polymerized species (Figure 20).

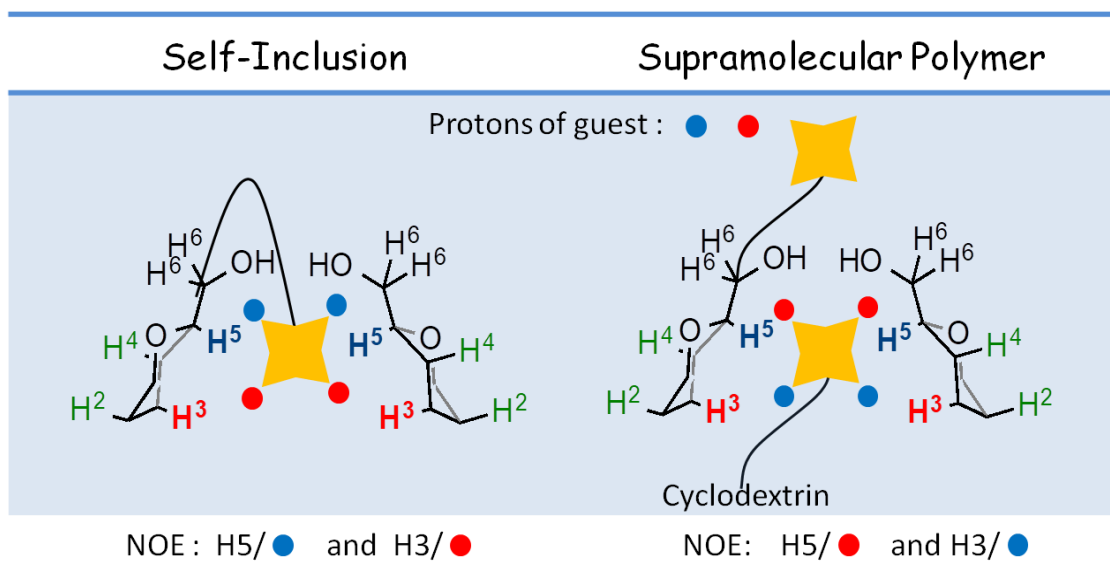


Figure 20: Verification of self-included species and the polymerized species by NMR-NOESY study.

2.5.1.3. NMR-Diffusion Ordered Spectroscopy (NMR-DOSY)

Two-dimensional NMR-DOSY becomes a powerful tool for characterization of supramolecular polymers [76] [77], which is a technique for qualitatively estimating the diffusion coefficient (D) of species in sample solution. A large diffusion coefficient corresponds to small supramolecular polymer, when lowering of the diffusion is associated to the growing size of the supramolecular assembly. Moreover, the size of supramolecular polymers can be calculated according to the Stokes-Einstein equation.

$$D = \frac{k_B T}{6\pi \eta r}$$

Where:

D Coefficient of diffusion (m s^{-1})

k_B Boltzmann constant (J K^{-1})

T Kelvin temperature (K)

η Viscosity of the solvent (Pa s)

r The radius of the spherical particle (m)

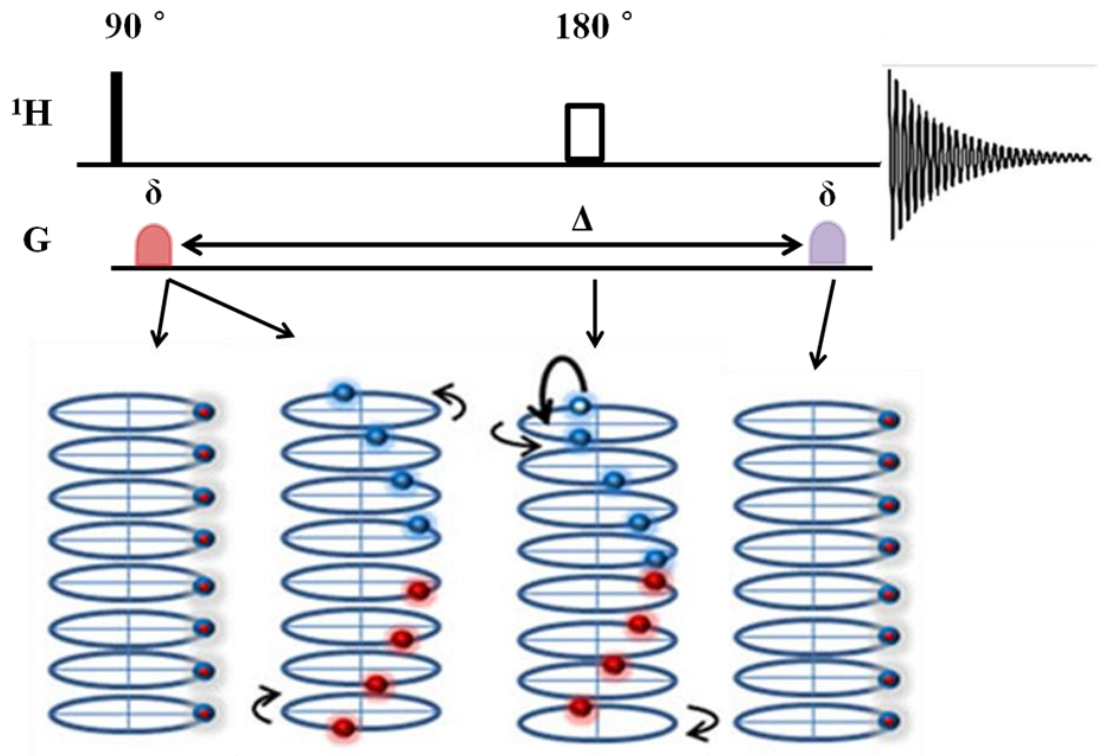
The result at the basis of the relationship mentioned above holds true for many systems. However, the disadvantage of this method is that a rough estimate of the average molar weight of the supramolecular polymer causes the different supramolecular polymer system to badly meet the requirements of the Stokes-Einstein equation model [20].

The DOSY mechanism is based on the Pulsed Field Gradient Spin Echo (PFG-SE) experiments [78]. First a 90° magnetic pulse ensures all spins to be placed in the same direction. Then applying a pulsed field gradient (PFG) of duration (δ) gives rise to a phase shift of the global magnetization. That is to say, the different vertical positions of the molecules in the NMR tube result in the application of different magnetic pulses. After diffusion delay, a period of $\Delta/2$, the same gradient of the pulsed field in the opposite direction then applied to reverse the magnetization.

In the absence of diffusion phenomenon, the spin echo obtained is the same as the beginning of the experiment (Figure 21-a); on the other hand, in the presence of diffusion phenomenon,

the faster the molecular diffusion in the tube, the smaller the spin echo obtained (Figure 21-b)
 [79] [80].

(a) NMR-DOSY without diffusion phenomenon



(b) NMR-DOSY with diffusion phenomenon

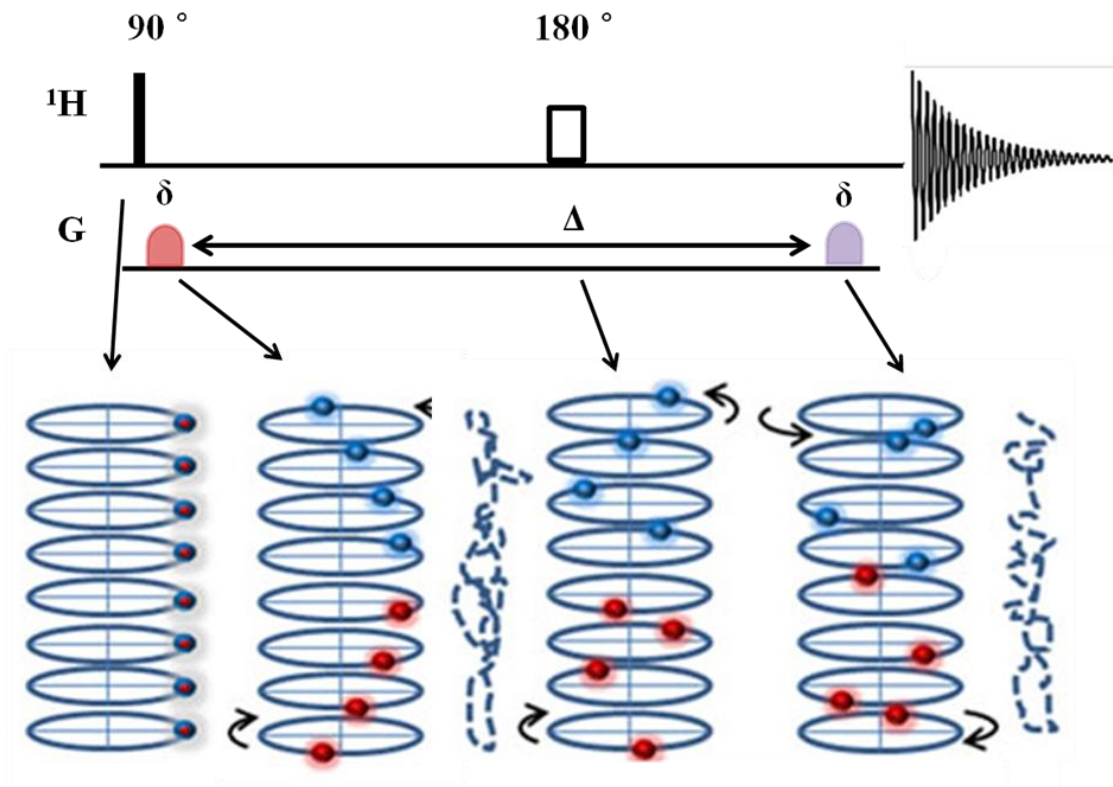


Figure 21: NMR-DOSY experiment without diffusion (a) and diffusion (b) ^[80].

Furthermore, there is an exponential function between the decrease of signal intensity and the diffusion coefficient (D). The relationship between them is as follows:

$$I = I_0 e^{\left(-D\gamma^2 g^2 \delta^2 \left(\Delta - \frac{\delta}{3}\right)\right)}$$

Where:

- I the current intensity or integral of a signal
- I_0 the reference intensity or integral of a signal
- D coefficient of diffusion (m s^{-1})
- γ the gyromagnetic ratio of the nucleus ($\text{rad s}^{-1} \cdot \text{T}^{-1}$)
- g the gradient pulse strength (T^2)
- δ the duration of the gradient pulse (s)
- Δ the diffusion delay time (s)

It is, therefore, possible to estimate the degree of polymerization through the diffusion coefficients, measuring at constant temperature and in the same solvent.

2.5.2. Isothermal Calorimetric Titration (ITC)

ITC ^[81] is a physical technique that allows to determine the interaction between two molecules thermodynamic parameters of interactions in solution, so it is the quantitative method of multiple molecules of supramolecular polymer systems and diverse bio-molecular interactions. This method works by directly measuring the absorbed or released heat during the two compounds binding process. Particularly, it is the only method that can give all binding parameters at the same time in a single experiment. The parameters involve binding constant, reaction stoichiometry, enthalpy (ΔH) and entropy (ΔS).

The device of the thermal core includes two isolated cells with an adiabatic shield (Figure 22-a). The two cells are filled with a certain concentration of the sample solution and the solvent as a reference, respectively. Taking a host-guest system as an example, firstly, two cells are set to the desired experimental temperature and kept at the same temperature during the whole experiment. Then, a given concentration of guest solution is loaded into the micro-syringe which locates above the sample cell. A series of heat changes in the cell during the formation of the inclusion complex caused by the injection are detected and measured

(Figure 22-b). ITC experiment not only characterizes the affinity constant between two molecules but also explains the mechanisms of molecular interactions.

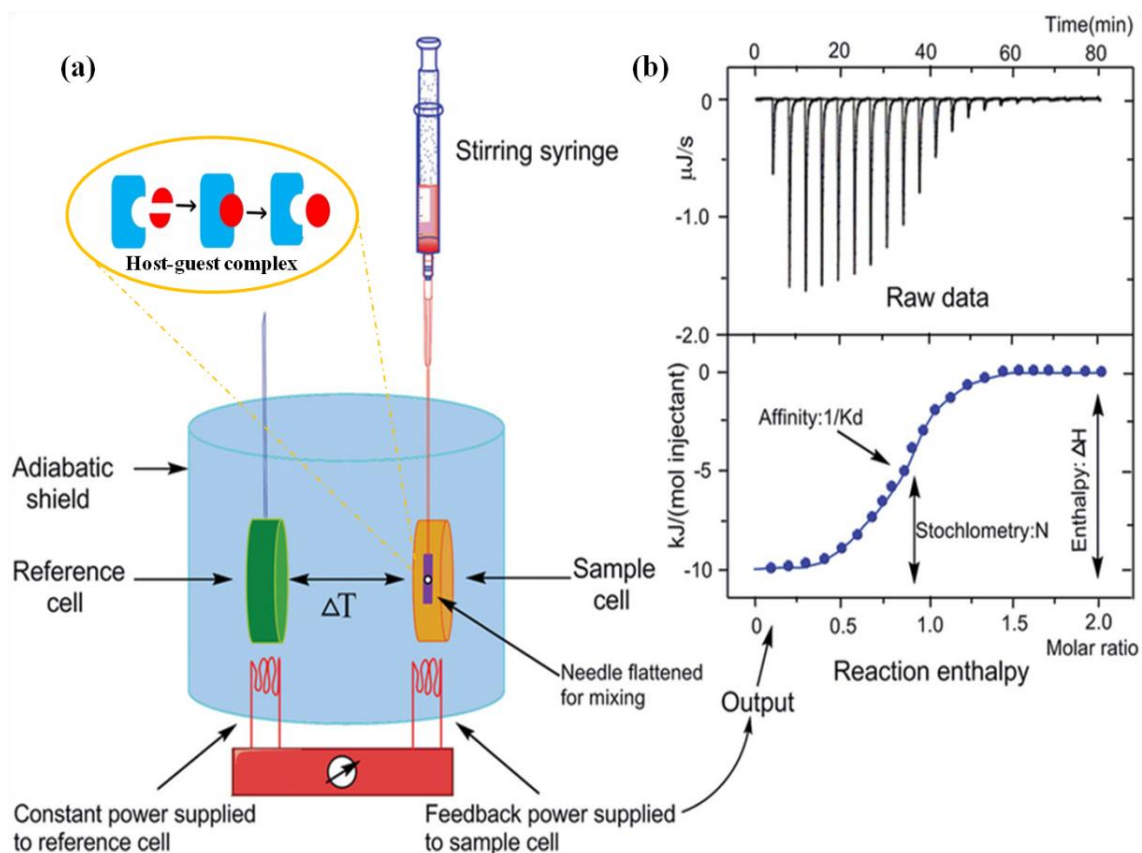


Figure 22: (a) Schematic of principle of an ITC experiment to characterize the interaction between two molecules (host-guest); (b) Results of various thermodynamic parameters ^[81].

2.5.3. Dynamic Light Scattering (DLS)

DLS is a well-established tool that provides information (hydrodynamic radius) about the particle size distribution of supramolecular polymers. This technique is suitable for particle with hydrodynamic radius in the range of 2-500 nm ^[82].

The principle of the DLS experiment is based on the difference in light diffusion as a function of the size of the molecules. The DLS experiment works by measuring the scattered laser light intensity during the illuminating the liquid sample over time. The molecules diffusion subjects to Brownian motion. As a result, it means the larger the particle, the slower the diffusion, and vice versa (Figure 23). This method only results in an approximation of the species size range rather than an exact value. In addition, the size distribution information of

small species solutions cannot be truly reflected due to the possibility of interference from a small amount of large particles in the solution. This might lead to misleading results for the size distribution of analytes by DLS ^[83].

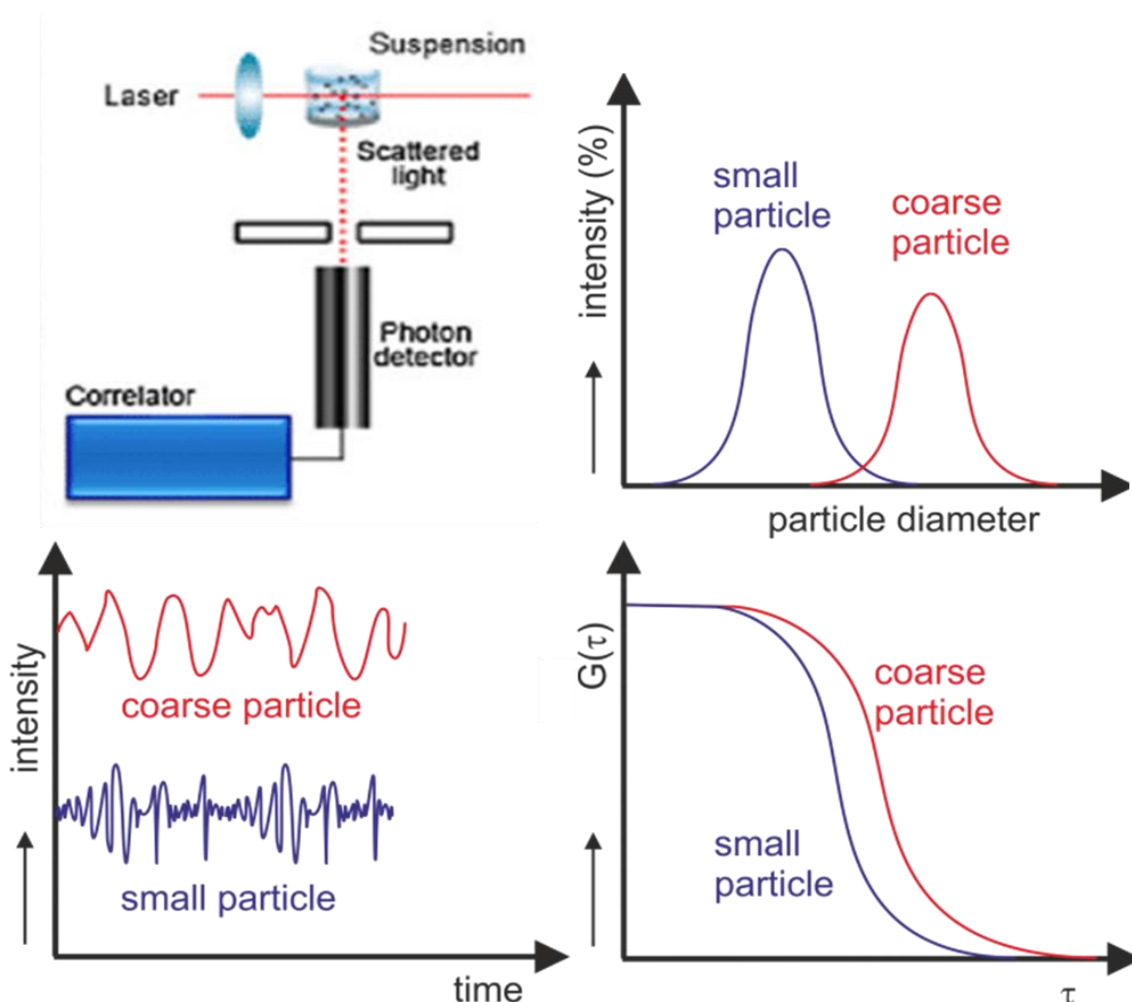


Figure 23: Measurement principle of DLS ^[83].

2.5.4. Viscometry

The measurement of viscosity (η) is a classic technique to characterize the polymerization process. The viscosity (dynamic or kinematic) measured by the viscometer depends on the type of viscometer used. There are many different types of viscometers, such as orifice viscometers, capillary viscometers, vibrational viscometers. Supramolecular polymer systems usually evaluate its dynamic viscosity rather than kinematic viscosity.

Generally, the dependence of this viscosity on the molecular weight (M) of the polymer can be described by the Mark-Houwink-Sakurada equation as following: $[\eta] = KM^\alpha$, in which K

and α are both experiential constants derived from calibration experiments that perform with a set of standard polymer samples with different molecular weights ^{[20] [84]}. Therefore, in most cases, viscosity measurement can only be used as a qualitative method for studying supramolecular polymerization ^[20].

2.5.5. Small-Angle Neutron Scattering (SANS)

Small-angle neutron scattering is an important technique that gives the opportunity to extract the size and shape of the supramolecular assembly ^[85]. A beam of neutron with a given wavelength is applied to the sample. The interaction of neutrons with the nuclei or with the magnetic momentum of unpaired electrons results in scattering in all spatial directions which are detected by the receiver in the form of spots. The scattered intensity outputted is only a function of the scattering vector q , whose modulus is defined as:

$$q = \frac{4\pi \sin \theta}{\lambda}$$

Where θ is the angle of deviation of incident light (rad) and λ is the wavelength of the neutron (m). The shape of the supramolecular assembly is deduced by effective cross-section from plotting $I(q) = f(q)$ ^{[86] [87] [88]}.

3. Cyclodextrins Based Supramolecular Polymers

3.1. Cyclodextrin (CD)

3.1.1. Structure and properties of cyclodextrin

The cyclodextrin was discovered by the French chemist Antoine Villiers. In 1891, during the study of starch degradation under the action of the bacillus amyloabacter ^[89], he successfully isolated a substance whose physicochemical properties were close to cellulose. After 15 years later, Franz Schardinger obtained two distinct crystals of this substance, which probably are the α -cyclodextrin and β -cyclodextrin at the basis of our current knowledge. Karl Johann Freudenberg firstly experimentally demonstrated the cyclic structure of cyclodextrins in 1936 ^[90]. Dexter French determined their molecular weights and discovered their exact chemical structure in 1942 ^{[91] [92] [93]}.

Cyclodextrins (CDs) are a class of cyclic oligomers composed of 6, 7, 8 glucopyranose units (4C_1 conformation) (named α -, β -, and γ -cyclodextrin, respectively) via α -1, 4-D-glycosidic bonds. Their three-dimensional structure is vividly described as a doughnut truncated cone. The dimensions of them increase with the number of unit contained in the structure. The specific diameters of cyclodextrins are approximately 4.7 Å-7.5 Å (narrow rim) and 5.3 Å-8.3 Å (wide rim), respectively. And the cavity depth of them is the same as 7.9 Å (Figure 24) ^{[94] [95] [96]}.

There are three free hydroxyl groups on each unit of a cyclodextrin: one primary hydroxyl group on the narrow rim and two secondary hydroxyl groups on the wide rim. The rigidity of a cyclodextrin depends on the hydrogen bond between the two secondary hydroxyl groups of adjacent rings, and the deviation of the coplanar O4 atom from the general mean plane is less than 0.25 Å ^[97]. The larger CDs become slightly twisted with low rigidity. In the structure of cyclodextrin, the H1, H2, and H4 protons are located at the exterior of the cyclodextrin molecule; the H3 protons placed near the narrow rim and the H5 protons placed near the wide rim point towards the interior of the cavity. Moreover, the solubility in water of cyclodextrins is 145 g L⁻¹, 18.5 g L⁻¹, and 232 g L⁻¹, respectively ^[94].

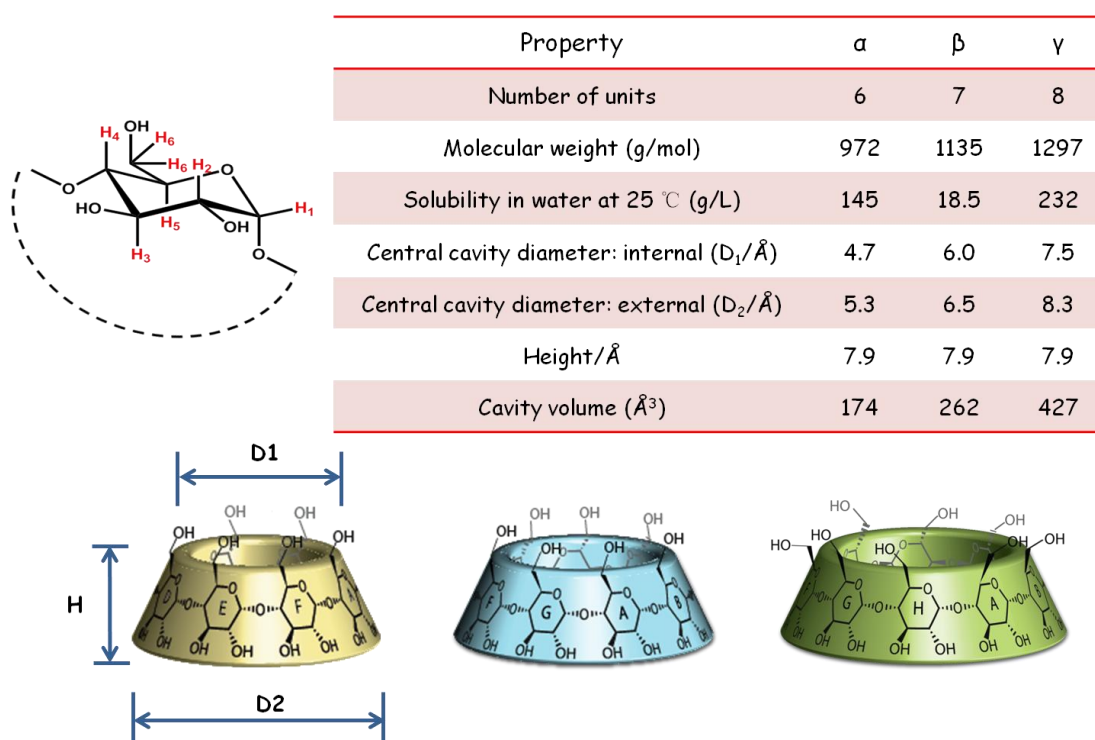


Figure 24: The characteristics of cyclodextrins.

3.1.2. Properties of cyclodextrin cavity

The CDs consist of a hydrophobic cavity and two hydrophilic shells. They can form inclusion complexes by entrapping organic molecules (guests) in the cavity of the cyclodextrins (hosts) (Figure 25). The first patent on inclusion complexes of the small compounds in CD cavities in water was registered in 1953 ^[98]. This property allows it endow great potential for application in pharmacy, food, chemistry, cosmetic and engineering.

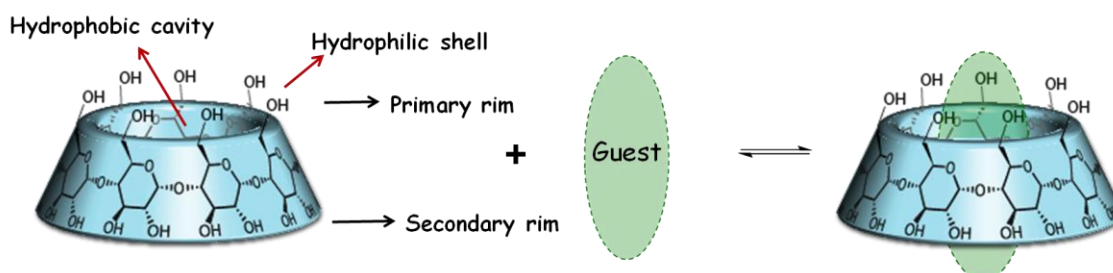


Figure 25: Inclusion complex formation.

3.1.2.1. Inclusion complex of cyclodextrins

Apart from consideration of the hydrogen bonding and the steric effect that requires the guest to match the cyclodextrin cavity, there are two important driving forces allowing cyclodextrin to encapsulate guests: (1) the van der Waals forces and (2) the hydrophobic effect.

(1) Van der Waals forces

All types of van der Waals forces (Keesom, Debye and London dispersion) participate in the construction of the cyclodextrin inclusion complex. The cyclodextrin as a polarized molecule exists a rather large dipole moment (10-20 D) and the direction of the dipole moment points from the secondary rim to the primary rim ^[99]. Hence, many guest molecules with dipole moments lead to an increase in the energy of the interaction within the cyclodextrin-guest system (Figure 26-a).

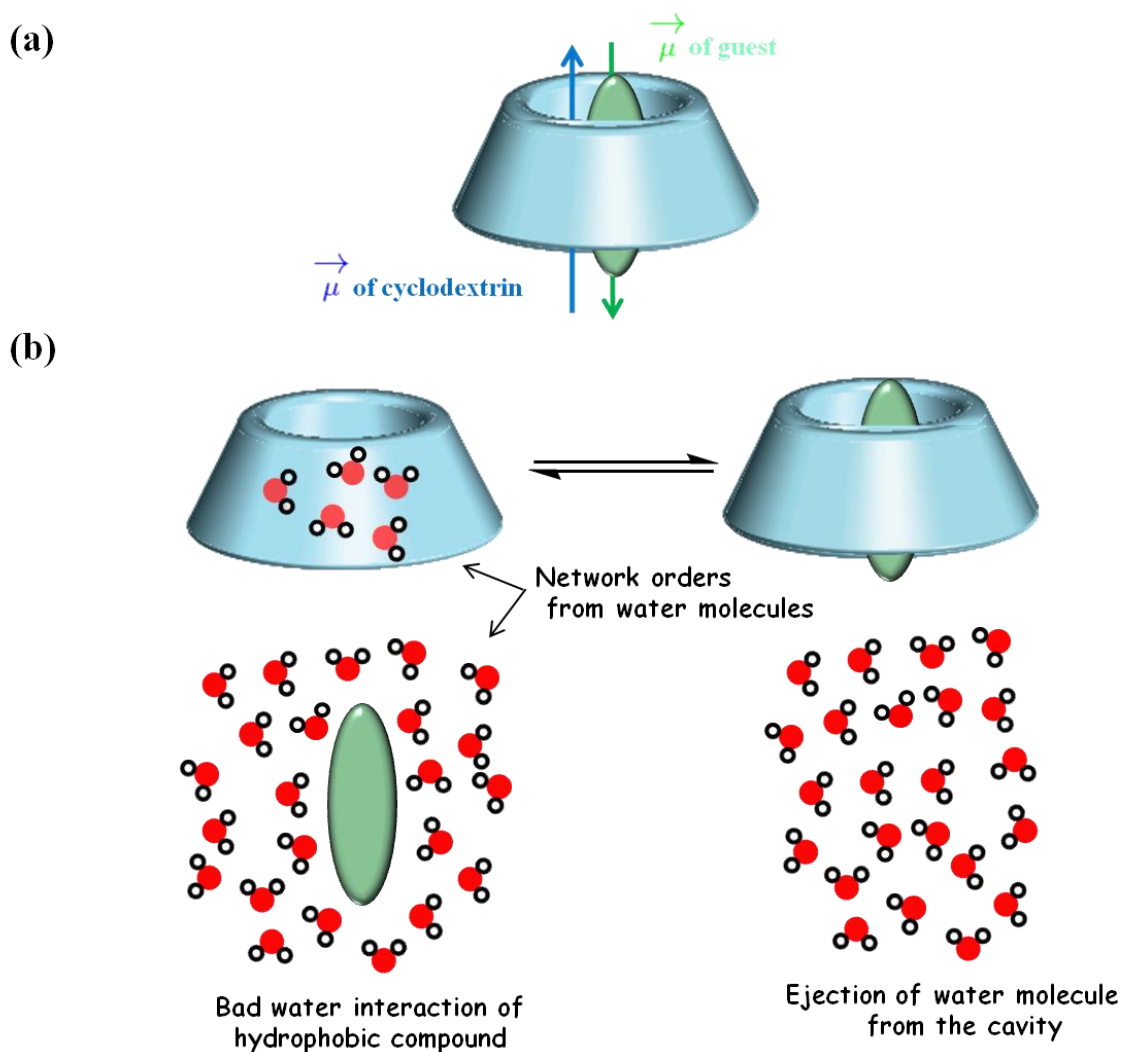


Figure 26: (a) Dipole-dipole interactions and (b) Hydrophobic effect involved in the formation of the inclusion complex.

(2) Hydrophobic effect

From mentioned previously in the part on non-covalent interactions, we are already familiar with the hydrophobic effect. In the cyclodextrin inclusion complexes process, this factor derives from that the water molecules distributions of the host-guest system are affected by the modification of interaction. The water is unfriendly with the cavity of the cyclodextrin because of the absent of electrostatic interaction or hydrogen bond between them. Similarly, the water is unfavorable with the hydrophobic guest. The entry of hydrophobic molecules into the cyclodextrin/solvent system causes the water molecules in the cavity to be squeezed out and rearranged (Figure 26-b).

3.1.2.2. Guest of inclusion complex of cyclodextrins

In the formation process of self-inclusion complexes, the size of the cavity is very important for organic guest selection. α -cyclodextrin tends to interact with azobenzene and its derivatives ($K = 10^4 \text{ M}^{-1}$), naphthalenes ($K = 10^2\text{-}10^3 \text{ M}^{-1}$), and phenyl derivatives ($K = 10^2\text{-}10^3 \text{ M}^{-1}$) [100]. β -cyclodextrin usually forms stable supramolecular polymer system with ferrocene, cholesterol, and adamantane. γ -cyclodextrin is apt to construct supramolecular polymers with pyrene, phenanthrene, and anthracene, etc [101].

Adamantane (Ada) as the most important guest in the cyclodextrin inclusion complex has been the subject of numerous studies. The basic carbon skeleton of adamantane is symmetrical and is analogous to the diamond crystal lattice. The diameter and the volume are approximately 7\AA and 180\AA^3 , respectively [101]. So it perfectly fits the cavity of β -cyclodextrin whose radii of available free space for guests are approximately 3.0\AA and 3.3\AA , respectively (Figure 27) [102] and no space for water molecules, forming a stable inclusion complex with a higher association constant (up to $4 \times 10^4 \text{ M}^{-1}$). The association constant still reaches $5 \times 10^3 \text{ M}^{-1}$ for γ -cyclodextrin. Since α -cyclodextrin small cavity can't completely wrap adamantane. Normally, α -cyclodextrin interacting with adamantane forms a 2:1 inclusion complex with an association constant of 10^2 M^{-1} [103] [104].

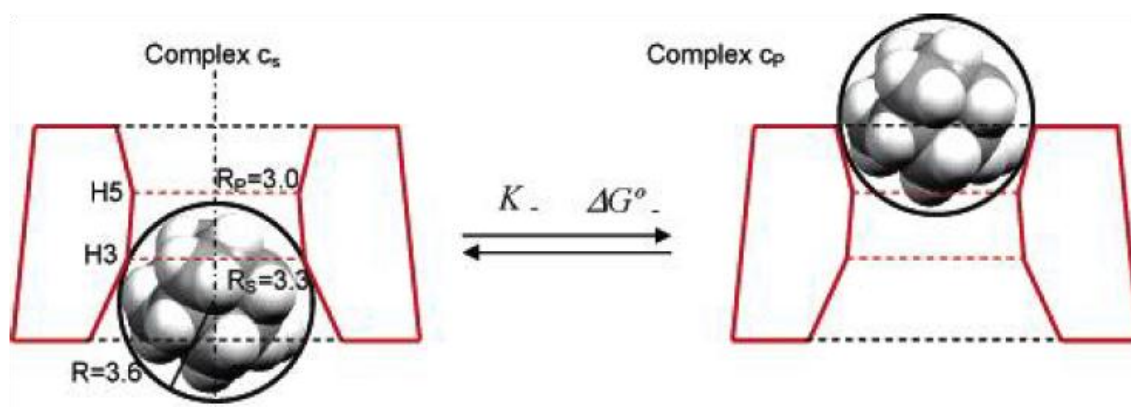


Figure 27: Equilibrium between expected β -cyclodextrin based inclusion complexes and adamantane derivatives, data in \AA [102].

3.1.3. Reactivity of cyclodextrins

The three hydroxyl groups (named position 2, position 3 and position 6) in the cyclodextrin differ in the reactivity (Figure 28). The position 2 is the most acidic ($\text{p}K_a = 12$) due to the influence of electron-withdrawing induction from the anomeric oxygen atoms and the

hydrogen bond between position 2 and position 3 of the adjacent unit. They can be easily deprotonated and the corresponding alkoxides are more nucleophilic. ^[105] The position 3 is the most crowded and activity of it is too low to be selectively functionalized. By comparison with the other two hydroxyl groups, the position 6 has the least steric effect and the highest nucleophilicity, allowing the primary rim of the cyclodextrin to selectively functionalize by adjusting the reactivity of the electrophile ^[106].

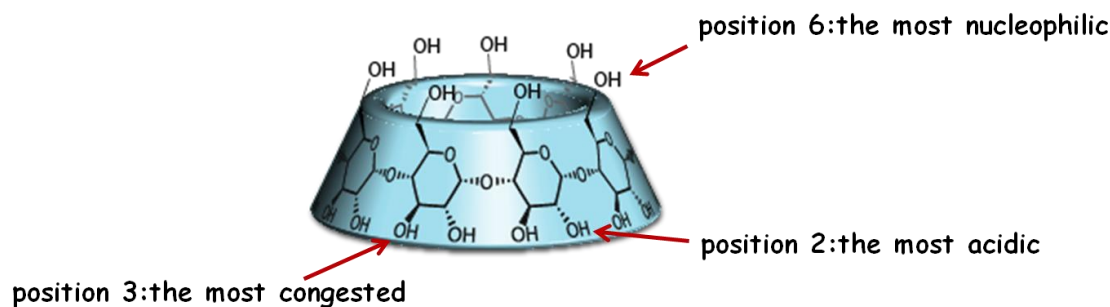


Figure 28: Reactivity of the different hydroxyls of cyclodextrin.

3.2. Supramolecular polymers based on cyclodextrin in solution

3.2.1. Supramolecular polymers of A_nB_m type

The Tato group developed a supramolecular copolymer containing dimers of adamantane and dimers of β -cyclodextrin via host-guest in aqueous solution. The inclusion of adamantyl groups was straightforwardly characterized by small angle X-ray scattering (SAXS), which measured the molecular weight of highly concentrated solutions of $(2.3 \pm 0.2) \times 10^3 \text{ g mol}^{-1}$. The result from dynamic light scattering (DLS) showed that the hydrodynamic radius of the complex was $12.5 \pm 0.5 \text{ \AA}$. The self-assembly was clearly pointed out. With the help of theoretical simulation, it was a shrunk oligomer with a polymerization degree of 8 (4 dimers of each species) rather than a cyclic conformation. Hence this design avoided the cyclic oligomers production and induced the formation of linear polymers (Figure 29-a) ^[107].

Another example of supramolecular polymer systems based on cyclodextrins AA-BB type was reported by Harada group. The highlight of this work was the use of a flexible spacer, polyethylene glycol (PEG), as a linker between monomers (Figure 29-b). The degree of polymerization reached 20 mers on accounts of the special design of monomer. The inclusion of adamantane through the secondary rim of the cyclodextrin had been estimated by

NMR-ROESY. The NMR-DOSY experiment inferred the diffusion coefficient as a function of concentration. Because of poor solubility, a VPO experiment had been employed to confirm a linear supramolecular polymer, calculated the molecular weight value of 1×10^4 g mol⁻¹ at 20 mM [108].

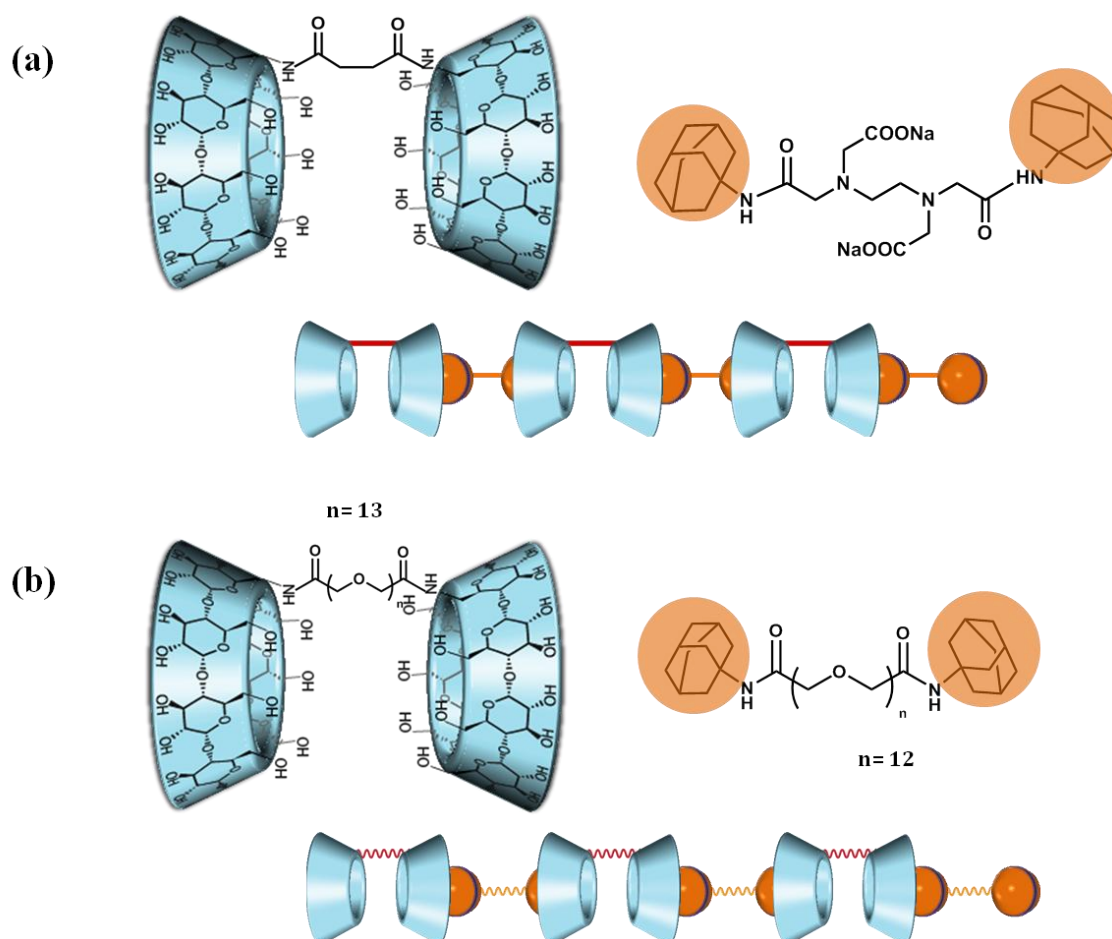


Figure 29: Supramolecular polymer systems based on cyclodextrins AA-BB type described by the groups of (a) Tato and (b) Harada.

The following two examples by Harada group illustrate that the flexible guest is controlling the type of supramolecular assembly.

The challenge of the work was to construct supramolecular polymers from two types of cyclodextrins and two adamantyl derivatives, the hosts being α - and β -cyclodextrins and the guests being cinnamoyl-adamantane and cinnamoyl-adamantane with protection group (Figure 30-a). The structure of the inclusion complexes of cyclodextrin with cinnamoyl-adamantane was investigated by NMR-ROESY, but this information wasn't sufficient to support supramolecular assembly. The answer was found by NMR-DOSY and a

competition study with adamantane. For the cinnamoyl-adamantane with a protecting group, the results showed that: (1) a significant change of $^1\text{H-NMR}$ spectrum in the presence of the competitive guest; (2) a slightly change of the diffusion coefficient with increasing concentration; for the cinnamoyl-adamantane without a protecting group, the results were exactly the opposite. The information indicated the formation of a self-included dimer and a supramolecular polymer by controlling the guest. AFM microscopy was employed to determine the appearance of the self-assembly and observed a huge difference in size of two species (20 nm and 250 nm) ^[109].

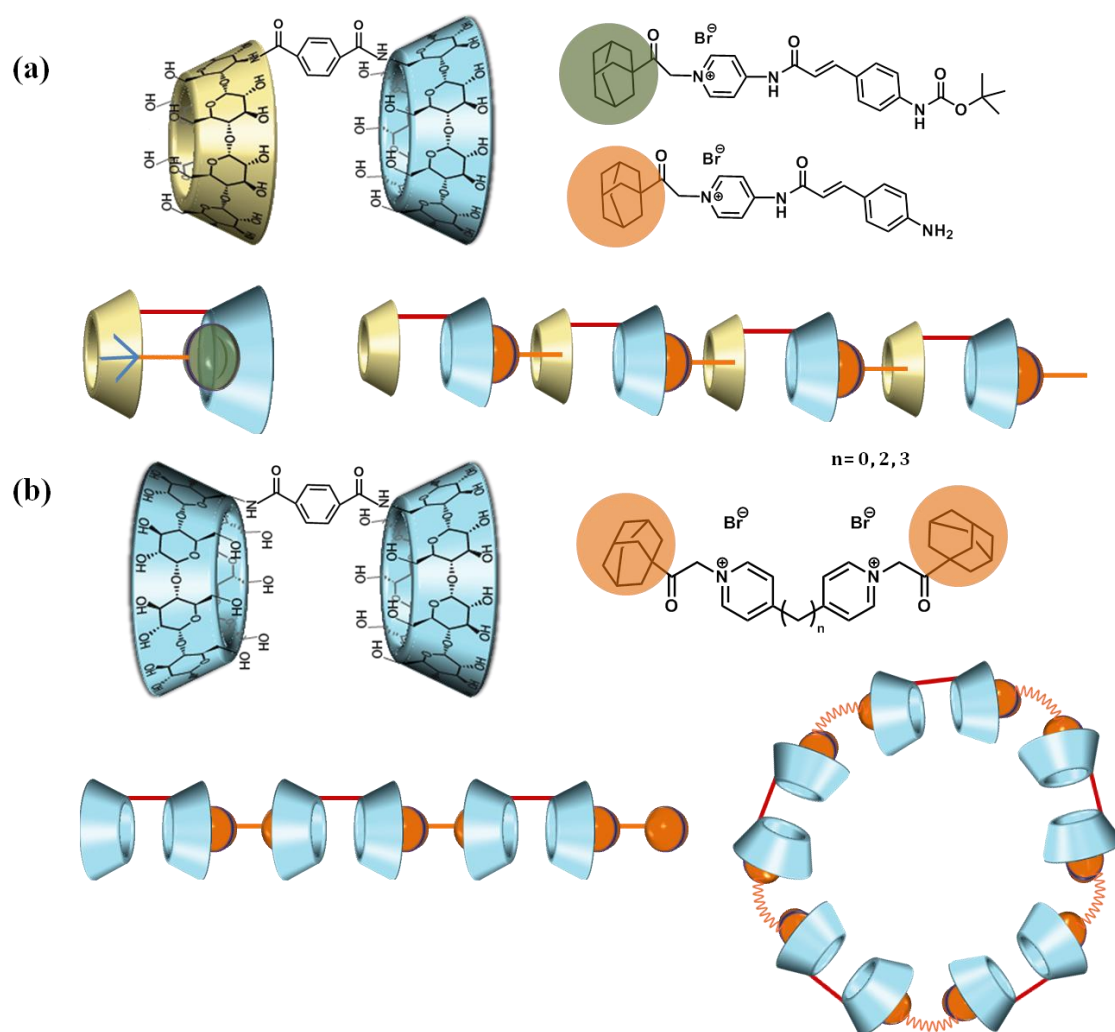


Figure 30: Supramolecular polymer systems based on cyclodextrins AA-BB type described by the group of Harada.

Another study employed the rigid or flexible guest to form different types of supramolecular assemblies. The construction of a supramolecular polymer involved a homoditopic host based

on β -cyclodextrin and a homoditopic guest based on adamantane (Figure 30-b). No matter what type of guest (rigid or flexible), it was demonstrated that the adamantane was included in the cavity of the cyclodextrin. For the rigid guest, the measurement result of the molecular weight was $9 \times 10^4 \text{ g mol}^{-1}$ at 15 mM, inferring the formation of a linear polymer. For the more flexible guests, another assembly behavior was highlighted. The VPO experiment result showed the molecular weight of assemblies in the range between 9.4×10^3 and $15 \times 10^3 \text{ g mol}^{-1}$ at 8 mM. The more flexible guests would favor the formation of cyclic polymers ^[110].

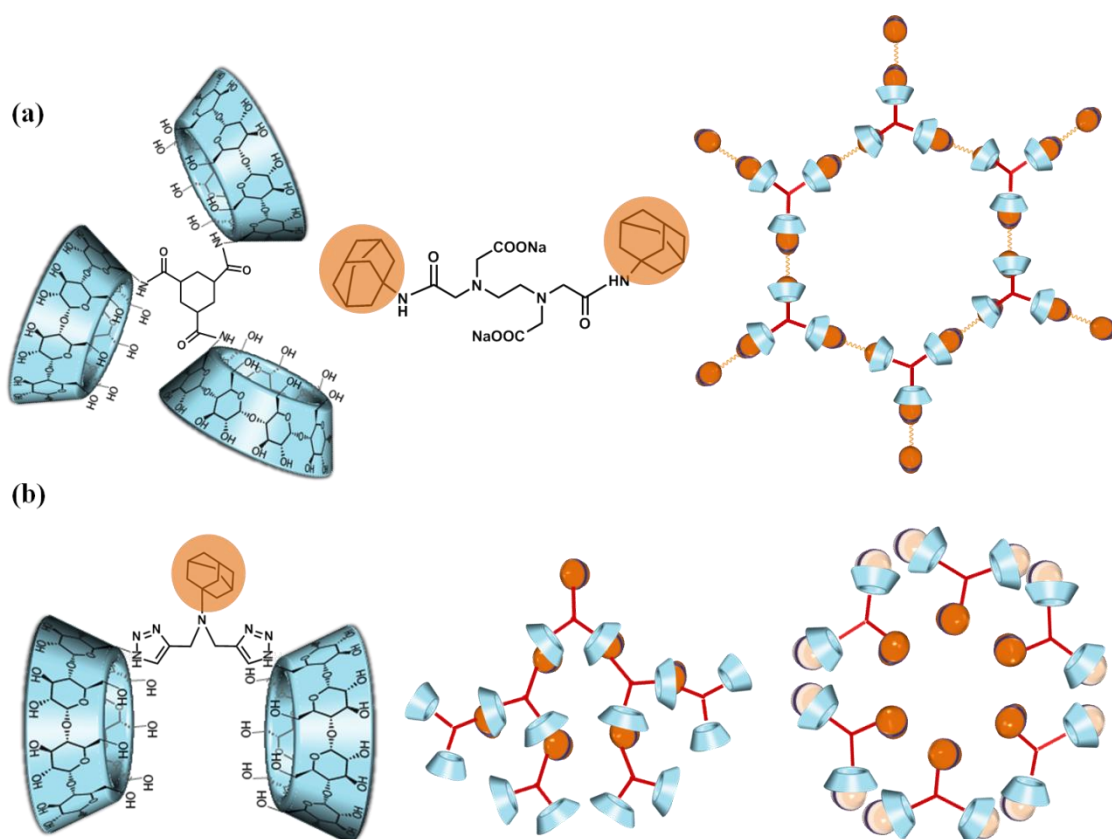


Figure 31: Supramolecular polymer systems based on cyclodextrins AA-BB type described by the groups of (a) Tato and (b) Zhang.

Some studies focused on non-covalent dendrimer structures based on tritopic monomers of cyclodextrin. Tato prepared a supramolecular polymer containing a homotritopic β -cyclodextrin based host and a homoditopic adamantane-based guest (Figure 31-a). The supramolecular assembly should be favored in dendrimer structure owing to a high association constant between adamantane and cyclodextrin ^[100]. Light scattering showed a supramolecular polymer with a hydrodynamic diameter of 1.42 nm and a molecular weight of $4.4 \times 10^3 \text{ g mol}^{-1}$. Furthermore, the dendrimer-like structure was observed by AFM ^[111].

Another example of branched polymer had been developed by Fan group. The special feature of this work is a complementary host–guest pair building into a monomer which carried two β -cyclodextrins and one adamantane via a triazole group (Figure 31-b). Its behavior was studied in a DMF/H₂O mixture (1: 1) solution. Although DMF is a bad solvent for the formation of inclusion complexes, the inclusion of adamantane in the cavity of cyclodextrin was proven by NMR-NOESY. The branched supramolecular polymer was observed by TEM. Besides, the change in morphology in the presence of the competitive guest (sodium adamantyl carboxylate) was also observed by TEM. Indeed, the competitive guest which is strongly bond to the cavity of β -cyclodextrin led to dissociation of the branched species and aggregating to form micelles via hydrophobic interaction ^[112].

From these examples, the cyclodextrin based supramolecular polymer is a rather difficult task. The assembled species still stays at a low level of the degree of polymerization. We need to strive to optimize the system in terms of structure, flexibility and solubility et.al to obtain “real” supramolecular polymers, endowing more function.

3.2.2. Supramolecular polymers of AB type

Ritter group prepared monomer functionalized on position 6 of β -cyclodextrin, employing the mono-azide and attaching a rigid fluorescent linker by click reaction. The NMR-ROESY result showed that the linker was included in the cavity of β -cyclodextrin in aqueous solution. This fact was also confirmed by the decrease in the fluorescence intensity of the complex in the presence of a competing guest (potassium adamantanecarboxylate), which indicated two information: (1) the stronger fluorescence accounted for the inclusion of the linker; (2) the competitive guest expelled the linker from the cavity because it perfectly adapted to the cavity of the β -cyclodextrin with a high association constant ^[100], leading to the fluorescence quenching. DLS studies showed a size change process from the 200 nm supramolecular polymer to the 5 nm self-contained complex in the presence of the competitive guest ^[113] (Figure 32-a). The same work from Harada group reported the preparation of supramolecular polymer from a functionalized β -cyclodextrin with an arm which composed of cinnamoyl and trinitrobenzene groups on the same position of β -cyclodextrin. The formation of the inclusion complex was confirmed by NMR-ROESY experiment and the VPO (Figure 32-b) ^[114].

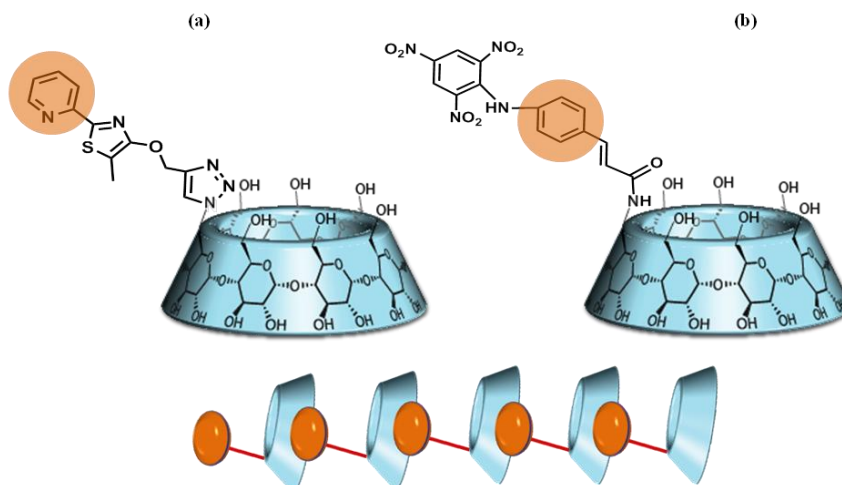


Figure 32: Systems developed for formation of supramolecular polymers with monomer based on β -CD (a) by Ritter group; (b) Harada group.

Harada et.al prepared a α -cyclodextrin derivative with a cinnamamide group as a guest part to construct a supramolecular polymer. In order to control the supramolecular structure by changing the position of the guest moiety in the cyclodextrin, this work adopted position 3 as a functionalization site rather than position 6. The inclusion of the guest moiety can be oriented to the primary rim of another cyclodextrin to avoid formation of oligomer (Figure 33). The NMR-DOSY studies showed the diffusion coefficient as a function of the concentration, which implied the larger supramolecular polymer formation. And a degree of polymerization of 12 for this polymer was calculated. The molecular weight measured by VPO was very similar to its formula ($1.6 \times 10^4 \text{ g mol}^{-1}$) [115].

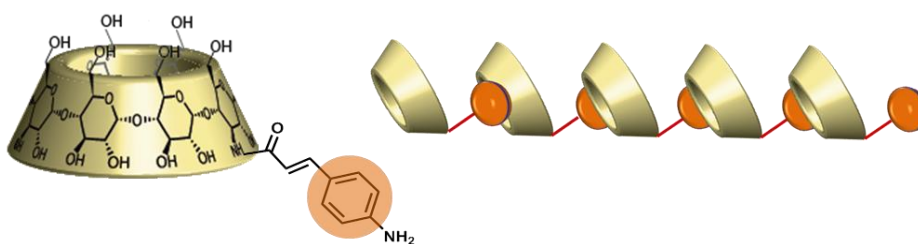


Figure 33: Systems developed for formation of supramolecular polymers with conjugates composed of α -CD by the Harada group.

Many researchers have attached the hydrophobic guest directly to the cyclodextrin. However, very little work has achieved the formation of polymers as described above, even if the

monomer structure is carefully designed. The size of the obtained polymers is not much different from that of monomers. These studies highlight several difficulties for the development of such polymers: (1) no guest perfectly fits cyclodextrin cavity compared to adamantane, resulting in the small association constant for the formation of polymers (main factor for α cyclodextrin); (2) the production of self-inclusion complex is inevitable when a more flexible arm is adopted. We will discuss this question again in part of Chapter 2.

4. Conclusion

In this chapter, various interactions for supramolecular polymerization have been summarized and the characterization methods of supramolecular polymers have been outlined. This knowledge about supramolecular polymers is very important and helpful to design the structure of monomers in order to achieve the construction of supramolecular polymers that are provided with a higher degree of polymerization and special function. Meanwhile, the preceding examples of cyclodextrin-based supramolecular polymers exploit the hydrophobic interactions and illustrate the feasibility of construction of a well-defined structure.

CHAPTER 2

DESIGN STRATEGY AND SYNTHESIS OF SUPRAMOLECULAR POLYMERS BASED ON BETA-CYCLODEXTRIN-ADAMANTANE IN AQUEOUS SOLUTION

1. Selective Functionalization of Cyclodextrins Debenzylation

1.1. Synthesis of cyclodextrin diol with diisobutylaluminum hydride

Cyclodextrin are consisted of n identical glucopyranose units with a C_n symmetry, possesses a unique three-dimensional architecture with a cavity, allowing it to show great potential for the construction of supramolecular polymers ^{[21] [116]}.

The Polyfunctionalization of C_n symmetrical cyclodextrin has a significant influence on its nature and applications. However, this task is a huge challenge for chemists due to the same chemical reactivity of each unit. In the past few decades, chemists have invested great great amounts of time and effort in the development of simple and efficient methods for the functionalization of one or more hydroxyl groups of cyclodextrins ^[117].

Our laboratory has developed a highly efficient method for functionalization of the primary rim of cyclodextrin, overcoming the problems of low regioselectivity, difficulty in purification, and low yields ^{[118] [119] [120] [121] [122] [123]}. This method is based on the selective deprotection of protected cyclodextrin in all its positions. In the case of α -cyclodextrin, the native cyclodextrin as start material firstly launches protection reaction with benzyl chloride and sodium hydride in DMSO ^[124], perbenzylated α -cyclodextrin allows its purification by silica gel chromatography because it is soluble in organic solvents.

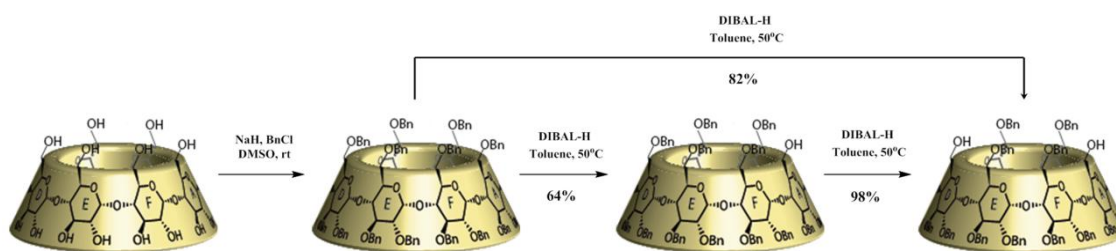


Figure 34: Synthesis route of the diol of prebenzylated α -CD.

Then, the corresponding diol of prebenzylated α -cyclodextrin is generated with a good yield of about 82% by the selective debenzylation reaction with an excess of DIBAL-H in toluene at 50°C. Interestingly, it is also possible to produce monol of prebenzylated α -cyclodextrin with a yield of about 64%, which depends on the dilute concentration of DIBAL-H and the reaction time. The monol can be converted into diol with a quantitative yield under action of

DIBAL-H, indicating the regioselective debenzoylation is a stepwise reaction (Figure 34). The results of selective deprotection of protected β -cyclodextrin are the same as the prebenzylated α -cyclodextrin (Figure 35).

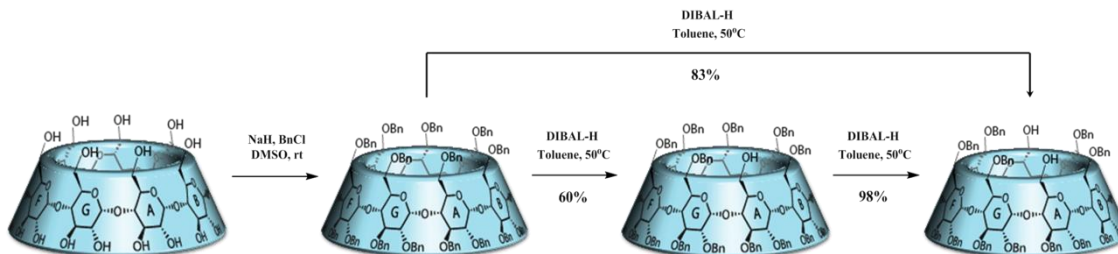


Figure 35: Synthesis route of the diol of prebenzylated β -CD.

1.2. Mechanism of DIBAL-H mediated debenzoylation

Our laboratory's early systematic study reported that at least two molecules were engaged in the selective debenzoylation reaction under the action of DIBAL-H. The alkyl ether didn't undergo debenzoylation even after 4 days, but the benzyl group of pyran ether was removed in 4 hours with a good yield (Figure 36). Therefore, the second oxygen atom on the molecular framework is required for chelation the aluminum atom.

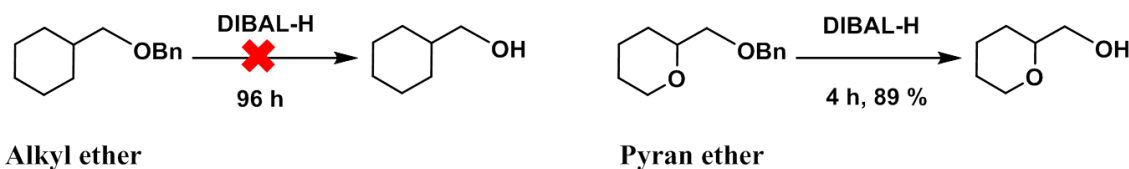


Figure 36: Debzoylation of alkyl ether and pyran ether by DIBAL-H.

The proposed mechanism for the debenzoylation of monosaccharides using DIBAL-H is described in Figure 37 ^[118]. In view of the above observations, it was assumed that the debenzoylation reaction process involved a minimum of two molecules of DIBAL-H. The first DIBAL-H molecule chelated with the oxygen atom of $-OBn$ group in position 6 and the endocyclic oxygen atom of the glucose unit to form the cyclic complex. Then the second DIBAL-H molecule coordinated with the less hindered oxygen (oxygen atom in position 6), forming the di-aluminum derivative. The process can be summarized that one DIBAL-H molecule acts as a Lewis acid to activate the C-O bond of benzyl ether and another of that acts as a deliverer of the hydride which attacks the benzylic carbon to obtain deprotected

product after hydrolysis.

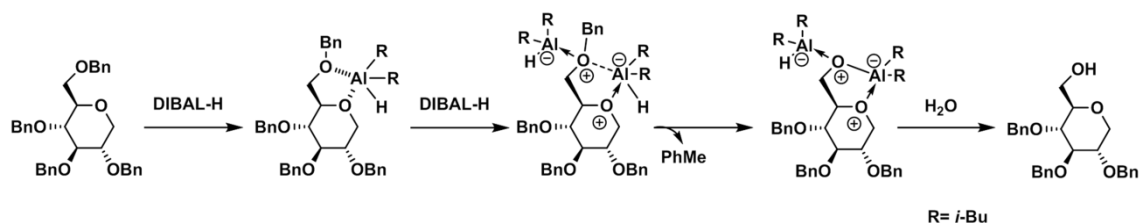


Figure 37: Proposed mechanism for debenzylation of monosaccharide using DIBAL-H.

1.3. Selectivity rationalization for α - and β -cyclodextrins debenzylation

The debenzylation mechanism of cyclodextrins under the action of DIBAL-H was proposed on the basis of the study on monosaccharide deprotection reaction. In the case of α -cyclodextrin, selective debenzylation only occurred on the primary rim rather than the congested secondary rim (Figure 38). The first debenzylation occurred on one of the sugar units (unit A). The hydroxyl group and two equivalents of DIBAL-H chelated in a similar “tweezer” pattern. The huge steric hindrance was sufficient to direct the second debenzylation on sugar unit D which was located diametrically opposed to sugar unit A position, giving a single regioisomer which was 6A, 6D-diol- α -cyclodextrin. The deprotection of prebenzylated β -cyclodextrin was following the same route.

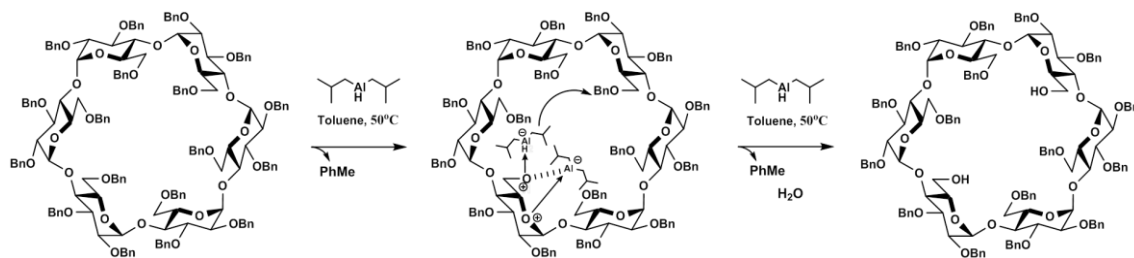


Figure 38: Regioselective debenzylation process of the α -cyclodextrin in the presence of DIBAL-H.

And our team has adopted this efficient method of selective debenzylation to achieve hexadifferentiated α -cyclodextrin on which six different groups possess different properties (Figure 39) [125]. It opened the way to synthesize all 7826 possible arranged α -cyclodextrin derivative. Therefore, this work provides cornerstones for building diverse supramolecular polymers.

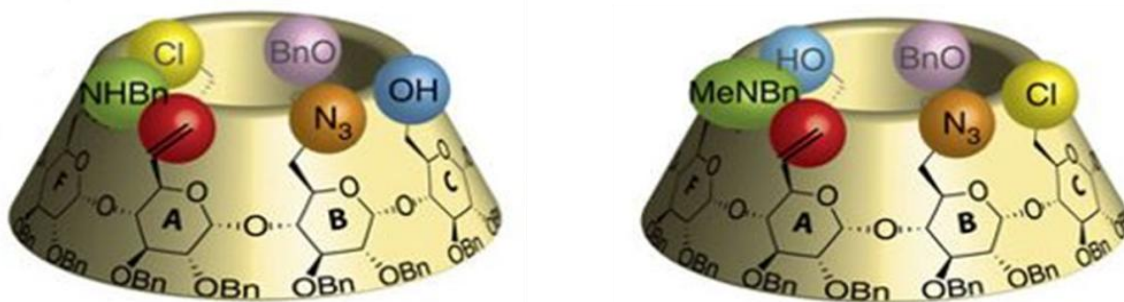


Figure 39: Hexa-hetero-functionalized of α -cyclodextrin ^[125].

2. Our Previous Work: Supramolecular Polymerization Based on β -Cyclodextrin Adamantane in Aqueous Solution

2.1. Initial considerations and preliminary experiences

The well-known high association constant (up to $4 \times 10^4 \text{ M}^{-1}$) ^[100] of adamantane for β -cyclodextrin should have been exploited to form the supramolecular polymers. Surprisingly, only a few examples which referred to construction of supramolecular polymers based on this cyclodextrin/adamantane system in solution are reported in the literature. The reason might be that the β -cyclodextrin-adamantane monomer with a flexible linker inevitably formed self-included conjugates inhibiting self-association to yield polymers ^[126], while that of with a rigid arm would favor to aggregate so as to be insoluble ^[127]. Hence, pertinent arm is very essential.

Our laboratory has attempted to polymerize AB monomers of cyclodextrins with functionalized adamantane ^[128], two cyclodextrin derivatives have been synthesized: (1) one bearing adamantane via a rigid triazole arm; (2) another bearing adamantane via a flexible succinimide arm. In addition, in order to control structure to construct supramolecular polymers, both arms were directly attached to the primary rim of cyclodextrin. It was impossible to study on self-assembly behavior of the triazole compound because it was insoluble in water. In the case of the succinimide compound, a surprising result was obtained: it formed a self-included species (Figure 40-a). This information was derived from the cross-correlation between the H-3 protons of the cyclodextrin and Hc-eq/Hb protons of the adamantane, as well as those between the H-5 protons of the cyclodextrin and Ha protons of the adamantane (Figure 40-b).

CHAPTER 2 DESIGN STRATEGY AND SYNTHESIS OF SUPRAMOLECULAR POLYMERS
BASED ON BETA-CYCLODEXTRIN-ADMANTANE IN AQUEOUS SOLUTION

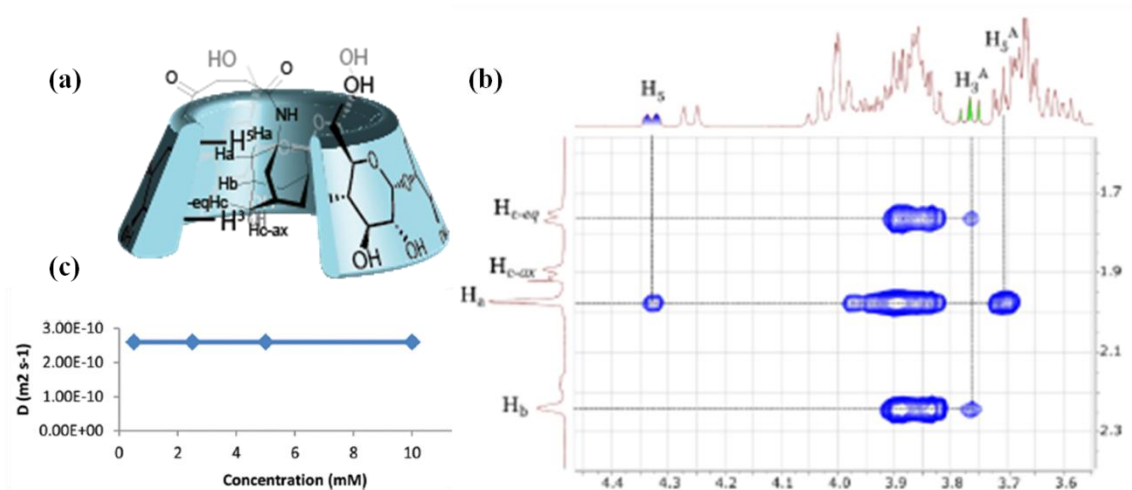


Figure 40: (a) Proposed structure of the self-inclusion species observed by NMR-ROESY; (b) NMR-ROESY spectrum of the self-included conjugate of β -CD with succinimide adamantyl moiety; (c) Diffusion coefficient of the species with variable concentration ^[128].

Self-inclusion state was confirmed again by NMR-DOSY experiment which showed constant value of diffusion coefficient whatever the concentration (Figure 40-c). There was no intermolecular assembly. The possible mechanism is proposed: so-called “tumbling”, involving a 360° reversal of adamantane guest attached to a sugar unit of the cyclodextrin-adamantane conjugate (Figure 41).

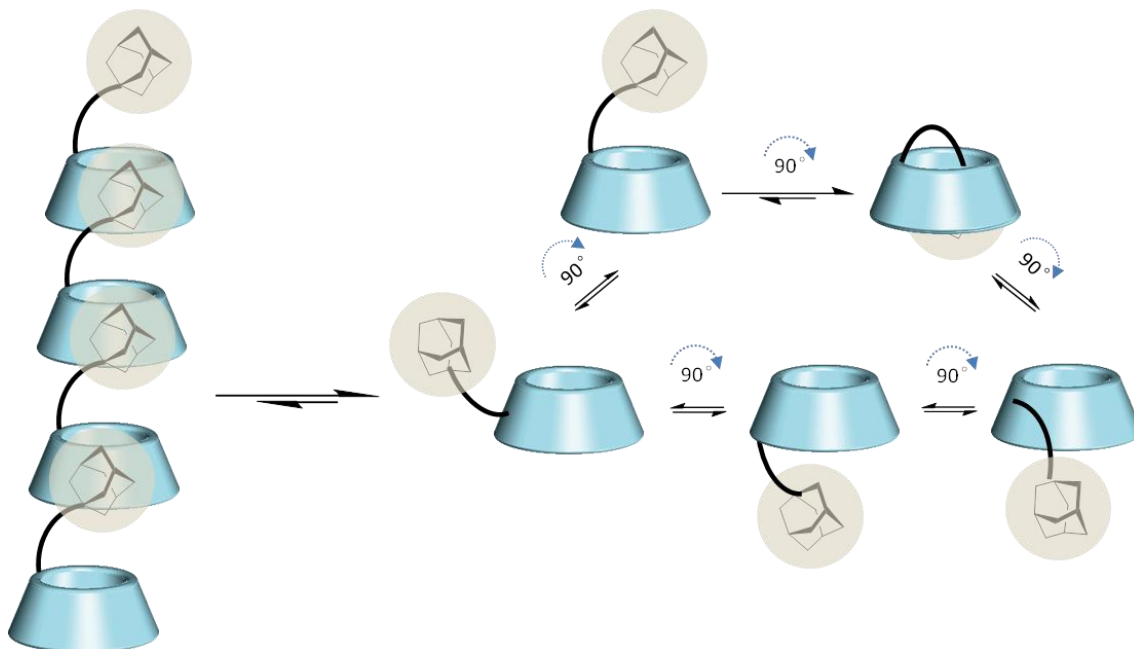


Figure 41: Competitive behavior between the phenomenon of "tumbling" and the formation of polymer.

2.2. Further experiences with new strategies

Following these studies, our laboratory has adopted new strategies to avoid self-inclusion by the phenomenon of tumbling and head-to-head dimerization---a bridging method has been developed for the formation of linear supramolecular polymers.

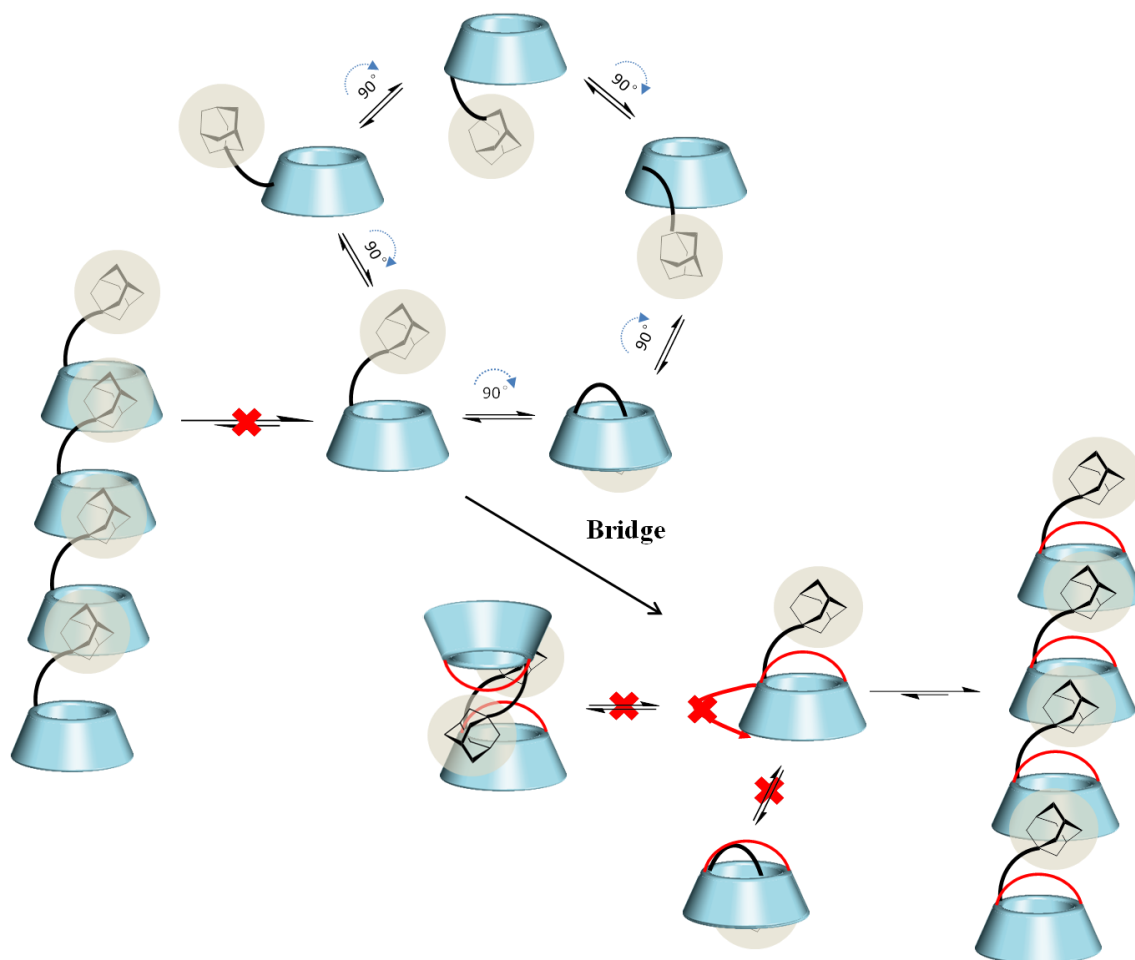


Figure 42: Bridging strategy on cyclodextrins.

This method involves the attachment of two diametrically opposite sugar units on the primary rim of the cyclodextrin via an alkyl chain bridge, one of which is functionalized by the adamantyl guest (Figure 42). In fact, the presence of the bridge blocks the primary rim of cyclodextrin and directly prevents the guest moiety from being included within the cavity of cyclodextrin. Besides, it is impossible to render the flipping of the sugar unit to which adamantane is attached, because it is bounded by another sugar unit of the cyclodextrin. And previous work from our laboratory showed that the hydrophobic arm on the primary rim of cyclodextrin led to an increase in binding association constant of adamantane in aqueous solution ^[128] ^[129]. Hence, our team synthesized such a cyclodextrin and studied its self-assembly ^[130] (Figure 43).

CHAPTER 2 DESIGN STRATEGY AND SYNTHESIS OF SUPRAMOLECULAR POLYMERS
BASED ON BETA-CYCLODEXTRIN-ADMANTANE IN AQUEOUS SOLUTION

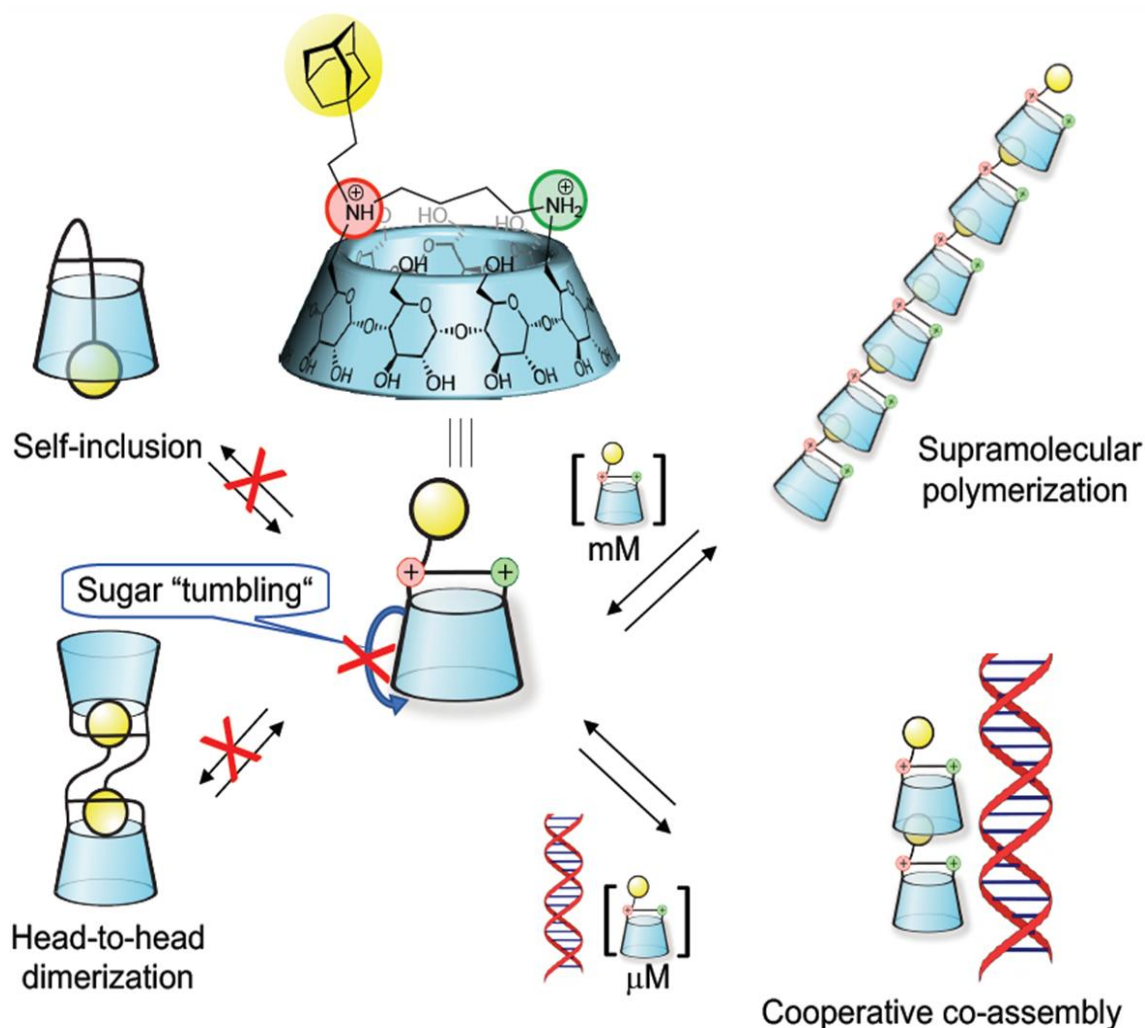


Figure 43: Bridged cyclodextrin derivative prevented self-inclusion that involved tumbling and head-to head dimerization, to allow supramolecular polymerization and cooperative assembly induced by siRNA ^[130].

The NMR-ROESY experiment confirmed the inclusion of adamantane in the cavity of the cyclodextrin. The strong cross-correlations between protons of adamantyl group and protons that pointed towards the interior of the cavity were observed, which indicated the inclusion of adamantane across the secondary rim of other cyclodextrins (Figure 44-a). The NMR-DOSY experiment also demonstrated the existence of a supramolecular polymer and estimated it composed of 9 repeat units (Figure 44-b). The self-assembly into a supramolecular polymer was fully understood through viscometry, ITC and SANS. The cooperatively interactions between self-assembled cyclodextrin and DNA was demonstrated by compaction experiments. Furthermore, this derivative possessed the ability to transfect siRNA in vitro without any toxicity. The self-assembling cyclodextrin was finally observed by cryo-microscopy. The bridged modified β -cyclodextrin derivative, as artificial tool, could mimic the assemblies of

Nature (Figure 44-c) ^[130].

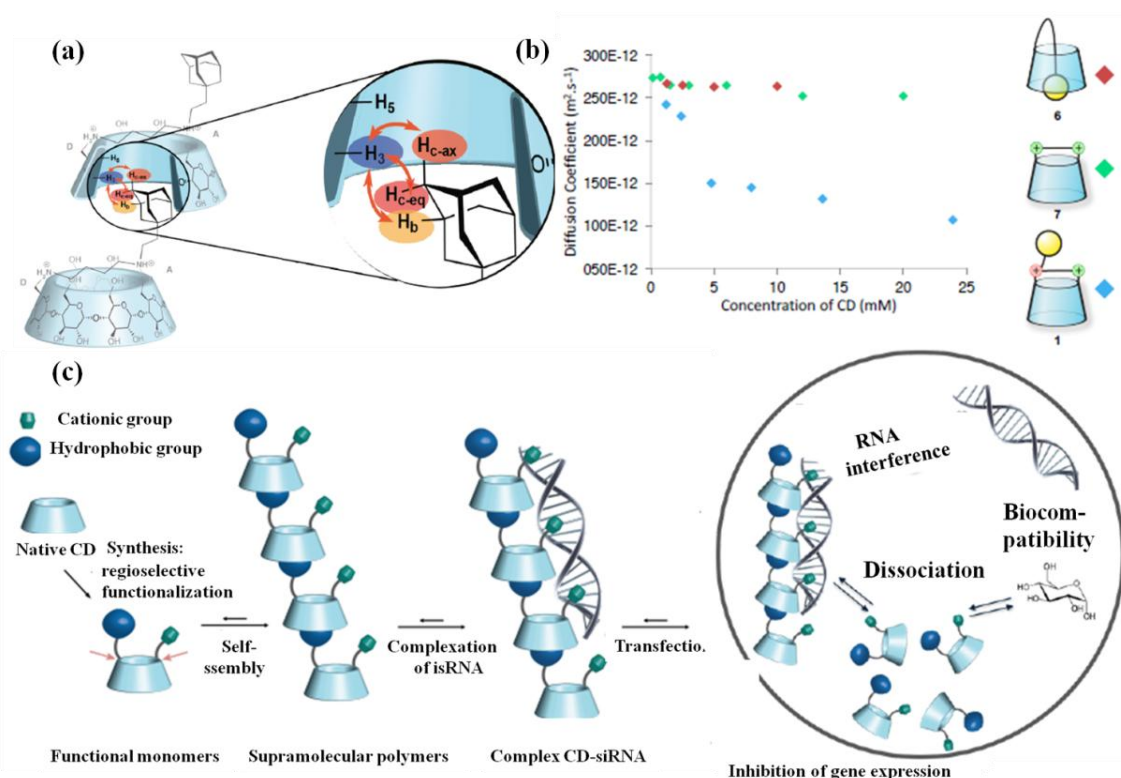


Figure 44: Bridged β -cyclodextrin derivative: (a) NMR-ROESY cross-correlations (600 MHz, D₂O, 300K); (b) diffusion coefficient with variable concentration by NMR-DOSY (600 MHz, D₂O, 300K); (c) schematic diagram of the supramolecular polymer formation and of interaction with siRNA & transfection ^[130].

In addition to the result of the four carbons bridge between the two amine groups on the position 6 of sugar units used in above system, I studied a set of alkyl-bridged modified β -cyclodextrin derivatives with different chain lengths from two to six carbons (four carbon: 5-a; two carbon: 5-b; three carbon: 5-c; five carbon: 5-d; six carbon: 5-e), which were synthesized in approximately 45% yield (Figure 45-a). The contributions of bridge length in β -cyclodextrin derivatives were studied by NMR experiment. The H-1 protons and H-5 protons of β -cyclodextrin as space-sensitive protons were slightly shielded. Moreover, a large chemical shift change (from 2.41 ppm to 1.35 ppm) was observed for the protons of the alkyl bridge, indicating that the longer the length of the bridge, the greater the interference with the cavity of the β -cyclodextrin (Figure 45-b). In conclusion, the bridge containing four carbons could enable the cavity of cyclodextrin to hold the truncated cone structure.

CHAPTER 2 DESIGN STRATEGY AND SYNTHESIS OF SUPRAMOLECULAR POLYMERS
 BASED ON BETA-CYCLODEXTRIN-ADMANTANE IN AQUEOUS SOLUTION

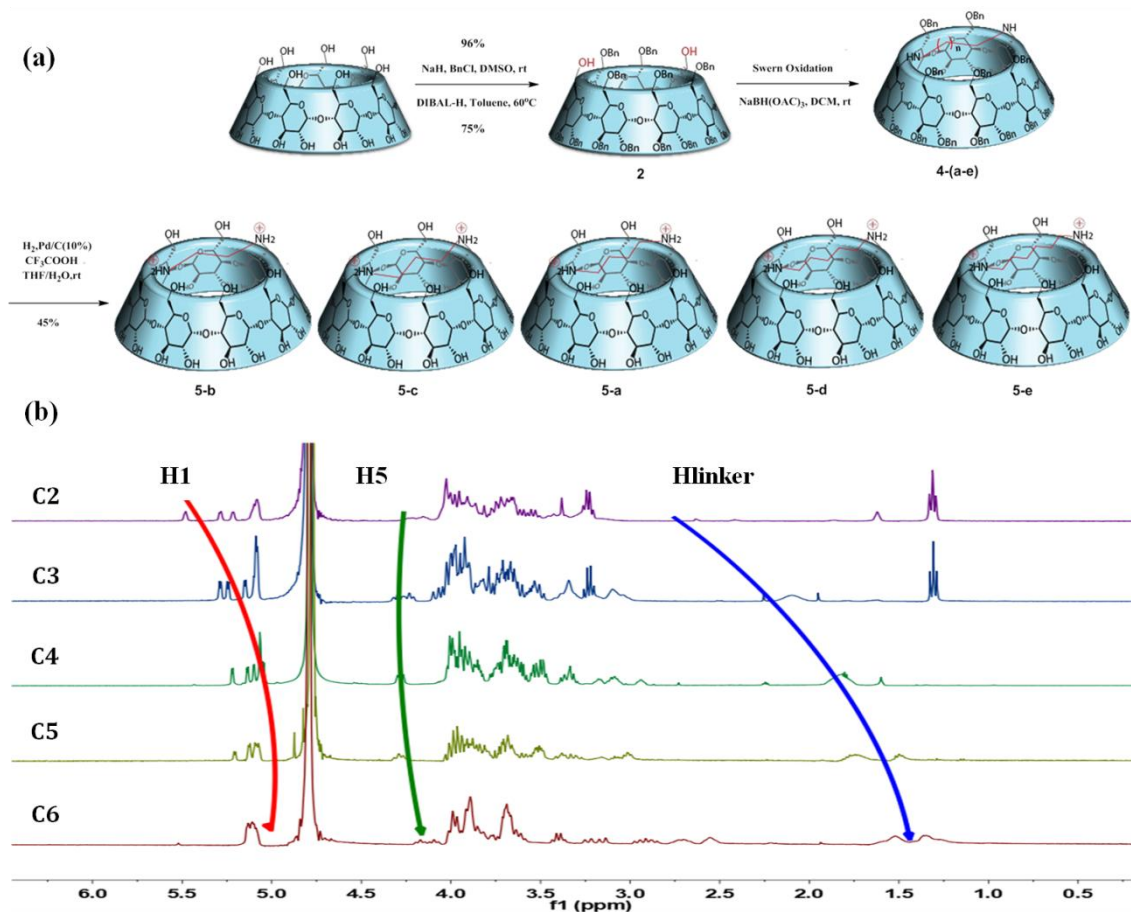


Figure 45: (a) Synthesis route and (b) ¹H-NMR spectrum (600 MHz, D₂O, 300K) of a set of alkyl bridged β -cyclodextrin derivatives with different chain lengths of 2-6 carbon atoms.

3. System Design

The above mentioned bridged β -cyclodextrin used as a AB monomer performed well: (1) self-assembly in a supramolecular polymer structure; (2) high degree of polymerization (DP) through β -cyclodextrin/adamantane interaction (DP: 9 repeat units at 24 mM); (3) great potential for application in the biological field. This was a very successful case of construction using an artificial molecular tool possessing properties to compete with that of Nature.

Hence, we will still retain the β -cyclodextrin-adamantane system to construct supramolecular polymers and try to optimize the design of the monomer using the bridging strategy to achieve a higher degree of polymerization. We have wondered if the guest position on the bridge had an influence on the size of the supramolecular polymer obtained. The truncated cone-shape of cyclodextrin gives a resultant dipole moment. This moment directed along the

axis of cyclodextrin and passed through the cavity of cyclodextrin allows the cavity interior in an electrical field ^[131]. Therefore the guest located the C_n symmetric center of the cyclodextrin could increase the axial host-guest interaction in order to form longer linear polymers.

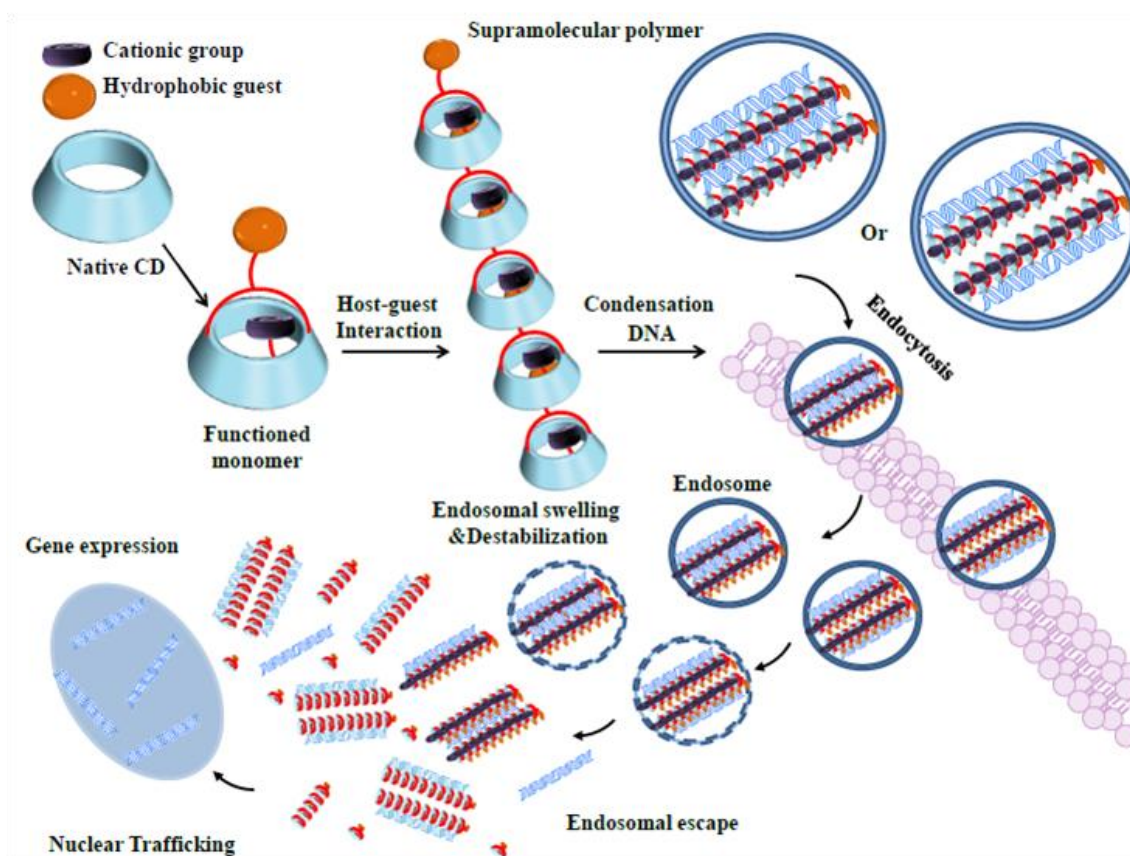


Figure 46: Design of system.

Our aim is to use the method of polyfunctionalisation CDs developed in the laboratory and the previous strategy to successfully avoid self-inclusion phenomenon: (1) to introduce adamantyl group located in the center of the cavity to trigger a higher level of the assembly; (2) to introduce amine group carrying several positive charges for the interaction with the gene template in aqueous solution. This work is expected to attain a higher degree of polymerization of supramolecular polymer, thereby displaying great performance in the gene condensation and gene delivery fields. It also provides us with the opportunity to adopt a simpler synthesis without the formation of multiple regioisomers. In addition, these amines will make it possible to functionalize the cyclodextrin into conjugates and to develop sophisticated functionalized cyclodextrins (Figure 46).

4. Synthesis of Functionalized CD/Adamantane Monomers

4.1. General retrosynthesis

The general retrosynthesis route is proposed in Figure 47. Several precursors are involved to synthesize the cationic bridged β -cyclodextrin molecular brick for construction supramolecular polymers. First, two triazoles bridged β -cyclodextrin should be prepared before tri-differentiated regioisomer of cyclodextrin with an amino function group from the debenzoylation reaction. The structure of the bridge shouldn't be affected by the deprotection reaction with DIBAL-H. Then the bridge with an adamantyl group is produced by the reductive amination reaction or the nucleophilic substitution reaction. Subsequently, cyclodextrin should be available at least two arms for this bridge bearing adamantane guest, so it is necessary to synthesize diol of cyclodextrin, itself polyfunctionalisation process is started from native cyclodextrin with aid of DIBAL-H described above.

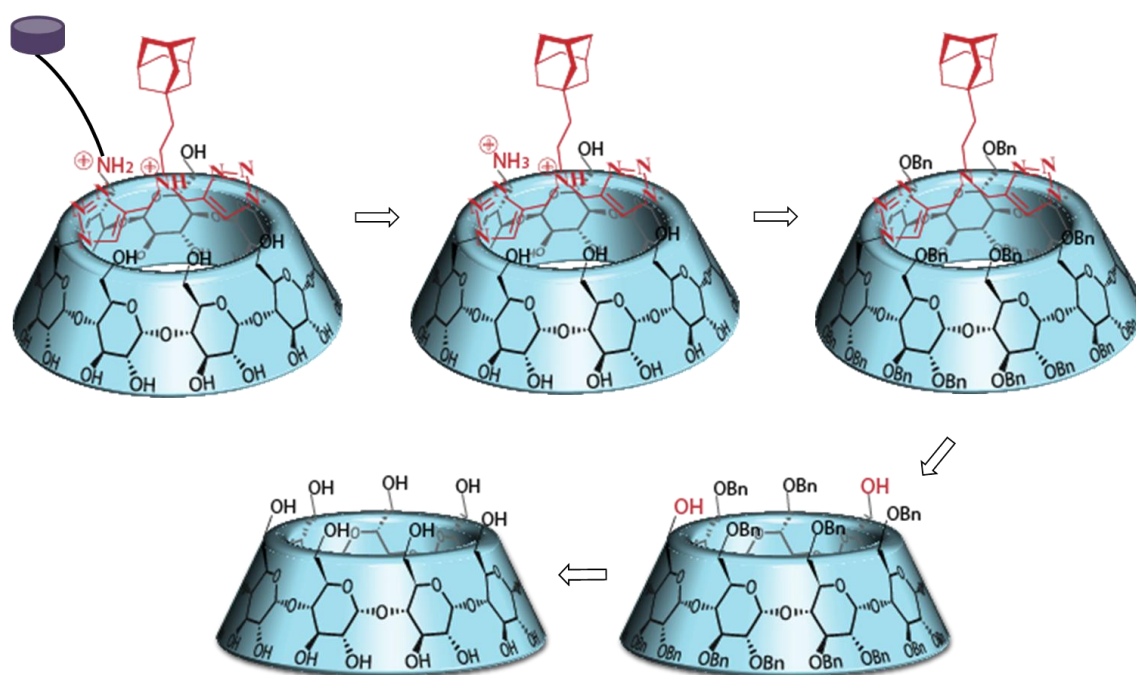


Figure 47: General retrosynthesis of functionalized cyclodextrin monomers.

4.2. Synthesis of the common precursor: bi-azide cyclodextrin

Before preparing a series of functionalized β -cyclodextrin/adamantane monomers, the compound (7) as a common precursor should be synthesized. According to the method

developed in the laboratory ^[121], its synthetic route was considered in Figure 48.

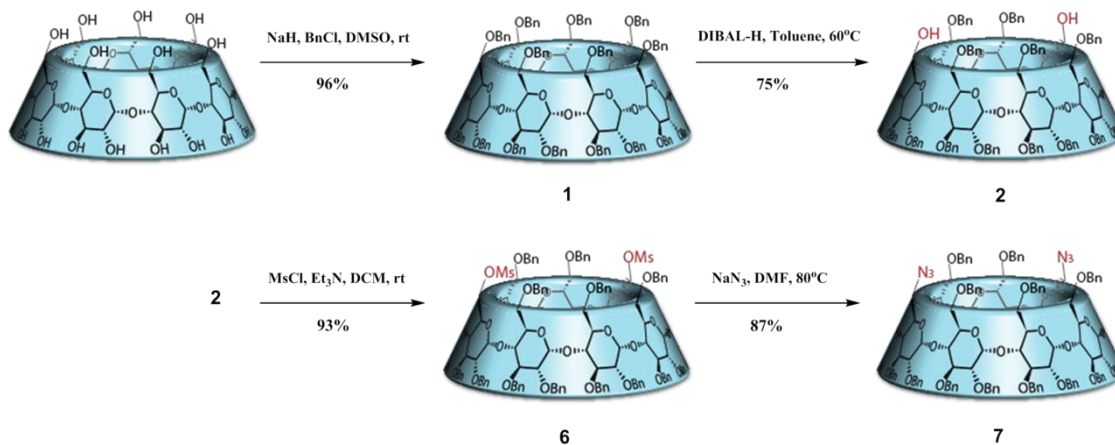


Figure 48: Synthesis of compound (7).

The synthesis of compound (7) began with prebenzylation reaction from the native β -cyclodextrin in the presence of benzyl chloride and sodium hydride. Then, treating the completely protected β -cyclodextrin in DIBAL-H, the selective regioisomer diol (2) was obtained with a yield of 72% over two steps. The precursor bi-azide β -cyclodextrin (7) was prepared through mesylation reaction and nucleophilic substitution reaction in a yield of 81% on two steps.

4.3. Synthesis of bridged neutral cyclodextrin/adamantane monomer

Next, we devoted our mind to synthesize the bridged neutral β -cyclodextrin monomer with an adamantyl group located in the center of the bridge. The synthesis of compounds was shown in Figure 49. The bridge with the adamantyl group (9) was obtained from adamantane acetaldehyde which was condensed on dipropargylamine in a reductive amination reaction with an excellent yield of 86%. From the compound (7), the Copper-catalyzed Azide–Alkyne Cycloaddition (CuAAC) reaction was carried out in the presence of the compound (9) to form the final protected compound (10) with a yield of 35%. Furthermore, the synthesis of the compound (10) was launched under the following two reaction conditions: conventional heating and microwave heating. The compared results showed that this reaction could be accelerated under the help of microwave and increased the conversion ratio of start material in short reaction time.

CHAPTER 2 DESIGN STRATEGY AND SYNTHESIS OF SUPRAMOLECULAR POLYMERS
 BASED ON BETA-CYCLODEXTRIN-ADMANTANE IN AQUEOUS SOLUTION

The compound (10) was deprotected by catalytic hydrogenation in the presence of palladium on carbon and TFA. Two compounds were obtained: the self-inclusion (11) and the bridged functionalized monomer (12) allowing supramolecular polymerization. After reverse phase purification, compound (11) with a yield of 28% and compound (12) with a yield of 58% were obtained (Figure 49).

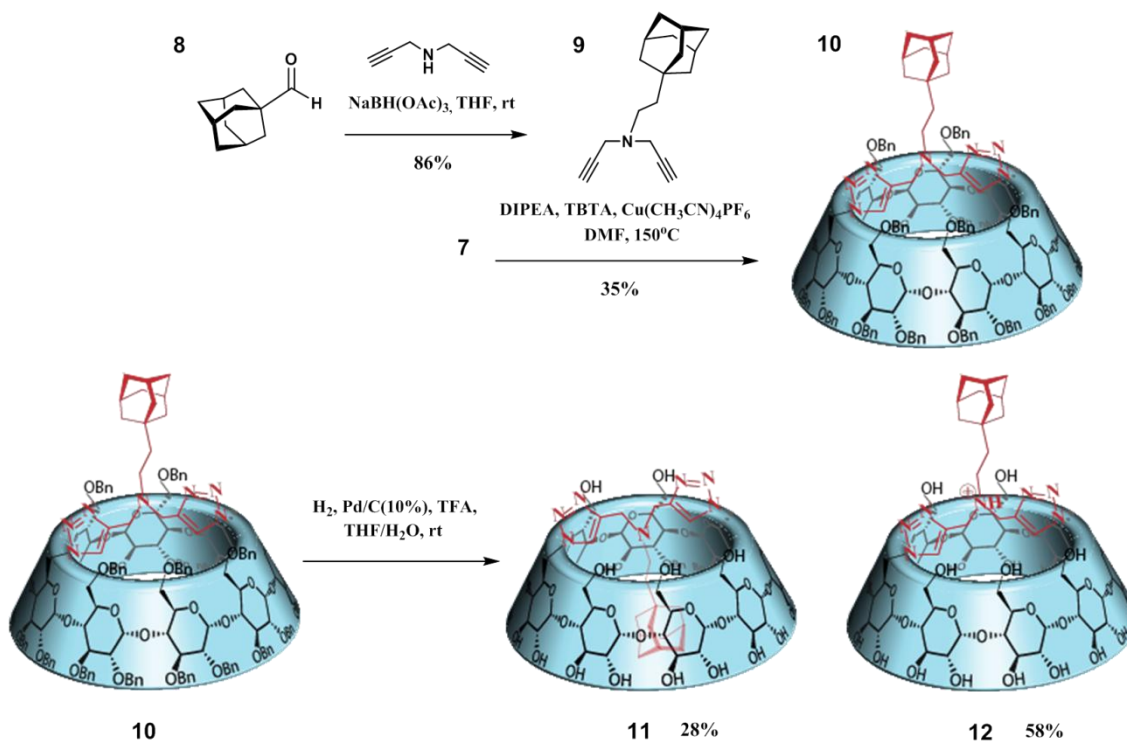


Figure 49: Synthesis of compound (11), (12).

Reversed-phase column chromatography is an effective method for the purification of cyclodextrin deprotected by catalytic hydrogenation. Because of cyclohexyl group as the result of benzyl group over-reduction in the hydrogenolysis reaction, a significant fraction (10-20%) of the starting material of the reaction converted to by-product. Purification became challenging task in the presence of this by-product. After many purification studies by HPLC, pure functionalized cyclodextrins in a great yield were obtained by a CombiFlash purification method with pre-packed C-18 column.

Besides, we further studied compound (10) by Infrared experiment (IR) to directly confirm that we obtained the compound with two triazoles. The IR spectra of species before and after CuAAC reaction were shown in Figure 50. Asymmetric stretching (2099 cm^{-1}) in the azide group (N_3) vibrations^[132] could be seen in the IR spectrum of starting material (7) but not in

the corresponding product (10), which indicated that the compound (10) was the ditriazole-substituted derivative.

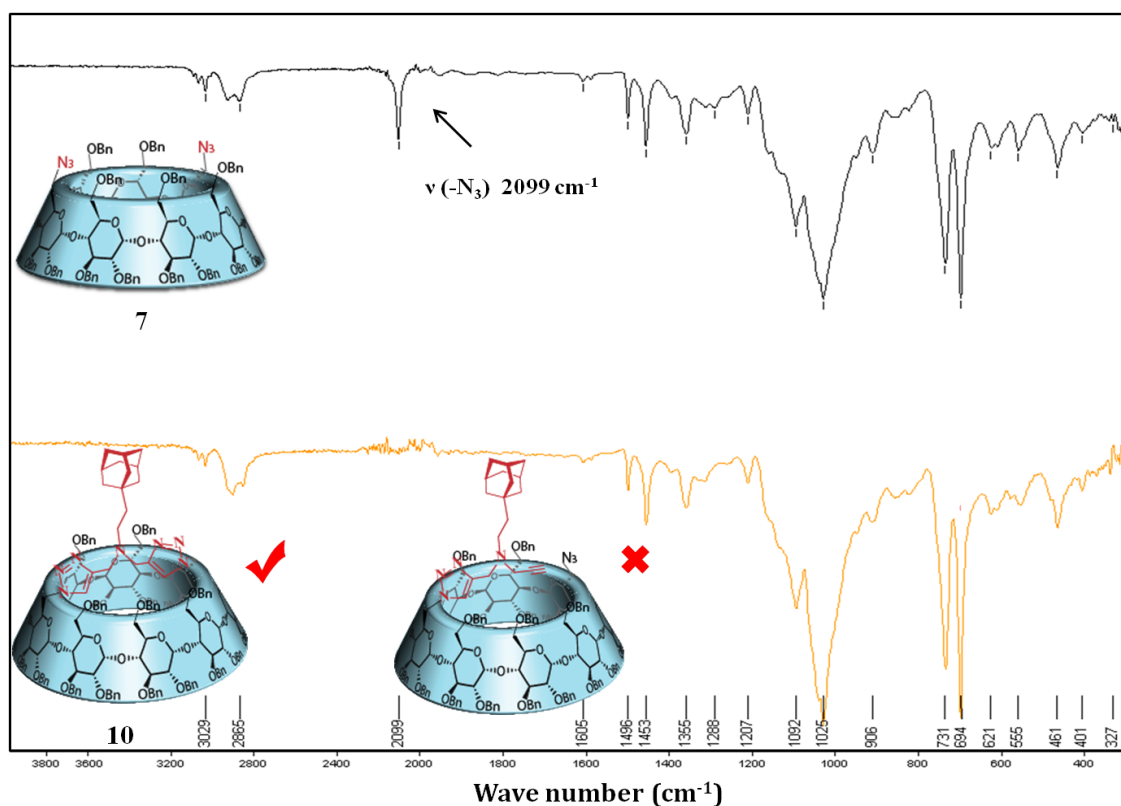


Figure 50: The IR spectra of species before (7) and after (10) CuAAC reaction.

4.4. Synthesis of bridged cationic cyclodextrin/adamantane monomer

In order to functionalize the bridged β -cyclodextrin/adamantane monomer via cationic groups, the synthesis of compound (19) was carried out (Figure 51).

The synthesis began with the perbenzylated functionalized β -cyclodextrin (10) to form a monol (16) using a synthetic method analogous to that of described above. The monol (16) was engaged in a mesylation and an azidation with a yield of 64% over two steps. The obtained corresponding compound (18) was then deprotected in the same manner as previously described by hydrogenation reaction to obtained mono-substituted ammonium bridged β -cyclodextrin/adamantane monomer with a final yield of 62%.

CHAPTER 2 DESIGN STRATEGY AND SYNTHESIS OF SUPRAMOLECULAR POLYMERS
BASED ON BETA-CYCLODEXTRIN-ADMANTANE IN AQUEOUS SOLUTION

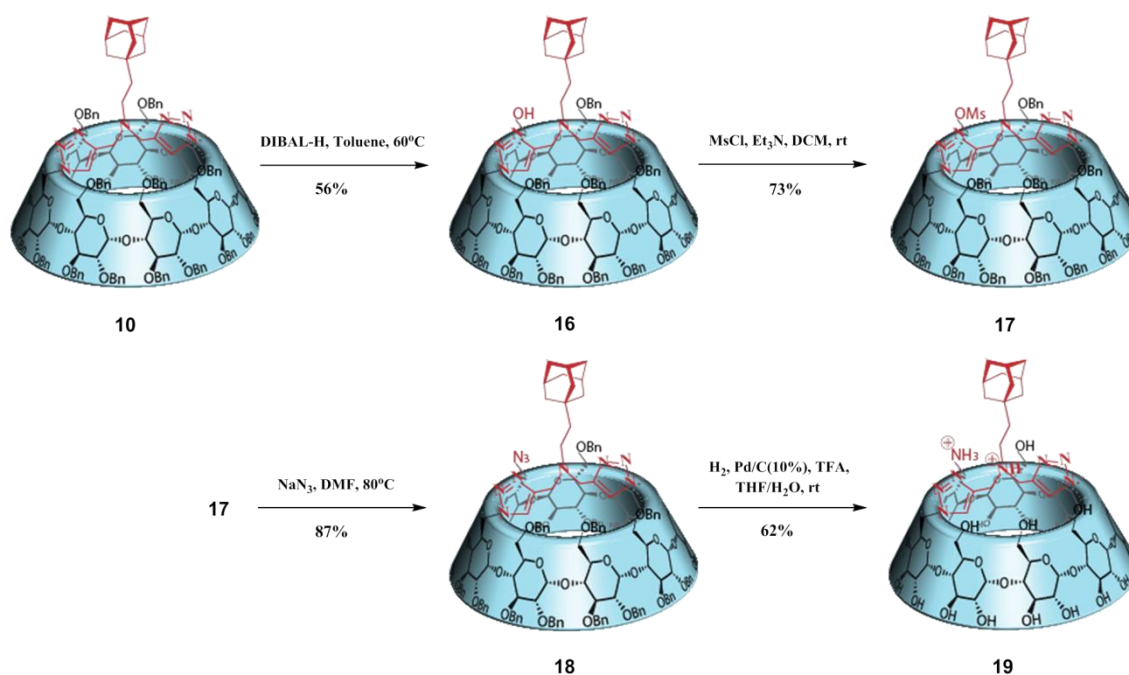


Figure 51: Synthesis of compound (19).

In fact, before we exploited this strategy to introduce a cationic functional group on the primary rim of the cyclodextrin, the di-triazoles bridge as another reaction site was also attempted to achieve this goal. Starting from functionalized compound (10), one approach involved pyridine iodo-triazole formation and coupling of propargylamine to produce a disubstituted ammonium β-cyclodextrin derivative. After many attempts, this strategy was proved unworkable due to steric hindrance of the cyclodextrin (Figure 52).

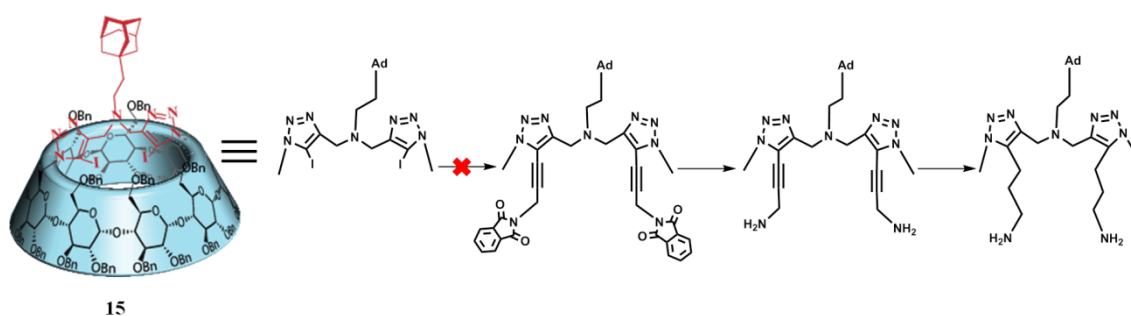


Figure 52: Proposed synthesis route to obtain disubstituted ammonium β-cyclodextrin derivative.

4.5. Synthesis of difunctionalized bridged cyclodextrin/adamantane monomer: functionalized 1-deoxyjirimycin derivative

In order to give bridged β-cyclodextrin/adamantane monomer more applications, the

synthesis of bridged β -cyclodextrin bearing an alkyl arm (22) with functionalized sugar (34) was developed.

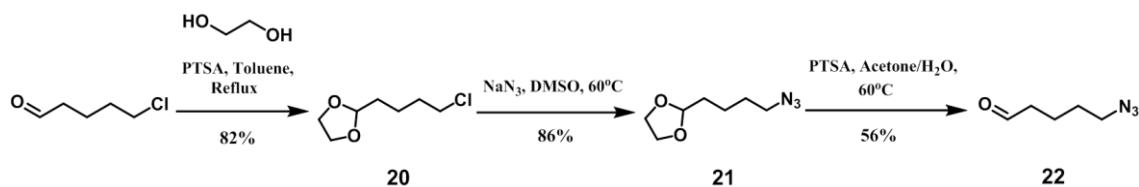


Figure 53: Synthesis of alkyl arm (22).

The alkyl arm and functionalized sugar were first prepared. The commercial derivative 5-chloropentanal with ethylene glycol in the presence of *p*-toluenesulfonic acid (PTSA), gave the compound (20) in a great yield of 82%, which then underwent a nucleophilic substitution reaction (NaN_3 , refluxed at 60°C for 24h) to produce the compound (21). The 5-azidopentanal (22) was prepared after deprotection (Figure 53).

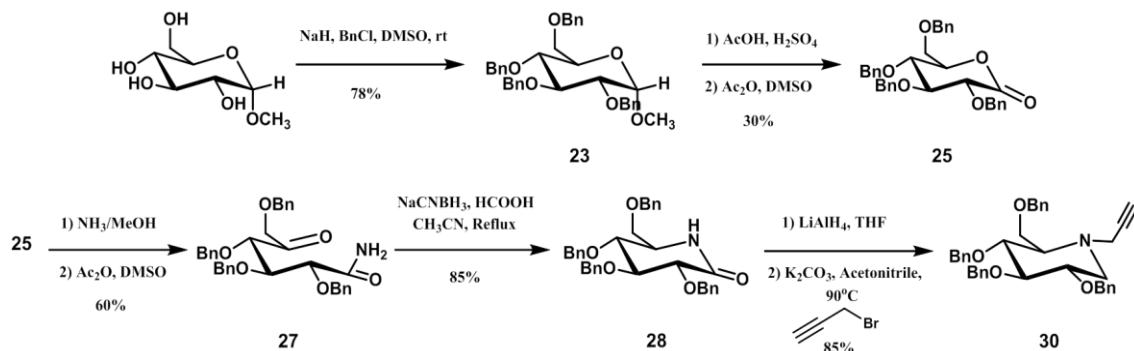


Figure 54: Synthesis of functionalized sugar (30).

In parallel, the perbenzylated sugar (23) could be obtained through carrying out the protected reaction in the presence of benzyl chloride and sodium hydride in DMSO from commercially available methyl α -D-glucopyranoside. Then the compound with the anomeric hydroxyl group was afforded by hydrolysis reaction under the action of acetic acid/sulfuric acid. The formed anomeric hydroxyl group was used to generate the compound (25) via the oxidation reaction. The compound (25) was treated with methanolic ammonia and oxidation to give the keto amide compound (27). The lactam (28) was synthesized by cyclization reaction under the reducing conditions in the presence of sodium cyanoborohydride and formic acid with a yield of 85%. Treatment of the lactam (28) with lithium aluminum hydride (LAH) provided perbenzyl-1-deoxynojirimycin compound, which then underwent nucleophilic substitution to

CHAPTER 2 DESIGN STRATEGY AND SYNTHESIS OF SUPRAMOLECULAR POLYMERS
BASED ON BETA-CYCLODEXTRIN-ADMANTANE IN AQUEOUS SOLUTION

afford the functionalized sugar (30) in a high yield of 85% over two steps (Figure 54) [133].

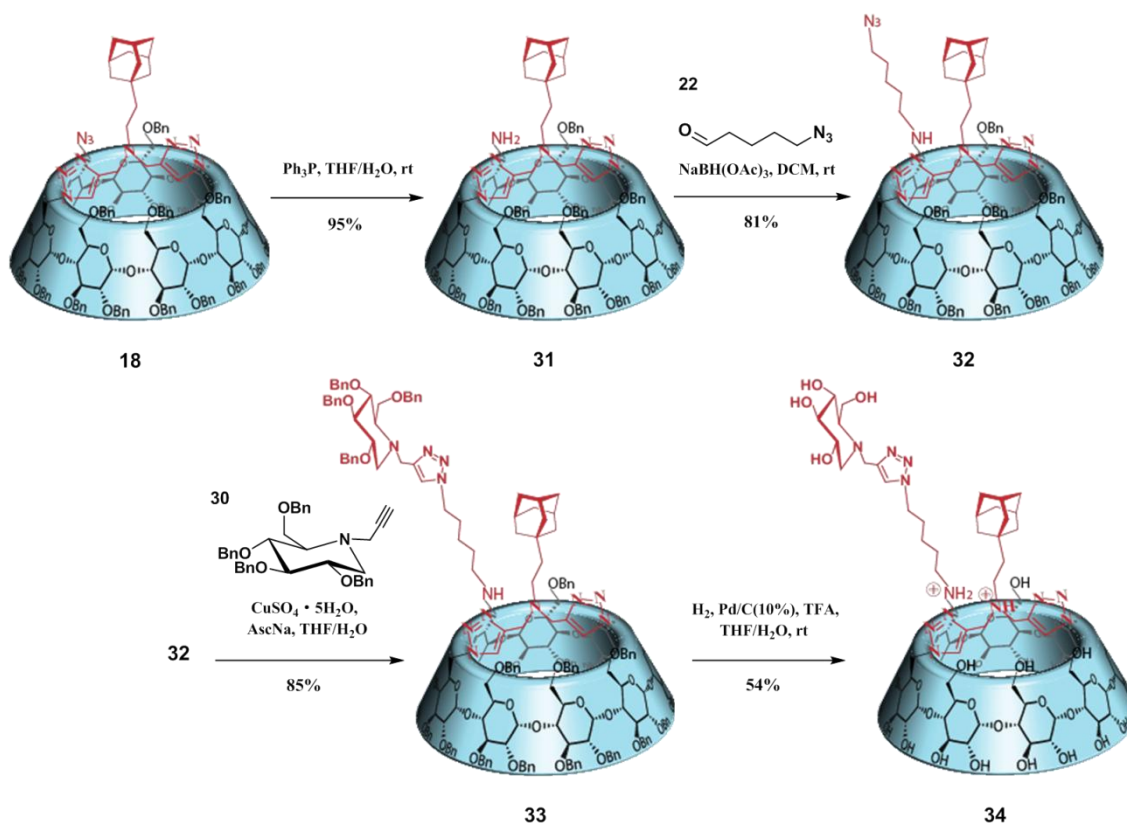


Figure 55: Synthesis of the bridged β -cyclodextrin linked to an alkyl arm with perbenzylated sugar (34).

Next, the mono-substituted azide bridged β -cyclodextrin (18) underwent a reduction reaction, with triphenylphosphine in $\text{THF}/\text{H}_2\text{O}$ to give the amino derivative (31) in 95% yield, which was subjected to the reductive amination in the presence of 5-azidopentanal (22) to furnish the corresponding bridged β -cyclodextrin with the alkyl arm (32), which attached the functionalized sugar (30) by the click reaction to yield the compound (33). Finally, treatment of the compound (33) with palladium on carbon and TFA provided deprotected bridged β -cyclodextrin binding the alkyl arm with functionalized sugar (34) in a final yield of 54% (Figure 55).

4.6. Conclusion of synthesized cyclodextrin/adamantane monomers

Thus, three functional monomers based on β -cyclodextrin could serve as molecular bricks for the construction of supramolecular polymers. The self-inclusion molecule (11) will also be studied to give us some information about the mechanism of supramolecular polymerization (Figure 56).

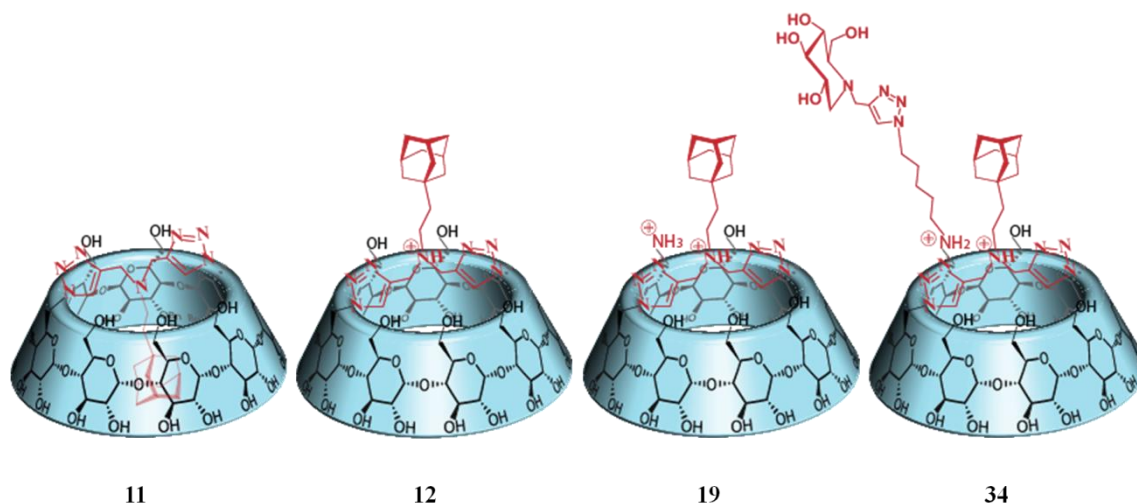


Figure 56: Final molecules (11), (12), (19) and (34).

5. Conclusion

With the aim to mimic biological macromolecules, we have carefully developed completely artificial small molecules based on the cyclodextrin-adamantane system. The bridging strategy is adopted to prepare β -cyclodextrin conjugates with hydrophobic moiety. The location of the adamantyl group is set in the center of the cyclodextrin cavity in order to obtain a higher degree of polymerization of supramolecular polymer. Besides, cationic groups are added to allow further applications in gene condensation and delivery fields, owing to their electrostatic interaction with the anionic phosphate groups of nucleic acids. Moreover, the introduction of sugar gives the possibility to form supramolecular polymers possessing more complex functions. Finally, four β -cyclodextrin conjugates have been synthesized and their ability to construct supramolecular polymers via host-guest interaction will be tested by using several characterization techniques.

CHAPTER 3

STUDY OF SUPRAMOLECULAR ASSEMBLIES

BASED ON BETA-CYCLODEXTRIN-ADAMANTANE

IN AQUEOUS SOLUTION

1. Characterization of the Supramolecular Assembly

1.1. Characterization of supramolecular assembly by $^1\text{H-NMR}$

The functionalized compounds synthesized were first studied in supramolecular assemblies by $^1\text{H-NMR}$. The dilution study made it possible to track the behavior of the different protons. The changes in chemical shift would show the formation of intermolecular complexes. As mentioned above, the degree of polymerization relied on concentration. The existence of an equilibrium state between two species was considered, involving in free monomers with and without intermolecular inclusion of the adamantyl group across the cavity of another monomer. Under low concentration, the spectrum would reflect the free monomer without any inclusion tendency; under high concentration, the spectrum would imply the high distribution of intermolecular complex formation. According to the previous work of our laboratory, the width of the signals could provide information about the species size. The signal of the corresponding polymer would be broader compared to the monomer signal.

We focused on the H-1 protons of the cyclodextrin to catch changes caused by dilution study. These protons were very sensitive to the inclination of adjacent sugar units, providing an idea as to the deformation of the cavity. More importantly, the H-1 protons allowed us to track them easily, which didn't overlap with other cyclodextrin protons in ranges of chemical shifts. Of course, the protons of the adamantane would be carefully followed to see whether self-inclusion or self-assembly process happen.

Firstly, a dilution study was carried out on the compound (11). The spectrum was quite fine at the highest concentration. However, no chemical shift changes or sharpening of the signals were observed even upon 20 times dilution (Figure 57). This was at odds with high concentration dependency to intermolecular complex formation.

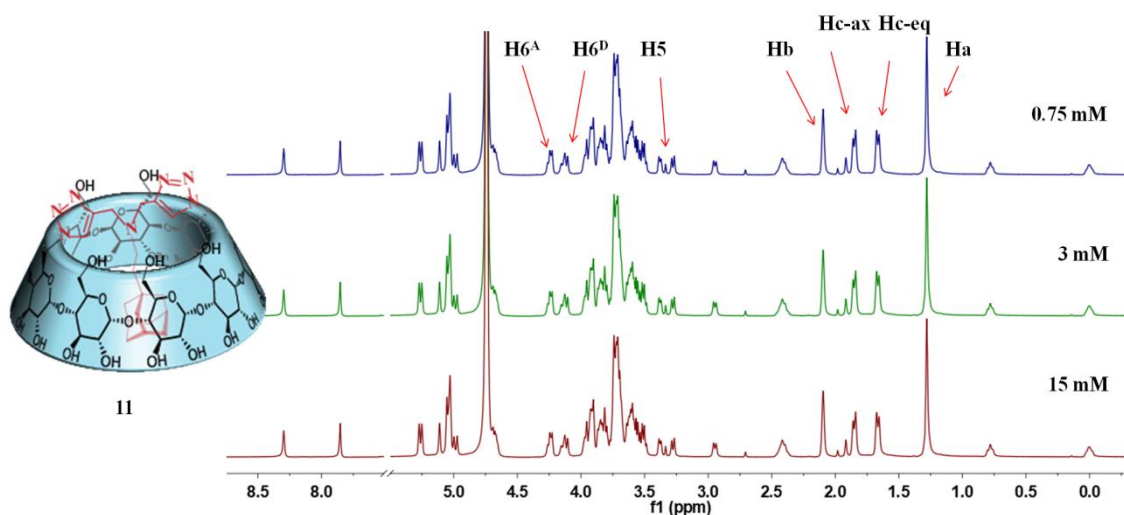
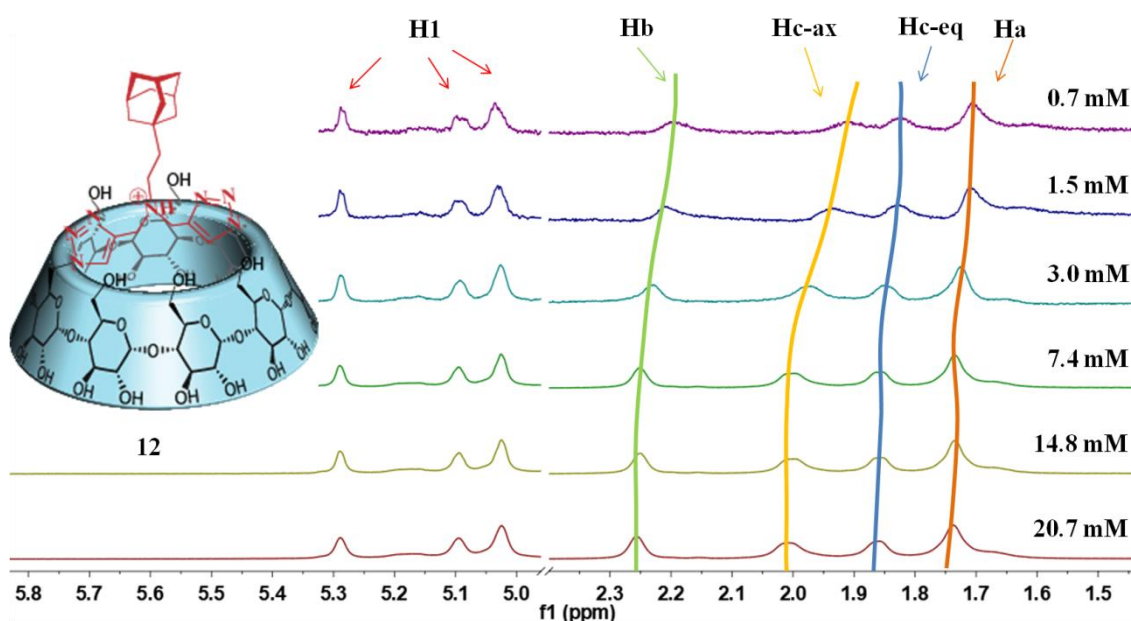


Figure 57: Dilution study by $^1\text{H-NMR}$ (D_2O , 600 MHz, 300 K) of compound (11).

Then, a dilution study was performed on the compound (12). The proton spectra didn't show a large difference in the correlations between concentration and chemical shift changes for cyclodextrin H-1 protons (Figure 58). Perhaps the H-1 protons, because they were located on the exterior surface of the truncated cone, experienced a marginal shift. But some variations of chemical shift for adamantane protons were observed, indicating a change in the environment around the adamantyl group. While the stable signal from 20.7 mM to 7.4 mM solution of compound (12), a sudden variation was fulfilled between 3.0 mM and 7.4 mM, which exhibited small upfield chemical shifts. This result suggested encapsulation of the adamantyl group into the cavity of the cyclodextrin.



CHAPTER 3 STUDY OF SUPRAMOLECULAR ASSEMBLIES BASED ON BETA-CYCLODEXTRIN-ADAMANTANE IN AQUEOUS SOLUTION

Figure 58: Dilution study by $^1\text{H-NMR}$ (D_2O , 600 MHz, 300 K) of compound (12).

This result was also demonstrated using $^1\text{H-NMR}$ through titration of the competitive guest to the compound (12) solution (Figure 59). Adamantylcarboxylate (AdCOONa), a soluble adamantane derivative, was chosen for this study. The chemical shift changes of protons were observed with successive additions of AdCOONa to a 12 mM solution of compound (12) in D_2O . The possible explanation was that the guest molecule attached to cyclodextrin was replaced from the cavity of the cyclodextrin by means of the competitive guest based on considerations of chemical equilibrium, suggesting the depolymerization of the supramolecular polymer. This study also made possible to estimate of the association constant between the bridged cyclodextrin and the adamantane.

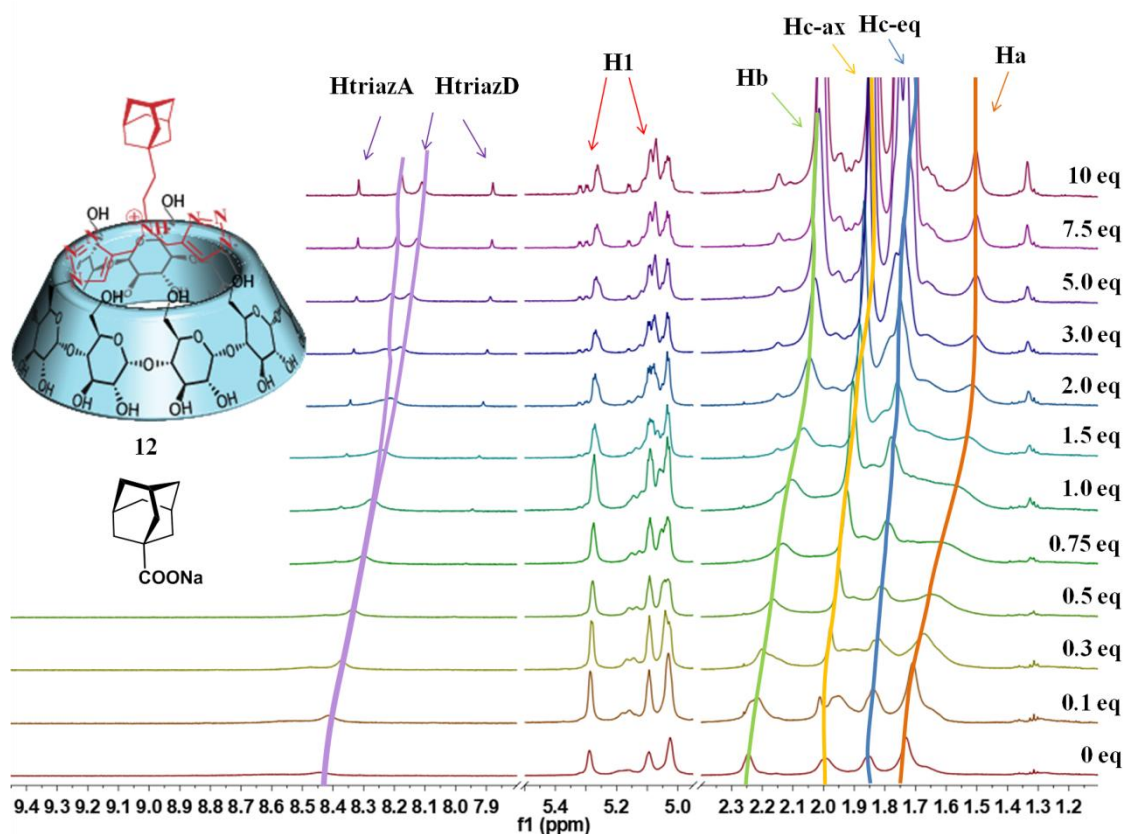


Figure 59: Titration study by $^1\text{H-NMR}$ (D_2O , 600 MHz, 300 K) in the presence of a competitive guest molecule (AdCOONa) of compound (12) at 12 mM.

A similar result of dilution study was obtained for compound (19). The splitting of H-1 protons peaks of cyclodextrin was observed, indicating the changes in the surrounding environment. Besides, a similar jump in chemical shifts of adamantyl protons was also noticed between 1.1 mM and 3.6 mM (Figure 60).

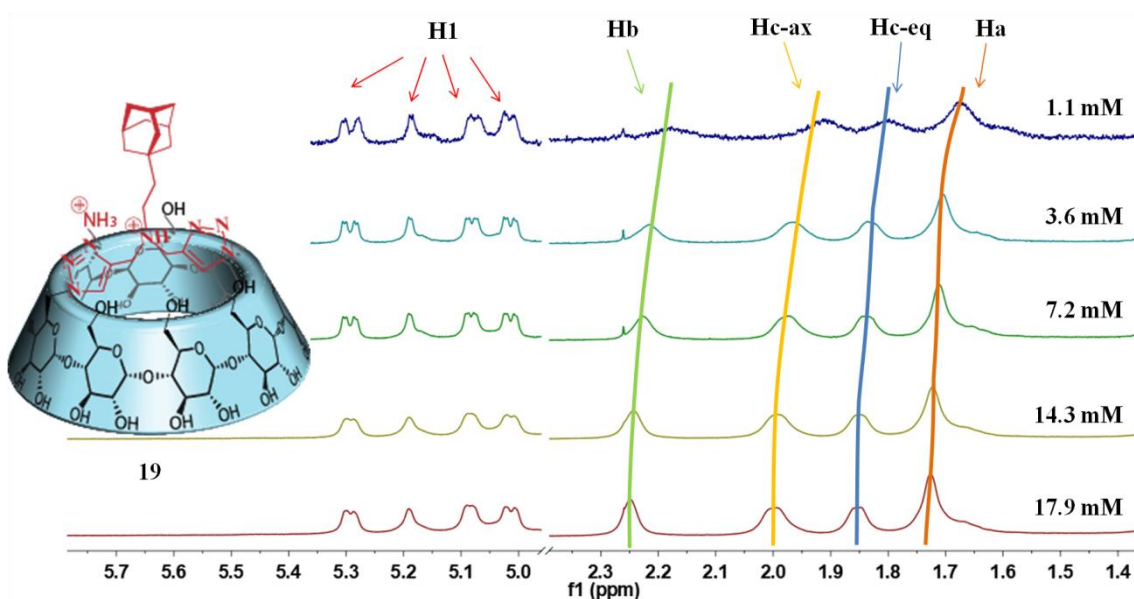


Figure 60: Dilution study by $^1\text{H-NMR}$ (D_2O , 600 MHz, 300 K) of compound (19).

And in the case of compound (34), the behavior of the formation of the supramolecular polymer wasn't affected by attaching the alkyl arm with small sugar molecule to functionalized bridged cyclodextrin. The chemical shift changes of adamantyl protons occurred between 1.9 mM and 3.9 mM (Figure 61). The performance of small upfield shifts from the sugar triazole protons, the H-1 protons and the adamantyl protons implied intermolecular association. In order to confirm our inference, the NMR-ROESY experiment was carried out to give directly powerful support as to self-assembly.

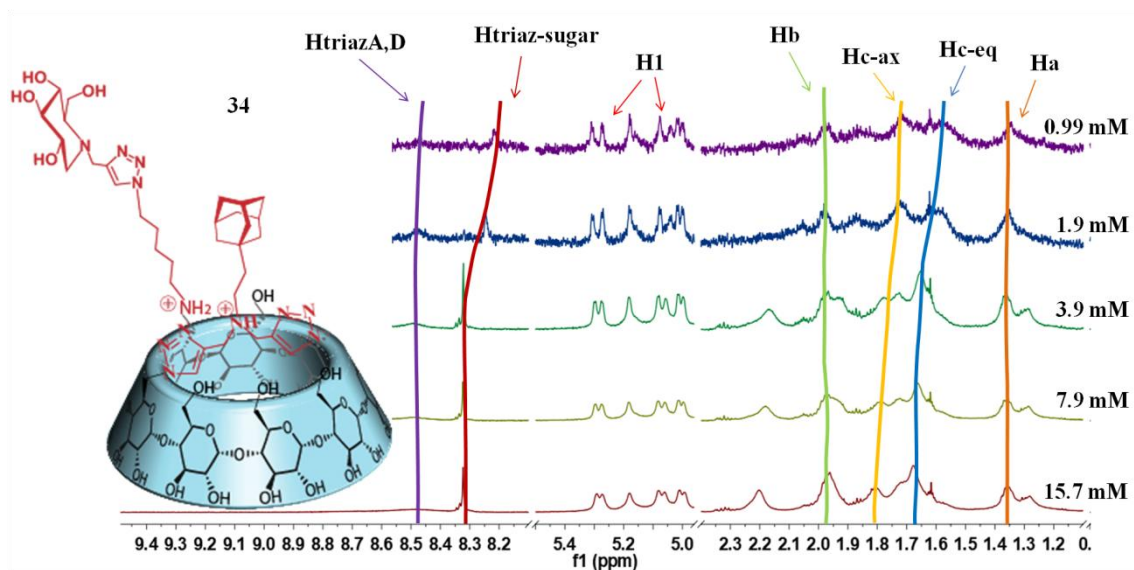


Figure 61: Dilution study by $^1\text{H-NMR}$ (D_2O , 600 MHz, 300 K) of compound (34).

1.2. Characterization of supramolecular assembly by NMR-ROESY

It was possible to observe the interactions between adamantane moiety and the cavity of the cyclodextrin by performing the NMR-ROESY experiment. The inclusion orientation of the guest in the cavity was confirmed, giving access to determine self-inclusion or self-assembly.

For compound (11), its cavity indeed included the adamantane. Surprisingly, the inclusion wasn't in the expected direction but upside down (Figure 62). The result of self-inclusion was confirmed by NMR-ROESY which clearly showed interaction between the H-3 protons of the cyclodextrin and Hc-eq/Hb protons of the adamantane, when the H-5 protons of the cyclodextrin interactions with Ha protons of the adamantane. Consequently compound (11) was in a self-inclusion form.

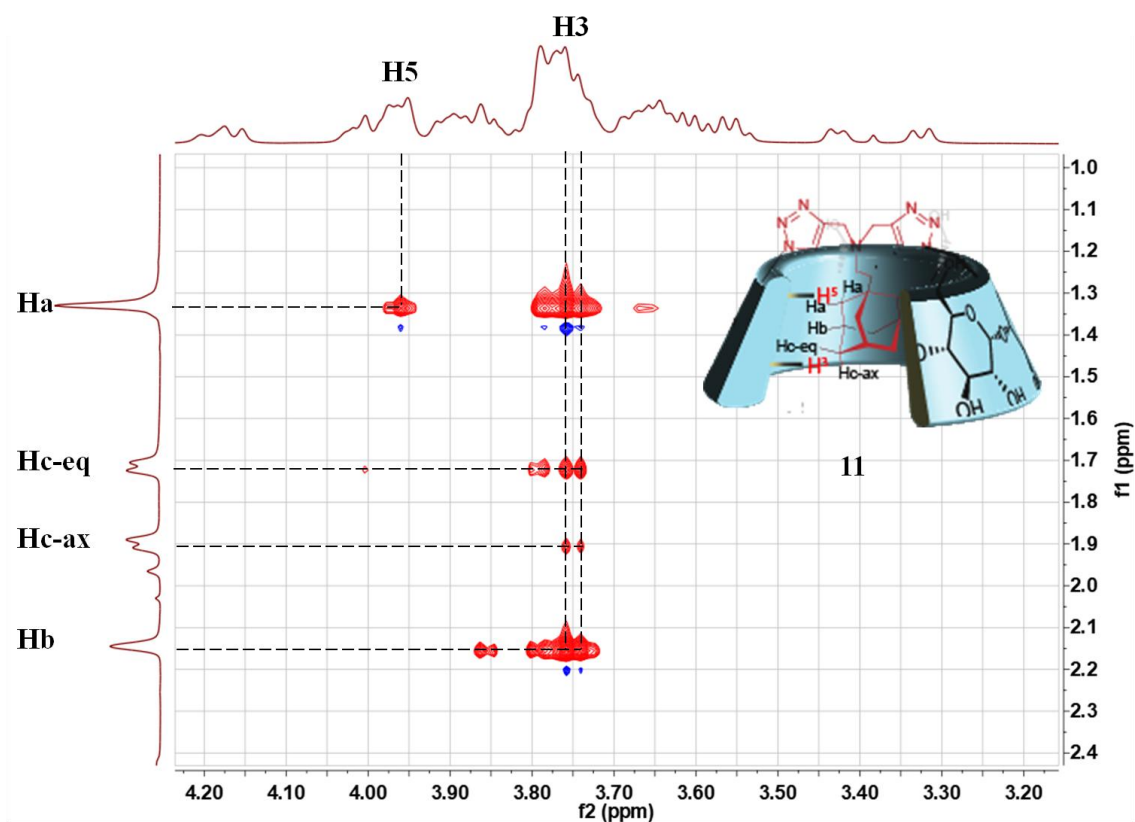


Figure 62: NMR-ROESY (D₂O, 600 MHz, 300 K) of compound (11).

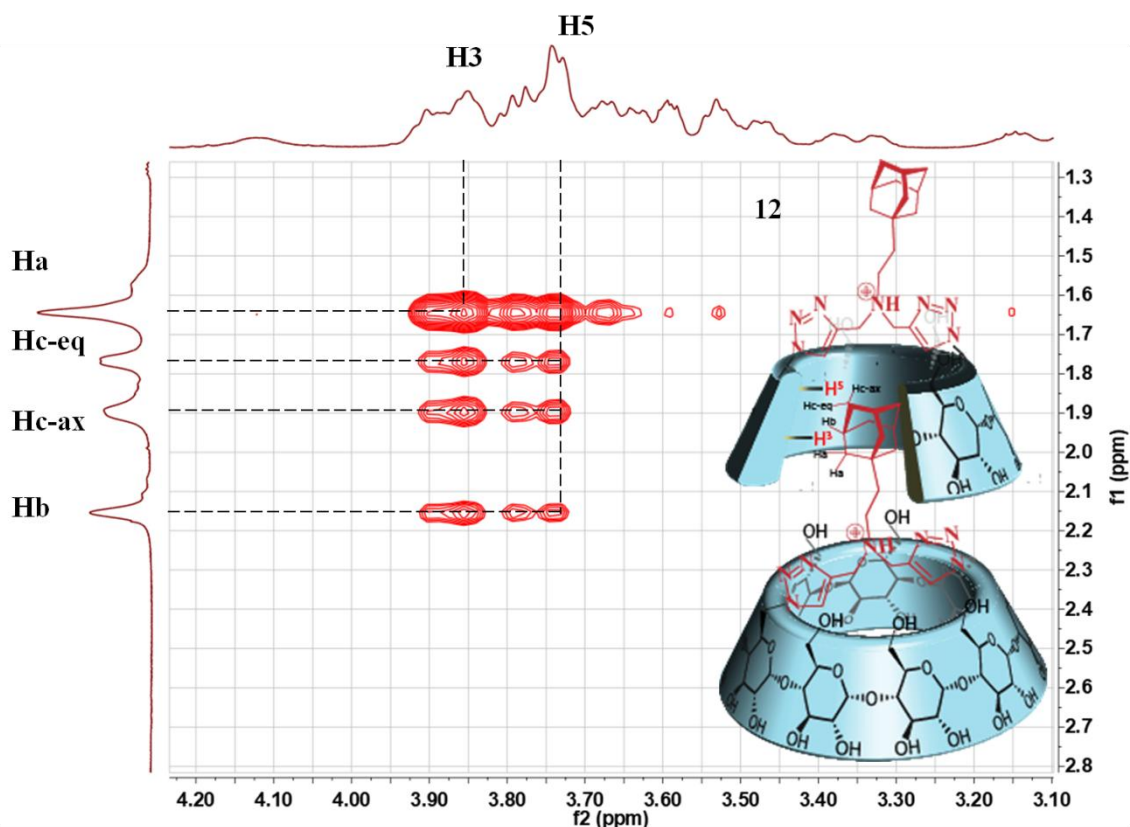


Figure 63: NMR-ROESY (D₂O, 600 MHz, 300 K) of compound (12).

A markedly different result was obtained for the other conformer (12). Several signals overlapped with that of Ha protons of the adamantyl group. Two other types of protons of the adamantyl group related to the interaction were focused on. The NMR-ROESY spectrum showed cross-correlations between adamantane protons (Hc and Hb) and H-5 protons of the cyclodextrin were observed (Figure 63). These results provided the evidence for the existence of inclusion of adamantane across the secondary rim of another cyclodextrin, with a complete insertion. In addition, no special cross-correlations for the protons of the triazole group were observed to determine their orientation.

With regard to the functionalized β -cyclodextrin derivative with the ammonium group (19) and with the alkyl arm bearing small sugar molecule (34), NMR-ROESY experiments were also carried out (Figure 64 and Figure 65). The same self-assembly behaviors were shown to draw the same conclusions.

CHAPTER 3 STUDY OF SUPRAMOLECULAR ASSEMBLIES BASED ON BETA-CYCLODEXTRIN-ADAMANTANE IN AQUEOUS SOLUTION

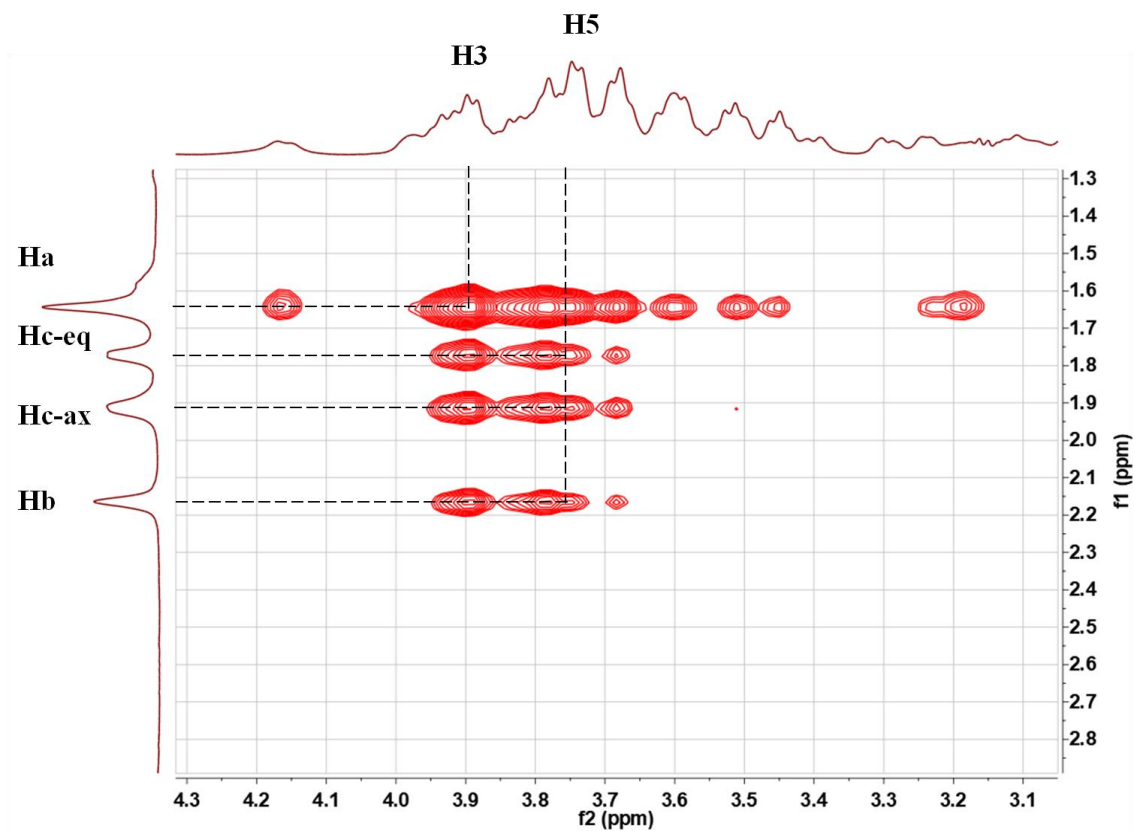


Figure 64: NMR-ROESY (D₂O, 600 MHz, 300 K) of compound (19).

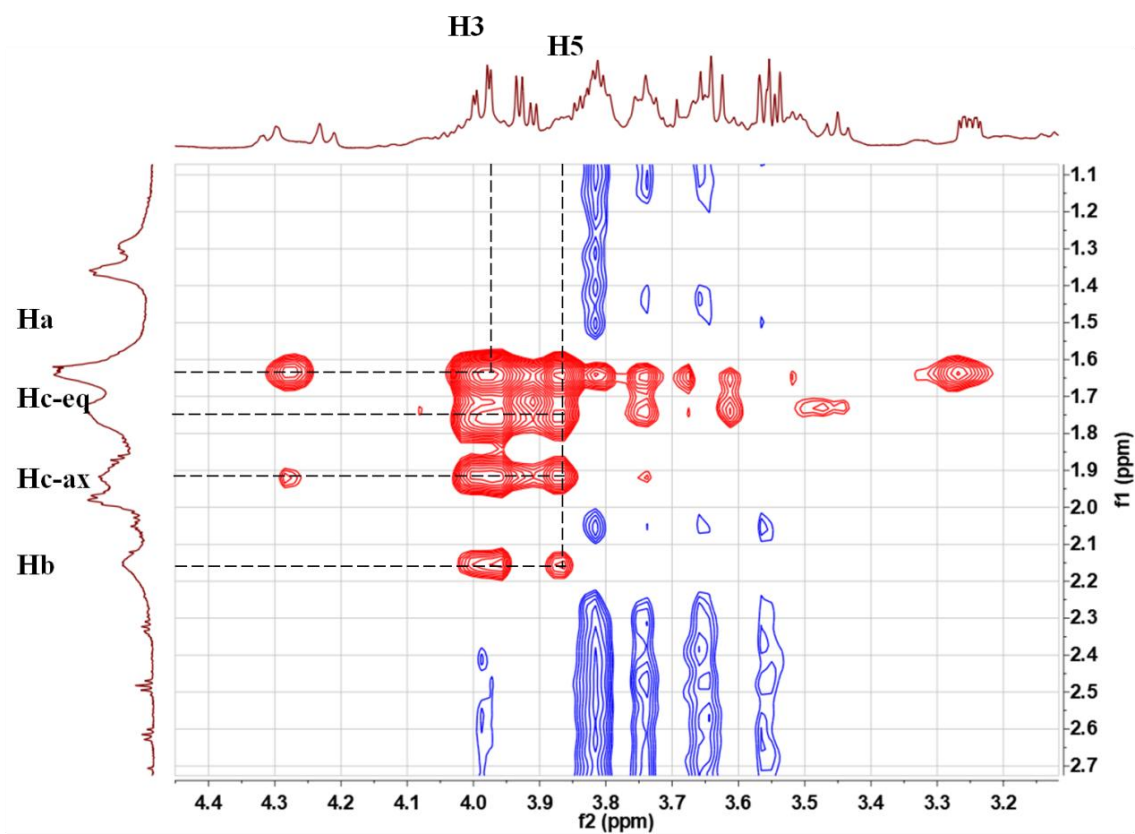


Figure 65: NMR-ROESY (D₂O, 600 MHz, 300 K) of compound (34).

1.3. Characterization of supramolecular assembly by NMR-DOSY

In a second step, two-dimensional NMR-DOSY studies were carried out to evaluate the size and the behavior of the self-assemblies of synthesized cyclodextrin monomers. An NMR-DOSY experiment was performed with compound (11) whose value of diffusion coefficient remained relatively constant, whatever the concentration. This tendency of the diffusion coefficient was similar to that of the self-included compound described in the literature ^[134] (Figure 66). Indeed, the constant value of the diffusion coefficient was in accordance with that of the native β -cyclodextrin ($D = 2.6 \times 10^{-10} \text{ m}^2 \text{ s}^{-1}$) over the same concentration range ^[135], allowing us to affirm the presence of a single monomer in aqueous solution. In contrast, for the other conformer (12), the diffusion coefficient tended to decrease non-linearly ($D = 1.1 \times 10^{-10} \text{ m}^2 \text{ s}^{-1}$ to $0.78 \times 10^{-10} \text{ m}^2 \text{ s}^{-1}$) as an increase in concentration (3.0 mM to 7.5 mM). The change as a concentration function indicated the polymerization of the repeat unit (Figure 66).

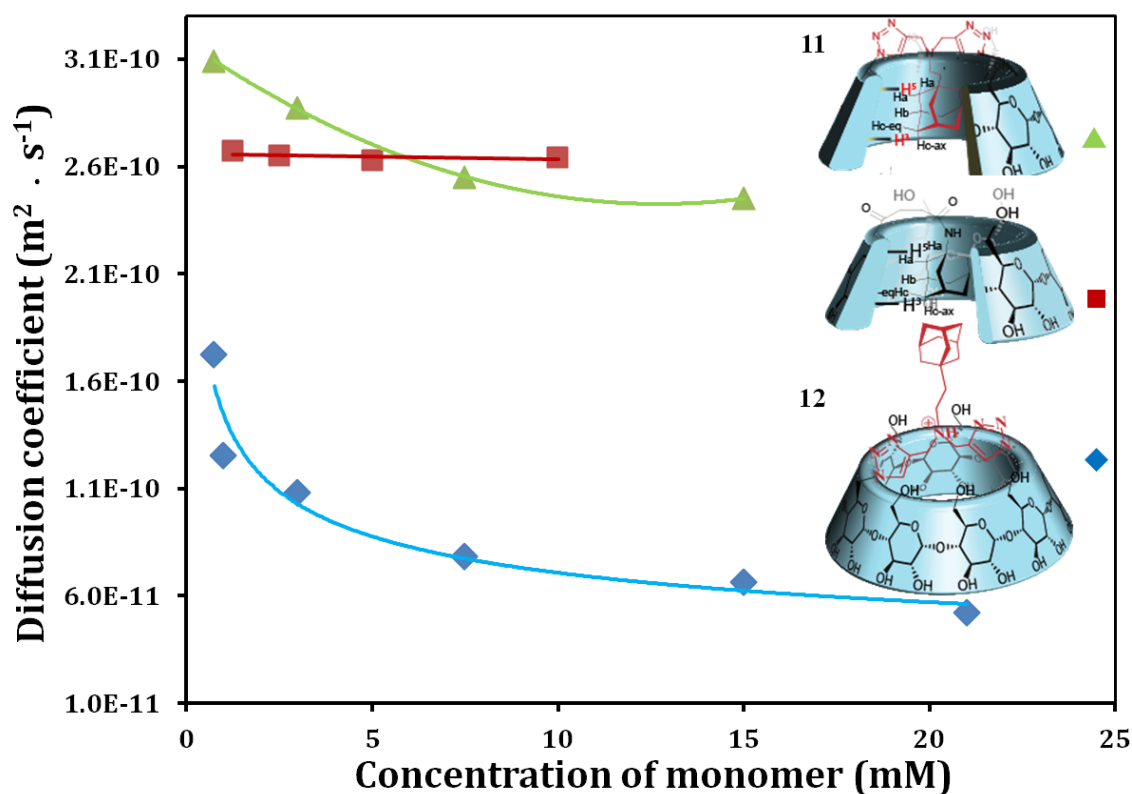


Figure 66: Diffusion coefficients measured by NMR-DOSY experiment (D_2O , 600 MHz, 300 K) of compounds (11), (12) and the self-included compound described in the literature.

Furthermore, the study of the diffusion coefficient of concentration-dependence would

provide information about the size of the model by calculation the degree of polymerization. It is assumed that the formed supramolecular polymer is a linear and model of a cylinder-like structure applied. The size of this model can be estimated by the Garcia de la Torre relationship ^[136]:

$$D = \frac{kT}{3\pi\eta L} \left[\ln \left(\frac{L}{d} \right) + \nu \right]$$

With:

$$\nu = 0.312 + 0.565 \frac{d}{L} - 0.100 \left(\frac{d}{L} \right)^2$$

Where:

D Translational diffusion coefficient (m² s⁻¹)

K Boltzmann constant (J K⁻¹)

T Temperature (K)

η Viscosity of the liquid (Pa s)

L Length of cylinder (m)

d Diameter of cylinder (m)

According to Garcia de la Torre et al. ^[136], introducing isolating the terms and a finite aspect ratio (p = L/d), the translational diffusion coefficient D can be expressed as:

$$\frac{3D\pi\eta d}{kT} = \frac{1}{p} \left[\ln(p) + 0.312 + \frac{0.565}{p} - \frac{0.100}{p^2} \right]$$

This equation can't have a solution, but we can draw its corresponding curve y = f(p). It is assumed that the distance of the repeat unit of monomer (12) of self-assembly polymer is 0.9 nm and the cylinder parameter of compound (12) is the same as for β-cyclodextrin (diameter of the β-cyclodextrin = 1.54 nm) ^[137]. It is then enough to calculate the value on the left-hand side of the equation from the obtained diffusion coefficient and graphically define the value of p corresponding to our system. Finally, the degree of polymerization (DP) at a given concentration was obtained (Figure 67).

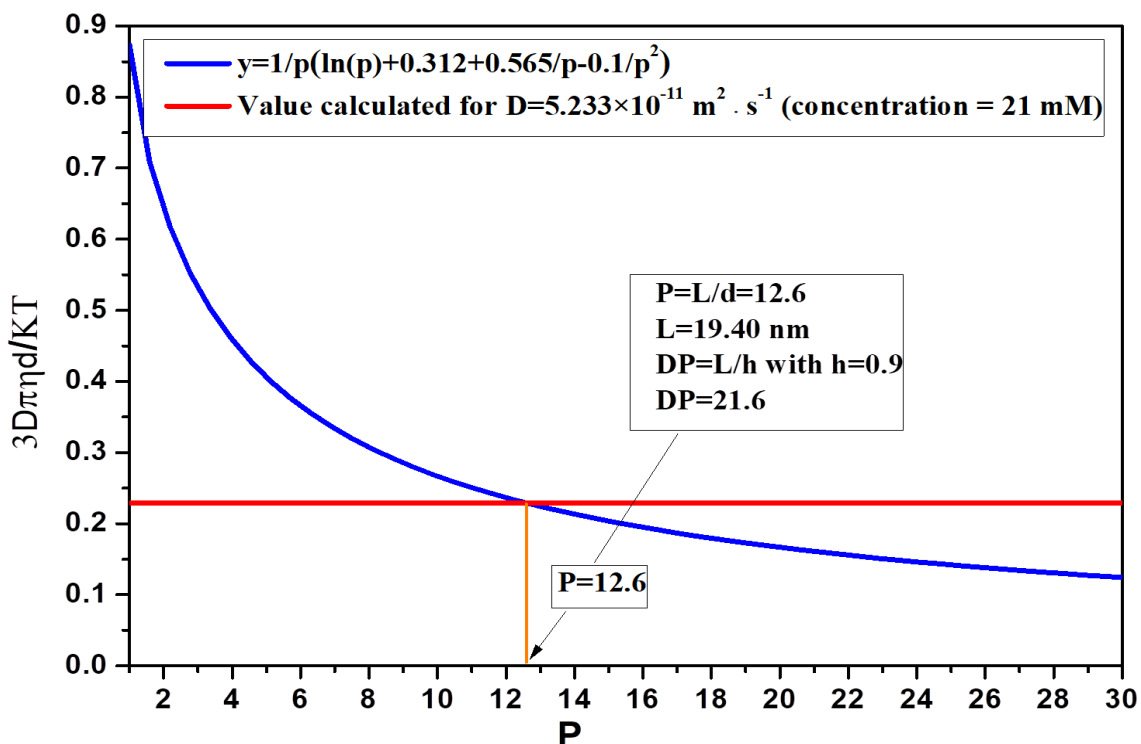
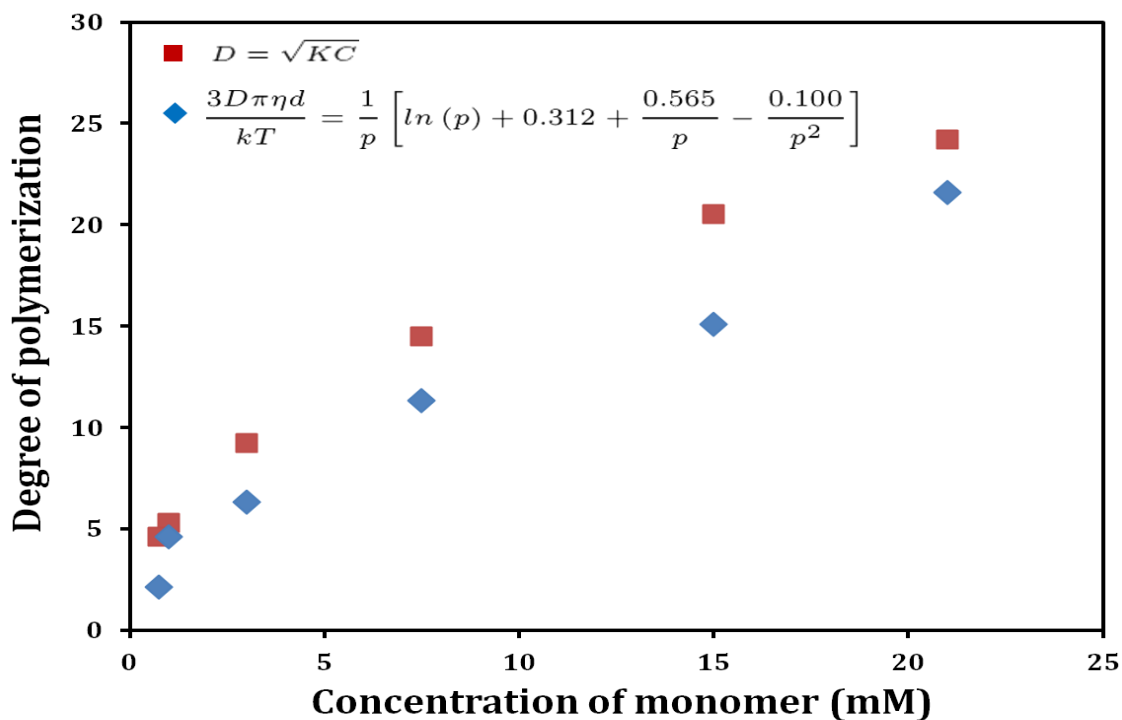


Figure 67: Example of the calculation of p for a solution of compound (12) at 21 mM.

Taking a solution of the compound (12) at 21 mM as an example calculated the degree of polymerization (Figure 67). The formed polymer composed of 22 monomers. The size of the formed supramolecular polymer was estimated according to the equation relating to the isodesmic model, 13 times longer than wide.



CHAPTER 3 STUDY OF SUPRAMOLECULAR ASSEMBLIES BASED ON BETA-CYCLODEXTRIN-ADAMANTANE IN AQUEOUS SOLUTION

Figure 68: Degree of polymerization values calculated for compound (12) following the Carothers equation and Tirado-Garcia de la Torre relationship.

And the value of the degree of polymerization for the compound (12) at each concentration was obtained according to the method of Tirado-Garcia de la Torre as shown in Figure 68. In addition, the association constant for cyclodextrin/adamantane system was 28000 M^{-1} (from ITC experiment, it will describe in the next section of this chapter), following the Carothers equation $DP \approx (KC)^{1/2}$ [21], the translated DP also obtained. The value of each concentration was a litter higher than that of following the relationship of Tirado-Garcia de la Torre. The possible explanation was slightly underestimation of the calculated DP in our work, taking no account of the length of the arm of connected the adamantane in the height of each unit.

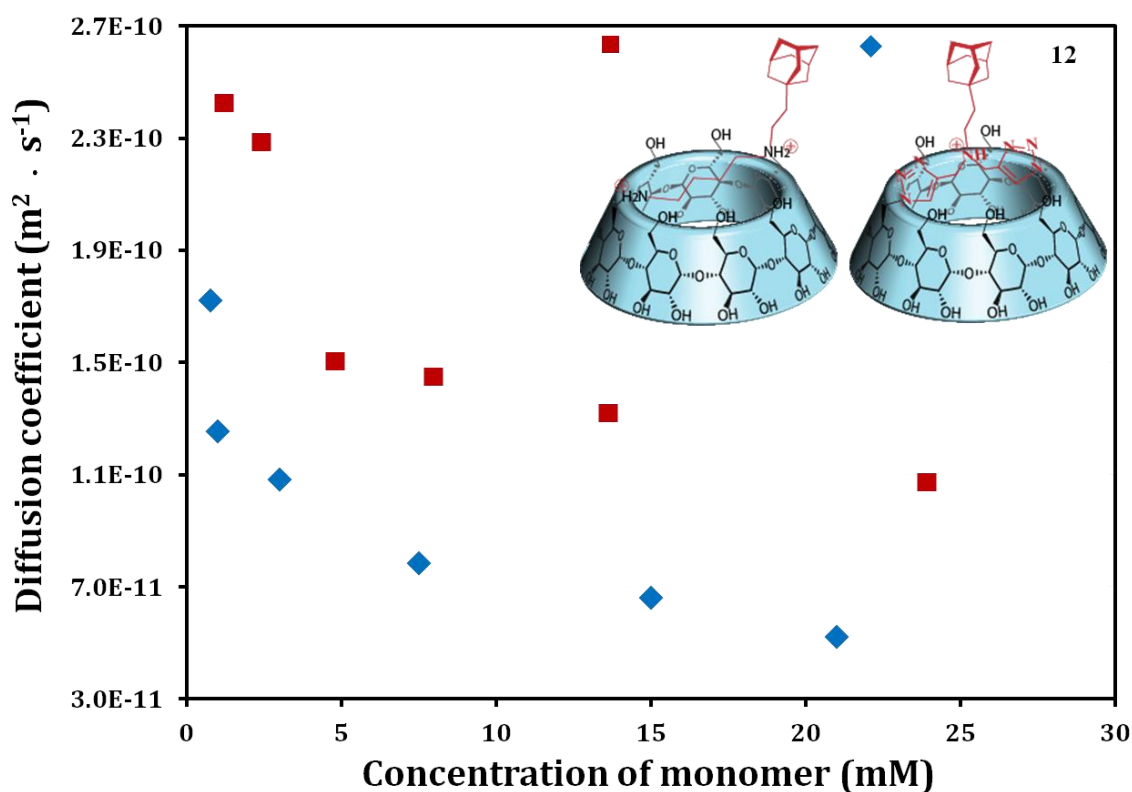


Figure 69: Diffusion coefficients measured by NMR-DOSY experiment (D_2O , 600 MHz, 300 K) of compound (12) and the bridged compound described in the literature.

Meanwhile, the comparison result of the diffusion coefficient between supramolecular polymer in my thesis and the bridged cyclodextrin derivative with adamantyl group described in the literature was shown in Figure 69 [130]. The length of polymer had a significant increase (22 repeat units and 9 repeat units correspond to the compound (12) in this thesis and the

compound mentioned in the literature). An optimization strategy that the position of adamantane was adjusted from one side to the center of the bridge was proved.

Finally, the NMR-DOSY experiment demonstrated the disassembly of polymer formed by compound (12) in the presence of the competitive guest (adamantyl carboxylate: AdCOONa). The data was collected by successive additions of AdCOONa to a 12 mM solution of compound (12) (Figure 70). A clear increase in diffusion coefficient ($5.23 \times 10^{-11} \text{ m}^2 \text{ s}^{-1}$ to $9.43 \times 10^{-11} \text{ m}^2 \text{ s}^{-1}$) with only an addition of 0.1 equivalents of the competitive guest was observed. This result demonstrated that the host-guest interaction played a key role in the formation of supramolecular polymers.

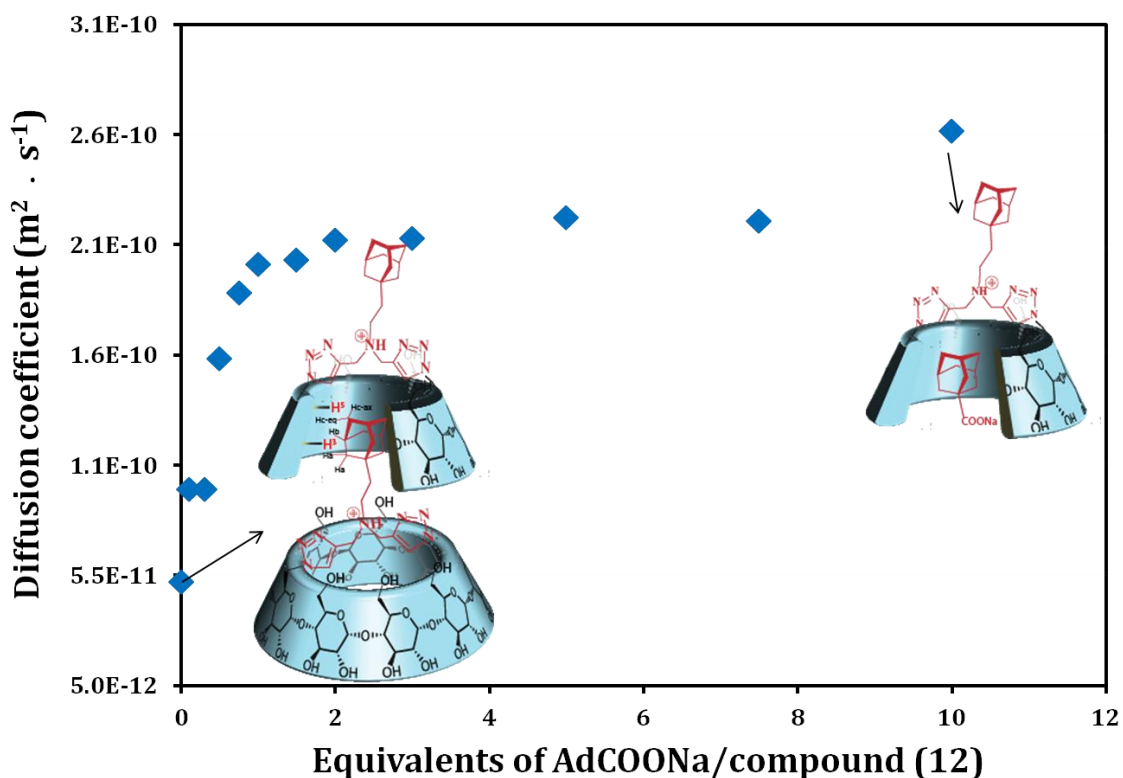


Figure 70: NMR-DOSY (D_2O , 600 MHz, 300 K) of successive addition of AdCOONa to a solution of compound (12) at 12 mM.

Similar NMR-DOSY studies were carried out on compound (19) and compound (34). The tendency of the diffusion coefficient of each compound was similar to that of the compound (12). The supramolecular polymers were formed with a characteristic of the non-linear decrease in the diffusion coefficient. The two compounds were in the form of self-assembly polymer (Figure 71).

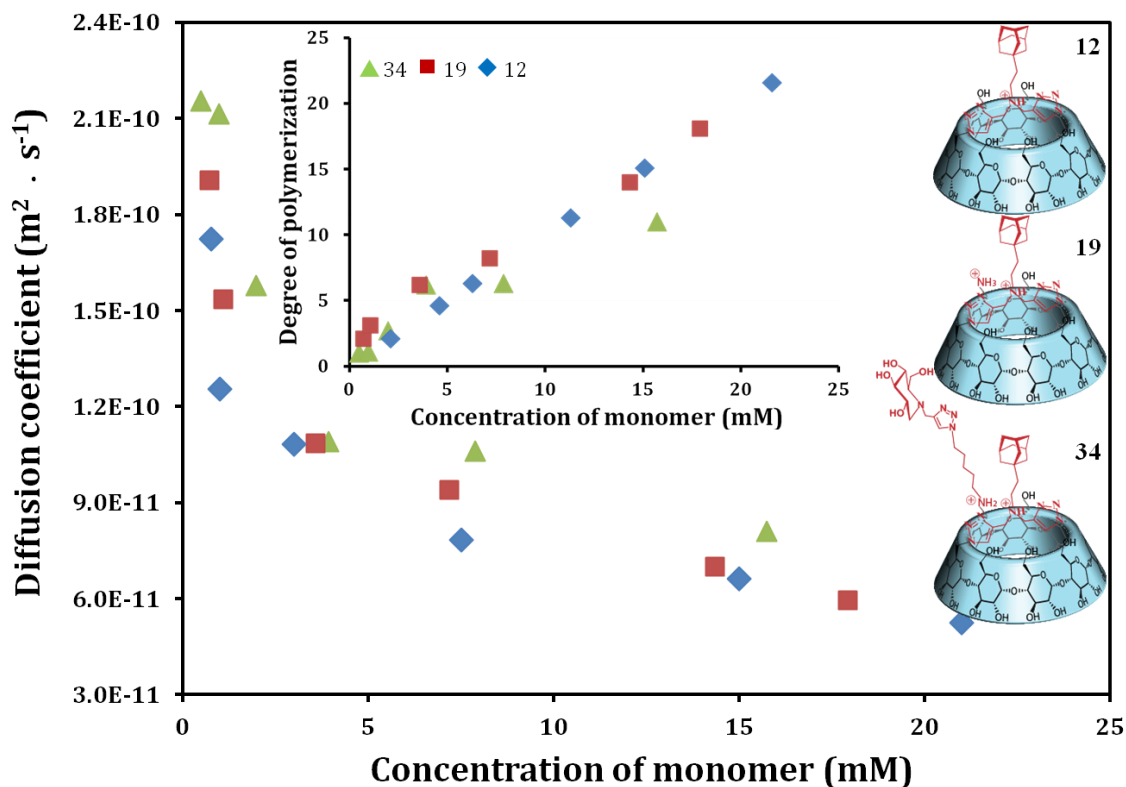


Figure 71: Diffusion coefficients measured by NMR-DOSY experiment (D₂O, 600 MHz, 300 K) of compounds (12), (19) and (34) (inset: translated degree of polymerization of compound (12), (19) and (34)).

1.4. Characterization of supramolecular assembly by ITC

ITC measurement can quantify the interaction of cyclodextrin with adamantane and knowledge of the association constants during polymerization. These experiments were performed by Ga ěle Pembouong who is one member of the polymer chemistry team of the IPCM.

The measurement was performed by successive injection of a 5 mM solution of compound (12) in the sample cell of ITC device. A significant heat increase was observed during the concentration-dependent dilution process. This implied that an exothermic process caused by disassembly of supramolecular polymer, which could be the evidence of the formation of the host-guest complex. In the application of the isometric model, the calculated association constant of monomer (12) was approximately $K = 28000 \text{ M}^{-1}$. The ITC results again demonstrated that the guest located in the center made it feasible to optimize the polymer system. However, due to an equipment problem, it was impossible to precisely abstract these values. This result hasn't been presented in this manuscript, but it should be obtained later.

For compound (11), the various NMR studies ruled out the presence of supramolecular polymer. Here we didn't characterize it by ITC. Based on their structures, we concluded that compounds (19) and (34) should also have their affinity in the same order of magnitude as compound (12). Currently, it is impossible to present relevant information of compound (19) and compound (34) in this thesis, but should be provided soon.

1.5. Characterization of supramolecular assembly by viscosity

Capillary viscosity experiment also was performed to study the self-assembly of synthesized monomers. As mentioned in chapter 1, the relationship of viscosity and molecular weight followed by the Mark-Houwink equation ($[\eta] = KM^\alpha$) which was an empirical equation^[20]. It was hard to find a suitable covalent model to get two empirical parameters (K , α) for the dynamic system. With regard to the supramolecular polymer, it was a supplementary means of characterization.

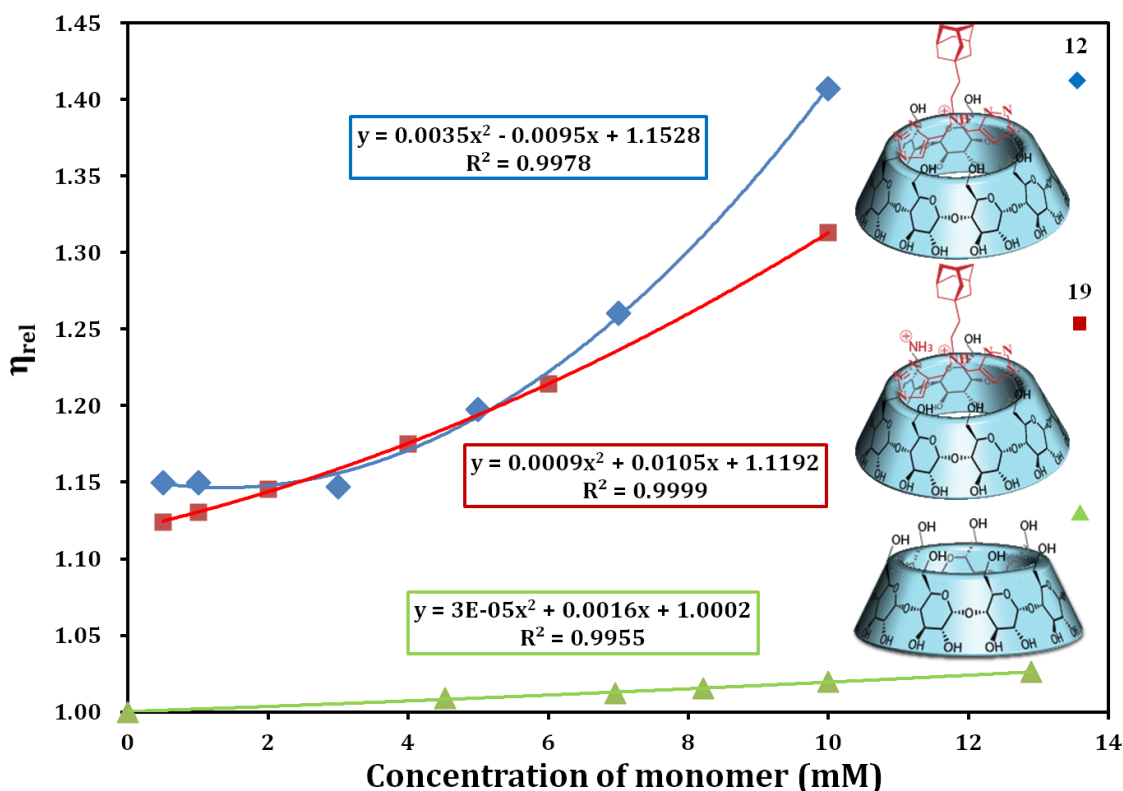


Figure 72: Study of the viscosity as a function of the concentration of compound (12), compound (19) and native β -cyclodextrin in water at 25 °C.

We only selected two compounds to characterize through this measurement. And among four synthesized monomers, supramolecular polymers formed by compound (12) and compound

(19) had better performances in size. The viscosity experiments were carried out on compound (12) and (19). Both compounds showed strong concentration-dependence of the relative viscosity compared to the native β -cyclodextrin (Figure 72) [138]. The non-linear increase indicated the self-assembly behavior of two compounds.

1.6. Characterization of supramolecular assembly by DLS

Dynamic light scattering (DLS) measurement is an intuitive way to determine the size distribution of the supramolecular assembly solution. Compounds (12) and (19) were studied by DLS. Their size distributions were observed at 150 nm on average. The hydrodynamic diameter (D_h) of the 15 mM solution of compound (12) and compound (19) were 156 nm and 148 nm, respectively. These values seem too high for supramolecular polymers composed of around 22 repeat units. The results were given for reference only, indicating the aggregation phenomenon of the two functionalized β -cyclodextrin derivatives. In most cases, since the DLS experiment was more sensitive to a small amount of large species present in the solution, the data obtained might mislead the true composition in solution.

2. Study Influence Factors on Polymerization of Supramolecular Polymer

According to the above-mentioned results of various characterization methods, it clearly proved that compounds (11) and (12) were conformers, self-included or self-assembled. It was an opportunity to examine the factors that influenced on self-inclusion versus supramolecular polymer formation. All the experiments were monitored by $^1\text{H-NMR}$ which could show the difference between two formations, as shown in Figure 73.

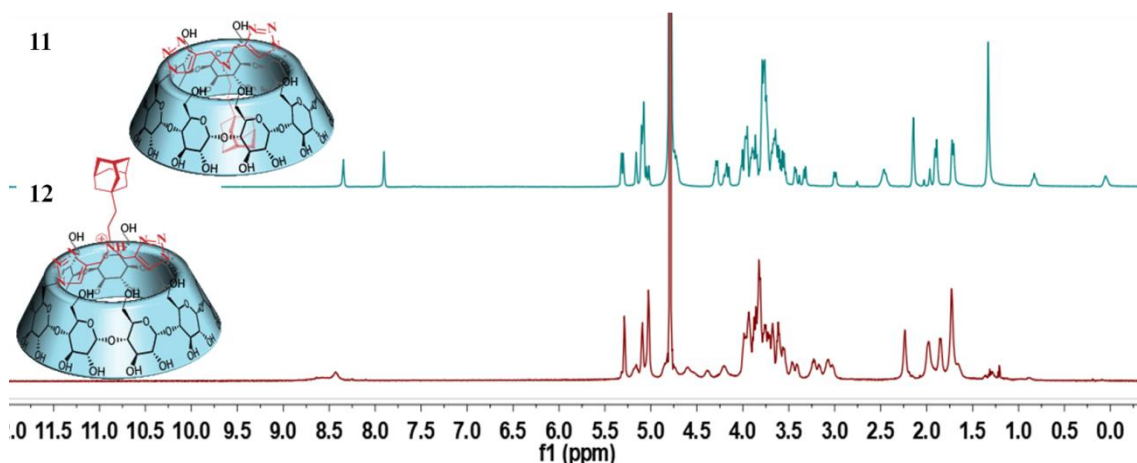


Figure 73: The ^1H -NMR spectra of compound (11) and compound (12).

The study of the factors influencing polymerization started with compound (11). Because of the basic group (amine group) in the compound (11), it was investigated at a concentration of 8 mM (Figure 74) in the presence of NaOD in water. The spectrum showed that the addition of NaOD didn't lead to the deprotonation of the ammonium group and the consequent conformational change. This result indicated that compound (11) was in the form of neutral derivative and the net charge was zero.

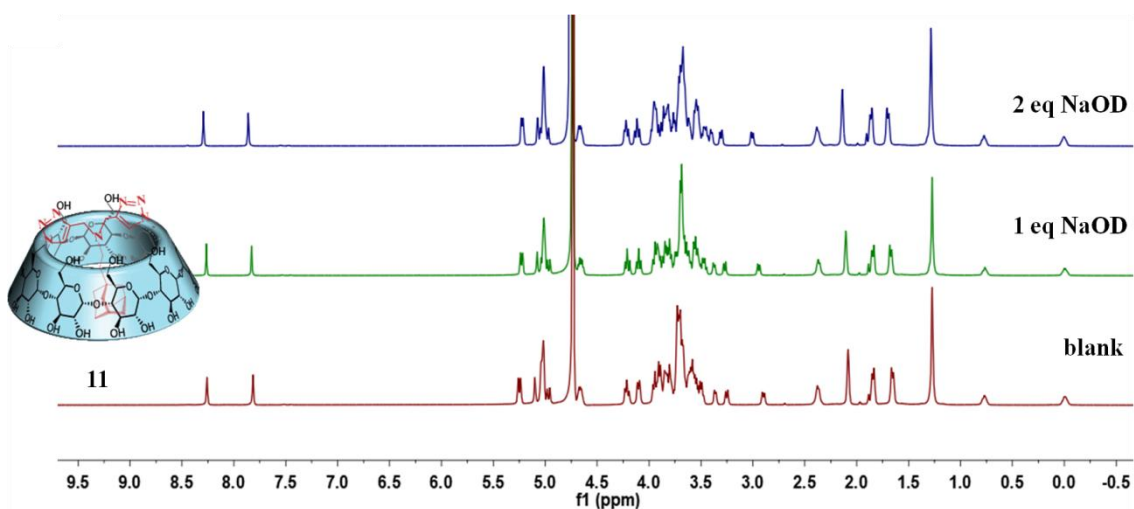


Figure 74: ^1H -NMR (D_2O , 600 MHz, 300 K) of successive addition of NaOD to a solution of compound (11) at 8 mM.

Hence, protonation monitoring in ^1H -NMR (Figure 75) was performed with a strong acid (TFA, $\text{pK}_a = 0.23$). Neutral monomer (11) could be converted into the corresponding positively charged monomer (13) by the addition of two equivalents of TFA. This was proved by the chemical shift changes in the ^1H -NMR spectrum. As the TFA was added, the protons of triazole group in the vicinity of the ammoniums was slightly deshielded, indicating the increase of the electron density of the positive charges. While the large downfield chemical shift changes of H-6 protons of the β -cyclodextrin and the small upfield chemical shift change of the adamantane proton (Ha) were observed, inferring that the ammonium protonation process allowed a deeper inclusion of the guest in the cavity.

CHAPTER 3 STUDY OF SUPRAMOLECULAR ASSEMBLIES BASED ON BETA-CYCLODEXTRIN-ADAMANTANE IN AQUEOUS SOLUTION

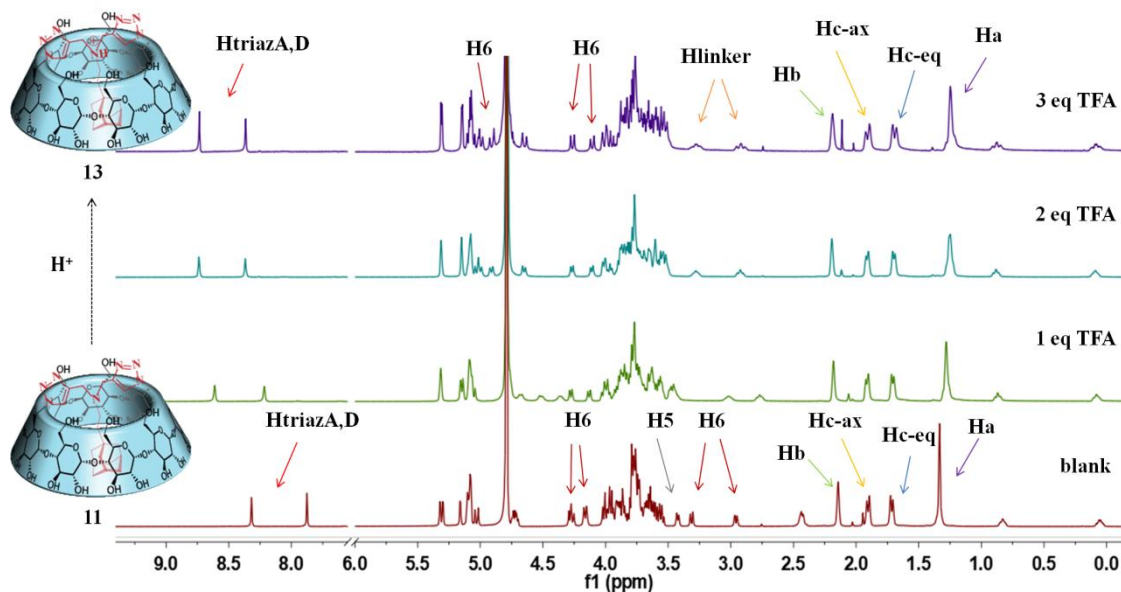


Figure 75: $^1\text{H-NMR}$ (D_2O , 600 MHz, 300 K) of successive addition of TFA to a solution of compound (11) at 8 mM.

NMR-ROESY spectrum of protonated monomer (13) was performed and showed that was still in self-included conformation (Figure 76). In addition, no significant conformational transitions were obtained under acidic conditions with high temperature ($90\text{ }^\circ\text{C}$) or over time (60 days).

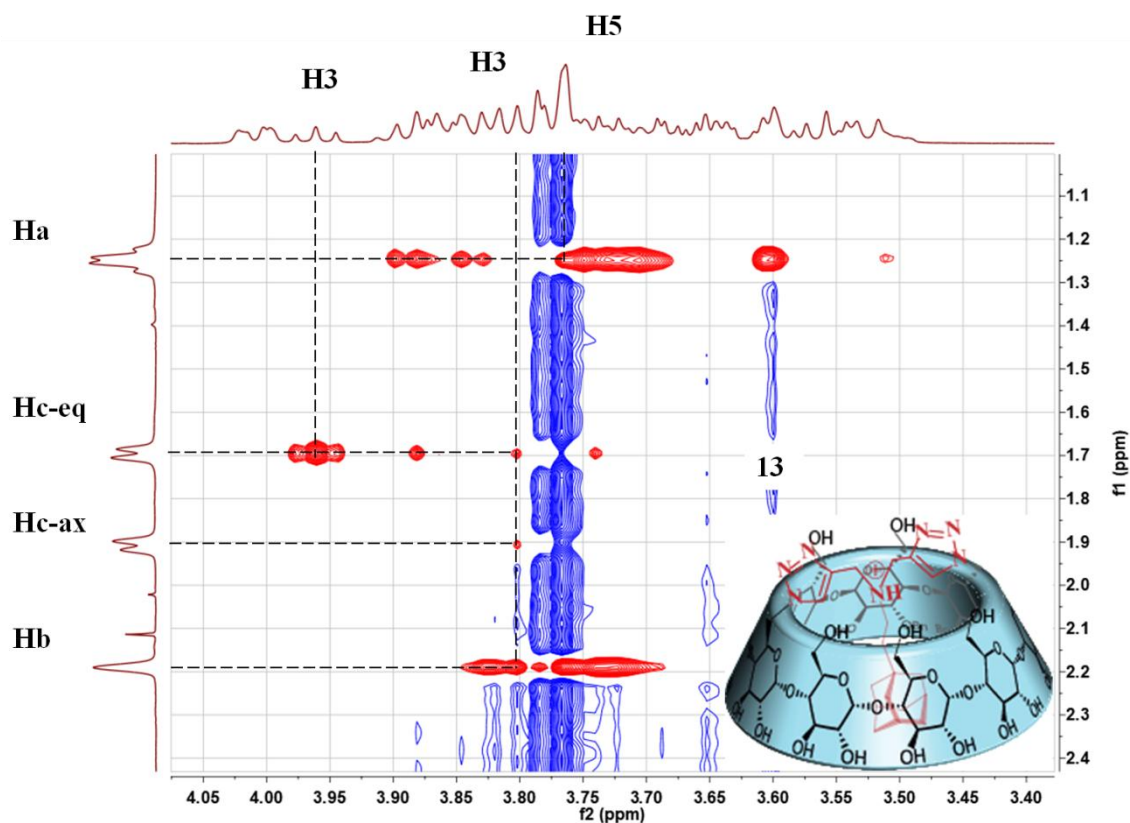


Figure 76: NMR-ROESY (D₂O, 600 MHz, 300 K) of compound (13).

Meanwhile, we observed a depolymerization of the self-assembled cyclodextrin (12), which appeared to be time-dependent and concentration-dependent. The percentage of monomer was investigated by ¹H-NMR at a 300K by monitoring the change of chemical shift of triazole proton in the transformation process from the supramolecular polymer state to the self-inclusion state.

For the observation of depolymerization by NMR, the characteristic resonances of the polymer at δ 8.67-8.21 ppm diminished until it disappeared, while the characteristic resonances of the monomer at δ 8.52 and 8.17 ppm occurred. Therefore, when the broad peak (8.67-8.21 ppm) of the triazole group is only present then we consider that all the monomer is assembled, namely 0% of monomer, as in the initial ¹H-NMR spectrum of compound (12); when the signal of the triazole group is completely split into two sharp peaks with a chemical shift of 0.35 ppm (8.52 ppm and 8.17 ppm, respectively) then all the monomer is self-included and therefore not assembled, namely 100% of monomer. The conversion ratio could be assessed by comparing the integration of the triazole proton of monomer to the sum of the triazole protons of monomer and polymer on the ¹H-NMR spectrum over time and was translated into the percentage of monomer. The formula is below:

$$\% \text{ self-included monomer} = \left[\frac{\text{integration area of monomer}}{\text{total integration area of (monomer + polymer)}} \right] \times 100\%$$

It was worth noting that values might have some inaccuracy. The peaks of the triazole group in the ¹H-NMR were difficult to accurately integrate, especially since very small and large peaks had to be compared. Furthermore, this quantitative analysis by the NMR technique followed with an assumption should be explicitly acknowledged. It was assumed that the polymer in which depolymerization occurred was only converted into self-included conformer. Two examples of these estimations were shown in Figures 77: (1) setting the integration area of triazole proton derived from the polymer to 2 when is shown separation integrals among polymer peak and monomer peaks (above in Figure 77); (2) setting the integration area of triazole proton derived from the part of monomer to 1 when is shown an overlap integral between polymer peak and a monomer peak (below in Figure 77).

CHAPTER 3 STUDY OF SUPRAMOLECULAR ASSEMBLIES BASED ON BETA-CYCLODEXTRIN-ADAMANTANE IN AQUEOUS SOLUTION

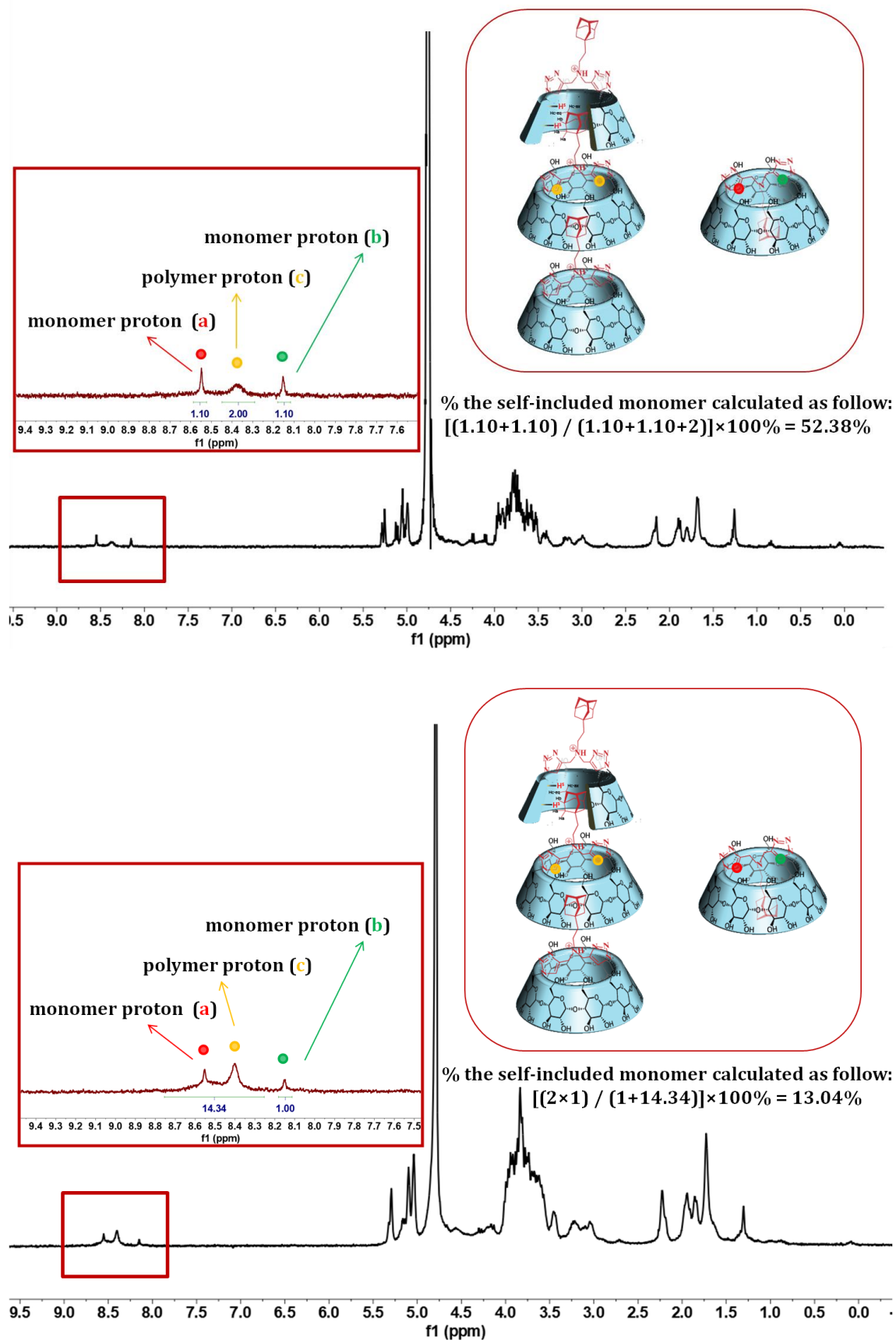


Figure 77: The ^1H -NMR spectra of compound (12) at 1.48 mM (above) and at 5 mM (below).

Concentration effect on the depolymerization of compound (12) was first studied. The studies of the assembly variation were carried out at 0.5 mM, 0.76 mM, 1.48 mM and 5 mM, respectively. Four plots of the percentage of monomer versus depolymerization time were made and displayed in Figure 78 (Appendix 1 and 2). We noticed that the depolymerization process for 0.5 mM solution reached completion in only 250 min. By comparison, even after 9780 min (almost one week) the depolymerization from polymer to monomer for 1.48 mM solution was not complete and around 5.43% of polymer remained. The 10-fold more concentrated solution exhibited great stability where just around 6.43% of the polymer was converted into monomer at one measurement point ($t = 5760$ min). Depolymerization was therefore dependent on the concentration.

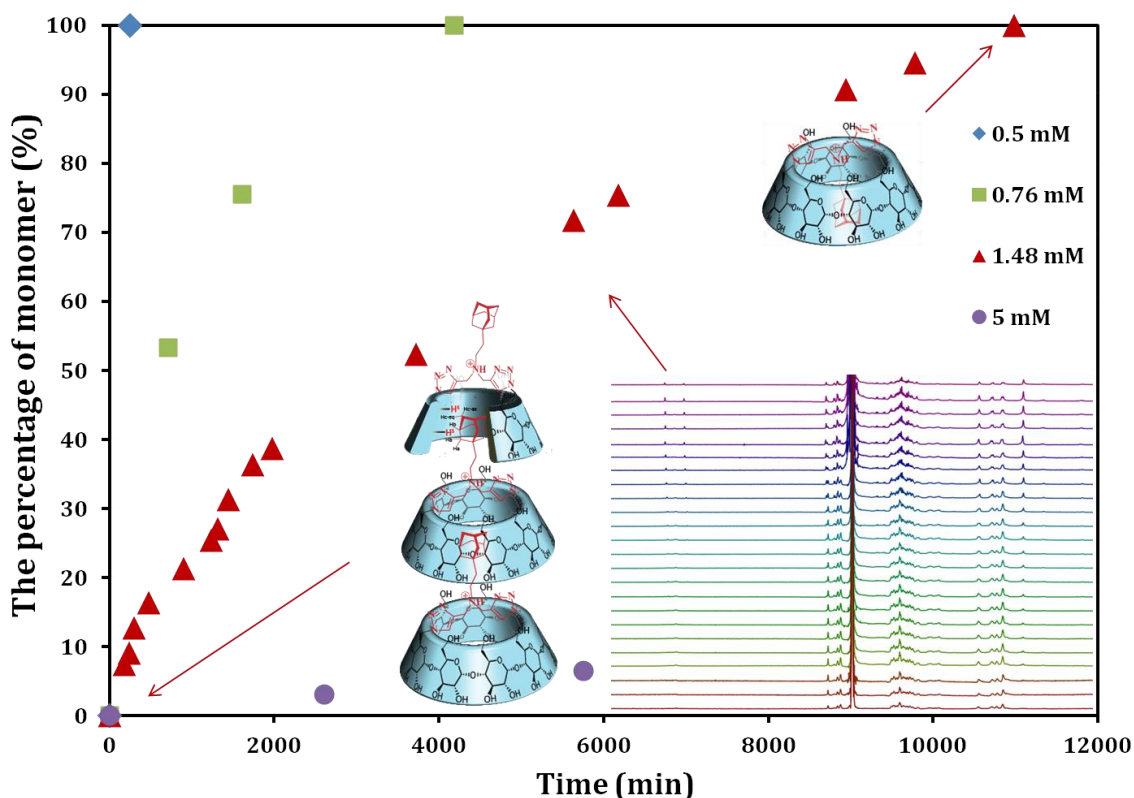


Figure 78: Time-conversion curves for depolymerization of supramolecular polymer formed by monomer (12) following different concentrations (inset: $^1\text{H-NMR}$ spectra of the solution at 1.48 mM over time).

Besides, this depolymerization behavior could also be accelerated with a base. In order to easily track the percentage of self-included monomer obtained by depolymerization, a 5 mM solution was chosen to systematically study in more detail at different equivalents of NaOD. The experiments were carried out on the 5 mM solution of monomer (12) with 0.15

CHAPTER 3 STUDY OF SUPRAMOLECULAR ASSEMBLIES BASED ON BETA-CYCLODEXTRIN-ADAMANTANE IN AQUEOUS SOLUTION

equivalents, 0.2 equivalents and 0.5 equivalents of NaOD, respectively. The results were summarized in Figure 79 (Appendix 3, 4, 5 and 6). The experiment performed in the absent of NaOD was shown as a reference.

The supramolecular polymer composed of monomer (12) with the base provided a higher depolymerization rate, while the self-included conformer was more favored under such conditions. Time-dependent depolymerization process in the presence of varying equivalents of NaOD suggested that the higher the base concentrations, the faster the conversion to the self-inclusion state. In other words, the result implied that the base effect stimulated the conformational change of the monomer (12).

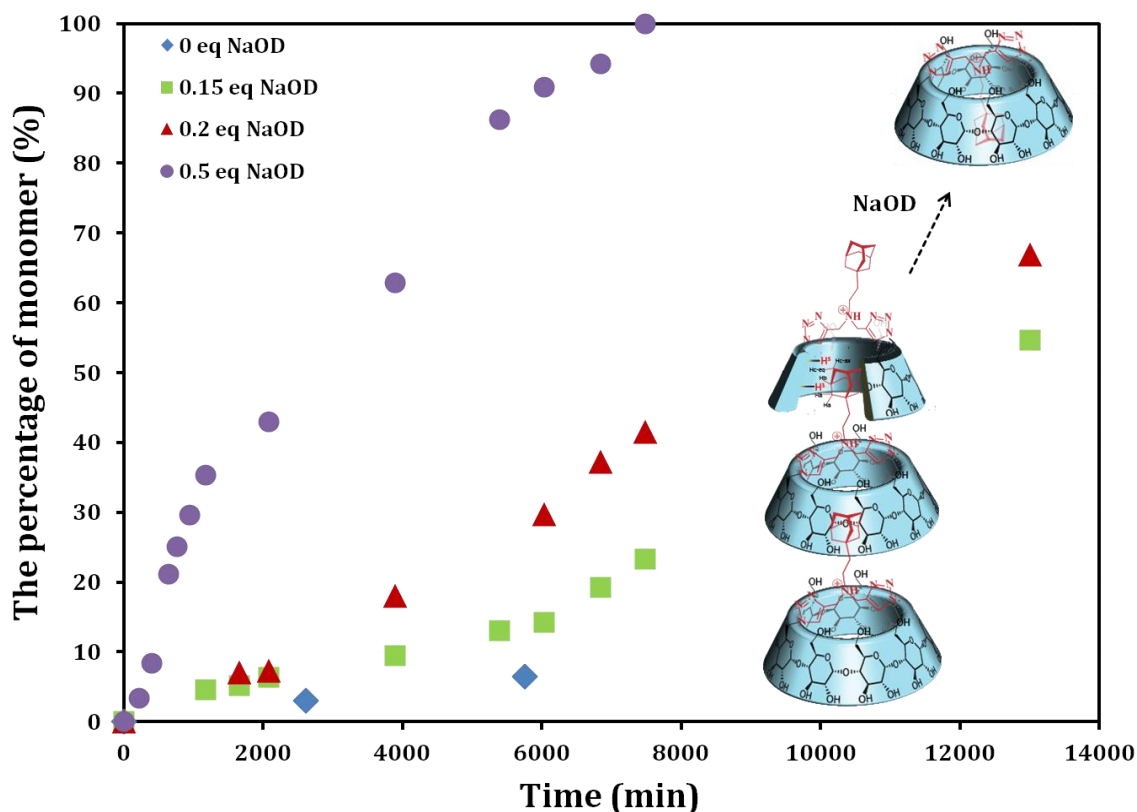


Figure 79: Time-conversion curves for depolymerization of supramolecular polymer formed by monomer (12) at a certain concentration (5 mM) following different equivalents of NaOD.

We further added 0.15 equivalents of NaOD into a series of different concentrations of monomer (12) solutions, and as expected, a faster self-inclusion was observed with a lower concentration of monomer (12) solution (Figure 80, Appendix 7, 8 and 9).

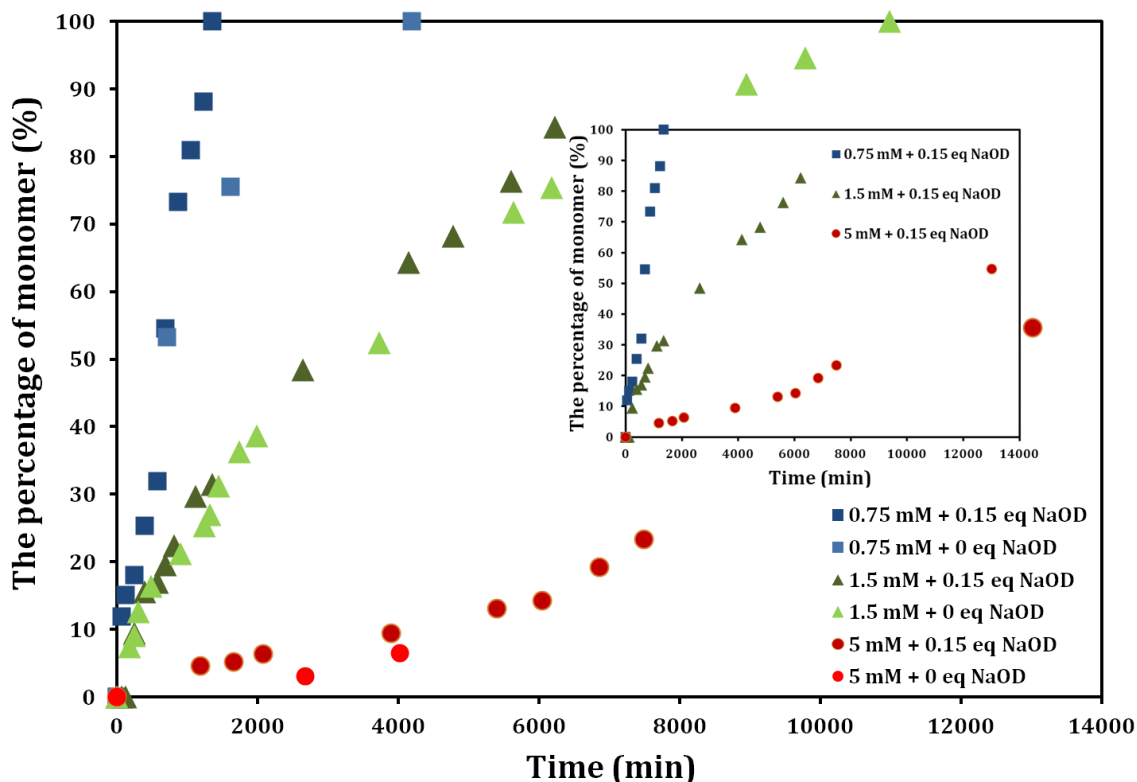


Figure 80: Time-conversion curves for depolymerization of supramolecular polymer formed by monomer (12) following different concentration in the presence of 0.15 equivalents of NaOD (inset: highlight the base effect).

Hence, it was worth investigating how to inhibit the depolymerization of polymers into self-included monomers. Acidic experiments attempted to struggle against the temporally controlled supramolecular organization of monomer (12). The experiments were performed on the monomer (12) solutions at 0.5 mM, 0.75 mM, 1.5 mM and 5 mM, respectively. These solutions in the presence of 3 equivalents of TFA were tracked by the $^1\text{H-NMR}$ experiment over a period of one week. The observation showed that even if 0.5 mM solution that completed the 100% conversion in 250 min was in a stable supramolecular polymer state under the acid condition, let alone a higher concentration of the solution. This result complied that the acid effect allowed the depolymerization process to slow down.

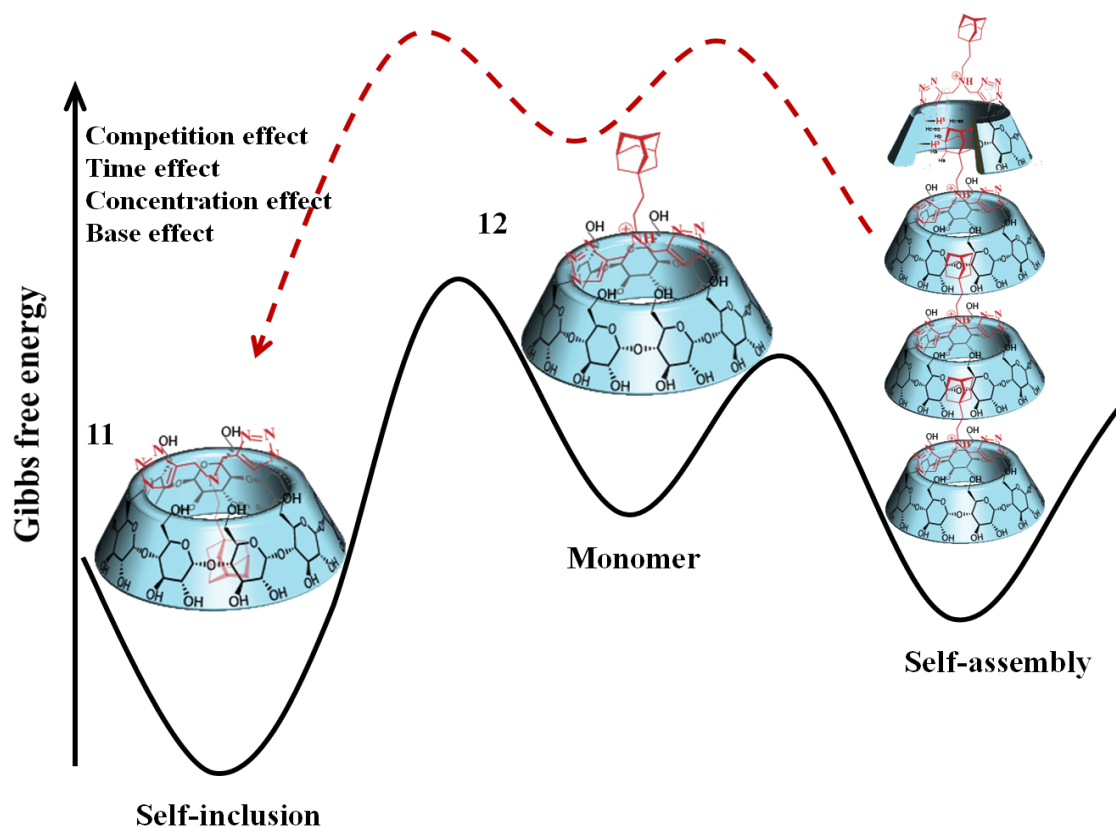


Figure 81: Schematic diagram of energetic pathway of supramolecular polymerization.

These results indicated that the supramolecular polymer was sensitive to both concentration and pH. The very high stability of the self-included conformer made the polymer meta-stable. The formation of supramolecular polymer might be ascribed to a combination of thermodynamics and kinetics factors ^{[21] [139] [140] [141] [142]}. So the possible explanation for the controlled supramolecular organization was that the monomer (12) was kinetically self-assembling, but thermodynamically driven to self-inclusion. The role of the pH had to be elucidated though, as self-inclusion seemed easier at fine pH (Figure 81).

3. Conclusion

The behaviors of the self-assembly of the synthesized β -cyclodextrin derivatives have been characterized by ¹H-NMR, NMR-ROESY, NMR-DOSY, ITC, viscosity and DLS. Three of them overcome the problem of the formation of self-inclusion in aqueous solution. Besides, one of three compounds is able to form a liner polymer up to 22 repeat units. We now have to operate the transfection study to confirm the ability of our designed molecule to act as transfection agents. Meanwhile, the self-inclusion can still be obtained even with the bridge.

Factors affecting the formation of the self-inclusion versus the supramolecular polymer are examined. Apart from a depolymerization caused by a competitive guest, we also observe depolymerizations with concentration and pH variation. The bases accelerate the transformation process and vice versa. This transformation process is almost irreversible.

CHAPTER 4

GENERAL CONCLUSION AND PERSPECTIVE

1. General Conclusion

Gene therapy is a potential method to treat certain disorders by replacing or altering the defective genes with normal ones. Gene condensation is the essential precondition to transferring genes into a target position, so the ability to pack large nucleic acid plasmids is critical to the design of a potential gene vector.

This thesis aimed to a higher degree of polymerization of supramolecular polymer employing host-guest interaction as the driving force, thereby showing great potential to act as a candidate for condensation and gene delivery.

To this goal, we prepared di-triazole-bridged β -cyclodextrin derivatives which contained an adamantane group to perform the primary host-guest interaction. In view of their interaction with genes, a cationic group was introduced. Furthermore, in this cyclodextrin/adamantane system, a sugar moiety was employed in order to perform more biological functions. The self-assembling capacity of three compounds was studied by $^1\text{H-NMR}$, NMR-ROESY, NMR-DOSY, ITC, viscometry and DLS. These studies confirmed the formation of supramolecular polymers of the three compounds. The goal was almost halfway done. We now have to test the ability to complex genes.

According to literature ^[130], the bridging could address all problems hindering the construction of supramolecular polymers. However, the self-inclusion compound was surprisingly still obtained with the present bridging strategy. The factors influencing self-inclusion versus supramolecular polymer formation were estimated. Apart from the depolymerization caused by a competitive guest ^{[134] [130] [143] [144] [145]}, we also obtained a depolymerization at lower concentration of monomer in short time. Moreover, the addition of a base accelerated the transformation process and vice versa. This transformation process was almost irreversible due to high stability of the self-included conformer.

2. Perspectives

As mentioned above, the bridge connecting the diametrically opposite sugar units of cyclodextrin didn't completely block the hydrophobic moiety outside of the cavity of the cyclodextrin, forcing it across the secondary rim of the cyclodextrin of another monomer to form self-assembled supramolecular polymer. Introduction a Y-shaped bridge to completely prevent the self-inclusion process was attempted. We carried out the synthesis of the compounds shown in Figure 82. We performed a click reaction in the presence of chlorinated alkyne (37) to obtain compound (38). It was reacted with DIBAL-H mediated debenzoylation reaction, giving compound (39) in 56% yield. However, there was some problem in attaching the adamantyl group by the reductive reaction, the Y-shaped bridge β -cyclodextrin derivative have not yet synthesized.

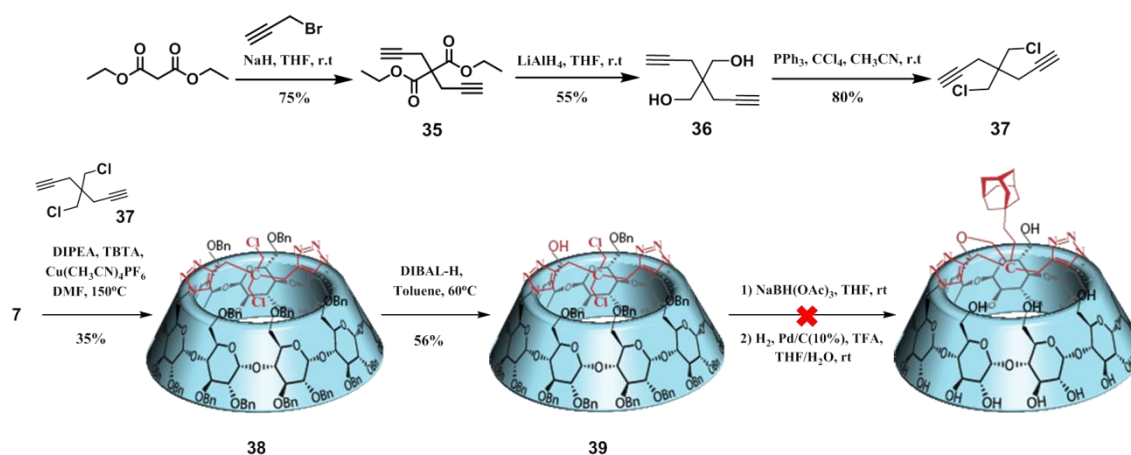
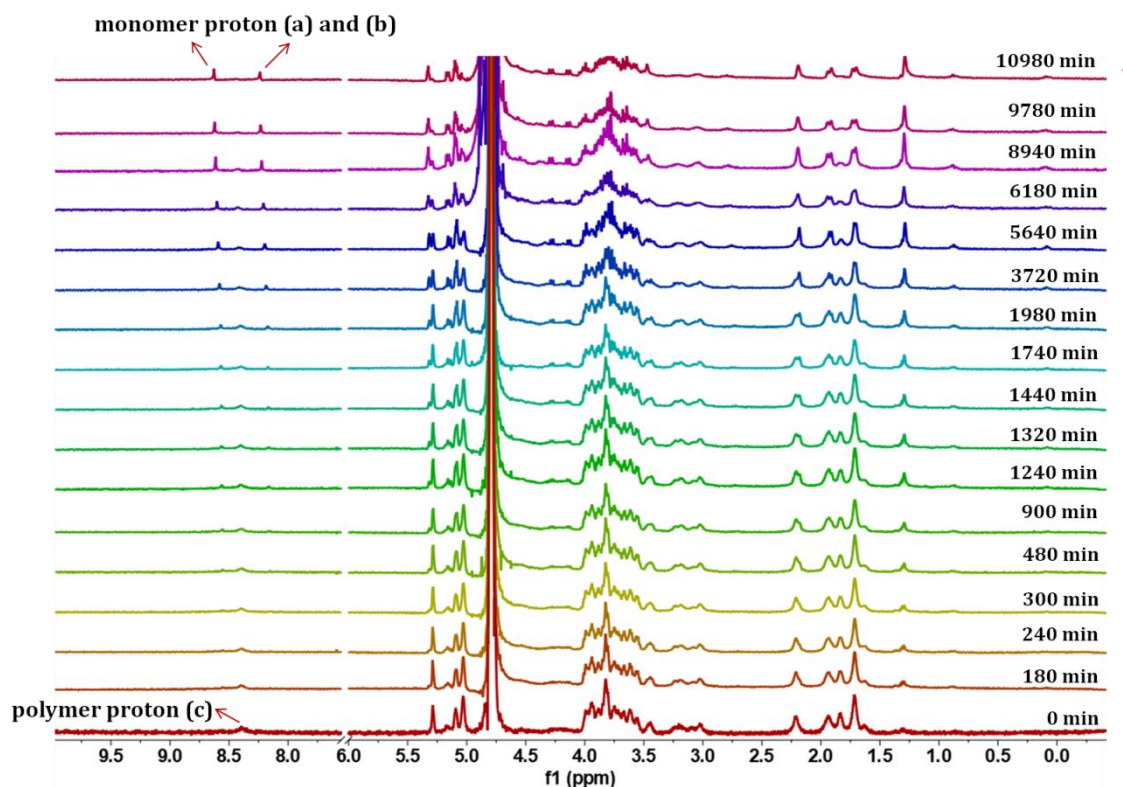


Figure 82: Synthesis of Y-shaped bridged β -cyclodextrin derivative.

APPENDIX

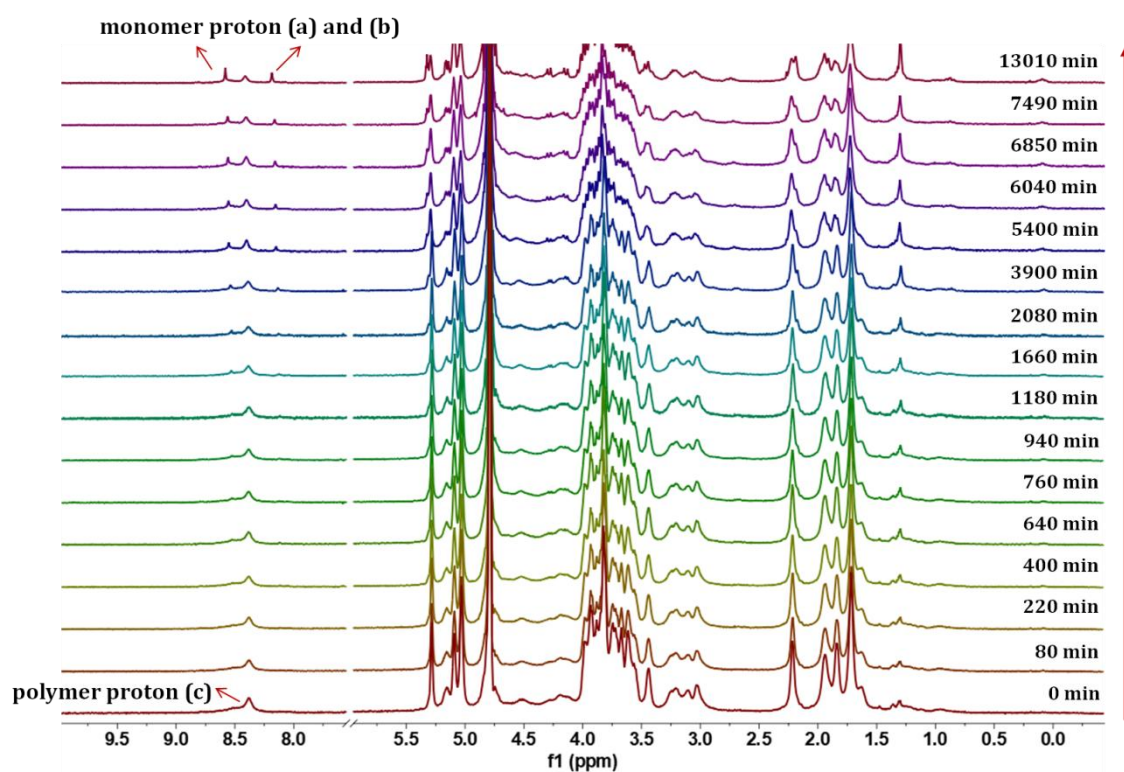
Appendix

Appendix 1: Time-dependent ^1H -NMR spectra of compound (12) in D_2O at 1.48 mM.

0.5 mM						
Time (min)	Integral a	Integral b	Integrals (a+b)	Total integrals (a+b+c)	% monomer	
0	0	0	0	2	0	
250	1	1	2	2	100	
0.76 mM						
Time (min)	Integral a	Integral b	Integrals (a+b)	Total integrals (a+b+c)	% monomer	
0	0	0	0	2	0	
710	1.15	1.13	2.28	4.28	53.27	
1610	3.10	3.08	6.18	8.18	75.55	
4190	1	1	2	2	100	
1.48 mM						
Time (min)	Integral a	Integral b	Integrals (a+b)	Total integrals (a+b+c)	% monomer	
0	0	0	0	2	0	
180	0.08	0.08	0.16	2.16	7.41	
240	0.10	0.10	0.20	2.20	9.09	
300	0.15	0.14	0.29	2.29	12.66	
480	0.19	0.20	0.39	2.39	16.32	
900	0.27	0.26	0.53	2.53	21.26	
1240	0.34	0.34	0.68	2.68	25.37	
1320	0.38	0.36	0.74	2.74	27.01	
1440	0.46	0.45	0.91	2.91	31.27	
1740	0.57	0.57	1.14	3.14	36.31	
1980	0.63	0.63	1.26	3.26	38.65	
3720	1.10	1.10	2.20	4.20	52.38	
5640	2.54	2.54	5.08	7.08	71.75	

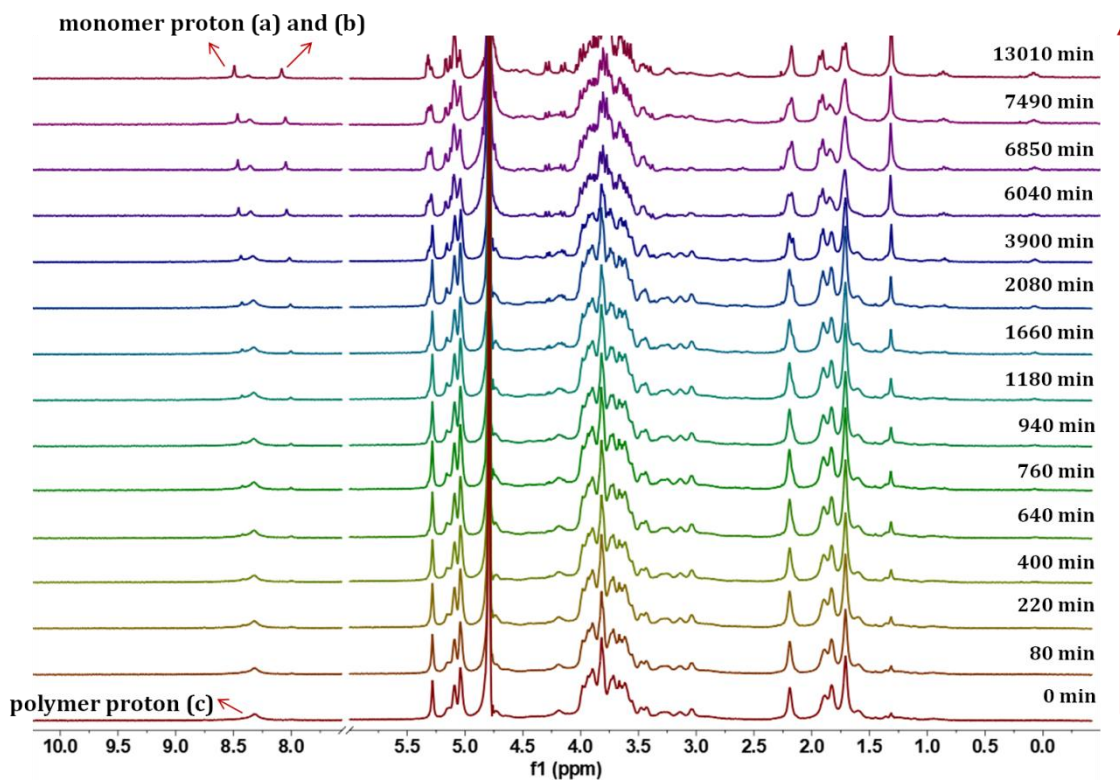
6180	3.08	3.06	6.14	8.14	75.43
8940	9.76	9.76	19.52	21.52	90.71
9780	17.38	17.43	34.81	36.81	94.57
10980	1	1	2	2	100
5 mM	Integral b	Integral (2×b)	Integrals (a+c)	Total integrals (a+b+c)	% monomer
Time (min)					
0	0	0	2	2	0
2610	0.03	0.06	1.94	1.97	3.05
5760	0.08	0.16	2.41	2.49	6.43

Appendix 2: Details of the percentage of monomer in compound (12) solution at different concentration during depolymerization.

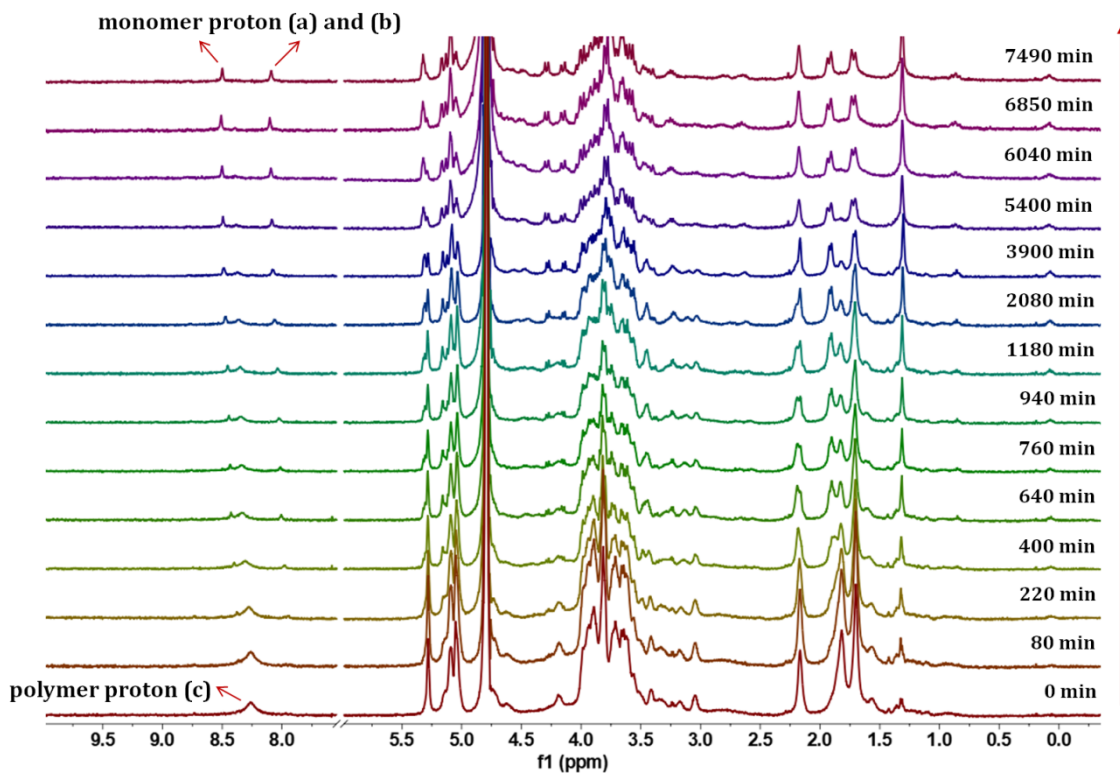


Appendix 3: Time-dependent $^1\text{H-NMR}$ spectra of compound (12) in D_2O at 5 mM in the presence of 0.15 equivalents NaOD.

APPENDIX



Appendix 4: Time-dependent $^1\text{H-NMR}$ spectra of compound (12) in D_2O at 5 mM in the presence of 0.2 equivalents NaOD.

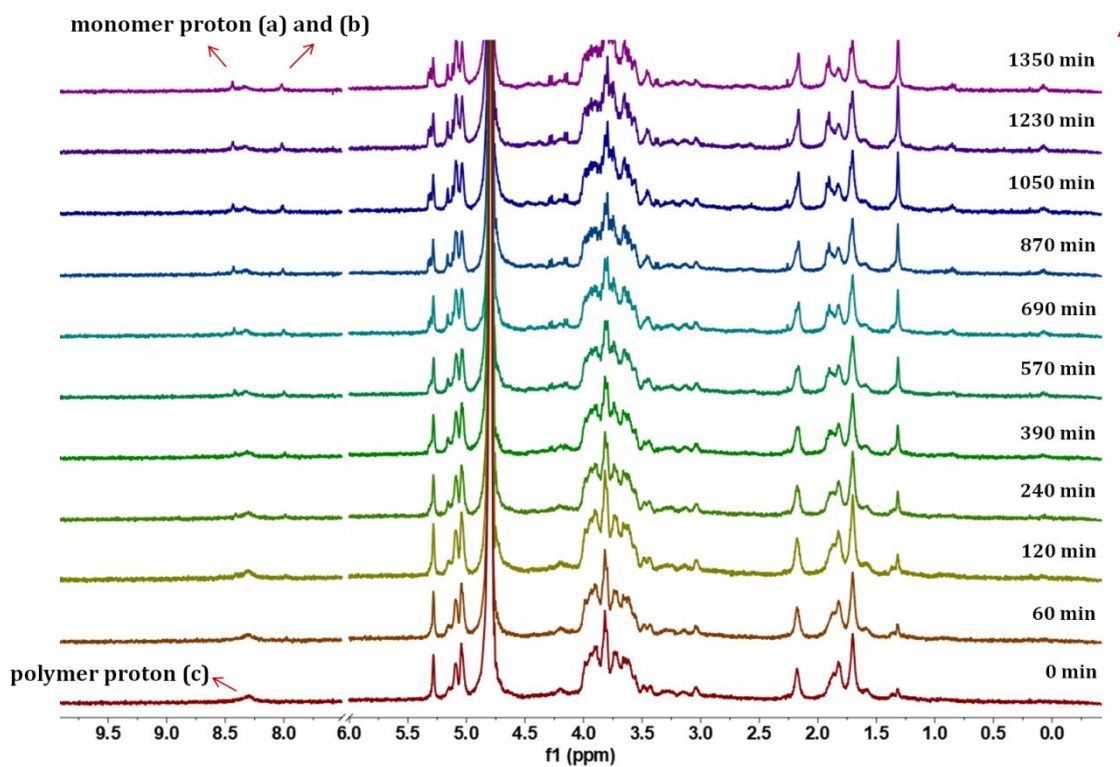


Appendix 5: Time-dependent $^1\text{H-NMR}$ spectra of compound (12) in D_2O at 5 mM in the presence of 0.5 equivalents NaOD.

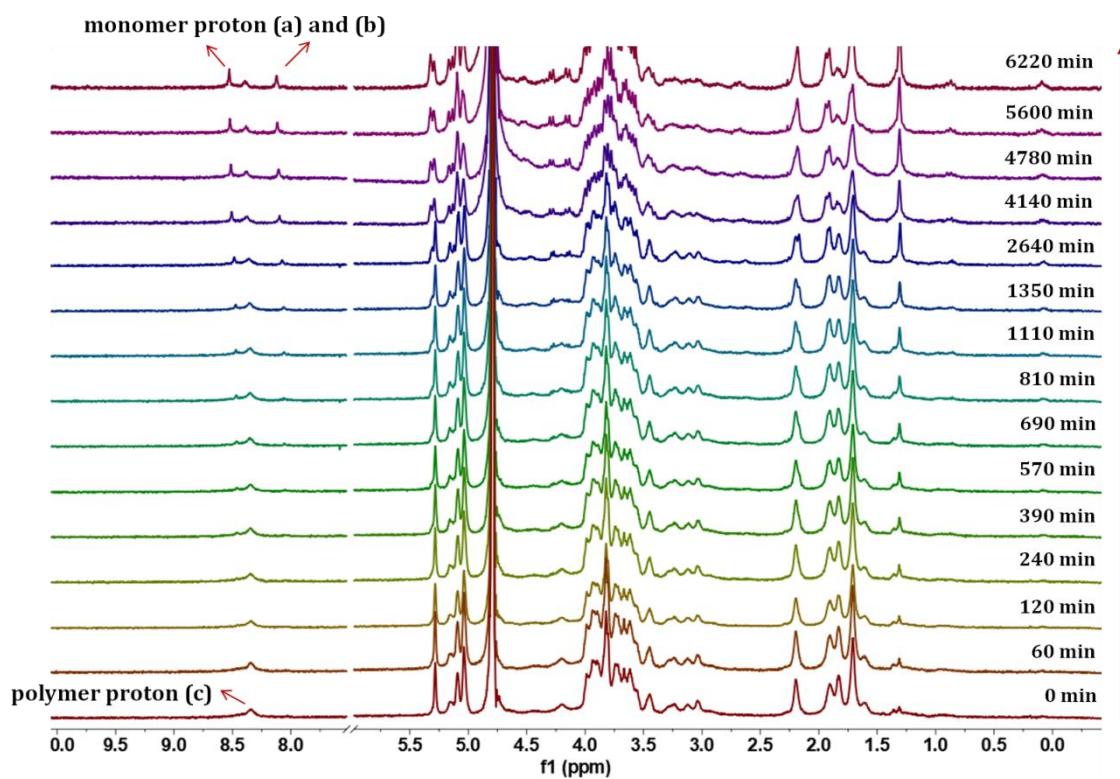
0.15 eq NaOD		Integral b	Integral (2×b)	Integrals (a+c)	Total integrals (a+b+c)	% monomer
Time (min)						
0	0	0	0	2	2	0
80	0	0	0	2	2	0
220	0	0	0	2	2	0
400	0	0	0	2	2	0
640	1	1	2	59.93	60.93	3.28
760	1	1	2	55.02	56.02	3.57
940	1	1	2	46.15	47.15	4.24
1180	1	1	2	42.72	43.72	4.57
1660	1	1	2	37.86	38.86	5.15
2080	1	1	2	30.55	31.55	6.34
3900	1	1	2	20.25	21.25	9.41
5400	1	1	2	14.34	15.34	13.04
6040	1	1	2	13.01	14.01	14.28
6850	1	1	2	9.41	10.41	19.21
7490	1	1	2	7.58	8.58	23.31
13010	1	1	2	2.66	3.66	54.65
0.2 eq NaOD		Integral b	Integral (2×b)	Integrals (a+c)	Total integrals (a+b+c)	% monomer
Time (min)						
0	0	0	0	2	2	0
80	0	0	0	2	2	0
220	0	0	0	2	2	0
400	1	1	2	55.88	56.88	3.52
640	1	1	2	53.19	54.19	3.69
760	1	1	2	48.00	49.00	4.08
940	1	1	2	39.62	40.62	4.92
1180	1	1	2	35.26	36.26	5.67
1660	1	1	2	27.33	28.33	7.06
2080	1	1	2	26.16	27.16	7.36
3900	1	1	2	10.12	11.12	17.99
6040	1	1	2	5.73	6.73	29.72
6850	1	1	2	4.37	5.37	37.24
7490	1	1	2	3.81	4.81	41.58
13010	1	1	2	2.02	3.02	66.89
0.5 eq NaOD		Integral b	Integral (2×b)	Integrals (a+c) or (a+b)	Total integrals (a+b+c)	% monomer
Time (min)						
0	0	0	0	2	2	0
80	0	0	0	2	2	0
220	1	1	2	57.42	58.42	3.42
400	1	1	2	22.84	23.84	8.39
640	1	1	2	8.47	9.47	21.12
760	1	1	2	6.97	7.97	25.09
940	1	1	2	5.75	6.75	29.63
1180	1	1	2	4.66	5.66	35.34
2080	1	1	2	3.36	4.66	42.92
3900	1	1	2	2.18	3.18	62.89
5400	6.24	6.24	12.48	12.49	14.49	86.20
6040	9.96	9.96	19.92	19.92	21.92	90.88
6850	16.36	16.36	32.72	32.72	34.72	94.24
7490	1	1	2	2	2	100

Appendix 6: Details of the percentage of monomer in 5 mM solution of compound (12) with different equivalents NaOD during depolymerization.

APPENDIX



Appendix 7: Time-dependent ^1H -NMR spectra of compound (12) in D_2O at 0.75 mM in the presence of 0.15 equivalents NaOD.



Appendix 8: Time-dependent ^1H -NMR spectra of compound (12) in D_2O at 1.5 mM in the presence of 0.15 equivalents NaOD.

0.75 mM					
0.15 eq NaOD	Integral b	Integral (2×b)	Integrals (a+c)	Total integrals (a+b+c)	% monomer
Time (min)					
0	0	0	2	2	0
60	1	2	15.81	16.81	11.90
120	1	2	12.31	13.31	15.03
240	1	2	10.10	11.10	18.02
390	1	2	6.89	7.89	25.35
570	1	2	5.26	6.26	31.95
690	1	2	2.67	3.67	54.50
870	1	2	1.73	2.73	73.26
1050	1	2	1.47	2.47	80.97
1230	1	2	1.27	2.27	88.11
1350	1	2	2	2	100
1.5 mM					
0.15 eq NaOD	Integral b	Integral (2×b)	Integrals (a+c)	Total integrals (a+b+c)	% monomer
Time (min)					
0	0	0	2	2	0
60	0	0	2	2	0
120	0	0	2	2	0
240	1	2	20.18	21.18	9.44
390	1	2	11.88	12.88	15.53
570	1	2	10.78	11.78	16.98
690	1	2	9.21	10.21	19.59
810	1	2	7.92	8.92	22.42
1110	1	2	5.75	6.75	29.63
1350	1	2	5.37	6.37	31.40
2640	1	2	3.13	4.13	48.43
4140	1	2	2.11	3.11	64.31
4780	1	2	1.93	2.93	68.26
5600	1	2	1.62	2.62	76.34
6220	1	2	1.37	2.37	84.39

Appendix 9: Details of the percentage of monomer in compound (12) solution with different concentration in the presence of 0.15 equivalents of NaOD during depolymerization.

EXPERIMENTAL PART

1. General Procedures

Reactants were purchased from commercial sources and used without further purification. The solvents were freshly distilled by standard methods: Dichloromethane from P₂O₅, THF from sodium/benzophenone, toluene, DMF and triethylamine were dried over molecular sieves. Thin Layer Chromatographies (TLC) was performed on Merck silica gel 60 F 254 and revealed with a UV lamp ($\lambda = 254$ nm) and KMnO₄, cerium molybdate or sulphuric acid staining. Flash Column Chromatographies were conducted on silica Geduran[®] Si 60Å (40–63 μ m) or silica Geduran[®] Si 60Å (63–200 μ m).

The CombiFlash Rf system was performed by injecting 5 mL of the filtered aqueous extract onto a RediSep Rf Gold C-18 reversed-phase column (20-40 μ m). Elution was performed by using pumps to deliver a constant flow rate of 20 mL/min. The solvent system consisted of acetonitrile (CH₃CN) and water always started with 0% of CH₃CN for 3 min to desalt the media then a specified gradient was applied for different product. The compounds including phenyl group were detected by UV at 210 nm.

High-Resolution Mass Spectrometry (HRMS) were recorded on a Bruker micrOTOF spectrometer, using Agilent ESI-L Low Concentration Tuning-Mix as reference.

Infrared (IR) spectra were recorded on a Bruker Tensor 27 (ATR diamond) spectrophotometer.

NMR spectra were recorded on a Bruker Avance II 600 MHz or Bruker AM-400 MHz using residual solvent signal as internal reference. Assignments of the signals were done using Heteronuclear Single Quantum Coherence spectroscopy (HSQC), Heteronuclear Multiple Bond Correlation (HMBC), COrrrelation SpectroscopY (COSY), TOtal Correlation SpectroscopY (TOCSY), Nuclear Overhauser Effect SpectroscopY (NOESY), Transverse Rotating-frame Overhauser Enhancement SpectroscopY (T-ROESY). Chemical shifts (δ) were reported in ppm and coupling constants (J) were given in Hertz (Hz).

DOSY NMR diffusion experiment was performed by using the using bipolar longitudinal eddy current delay with gradients (LEDBPGP) sequence. Spectra were acquired with gradient pulses (δ) of 2 ms ranging in strength from 0.28 to 5.26 g/mm for the BBFO 5 mm NMR probe. A diffusion delay from 50 to 200 ms was set and diffusion coefficients (D) were calculated from mono-exponential decays using Bruker Topspin 3.0 software.

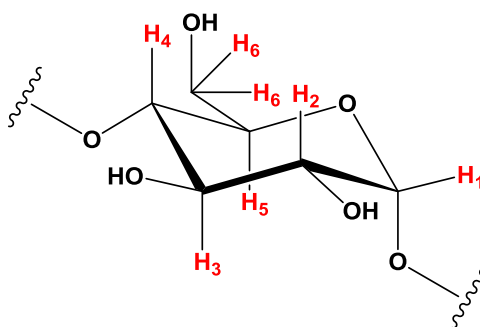
Isothermal Titration Calorimetry (ITC) experiments were recorded at 20 °C with a VP-ITC instrument from Malvern Instruments. The results were analyzed by “Origin for ITC” instrument software supplied with VP-ITC Microcalorimeter.

Viscosimetry experiments were performed at 20 °C on an automatic Anton-PaarAMVn viscometer using a capillary with an inner diameter of 1.6 mm containing a 1.5 mm diameter of the ball. The six times of falling time of the ball for each sample were recorded at a tilted angle (20 °). The corresponding average flow time of water was converted into the relative viscosity.

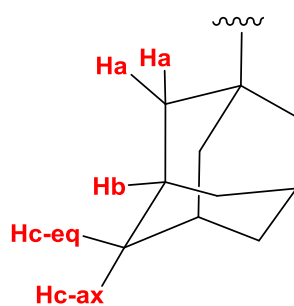
Dynamic Light Scattering (DLS) experiments were recorded on Malvern Zetasizer Nano S90 with a 5 mW He-Ne laser at a wavelength of 633 nm and a Peltier temperature controller to measure the particle size distribution of the objects in solution.

2. Nomenclature For Protons:

Cyclodextrin carbohydrate unit:

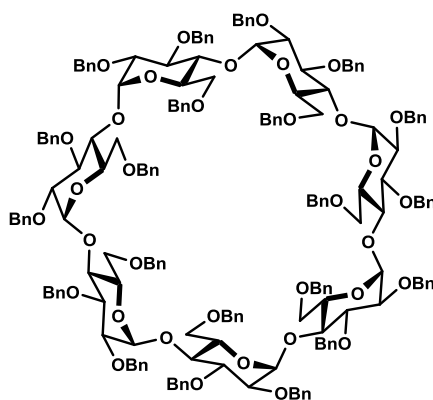


Adamantyl moiety:



3. Synthesis

2^{A-G}, 3^{A-G}, 6^{A-G}-per-O-Benzyl- β -cyclodextrin (1)



Chemical Formula: C₁₈₉H₁₉₆O₃₅
Exact Mass: 3025.3557

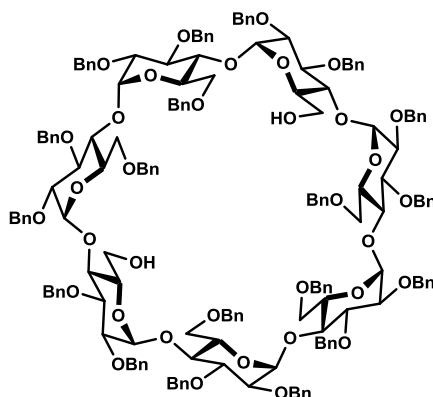
Before being used the β -cyclodextrin was lyophilized overnight. NaH (7.46 g, 310 mmol, 42 eq) (60% w/w) was added portionwise to a stirred solution of dried β -cyclodextrin (8.4 g, 7.4 mmol, 1 eq) in DMSO (150 mL) at room temperature under argon. Then benzyl chloride (36 mL, 310 mmol, 42 eq) was added dropwise over 2 h. The reaction was followed by TLC, and finished overnight. The mixture was neutralized by MeOH (10 mL) added carefully and was diluted with water (300 mL). The aqueous phase was extracted by diethyl ether (3×150 mL), and the combined organic layers were dried over MgSO₄, filtered and concentrated in vacuo. The residue was purified over silica gel chromatography (cyclohexane/EtOAc 98:2 then 5:1 then 3:1) to afford perbenzylated β -cyclodextrin 1 (16.9 g, 96% yield) as the white foam.

The structure of the product was confirmed by comparison with the literature ^[118].

EXPERIMENTAL PART

6^A, 6^D-Dideoxy-6^A, 6^D-diol-

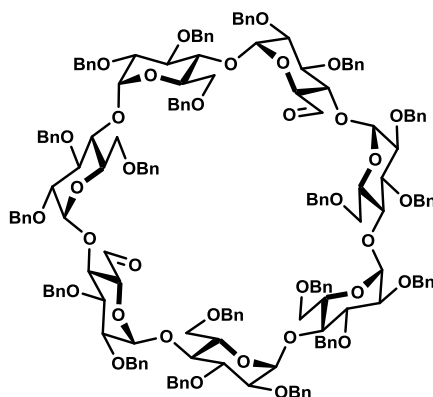
2^{A-G}, 3^{A-G}, 6^B, 6^C, 6^E, 6^F, 6^G-nonadeca-O-benzyl-β-cyclodextrin (2)



Chemical Formula: C₁₇₅H₁₈₄O₃₅
Exact Mass: 2845.2618

To a stirred solution of perbenzylated β-cyclodextrin 1 (10 g, 3.3 mmol, 1 eq) in toluene (23 mL) was added DIBAL-H (1.5 M in toluene, 45 mL, 66 mmol, 20 eq) was added dropwise at room temperature. The reaction mixture was heated at 60°C and put under nitrogen flux. The reaction mixture was monitored by TLC (cyclohexane/EtOAc 7:3). The reaction mixture was carefully and slowly poured in an ice/water bath (300mL) while stirring frequently. Ethyl acetate (400 mL) and HCl solution (1 M in water, 150 mL) were then added. The mixture was stirred for 3 h and then the aqueous phase was extracted with ethyl acetate (3×400 mL), and the combined organic layers were washed with brine, dried over MgSO₄, filtered and concentrated under vacuum. The residue was purified over silica gel chromatography (cyclohexane/EtOAc 3:1) to afford diol 2 (7.05 g, 75% yield) as the white foam.

The structure of the product was confirmed by comparison with the literature [146].

6^A, 6^D-Dideoxy-6^A, 6^D-dialdehyde-**2^{A-G}, 3^{A-G}, 6^B, 6^C, 6^E, 6^F, 6^G-nonadeca-O-benzyl-β-cyclodextrin (3)**

Chemical Formula: C₁₇₅H₁₈₀O₃₅
Exact Mass: 2841.2305

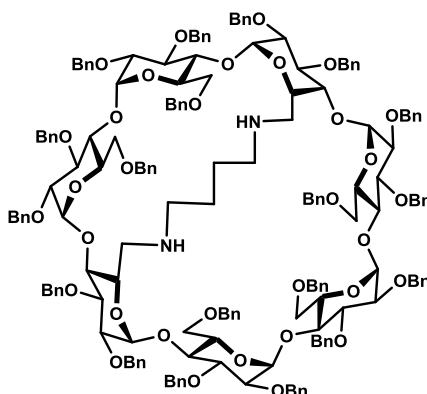
Oxalyl dichloride (3 mL, 35.5 mmol, 10 eq) was dissolved in DCM (30 ml) under argon atmosphere at -78°C. A solution of (methylsulfinyl)methane (5 mL, 70.4 mmol, 20 eq) in DCM (30 mL) was added dropwise to the cooled solution for about 30 min. Then, the reaction mixture was stirred about 30 min. Diol β-cyclodextrin 2 (10.5 g, 3.69 mmol, 1 eq) was dissolved in DCM (40 mL) and was added slowly to the above solution. After stirred 1h30min, triethylamine (10 mL, 72.1mmol, 20 eq) was added. And the solution was stirred overnight and warmed slowly to room temperature. The reaction progress was monitored by TLC. Finally, the solution was quenched with H₂O (300 mL). The reaction solution was diluted in DCM and the aqueous phase was extracted with DCM (3×200 mL), and the combined organic layers were washed with water, dried over MgSO₄, filtered and concentrated in vacuo. The residue was purified over silica gel chromatography (cyclohexane/EtOAc 4:1) to afford dialdehyde β-cyclodextrin 3 (8.39 g, 80% yield) as the white foam.

The structure of the product was confirmed by comparison with the literature ^[147].

EXPERIMENTAL PART

6^A, 6^D-Dideoxy-6^A, 6^D-diamino-N, N'-butyl-

2^{A-G}, 3^{A-G}, 6^B, 6^C, 6^E, 6^F, 6^G-nonadeca-O-benzyl-β-cyclodextrin (4-a)

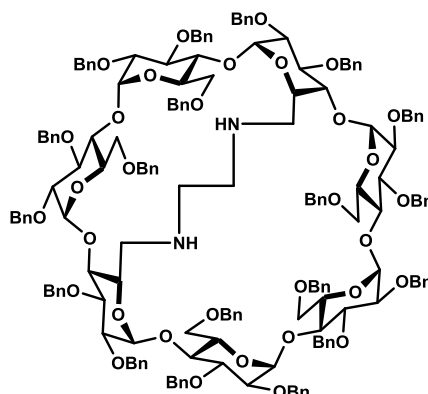


Chemical Formula: C₁₇₉H₁₉₂N₂O₃₃
Exact Mass: 2897.3407

To a solution of dialdehyde β-cyclodextrin 3 (1.1 g, 0.387 mmol, 1 eq) in dry DCM (20 mL) was added butane-1,4-diamine (50 μL, 0.477 mmol, 1.2 eq) at room temperature under nitrogen, and the mixture was stirred for 2 h. NaBH(OAc)₃ (0.418 g, 1.97 mmol, 5 eq) was added and the mixture was stirred for 3 h. AcOEt (70 mL) and the saturated aqueous solution of NaHCO₃ (70 mL) were then added. The mixture was stirred for 30 min and then the aqueous phase was extracted with ethyl acetate (3×70 mL), and the combined organic layers were washed with the saturated aqueous solution of NaHCO₃, brine, dried over MgSO₄, filtered and concentrated in vacuo. The residue was purified over silica gel chromatography (cyclohexane/EtOAc 4:1 then 3:2) to afford bridged diamine β-cyclodextrin 4-a (0.64 g, 57% yield) as the white foam.

The structure of the product was confirmed by comparison with the literature [130].

**6^A, 6^D-Dideoxy-6^A, 6^D-diamino-N, N'-ethyl-
2^{A-G}, 3^{A-G}, 6^B, 6^C, 6^E, 6^F, 6^G-nonadeca-O-benzyl-β-cyclodextrin (4-b)**



Chemical Formula: C₁₇₇H₁₈₈N₂O₃₃
Exact Mass: 2869.3094

Dialdehyde β-cyclodextrin 3 (390 mg, 0.137 mmol, 1 eq) was dissolved in DCM (15 mL). Ethylenediamine (10 μL, 0.149 mmol, 1.1 eq) was added and the mixture was stirred for 2 h. NaBH(OAc)₃ (145 mg, 0.686 mmol, 5 eq) was added and the mixture was stirred for 3 h. A saturated solution of NaHCO₃ (70 mL) and ethyl acetate (70 mL) were added and the mixture was stirred for 30 min. The aqueous phase was extracted with ethyl acetate (3×70 mL), and the combined organic layers were washed with the saturated aqueous solution of NaHCO₃, brine, dried over MgSO₄, filtered and concentrated in vacuo. The obtained residue was purified by silica gel chromatography (cyclohexane/EtOAc 3:1 then 2:1) to give bridged diamine β-cyclodextrin 4-b (230 mg, 58% yield) as the white foam.

¹H NMR (400 MHz, CDCl₃, 300K): δ = 7.41-6.75 (m, 95H, 95×H_{Ph}), 5.82 (d, ³J_{H1-H2} = 4.0 Hz, 1H, 1×H1), 5.36 (d, ²J = 10.8 Hz, 1H, 1×CHH-Ph), 5.31-5.22 (m, 2H, 1×H1, 1×CHH-Ph), 5.21-5.08 (m, 3H, 1×H1, 2×CHH-Ph), 5.05 (d, ²J = 11.2 Hz, 1H, 1×CHH-Ph), 4.83-4.51 (m, 13H, 9×CHH-Ph, 4×H1), 4.48-4.20 (m, 24H, 24×CHH-Ph), 4.14 (dd, ²J_{H6-H6'} = 11.2 Hz, ³J_{H6-H5} = 3.2 Hz, 1H, 1×H6), 4.09-3.77 (m, 22H, 7×H3, 6×H4, 5×H5, 4×H6), 3.74-3.68 (m, 2H, 2×H5), 3.65-3.54 (m, 5H, 1×H4, 4×H6), 3.48-3.22 (m, 9H, 7×H2, 1×H4, 1×H6), 2.98 (d, ³J_{H6-H5} = 13.2 Hz, 1H, 1×H6), 2.85 (d, ³J_{H6-H5} = 11.2 Hz, 1H, 1×H6), 2.65-2.42 (m, 3H, 1×H6, 2×CHH-NH), 2.41-2.21 (m, 3H, 1×H6, 2×CHH-CH₂-NH).

¹³C NMR (100 MHz, CDCl₃, 300K): δ = 129.24-125.53 (95C, CH-Ar), 99.13, 99.01, 98.93, 98.64, 97.88, 97.70, 96.79 (7×C1), 82.07 (C3), 81.46 (C4), 81.12-80.02 (10C, 6×C3, 4×C4), 79.88 (C2), 78.70-77.32 (7C, 1×C4, 6×C2), 76.60-76.22 (4×CH₂-Ph), 75.12 (CH₂-Ph), 74.85 (C4), 74.64 (CH₂-Ph), 73.79-72.39 (13×CH₂-Ph), 72.12-71.59 (5×C5), 70.57 (C5), 70.09 (C5), 69.77 (C6), 69.60 (2×C6), 69.29 (C6), 68.81 (C6), 68.38 (C6), 52.07 (C6), 50.42 (CH₂-NH),

EXPERIMENTAL PART

49.45 (CH₂-NH).

HMRS (ESI): calculated for [C₁₇₇H₁₈₈N₂O₃₃+H]⁺ 2870.3167; found 2870.3151.

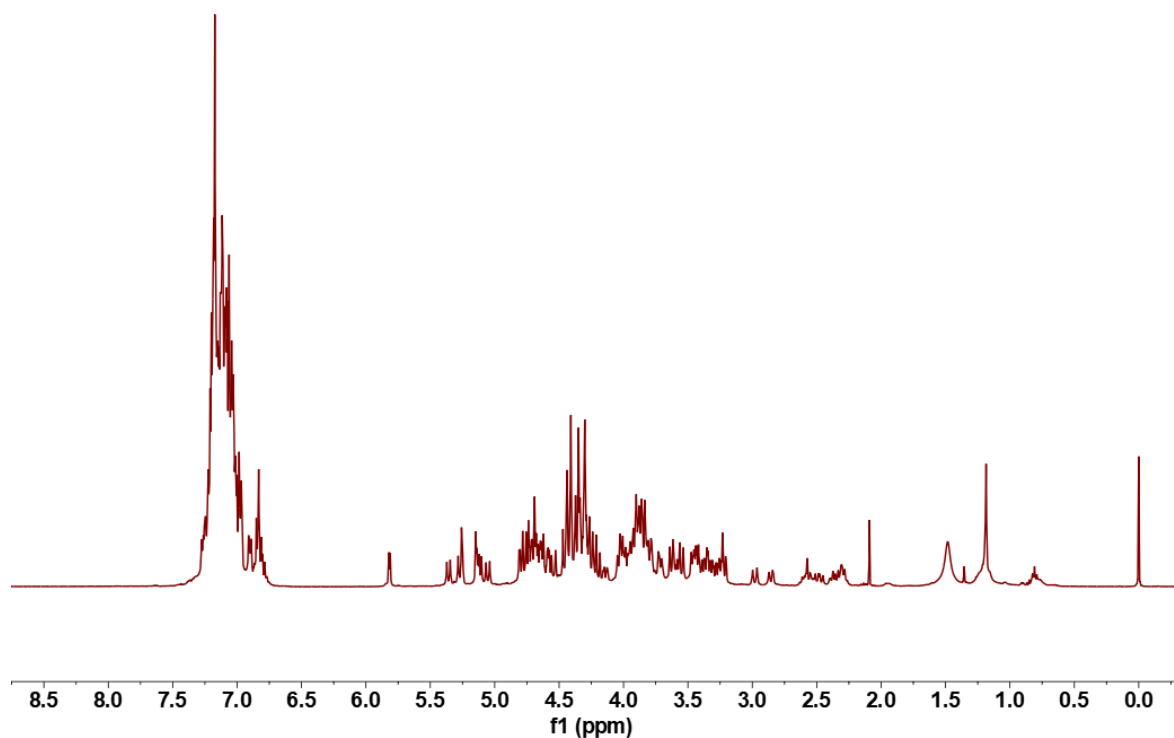


Figure 1: ¹H NMR (400 MHz, CDCl₃, 300K) of compound 4-b

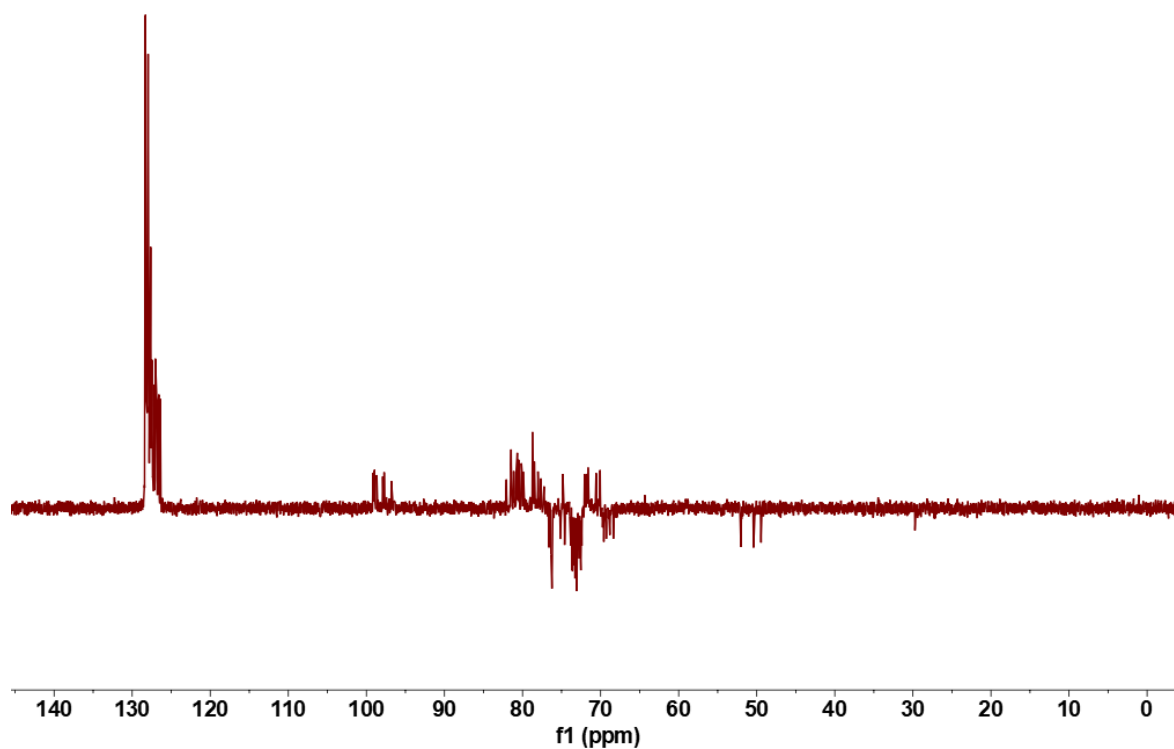
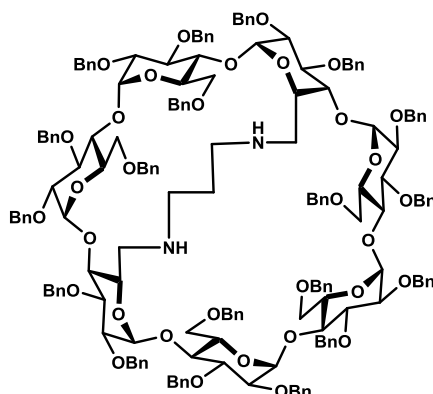


Figure 2: ¹³C NMR-DEPT 135 (100 MHz, CDCl₃, 300K) of compound 4-b

6^A, 6^D-Dideoxy-6^A, 6^D-diamino-N, N'-propyl-**2^{A-G}, 3^{A-G}, 6^B, 6^C, 6^E, 6^F, 6^G-nonadeca-O-benzyl-β-cyclodextrin (4-c)**

Chemical Formula: C₁₇₈H₁₉₀N₂O₃₃
Exact Mass: 2883.3251

To a solution of dialdehyde β-cyclodextrin 3 (361 mg, 0.127 mmol, 1 eq) in dry DCM (15 mL) was added 1,3-diaminopropane (12.7 μL, 0.152 mmol, 1.2 eq) at room temperature under nitrogen, and the mixture was stirred for 2 h. NaBH(OAc)₃ (135 mg, 0.635 mmol, 5 eq) was added and the mixture was stirred for 3 h. Ethyl acetate (70 mL) and the saturated aqueous solution of NaHCO₃ (70 mL) were then added. The mixture was stirred for 30 min and then the aqueous phase was extracted with AcOEt (3×70 mL), and the combined organic layers were washed with the saturated aqueous solution of NaHCO₃, brine, dried over MgSO₄, filtered and concentrated in vacuo. The residue was purified over silica gel chromatography (cyclohexane/EtOAc 4.5:1 then 4:1 then 3:1) to afford bridged diamine β-cyclodextrin 4-c (225 g, 61% yield) as the white foam.

¹H NMR (400 MHz, CDCl₃, 300K): δ = 7.31-6.80 (m, 92H, 92×H_{Ph}), 6.76-6.65 (s, 3H, 3×H_{ph}), 5.69 (d, ³J_{H1-H2} = 4.1 Hz, 1H, 1×H1), 5.63 (d, ³J_{H1-H2} = 4.0 Hz, 1H, 1×H1), 5.39 (d, ²J = 10.8 Hz, 1H, 1×CHH-Ph), 5.26 (d, ²J = 10.8 Hz, 1H, 1×CHH-Ph), 5.18-5.07 (m, 3H, 3×CHH-Ph), 4.86-4.70 (m, 7H, 3×H1, 4×CHH-Ph), 4.70-4.55 (m, 7H, 2×H1, 5×CHH-Ph), 4.55-4.28 (m, 17H, 17×CHH-Ph), 4.28-4.18 (m, 8H, 1×H6, 7×CHH-Ph), 4.13-4.05 (m, 3H, 1×H5, 2×H6), 4.05-3.69 (m, 16H, 7×H3, 4×H4, 5×H5), 3.69-3.26 (m, 14H, 5×H2, 3×H4, 1×H5, 5×H6), 3.24-3.16 (m, 2H, 2×H2), 2.89-2.72 (t, 2H, 1×H6, 1×CHH-NH), 2.60-2.38 (m, 3H, 2×H6, 1×CHH-NH), 2.35-2.19 (m, 3H, 1×H6, 2×CHH-NH), 1.19 (br. m, 2H, 2×CHH-CH₂-NH).

¹³C NMR (100 MHz, CDCl₃, 300K): δ = 128.57-126.65 (95C, CH-Ar), 101.53 (C1), 99.18 (C1), 98.98 (C1), 98.07 (C1), 97.92 (2×C1), 97.90 (C1), 83.12 (2×C4), 81.77-76.95 (20C, 7×C2, 7×C3, 6×C4), 76.44, 76.25, 76.01, 75.72 (4×CH₂-Ph), 73.83-72.34 (15×CH₂-Ph), 72.03-71.77 (5×C5), 69.60 (2×C6), 69.54 (C5), 68.92 (C6), 68.56 (C6), 67.85 (C6), 67.00 (C5), 52.59 (C6),

EXPERIMENTAL PART

51.81 (C6), 46.93 (2×CH₂-NH), 29.91 (CH₂-CH₂-NH).

HMRS (ESI): calculated for [C₁₇₈H₁₉₀N₂O₃₃+H]⁺ 2884.3324; found 2884.3391.

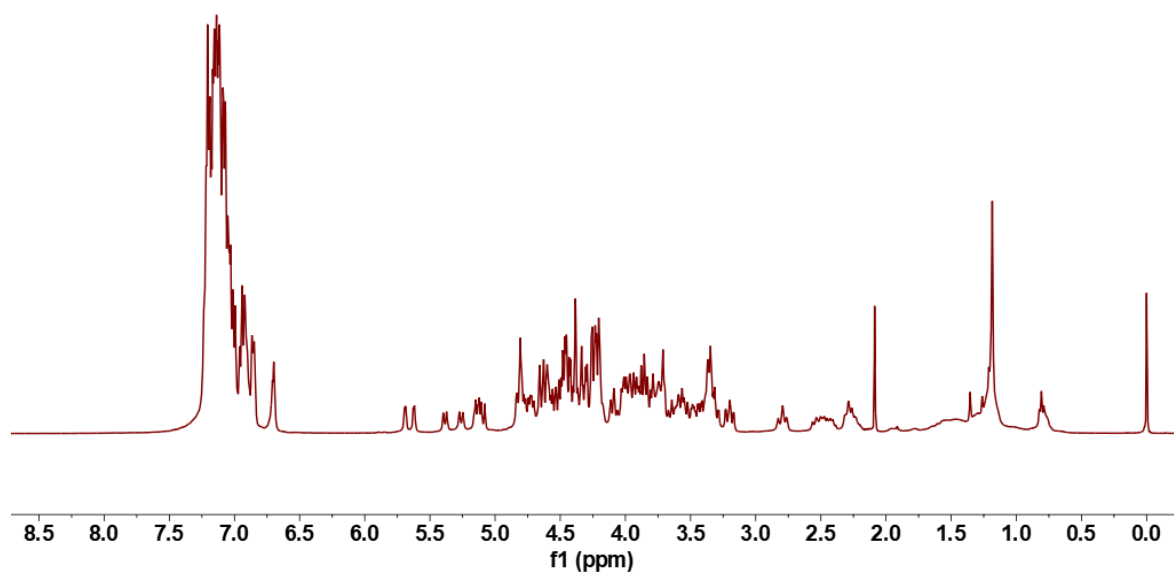


Figure 3: ¹H NMR (400 MHz, CDCl₃, 300K) of compound 4-c

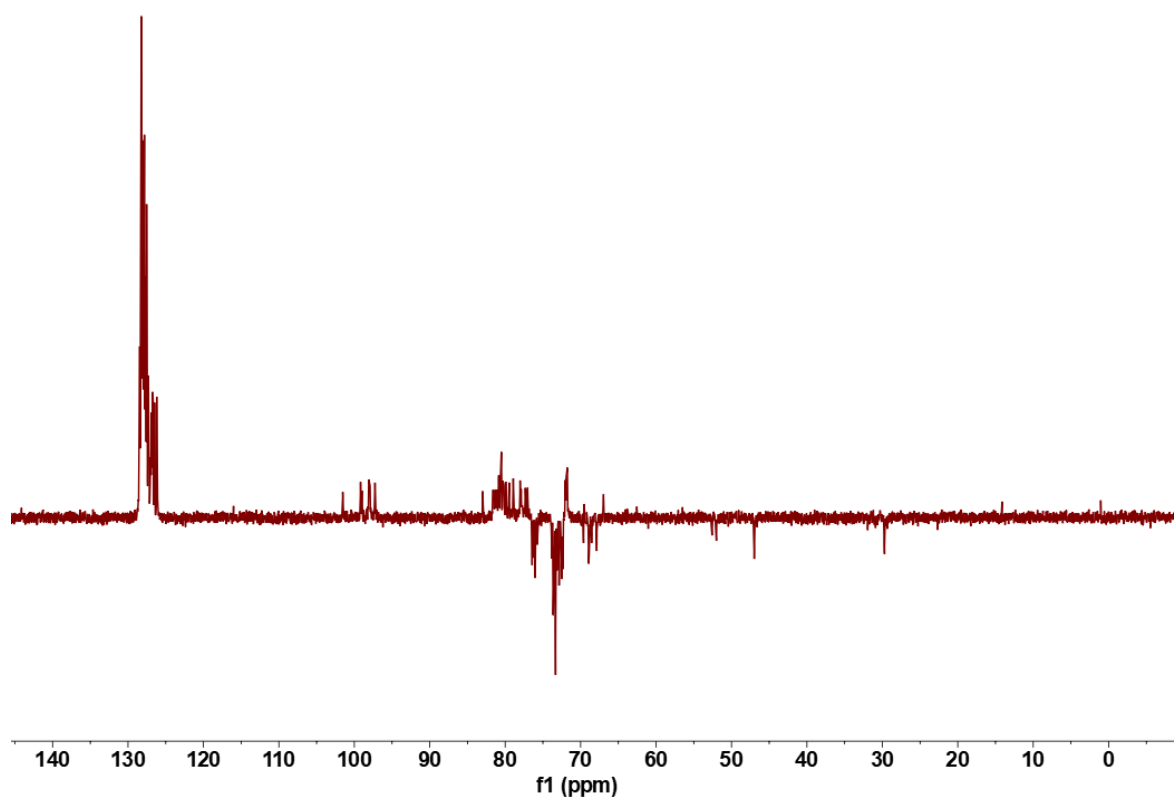
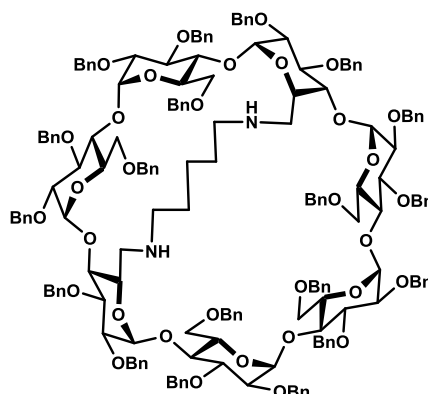


Figure 4: ¹³C NMR-DEPT 135 (100 MHz, CDCl₃, 300K) of compound 4-c

6^A, 6^D-Dideoxy-6^A, 6^D-diamino-N, N'-pentyl-**2^{A-G}, 3^{A-G}, 6^B, 6^C, 6^E, 6^F, 6^G-nonadeca-O-benzyl-β-cyclodextrin (4-d)**

Chemical Formula: C₁₈₀H₁₉₄N₂O₃₃
Exact Mass: 2911.3564

Dialdehyde β-cyclodextrin 3 (361 mg, 0.127 mmol, 1 eq) was dissolved in DCM (15 mL). 1, 5-diaminopropane (17.8 μL, 0.152 mmol, 1.2 eq) was added and the mixture was stirred for 2 h. NaBH(OAc)₃ (135 mg, 0.635 mmol, 5 eq) was added and the mixture was stirred for 3 h. A saturated solution of NaHCO₃ (70 mL) and EtOAc (70 mL) were added and the mixture was stirred for 30 min. The aqueous phase was extracted with ethyl acetate (3×70 mL), and the combined organic layers were washed with the saturated aqueous solution of NaHCO₃, brine, dried over MgSO₄, filtered and concentrated in vacuo. The obtained residue was purified by silica gel chromatography (cyclohexane/EtOAc 5:1 then 4.5:1 then 4:1) to give bridged diamine β-cyclodextrin 4-d (203 mg, 55% yield) as the white foam.

¹H NMR (400 MHz, CDCl₃, 300K): δ = 7.38-6.81 (m, 95H, 95×H_{Ph}), 5.63 (d, ³J_{H1-H2} = 4.4 Hz, 1H, 1×H1), 5.45-5.37 (m, 2H, 1×H1, 1×CHH-Ph), 5.25-5.11 (m, 5H, 1×H1, 4×CHH-Ph), 5.00-4.94 (dd, ³J_{H1-H2} = 3.6 Hz, ²J_{H3-H2} = 6.8 Hz, 2H, 2×H1), 4.80-4.59 (m, 12H, 2×H1, 10×CHH-Ph), 4.57-4.23 (m, 23H, 23×CHH-Ph), 4.23-4.12 (m, 3H, 1×H5, 2×H6), 4.12-3.77 (m, 20H, 7×H3, 5×H4, 6×H5, 2×H6), 3.71-3.61 (m, 3H, 3×H6), 3.60-3.39 (m, 9H, 5×H2, 2×H4, 2×H6), 3.35-3.22 (m, 3H, 2×H2, 1×H6), 2.92 (d, ³J_{H6-H5} = 11.6 Hz, 1H, 1×H6), 2.81 (d, ³J_{H6-H5} = 11.6 Hz, 1H, 1×H6), 2.60-2.47 (br. m, 2H, 2×H6), 2.37 (br. m, 2H, 2×CHH-NH), 2.27 (br. m, 2H, 2×CHH-NH), 2.01 (br. m, 1H, 1×CHH-CH₂-NH), 1.61 (br. m, 1H, 1×CHH-CH₂-NH), 1.43 (br. m, 1H, 1×CHH-CH₂-NH), 1.31 (br. m, 1H, 1×CHH-CH₂-NH), 1.28 (br. m, 1H, 1×CHH-CH₂-CH₂-NH), 1.25 (br. m, 1H, 1×CHH-CH₂-CH₂-NH).

¹³C NMR (100 MHz, CDCl₃, 300K): δ = 128.28-125.80 (95C, CH-Ar), 100.28, 98.80, 98.57, 98.48, 98.18, 98.12 97.57 (7×C1), 82.23-79.49 (12C, 7×C3, 5×C4), 79.49-77.23 (7×C2), 78.97 (C4), 78.27 (C4), 76.67-76.19 (4×CH₂-Ph), 73.49-72.27 (15×CH₂-Ph), 72.45-69.86

EXPERIMENTAL PART

(6×C5), 69.20 (C5), 69.01 (C6), 68.86 (C6), 68.49 (2×C6), 68.34 (C6), 52.38 (C6), 49.80 (C6), 48.95 (CH₂-NH), 48.61 (CH₂-NH), 32.32 (CH₂-CH₂-NH), 29.40 (CH₂-CH₂-NH), 24.44 (CH₂-CH₂-CH₂-NH).

HMRS (ESI): calculated for [C₁₈₀H₁₉₄N₂O₃₃+H]⁺ 2912.3637; found 2912.3686.

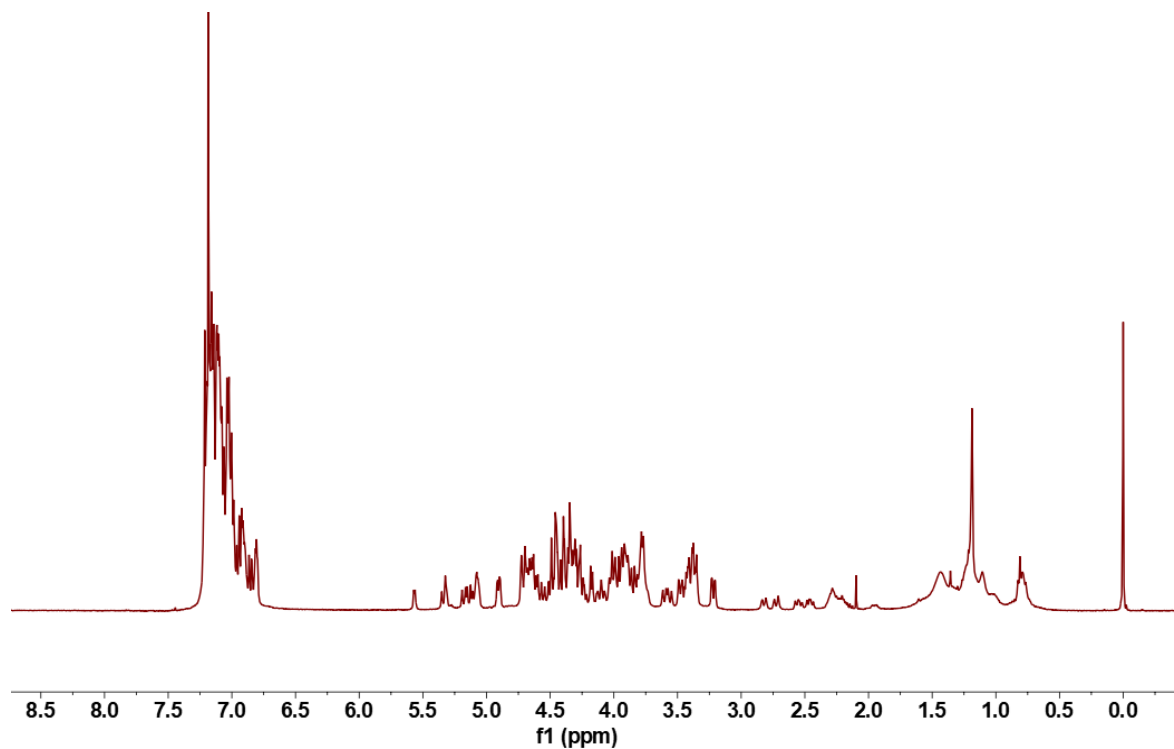


Figure 5: ¹H NMR (400 MHz, CDCl₃, 300K) of compound 4-d

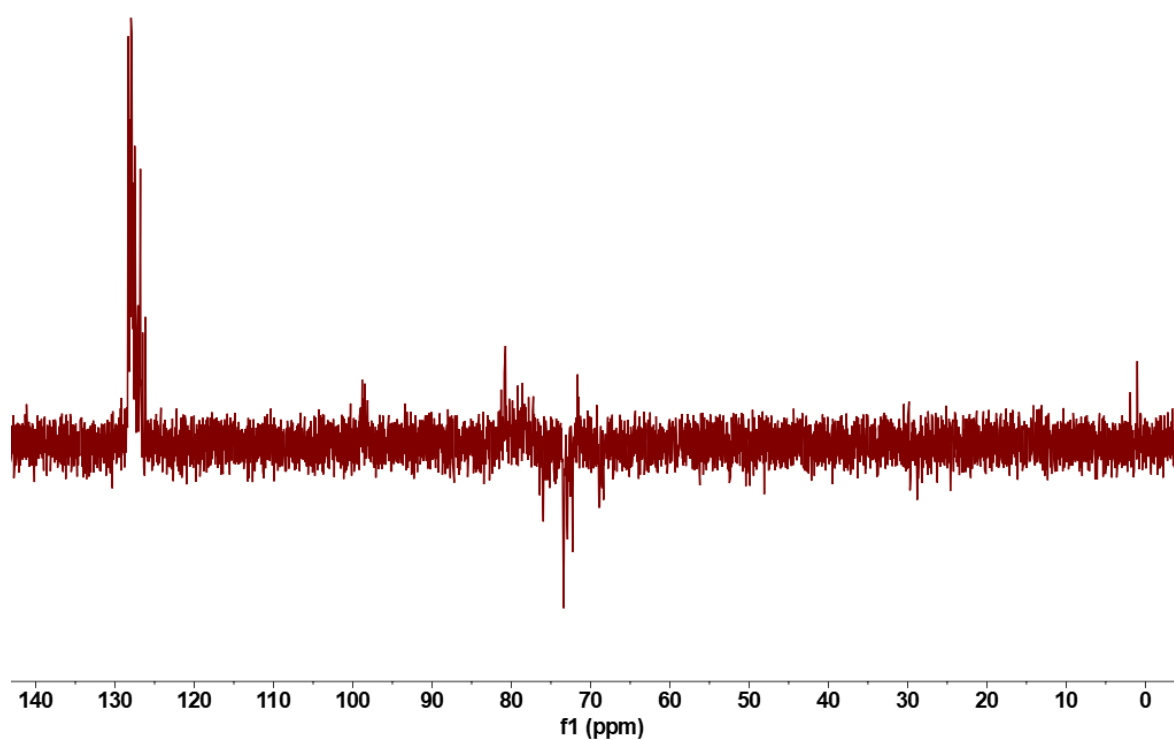
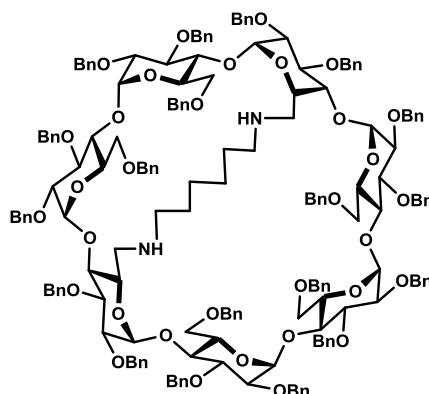


Figure 6: ¹³C NMR-DEPT 135 (100 MHz, CDCl₃, 300K) of compound 4-d

6^A, 6^D-Dideoxy-6^A, 6^D-diamino-N, N'-hexyl-**2^{A-G}, 3^{A-G}, 6^B, 6^C, 6^E, 6^F, 6^G-nonadeca-O-benzyl-β-cyclodextrin (4-e)**

Chemical Formula: C₁₈₁H₁₉₆N₂O₃₃
Exact Mass: 2925.3720

Dialdehyde β-cyclodextrin 3 (390 mg, 0.137 mmol, 1 eq) was dissolved in DCM (15 mL). A solution of 1, 6-diaminopropane (200 mg, 0.172 mmol, 1.2 eq) in dichloromethane (3 mL) was added and the mixture was stirred for 2 h. NaBH(OAc)₃ (145 mg, 0.686 mmol, 5 eq) was added and the mixture was stirred for 3 h. A saturated solution of NaHCO₃ (70 mL) and ethyl acetate (70 mL) were added and the mixture was stirred for 30 min. The aqueous phase was extracted with ethyl acetate (3×70 mL), and the combined organic layers were washed with the saturated aqueous solution of NaHCO₃, brine, dried over MgSO₄, filtered and concentrated in vacuo. The obtained residue was purified by silica gel chromatography (cyclohexane/EtOAc 5:1 then 4.5:1 then 4:1) to give bridged diamine β-cyclodextrin 4-e (227 mg, 57% yield) as the white foam.

¹H NMR (400 MHz, CDCl₃, 300K): δ = 7.29-6.82 (m, 95H, 95×H_{Ph}), 5.44 (d, ³J_{H1-H2} = 2.4 Hz, 1H, 1×H1), 5.26-5.10 (m, 5H, 2×H1, 3×CHH-Ph), 5.06 (d, ²J = 10.0 Hz, 1H, 1×CHH-Ph), 5.02-4.95 (dd, ³J_{H1-H2} = 3.6 Hz, ²J_{H3-H2} = 9.6 Hz, 2H, 2×H1), 4.92 (d, ²J = 10.4 Hz, 1H, 1×CHH-Ph), 4.75-4.57 (m, 11H, 2×H1, 9×CHH-Ph), 4.54-4.20 (m, 24H, 24×CHH-Ph), 4.14-4.05 (m, 3H, 3×H6), 4.02-3.76 (m, 20H, 7×H3, 5×H4, 6×H5, 2×H6), 3.68-3.54 (m, 3H, 1×H5, 2×H6), 3.51-3.54 (m, 10H, 5×H2, 2×H4, 3×H6), 3.29-3.32 (m, 2H, 2×H2), 2.97 (d, ³J_{H6-H5} = 12.4 Hz, 1H, 1×H6), 2.82 (d, ³J_{H6-H5} = 10.0 Hz, 1H, 1×H6), 2.63 (br. m, 1H, 1×H6), 2.48-2.30 (br. m, 3H, 1×H6, 2×CHH-NH), 2.30-2.15 (br. m, 2H, 2×CHH-NH), 1.97 (br. m, 1H, 1×CHH-CH₂-NH), 1.55 (br. m, 5H, 1×CHH-CH₂-NH, 2×CHH-CH₂-NH, 2×CHH-CH₂-CH₂-NH), 1.18 (br. m, 2H, 2×CHH-CH₂-CH₂-NH).

¹³C NMR (100 MHz, CDCl₃, 300K): δ = 128.12-126.44 (95C, CH-Ar), 99.39 (C1), 99.30 (C1), 99.07 (C1), 98.72 (2×C1), 98.57 (2×C1), 81.47 (C4), 81.43-80.27 (11C, 7×C3, 2×C4, 2×C2),

EXPERIMENTAL PART

79.96-77.49 (11C, 5×C2, 3×C4, 1×C5), 76.46, 76.15, 75.91, 75.52, 74.79 (4×CH₂-Ph), 73.68-72.26 (15×CH₂-Ph), 72.02-71.53 (4×C5), 70.81 (C6), 69.87 (2×C5), 69.24 (C6), 68.99 (C6), 68.82 (C6), 68.60 (C6), 51.97 (C6), 51.74 (C6), 49.22 (CH₂-NH), 48.36 (CH₂-NH), 29.82 (CH₂-CH₂-NH), 29.28 (CH₂-CH₂-NH), 26.16 (2×CH₂-CH₂-CH₂-NH).

HMRS (ESI): calculated for [C₁₈₁H₁₉₆N₂O₃₃+H]⁺ 2926.3793; found 2926.3840.

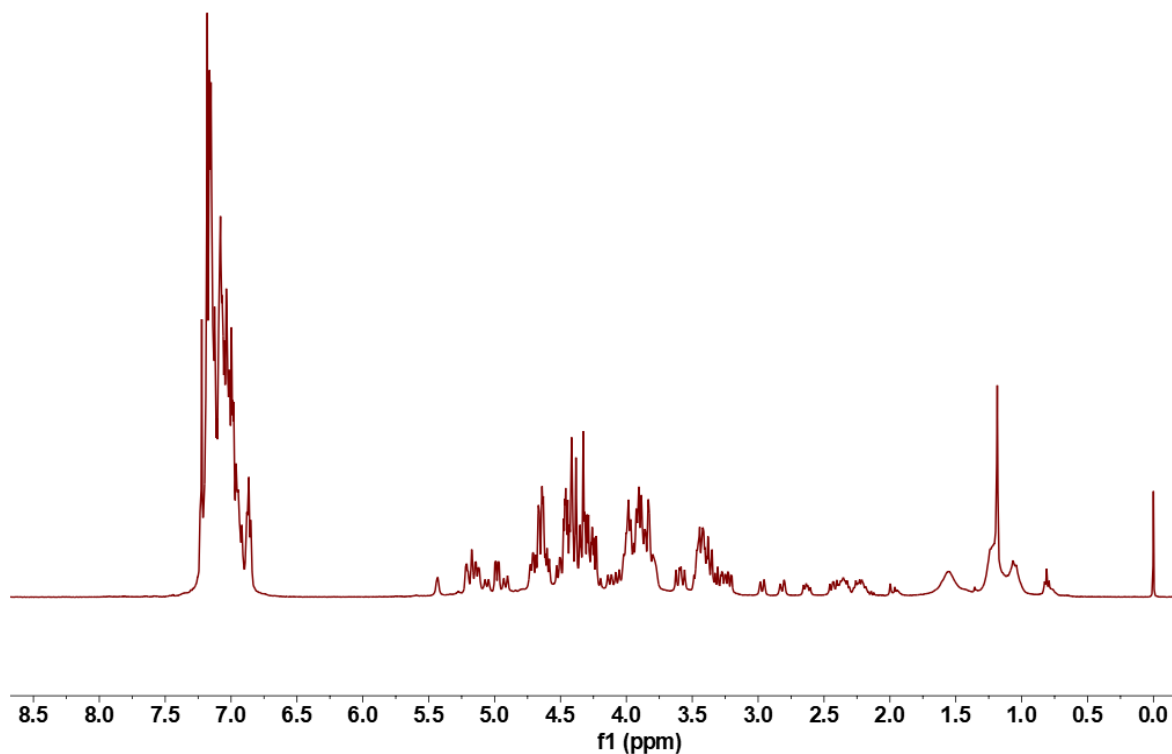


Figure 7: ¹H NMR (400 MHz, CDCl₃, 300K) of compound 4-e

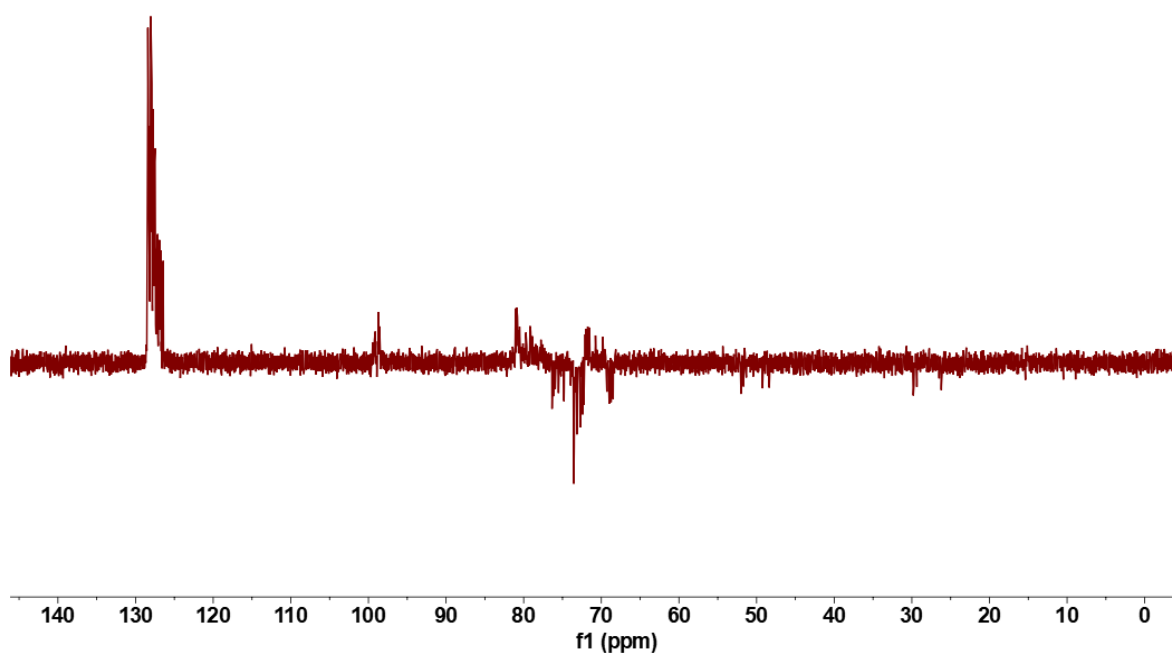
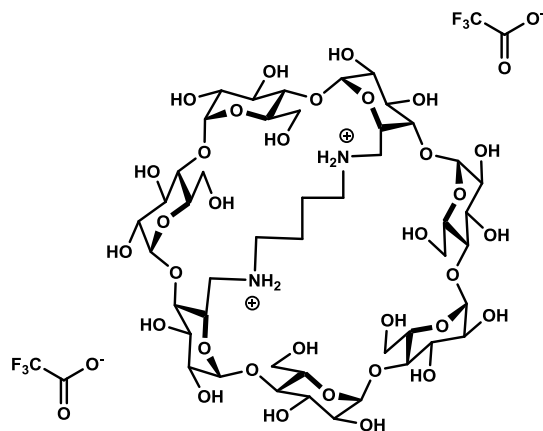


Figure 8: ¹³C NMR-DEPT 135 (100 MHz, CDCl₃, 300K) of compound 4-e

**6^A, 6^D-Dideoxy-6^A, 6^D-diammonio-N, N'-butyl-β-cyclodextrin bis-trifluoroacetate
(5-a)**



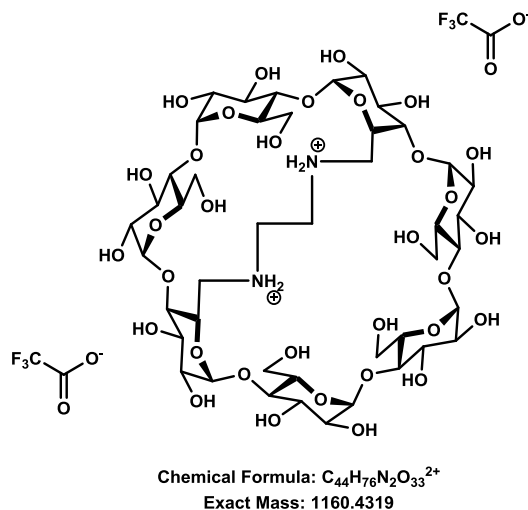
Chemical Formula: $C_{46}H_{80}N_2O_{33}^{2+}$
Exact Mass: 1188.4632

The perbenzylated bridged diamine β-cyclodextrin 4-a (200 mg, 0.069 mmol, 1 eq) was dissolved in THF/H₂O (3:1, 40 mL). 2, 2, 2-trifluoroacetic acid (43 μL, 0.552 mmol, 8 eq) and Pd/C (315 mg, 2.97 mmol, 43 eq) was added. The mixture was purged 3 times with argon and 3 times with hydrogen. The reaction mixture was monitored by MS, and then the mixture was purged under nitrogen, filtered through a pad of Celite and washed with MeOH/H₂O. The organic solvents were evaporated under vacuum and the residue was purified by a RediSep Rf Gold C-18 reversed-phase column using a gradient of ACN/water (%ACN: 0 => 5% in 10 min). The desired product 5-a was obtained as the white amorphous powder (32.8 mg, 40% yield) after freeze drying.

The structure of the product was confirmed by comparison with the literature ^[130].

EXPERIMENTAL PART

**6^A, 6^D-Dideoxy-6^A, 6^D-diammonio-N, N'-ethyl-β-cyclodextrin bis-trifluoroacetate
(5-b)**



The perbenzylated bridged diamine β-cyclodextrin 4-b (170 mg, 0.059 mmol, 1 eq) was dissolved in THF/H₂O (3:1, 44 mL). 2, 2, 2-trifluoroacetic acid (36 μL, 0.474 mmol, 8 eq) and Pd/C (217 mg, 2.55 mmol, 43 eq) was added. The mixture was purged 3 times with argon and 3 times with hydrogen. The reaction mixture was monitored by MS, and then the mixture was purged under nitrogen, filtered through a pad of Celite and washed with MeOH/H₂O. The organic solvents were evaporated under vacuum and the residue was purified by a RediSep Rf Gold C-18 reversed-phase column using a gradient of ACN/water (%ACN: 0 => 5% in 10 min). The desired product 5-b was obtained as the white amorphous powder (30.1 mg, 44% yield) after freeze drying.

¹H NMR (400 MHz, D₂O, 300K): δ = 5.48 (d, ³J_{H1-H2} = 3.6 Hz, 1H, 1×H1), 5.29 (d, ³J_{H1-H2} = 3.6 Hz, 1H, 1×H1), 5.22 (d, ³J_{H1-H2} = 3.6 Hz, 1H, 1×H1), 5.15-5.04 (m, 4H, 4×H1), 4.29-4.13 (m, 18H, 7×H3, 2×H4, 5×H5, 4×H6), 3.80-3.63 (m, 10H, 7×H2, 3×H6), 3.63-3.49 (m, 4H, 4×H4), 3.49-3.33 (m, 4H, 1×H4, 3×H6), 3.32-3.20 (m, 4H, 4×H6), 1.63 (s, 1H, 1×CHH-NH), 1.36-1.29 (m, 3H, 3×CHH-NH).

HMRS (ESI): calculate for [C₄₄H₇₄N₂O₃₃+H]⁺ 1159.4247; found 1159.3843.

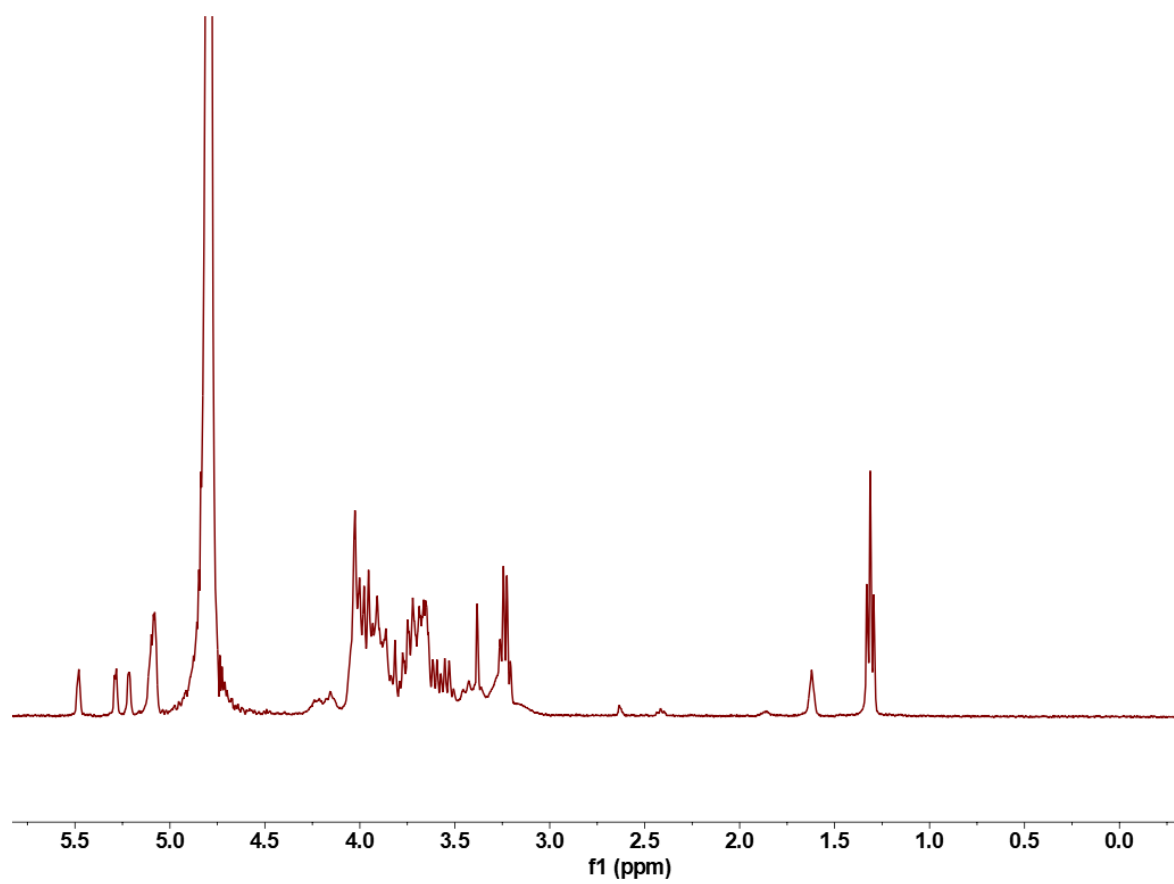
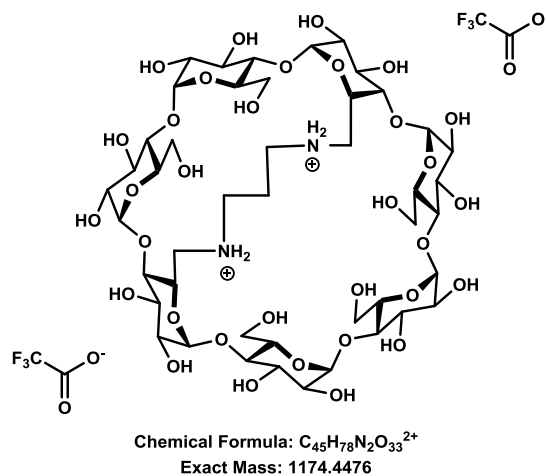


Figure 9: ¹H NMR (400 MHz, D₂O, 300K) of compound 5-b

EXPERIMENTAL PART

6^A, 6^D-Dideoxy-6^A, 6^D-diammonio-N, N'-propyl-β-cyclodextrin bis-trifluoroacetate (5-c)



The perbenzylated bridged diamine β-cyclodextrin 4-c (150 mg, 0.052 mmol, 1 eq) was dissolved in THF/H₂O (3:1, 40 mL). 2, 2, 2-trifluoroacetic acid (32 μL, 0.416 mmol, 8 eq) and Pd/C (238 mg, 2.24 mmol, 43 eq) was added. The mixture was purged 3 times with argon and 3 times with hydrogen. The reaction mixture was monitored by MS, and then the mixture was purged under nitrogen, filtered through a pad of Celite and washed with MeOH/H₂O. The organic solvents were evaporated under vacuum and the residue was purified by a RediSep Rf Gold C-18 reversed-phase column using a gradient of ACN/water (%ACN: 0 => 5% in 10 min). The desired product 5-c was obtained as the white amorphous powder (25.6 mg, 42% yield) after freeze drying.

¹H NMR (400 MHz, D₂O, 300K): δ = 5.29 (d, ³J_{H1-H2} = 3.6 Hz, 1H, 1×H1), 5.24 (d, ³J_{H1-H2} = 4.0 Hz, 1H, 1×H1), 5.15 (d, ³J_{H1-H2} = 3.6 Hz, 1H, 1×H1), 5.13-5.05 (m, 4H, 4×H1), 4.37-4.18 (m, 3H, 3×H5), 4.13-3.47 (m, 33H, 7×H2, 7×H3, 7×H4, 4×H5, 8×H6), 3.43-3.29 (m, 4H, 4×H6), 3.27-3.14 (m, 2H, 2×H6), 3.14-2.99 (br. m, 3H, 2×CHH-NH, 1×CHH-CH₂-NH), 2.19-1.99 (br. m, 3H, 2×CHH-NH, 1×CHH-NH).

HMRS (ESI): calculate for [C₄₅H₇₆N₂O₃₃+H]⁺ 1173.4403; found 1173.3237.

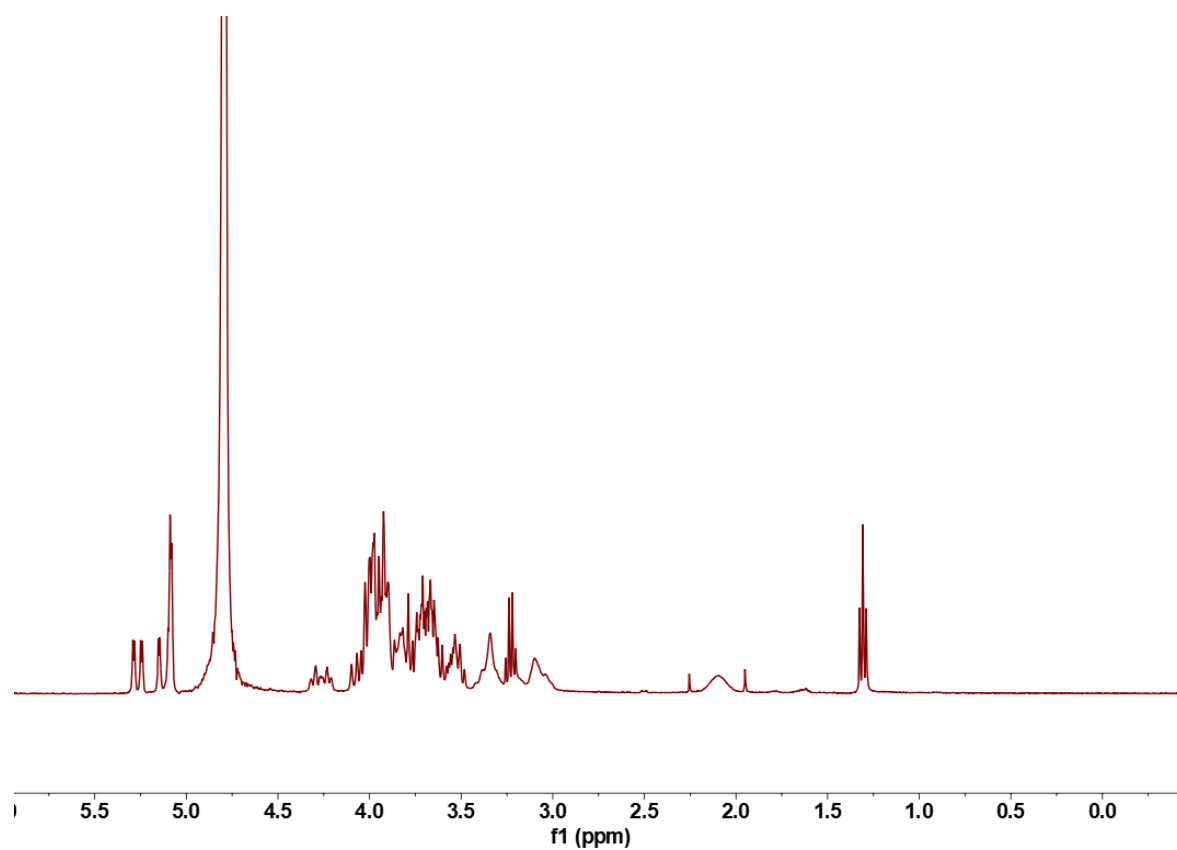
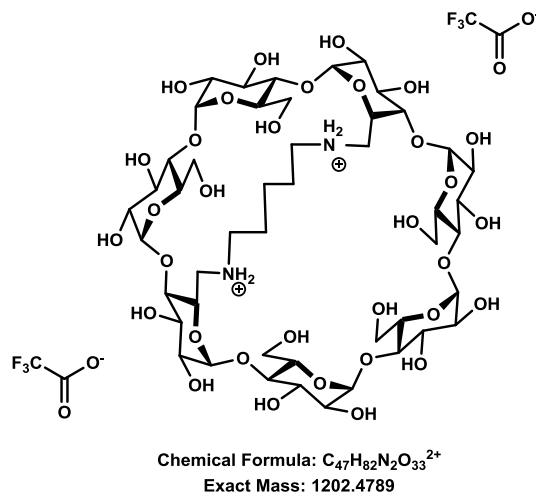


Figure 10: ¹H NMR (400 MHz, D₂O, 300K) of compound 5-c

EXPERIMENTAL PART

6^A, 6^D-Dideoxy-6^A, 6^D-diammonio-N, N'-pentyl-β-cyclodextrin bis-trifluoroacetate (5-d)



The perbenzylated bridged diamine β-cyclodextrin 4-d (160 mg, 0.055 mmol, 1 eq) was dissolved in THF/H₂O (3:1, 40 mL). 2, 2, 2-trifluoroacetic acid (35 μL, 0.439 mmol, 8 eq) and Pd/C (251 mg, 2.36 mmol, 43 eq) was added. The mixture was purged 3 times with argon and 3 times with hydrogen. The reaction mixture was monitored by MS, and then the mixture was purged under nitrogen, filtered through a pad of Celite and washed with MeOH/H₂O. The organic solvents were evaporated under vacuum and the residue was purified by a RediSep Rf Gold C-18 reversed-phase column using a gradient of ACN/water (%ACN: 0 => 5% in 10 min). The desired product 5-d was obtained as the white amorphous powder (29.7mg, 45% yield) after freeze drying.

¹H NMR (400 MHz, D₂O, 300K): δ =5.13 (d, ³J_{H1-H2} =3.6 Hz, 1H, 1×H1), 5.07-4.98 (m, 6H, 6×H1), 4.27-4.18 (m, 3H, 3×H6), 3.98-3.39 (m, 35H, 7×H2, 7×H3, 7×H4, 7×H5, 7×H6), 3.36-3.18 (m, 4H, 4×H6), 3.06-2.88 (m, 6H, 4×CHH-NH, 2×CHH-CH₂-NH), 1.43 (m, 4H, 2×CHH-CH₂-NH, 2×CHH-CH₂-CH₂-NH).

HMRS (ESI): calculate for [C₄₇H₈₀N₂O₃₃+H]⁺ 1201.4716; found 1201.6977.

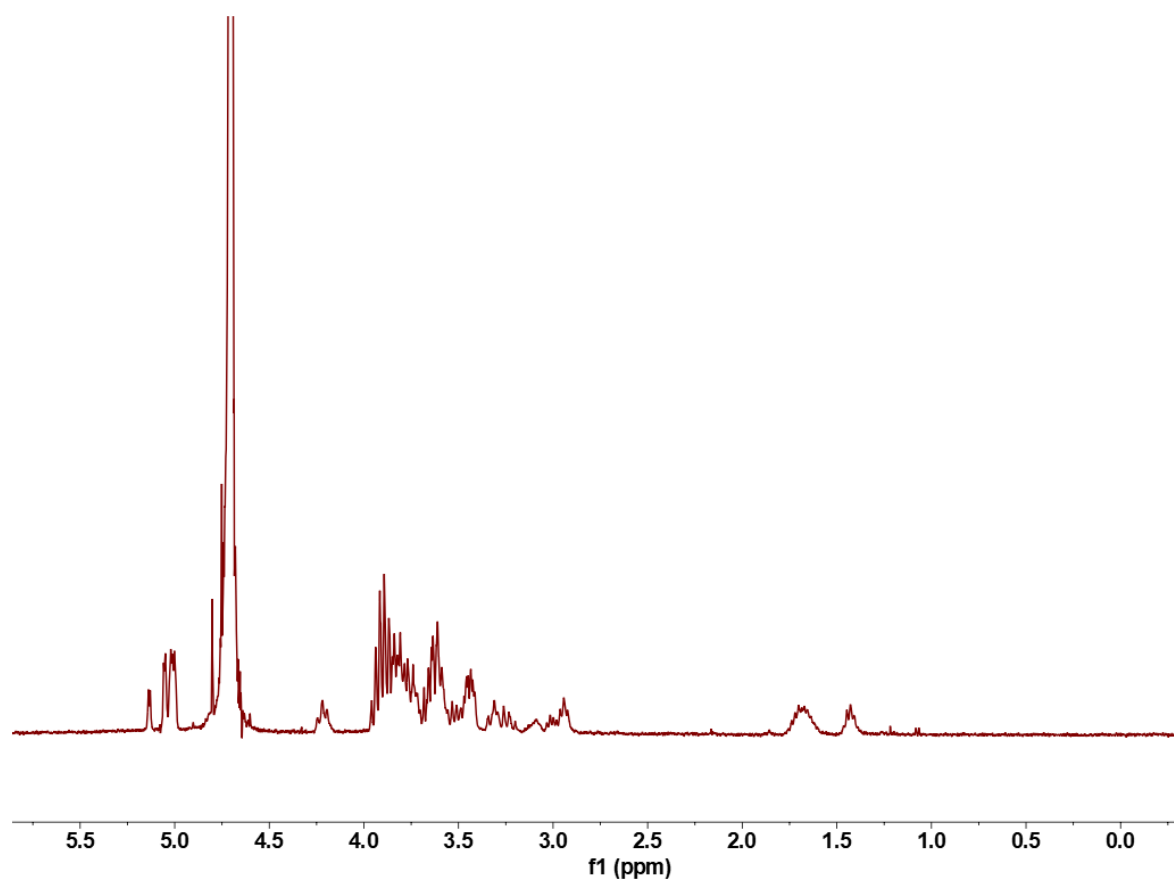
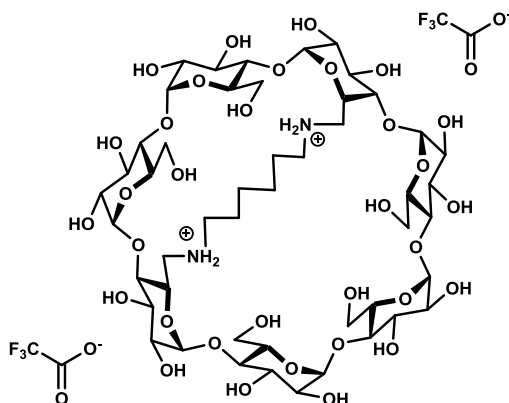


Figure 11: ^1H NMR (400 MHz, D_2O , 300K) of compound 5-d

EXPERIMENTAL PART

6^A, 6^D-Dideoxy-6^A, 6^D-diammonio-N, N'-hexyl-β-cyclodextrin bis-trifluoroacetate (5-e)



Chemical Formula: $C_{48}H_{84}N_2O_{33}^{2+}$
Exact Mass: 1216.4945

The perbenzylated bridged diamine β-cyclodextrin 4-e (150 mg, 0.051 mmol, 1 eq) was dissolved in THF/H₂O (3:1, 40 mL). 2, 2, 2-trifluoroacetic acid (32 μL, 0.410 mmol, 8 eq) and Pd/C (235 mg, 2.20 mmol, 43 eq) was added. The mixture was purged 3 times with argon and 3 times with hydrogen. The reaction mixture was monitored by MS, and then the mixture was purged under nitrogen, filtered through a pad of Celite and washed with MeOH/H₂O. The organic solvents were evaporated under vacuum and the residue was purified by a RediSep Rf Gold C-18 reversed-phase column using a gradient of ACN/water (%ACN: 0 => 5% in 10 min). The desired product 5-e was obtained as the white amorphous powder (28.3 mg, 45% yield) after freeze drying.

¹H NMR (400 MHz, D₂O, 300K): δ =5.20-5.03 (m, 7H, 7×H1), 4.22-4.06 (m, 2H, 2×H6), 4.03-3.56 (m, 34H, 7×H2, 7×H3, 5×H4, 7×H5, 8×H6), 3.48-3.33 (m, 2H, 2×H4), 3.24 (d, ³J_{H6-H5} =14.8 Hz, 1H, 1×H6), 3.16 (d, ³J_{H6-H5} =15.2 Hz, 1H, 1×H6), 3.00-2.82 (m, 2H, 2×H6), 2.72(br. m, 2H, 2×CHH-NH), 2.56(br. m, 2H, 2×CHH-NH), 1.67-1.44 (m, 4H, 4×CHH-CH₂-NH), 1.44-1.22 (m, 4H, 4×CHH-CH₂-CH₂-NH).

HMRS (ESI): calculated for [C₄₇H₈₂N₂O₃₃+H]⁺ 1215.4873; found 1215.4889.

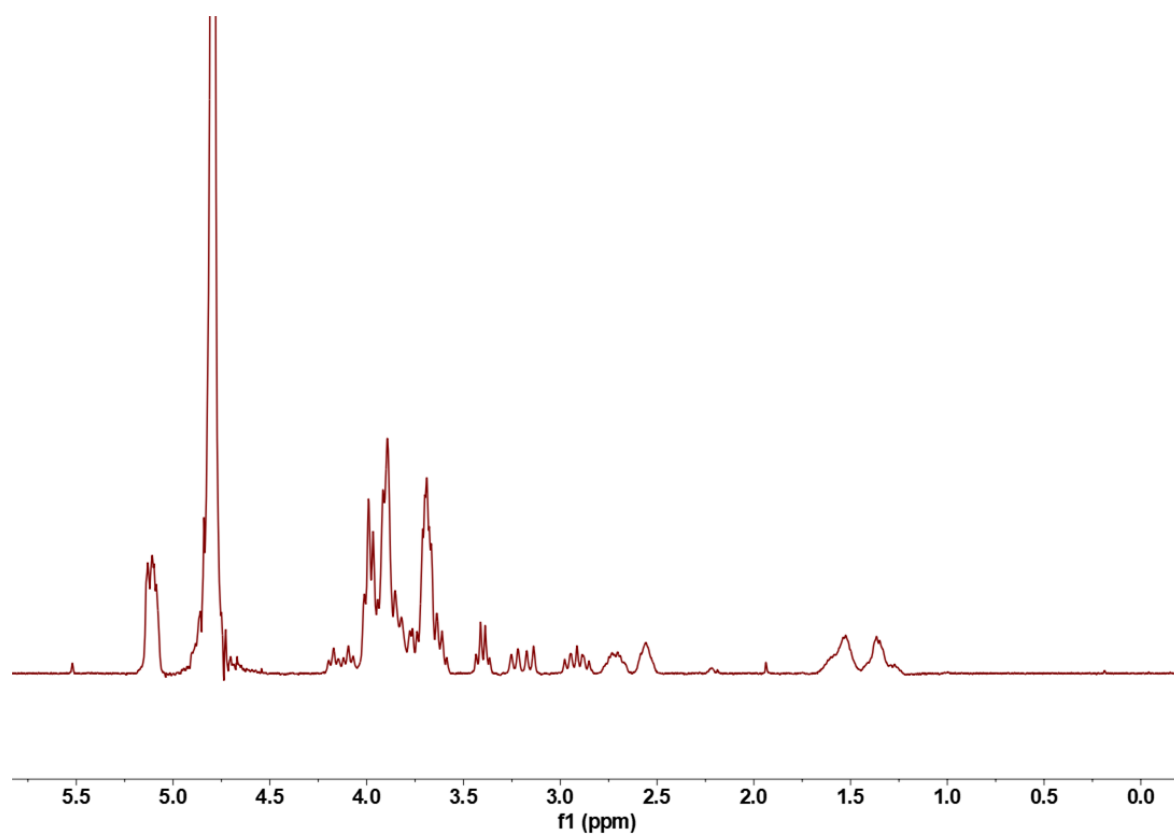
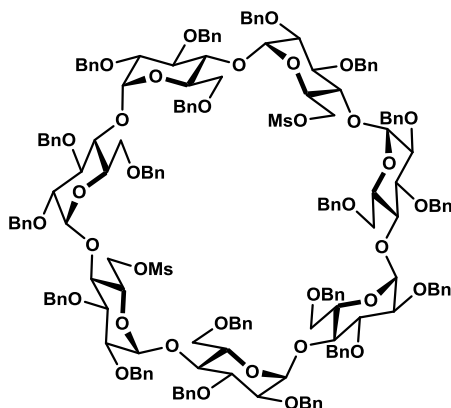


Figure 12: ^1H NMR (400 MHz, D_2O , 300K) of compound 5-e

EXPERIMENTAL PART

6^A, 6^D-Dideoxy-6^A, 6^D-methanesulfonyl-

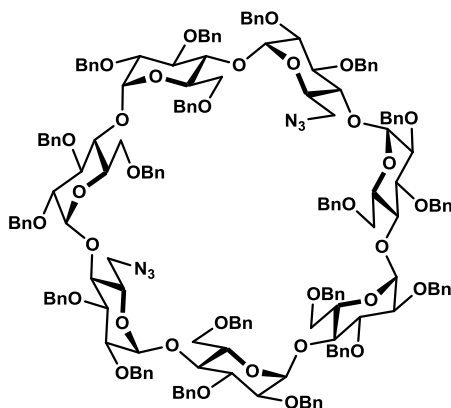
2^{A-G}, 3^{A-G}, 6^B, 6^C, 6^E, 6^F, 6^G-nonadeca-O-benzyl-β-cyclodextrin (6)



Chemical Formula: C₁₇₇H₁₈₈O₃₉S₂
Exact Mass: 3001.2169

To a cooled solution (0°C) of diol β-cyclodextrin 2 (4 g, 1.41 mmol, 1 eq) in CH₂Cl₂ (18 mL) followed by triethylamine (0.78 mL, 5.62 mmol, 4 eq) and mesyl chloride (0.44 mL, 5.62 mmol, 4 eq) sequentially added. The mixture solution was stirred at room temperature under nitrogen atmosphere, and reaction progress was monitored by TLC (cyclohexane/EtOAc 65:35) after 1 h. Finally, the mixture solution was quenched with H₂O and diluted with CH₂Cl₂ (10 mL). The aqueous phase was extracted with CH₂Cl₂ (3×20 mL), and the combined organic layers were washed with water, brine, passed over MgSO₄, filtered and concentrated in vacuo. The residue was purified over silica gel chromatography (cyclohexane/EtOAc 9:1 then 3:1) to afford desired product 6 (3.7 mg, 93% yield) as the white foam.

The structure of the product was confirmed by comparison with the literature ^[148].

6^A, 6^D-Dideoxy-6^A, 6^D-azido-**2^{A-G}, 3^{A-G}, 6^B, 6^C, 6^E, 6^F, 6^G-nonadeca-O-benzyl-β-cyclodextrin (7)**

Chemical Formula: $C_{175}H_{182}N_6O_{33}$
Exact Mass: 2895.2748

Product 6 (3.7 g, 1.23 mmol, 1 eq) was solubilized in dry DMF (21 mL) under argon atmosphere, sodium azide (0.64 g, 9.87 mmol, 8 eq) was added. The mixture solution was stirred at 80°C. The reaction progress was monitored by TLC (cyclohexane/ EtOAc 85:15) after 2 h. Water (50 mL) and EtOAc (50 mL) were added, and the aqueous phase was extracted with EtOAc (3×70 mL), and the combined organic layers were washed with 1:1 water/brine solution, dried over $MgSO_4$, filtered and concentrated in vacuo. The obtained residue was purified by silica gel chromatography (cyclohexane/EtOAc 85:15) to give product 7 (3.1 g, 87% yield) as the white foam.

¹H NMR (400 MHz, $CDCl_3$, 300K): δ = 7.42-7.00 (m, 95H, 95× H_{Ph}), 5.20 (d, $^3J_{H1-H2}$ = 4.8 Hz, 1H, 1×H1), 5.29-5.07 (m, 9H, 5×H1, 4×CHH-Ph), 5.05-4.98 (m, 2H, 1×H1, 1×CHH-Ph), 4.90-4.71 (m, 9H, 9×CHH-Ph), 4.67-4.57 (m, 2H, 2×CHH-Ph), 4.56-4.35 (m, 22H, 22×CHH-Ph), 4.20-3.84 (m, 25H, 7×H3, 5×H4, 7×H5, 6×H6), 3.76-3.41 (m, 17H, 7×H2, 2×H4, 8×H6).

¹³C NMR (100 MHz, $CDCl_3$, 300K): δ = 128.51-126.77 (95C, CH-Ar), 98.75, 98.63, 98.58, 98.53, 98.27, 98.09, 97.92 (7×C1), 81.73-76.67 (21C, 7×C2, 7×C3, 7×C4), 75.89, 75.73, 75.65, 75.35, 75.24 (5×CH₂-Ph), 74.85 (2×CH₂-Ph), 73.71-72.36 (12×CH₂-Ph), 71.94-71.33 (5×C5), 71.06-70.61 (2×C5), 69.48 (2×C6), 69.28 (2×C6), 68.98 (2×C6), 52.25 (C6).

HMRS (ESI): calculated for $[C_{175}H_{182}N_6O_{33}+Na]^+$ 2918.2640; found 2918.2699.

EXPERIMENTAL PART

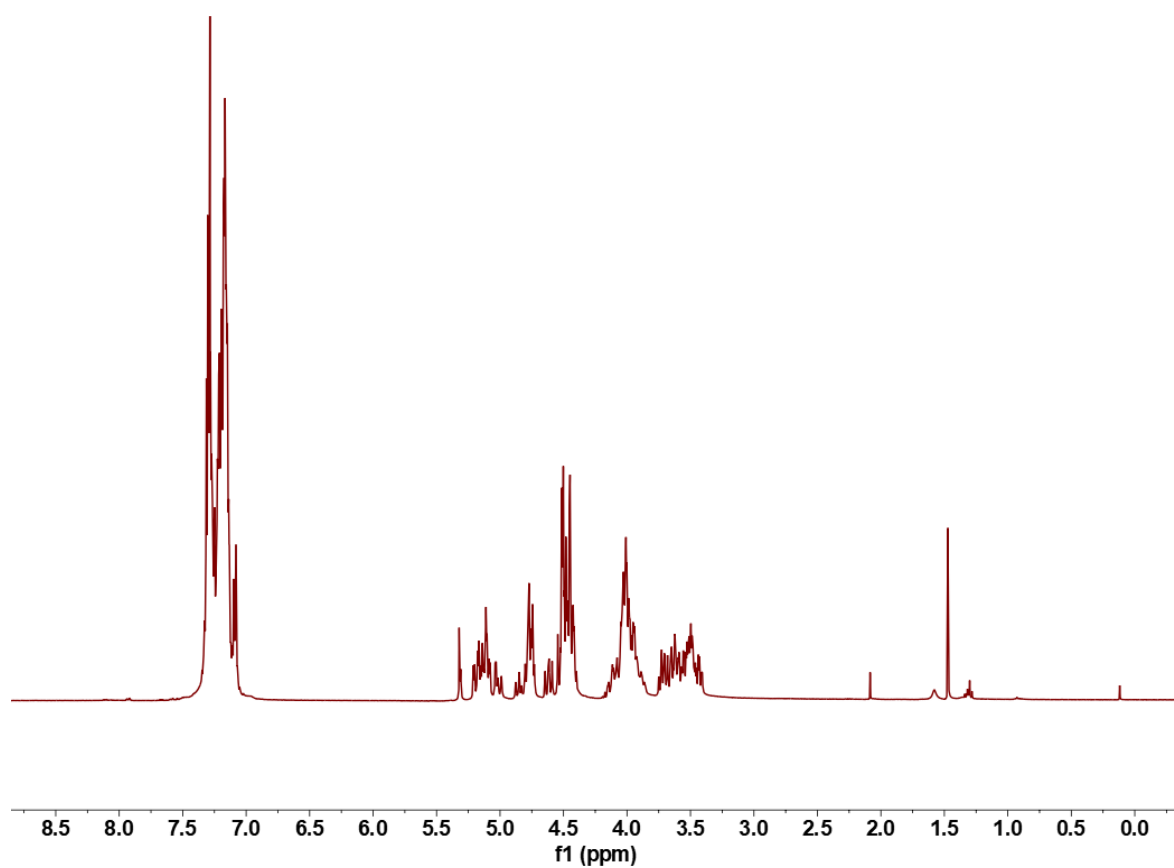


Figure 13: ¹H NMR (400 MHz, CDCl₃, 300K) of compound 7

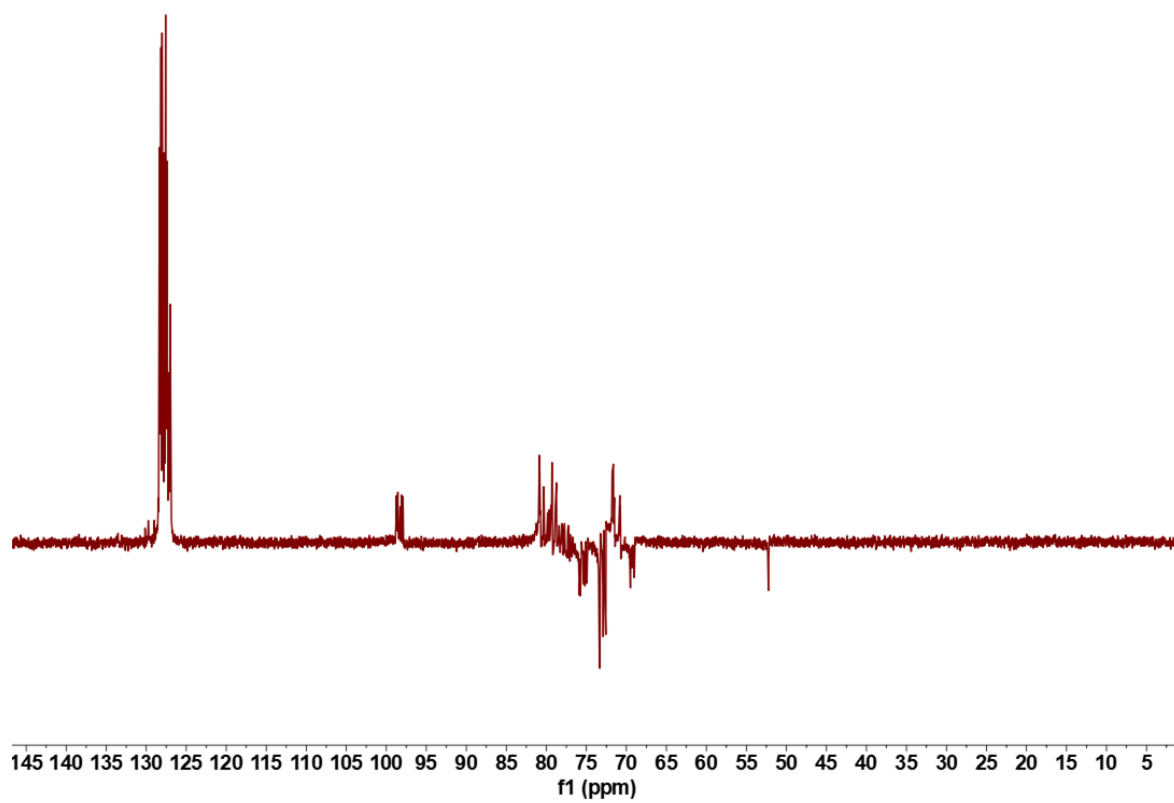
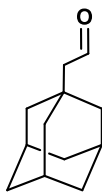


Figure 14: ¹³C NMR-DEPT 135 (100 MHz, CDCl₃, 300K) of compound 7

2-((3r, 5r, 7r)-Adamantan-1-yl)acetaldehyde (8)

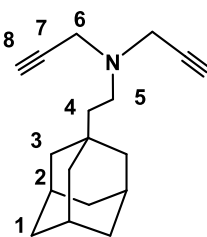
Chemical Formula: C₁₂H₁₈O
Exact Mass: 178.1358

To a flask containing 2-adamantyl-ethanol (1.01 g, 5.60 mmol, 1 eq) in dichloromethane (35 mL) was added TEMPO (88 mg, 0.560 mmol, 0.1 eq) followed by iodobenzene diacetate (2.0 g, 6.16 mmol, 1.1 eq). The mixture reaction was stirred for 3 h and then diluted with dichloromethane (20 mL). The saturated aqueous solution of Na₂S₂O₃ (20 mL) was then added. The mixture was stirred for 30 min and then the aqueous phase was extracted with dichloromethane (3×50 mL), and the combined organic layers were washed with the saturated aqueous solution of NaHCO₃, brine, dried over MgSO₄, filtered and concentrated in vacuo. The residue was purified over silica gel chromatography (Et₂O/pentane 1:30) to provide adamantylacetaldehyde 8 (0.77 g, 77.1% yield) as the colorless oil that was stored at -20°C under argon to prevent any further oxidation.

The structure of the product was confirmed by comparison with the literature ^[149].

EXPERIMENTAL PART

N-(2-((3r, 5r, 7r)-Adamantan-1-yl)ethyl)-N-(prop-2-yn-1-yl)prop-2-yn-1-amine (9)



Chemical Formula: C₁₈H₂₅N
Exact Mass: 255.1987

To a solution of adamantylacetaldehyde 8 (770 mg, 4.32 mmol, 1 eq) in dry THF (24 mL) was added dipropargylamine (0.45 mL, 4.32 mmol, 1 eq) followed by NaBH(OAc)₃ (1.373 g, 6.48 mmol, 1.5 eq) at room temperature under nitrogen, and the mixture was stirred for 2 h. Ethyl acetate (30 mL) and the saturated aqueous solution of NaHCO₃ (30 mL) were then added. The mixture was stirred for 30 min and then the aqueous phase was extracted with ethyl acetate (3×50 mL), and the combined organic layers were washed with the saturated aqueous solution of NaHCO₃, brine, dried over MgSO₄, filtered and concentrated in vacuo. The residue was purified over silica gel chromatography (cyclohexane/EtOAc 5:1) to afford desired dialkyne product 9 (946 mg, 86% yield) as the pale oil.

¹H NMR (400 MHz, CDCl₃, 300K): δ =3.44 (s, 4H, 4H-6), 2.55 (m, 2H, 2H-5), 2.21 (t, *J* =2.4 Hz, 2H, 2H-8), 1.94 (s, 3H, 3H-2), 1.73-1.60 (m, 6H, 6H-1), 1.51 (d, *J* =2.4 Hz, 6H, 6H-3), 1.30-1.23 (m, 2H, 2H-4).

¹³C NMR (100 MHz, CDCl₃, 300K): δ =78.85 (C-7), 72.84 (C-8), 47.38 (C-5), 42.27 (C-3), 42.08 (C-6), 41.54 (C-4), 37.12 (C-1) 31.84 (Cquat-Ad), 28.65 (C-2).

HMRS (ESI): calculated for [C₁₈H₂₅N+H]⁺ 256.2060; found 256.2077.

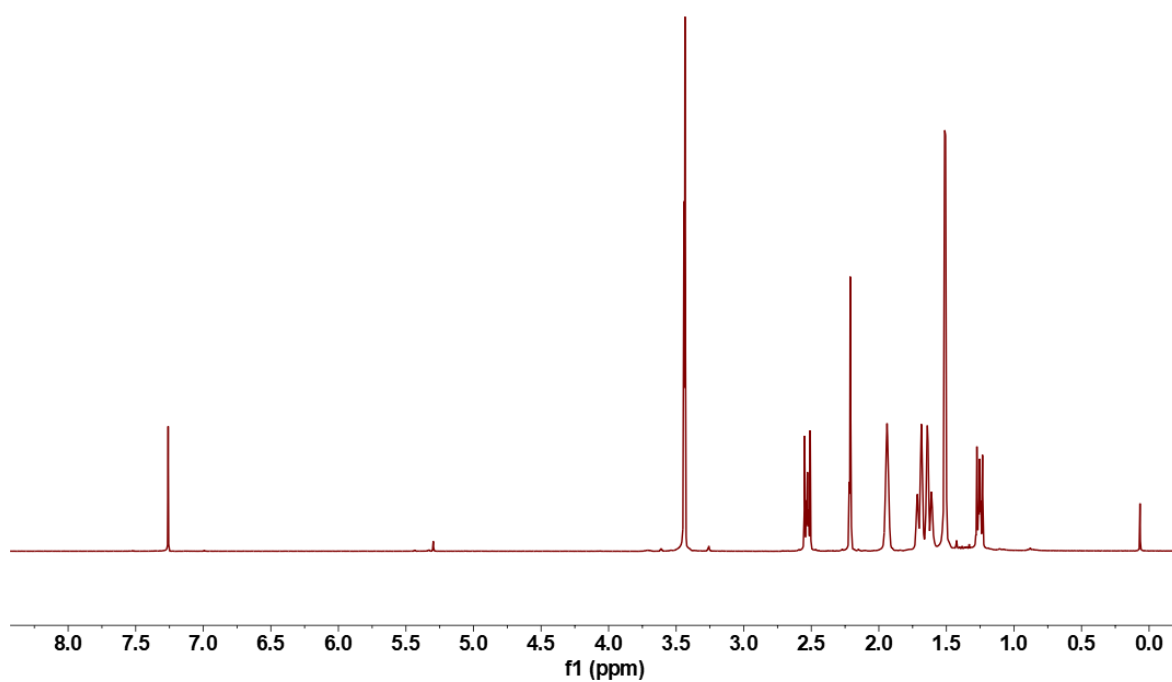


Figure 15: ¹H NMR (400 MHz, CDCl₃, 300K) of compound 9

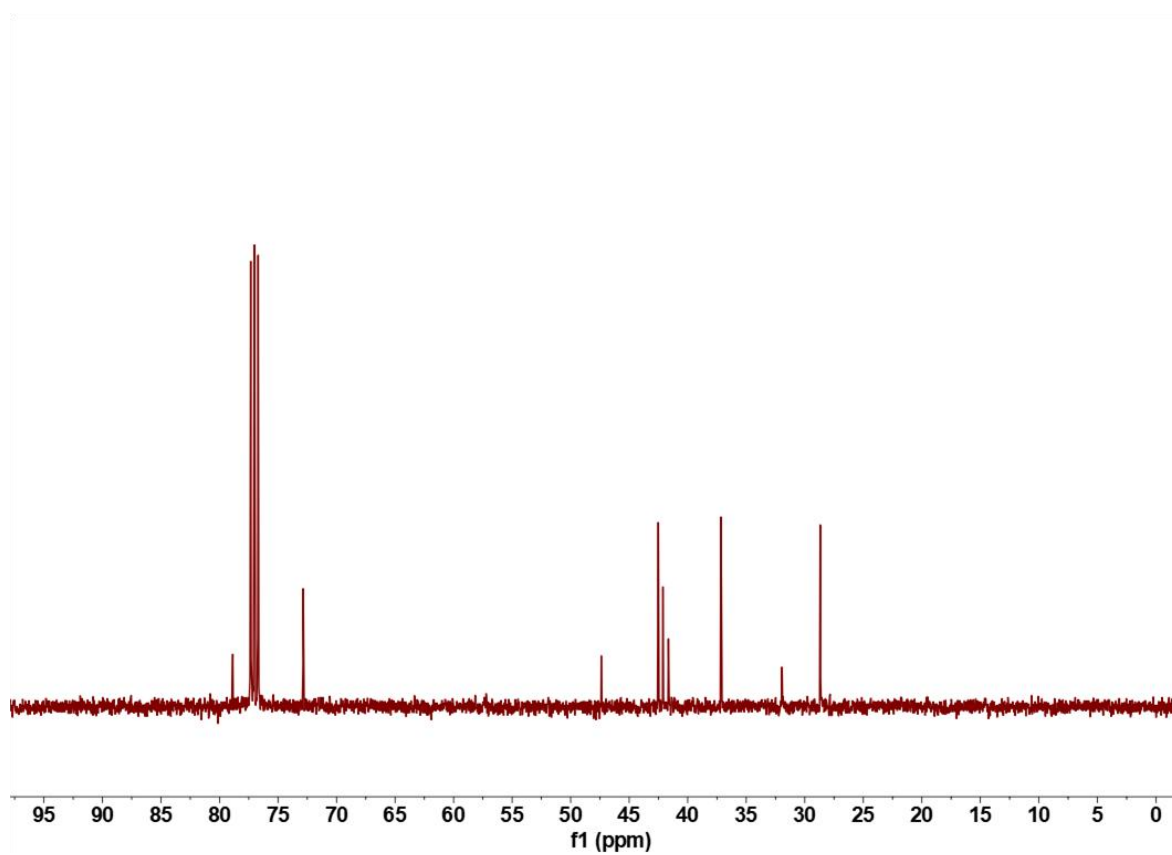
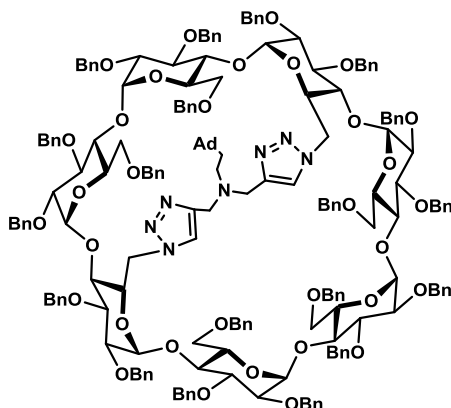


Figure 16: ¹³C NMR (100 MHz, CDCl₃, 300K) of compound 9

EXPERIMENTAL PART

**6^A, 6^D-Dideoxy-6^A, 6^D-di-triazole-bridged-N-ethyladamantyl-
2^{A-G}, 3^{A-G}, 6^B, 6^C, 6^E, 6^F, 6^G-nonadeca-O-benzyl-β-cyclodextrin (10)**



Chemical Formula: C₁₉₃H₂₀₇N₇O₃₃
Exact Mass: 3150.4735

To a solution of product 7 (1 g, 0.345 mmol, 1 eq) in 12 mL DMF followed by dialkyne product 9 (88 mg, 0.345 mmol, 1 eq) and DIPEA (24 μL, 0.138 mmol, 0.4 eq) was added. A mixture of TBTA (73 mg, 0.138 mmol, 0.4 eq) and Cu(CH₃CN)₄PF₆ (51 mg, 0.138 mmol, 0.4 eq) in 1 mL DMF was added. The mixture solution was stirred at 150°C under argon atmosphere for 1 h. Finally, the mixture solution was diluted with Et₂O (100 mL). The organic solution was washed with 1:1 water/brine solution (2×100 mL), HCl solution (1 M in water, 100 mL), the saturated aqueous solution of NaHCO₃ (100 mL), then passed over MgSO₄, filtered and concentrated in vacuo. The residue was purified over silica gel chromatography (cyclohexane/EtOAc 7:3) to afford desired compound 10 (381 mg, 35% yield) as the white foam.

¹H NMR (400 MHz, CDCl₃, 300K): δ = 7.70 (s, 1H, 1×H_{triazA}), 7.62 (s, 1H, 1×H_{triazD}), 7.29-7.08 (m, 95H, 95×H_{Ph}), 5.37-5.19 (m, 6H, 2×H1, 1×H6, 3×CHHPh), 5.12-5.08 (m, 3H, 2×H1, 1×CHHPh), 5.01-4.98 (m, 2H, 2×CHHPh), 4.90-4.70 (m, 14H, 3×H1, 11×CHHPh), 4.64-4.55 (m, 4H, 1×H5, 3×CHHPh), 4.52-4.30 (m, 17H, 1×H5, 16×CHHPh), 4.28-4.14 (m, 8H, 2×H3, 2×H5, 3×H6, 1×CHHPh), 4.09-3.94 (m, 7H, 5×H3, 1×H4, 1×CHHPh), 3.87-3.65 (m, 12H, 4×H4, 3×H5, 5×H6), 3.56-3.34 (m, 11H, 7×H2, 2×H4, 2×CHH_{triaz}), 3.31-3.28 (m, 2H, 1×H6, 1×CHH_{triaz}), 3.13-3.06 (m, 3H, 2×H6, 1×CHH_{triaz}), 2.81 (m, 2H, 2×H6), 2.51 (td, ²J = 11.7 Hz, ³J = 5.0 Hz, 1H, 1×N-CHH-CH₂-Ad), 2.17 (td, ²J = 11.8 Hz, ³J = 4.8 Hz, 1H, 1×N-CHH-CH₂-Ad), 1.97 (s, 3H, H_b), 1.76-1.62 (m, 9H, H_c, 3×H_a), 1.47 (m, 1H, 1×N-CH₂-CHH-Ad), 1.34-1.24 (m, 4H, 3×H_a, 1×N-CH₂-CHH-Ad).

¹³C NMR (100 MHz, CDCl₃, 300K): δ = 128.32-126.61 (95C, CH-Ar), 126.12 (C_{triazA}), 125.90 (C_{triazD}), 101.70, 101.13, 100.77, 99.87, 99.61, 99.35, 99.10 (7×C1), 82.49 (C2), 82.08 (C4),

81.53 (C4), 81.26 (C4), 80.98 (C3), 80.45 (C3), 80.28 (C3), 80.20 (2C, 1×C3, 1×C4), 79.98 (C3), 79.85 (2×C3), 79.53 (C2), 79.44 (C2), 79.37 (C2), 79.13 (2C, 1×C2, 1×C4), 77.85 (C2), 77.47 (C2), 77.22 (C2), 76.25 (2C), 75.90, 75.83, 75.43, 75.22, 74.56, 74.13, 73.40, 73.35, 73.19, 73.08, 72.84, 72.80, 72.71 (2C), 72.41, 72.21, 72.08 (19×CH₂-Ph), 71.77 (C5), 71.65 (C5), 71.40 (2×C5), 71.38 (C4), 71.26 (2×C5), 70.46 (C5), 69.88, 69.24, 68.85, 67.67, 67.42, 53.04, 52.61 (7×C6), 48.46 (N-CH₂-CH₂-Ad), 45.67 (CH₂triazA), 44.82 (CH₂triazD), 42.63 (Ca), 42.27 (N-CH₂-CH₂-Ad), 37.19 (Cc), 28.72 (Cb).

HMRS (ESI): calculated for [C₁₉₃H₂₀₇N₇O₃₃+Na]⁺ 3173.4627; found 3173.4678.

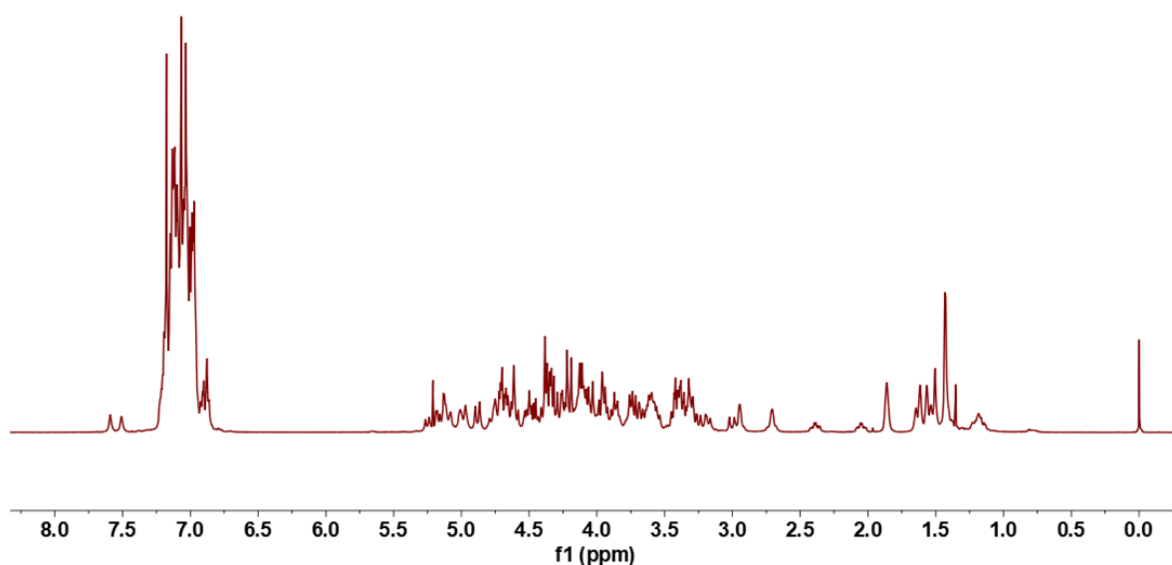


Figure 17: ¹H NMR (400 MHz, CDCl₃, 300K) of compound 10

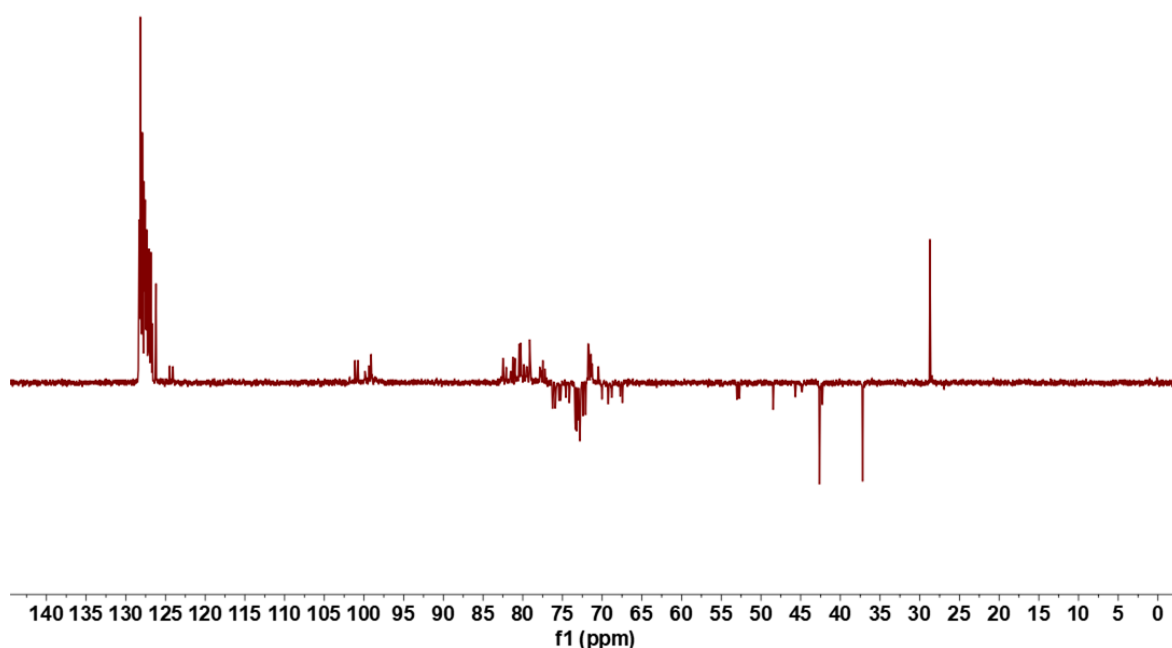
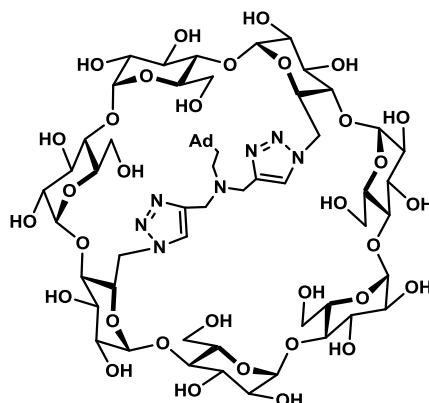


Figure 18: ¹³C NMR-DEPT 135 (100 MHz, CDCl₃, 300K) of compound 10

Procedure to obtain (11), (12) and (13)

The perbenzylated product 10 (200 mg, 0.063 mmol, 1 eq) was dissolved in THF/H₂O (3:1, 40 mL). 2, 2, 2-trifluoroacetic acid (39 μ L, 0.508 mmol, 8 eq) and Pd/C (290 mg, 2.73 mmol, 43 eq) was added. The mixture was purged 3 times with argon and 3 times with hydrogen. The reaction mixture was monitored by MS, and when the reaction completely finished: (a) then the mixture was purged under nitrogen, filtered through a pad of Celite and washed with MeOH/H₂O (3 \times 100 mL). The organic solvents were evaporated under vacuum and the residue was purified by a RediSep Rf Gold C-18 reversed-phase column using a gradient of ACN/water (%ACN: 0 => 5% in 10 min). The self-included derivative 11 was obtained as the white amorphous powder (25.6 mg, 28% yield) after freeze drying; (b) the reaction mixture was purged under nitrogen, filtered through a μ -filter (0.2 μ m-polyester). The organic solvent was evaporated under vacuum and the residue was lyophilized. The crude product was purified by a RediSep Rf Gold C-18 reversed-phase chromatography to afford the deprotected ditriazole-bridged N-ethyladamantyl- β -cyclodextrin 12 as the white amorphous powder (53.0 mg, 58% yield) after freeze drying; (c) the entirely protonated self-included derivative 13 was afforded by the self-included derivative 11 with 3 equivalent of 2, 2, 2-trifluoroacetic acid (TFA).

Self-included derivative

6^A, 6^D-Dideoxy-6^A, 6^D-di-triazole-bridged-N-ethyladamantyl- β -cyclodextrin (11)

Chemical Formula: $C_{60}H_{93}N_7O_{33}$
Exact Mass: 1439.5814

¹H NMR (600 MHz, D₂O, 300K): δ = 8.29 (s, 1H, 1 \times H_{triazA}), 7.85 (s, 1H, 1 \times H_{triazD}), 5.31 (d, 2H, 2 \times H1), 5.24-4.98 (m, 7H, 5 \times H1, 2 \times H6), 4.76 (m, 2H, 2 \times H6), 4.37-4.14 (m, 4H, 4 \times H6), 4.06-3.51 (m, 35H, 7 \times H2, 7 \times H3, 7 \times H4, 6 \times H5, 4 \times H6, 4 \times CHH_{triaz}), 3.45-3.26 (m, 2H, 1 \times H5, 1 \times H6), 3.00 (d, ³J_{H6-H5} = 8.0 Hz, 1H, 1 \times H6), 2.46 (br. m, 2H, 2 \times N-CHH-CH₂-Ad), 2.15 (s, 3H, Hb), 1.89 (br. m, 3H, Hc), 1.71 (br. m, 3H, Hc), 1.33 (br. m, 6H, Ha), 0.83 (br. m, 1H, 1 \times N-CH₂-CHH-Ad), 0.05 (br. m, 1H, 1 \times N-CH₂-CHH-Ad).

¹³C NMR (151 MHz, D₂O, 300K): δ = 128.98 (C_{triazA}), 123.21 (C_{triazD}), 102.79 (2 \times C1), 102.58 (C1), 102.55 (C1), 102.44 (2 \times C1), 102.08 (C1), 83.62 (C4), 83.48 (C4), 82.73 (C4), 82.16 (C4), 81.69 (C4), 81.55 (C4), 81.44 (C4), 74.98-71.49 (21C, 7 \times C2, 7 \times C3, 7 \times C5), 61.21 (C6), 60.83 (C6), 60.08 (2 \times CH₂_{triaz}), 58.85 (C6), 53.87 (C6), 52.14 (C6), 51.48 (C6), 51.42 (C6), 47.77 (N-CH₂-CH₂-Ad), 45.15 (N-CH₂-CH₂-Ad), 43.17 (Ca), 36.07 (Cc), 27.61 (Cb).

HMRS (ESI): calculated for [C₆₀H₉₃N₇O₃₃+H]⁺ 1440.5887; found 1440.5890.

EXPERIMENTAL PART

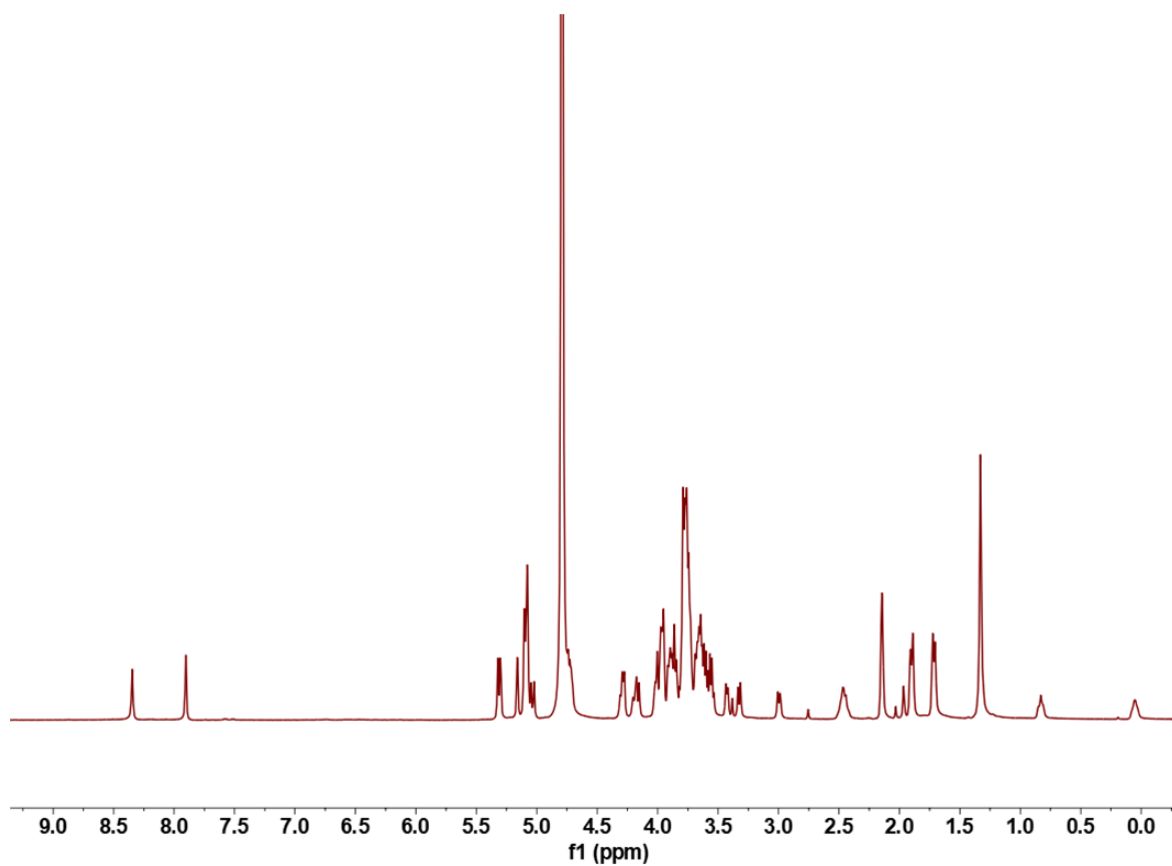


Figure 19: ¹H NMR (600 MHz, D₂O, 300K) of compound 11

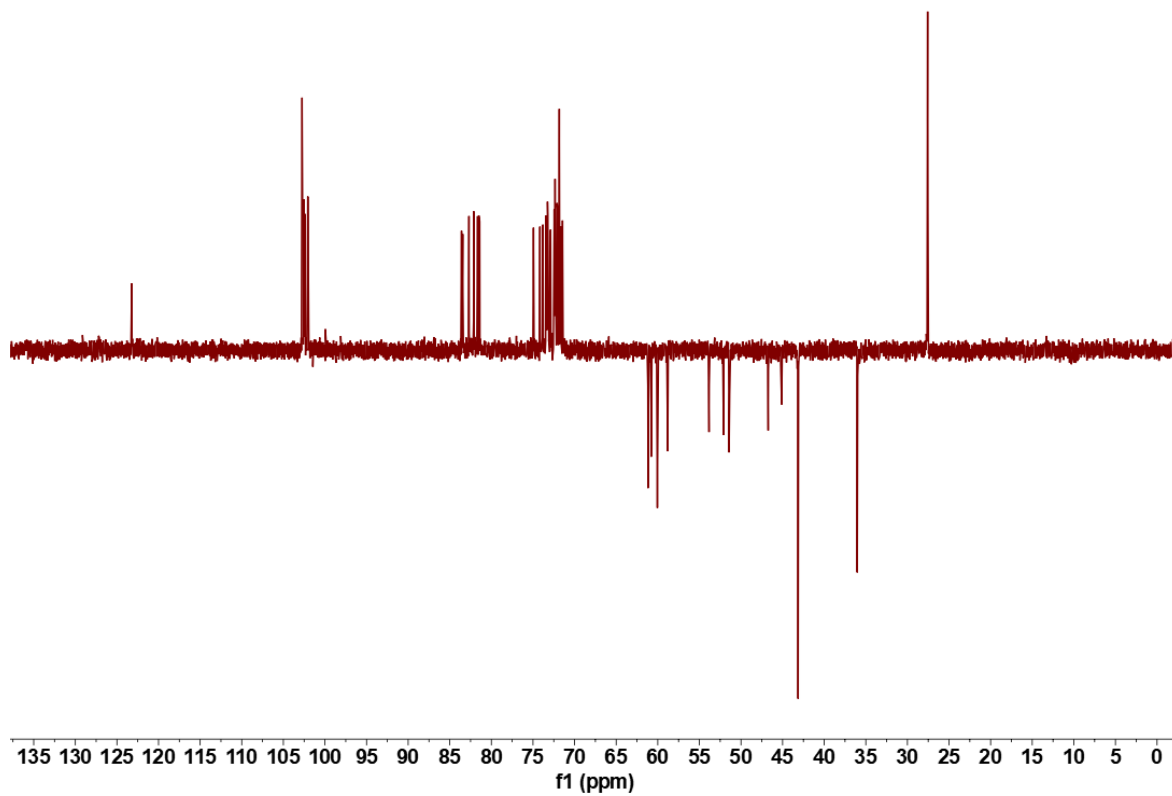
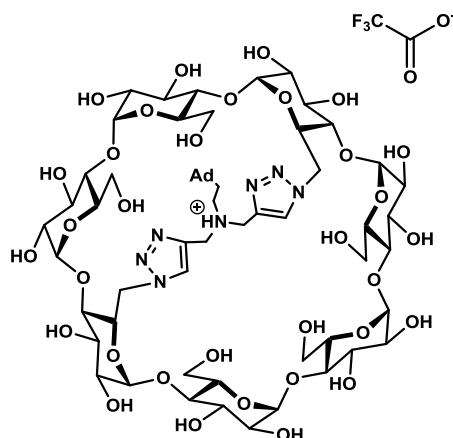


Figure 20: ¹³C NMR-DEPT 135 (151 MHz, D₂O, 300K) of compound 11

Monomer**6^A, 6^D-Dideoxy-6^A, 6^D-di-triazole-bridged-N-ethyladamantyl-β-cyclodextrin trifluoroacetate (12)**

Chemical Formula: $C_{60}H_{94}N_7O_{33}^+$
Exact Mass: 1440.5887

¹H NMR (600 MHz, D₂O, 300K): δ = 8.67-8.21 (br. m, 2H, 2× H_{triaz}), 5.26-5.15 (m, 2H, 2×H1), 5.15-4.85 (m, 7H, 5×H1, 2×H6), 4.84-4.60 (m, 2H, 2×H6), 4.00-3.25 (m, 38H, 7×H2, 7×H3, 7×H4, 7×H5, 10×H6), 3.23-2.85 (m, 6H, 4×CHH_{triaz}, 2×N-CHH-CH₂-Ad), 2.16 (s, 3H, H_b), 1.90 (br. m, 3H, H_c), 1.77 (br. m, 3H, H_c), 1.71-1.47 (br. m, 8H, H_a, 2×N-CH₂-CHH-Ad).

¹³C NMR (151 MHz, D₂O, 300K): δ = 128.41 (C_{triaz}), 127.76 (C_{triaz}), 102.51 (C1), 102.40 (C1), 102.22 (C1), 102.00 (C1), 101.71 (C1), 100.89 (2×C1), 83.53, 83.19, 82.29, 81.98, 81.49, 81.25, 80.18 (7×C4), 74.36-71.49 (21C, 7×C2, 7×C3, 7×C5), 61.70, 61.54, 60.75, 60.52, 60.16 (5×C6), 59.09 (CH₂triaz), 59.04 (CH₂triaz), 51.83 (2×C6), 49.22 (N-CH₂-CH₂-Ad), 41.76 (Ca), 36.98 (Cc), 28.43 (Cb), 27.87 (N-CH₂-CH₂-Ad).

HMRS (ESI): calculated for $[C_{60}H_{93}N_7O_{33}+H]^+$ 1440.5887; found 1440.5890.

EXPERIMENTAL PART

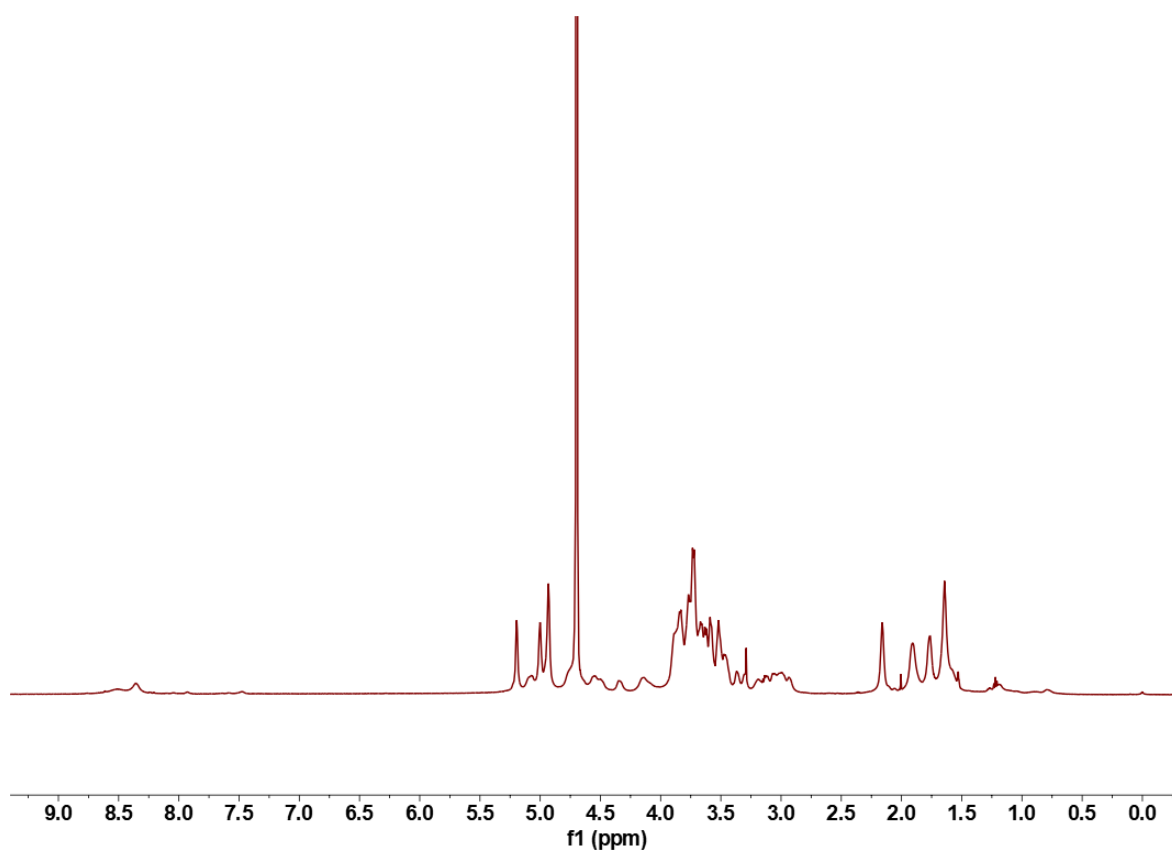


Figure 21: ^1H NMR (600 MHz, D_2O , 300K) of compound 12

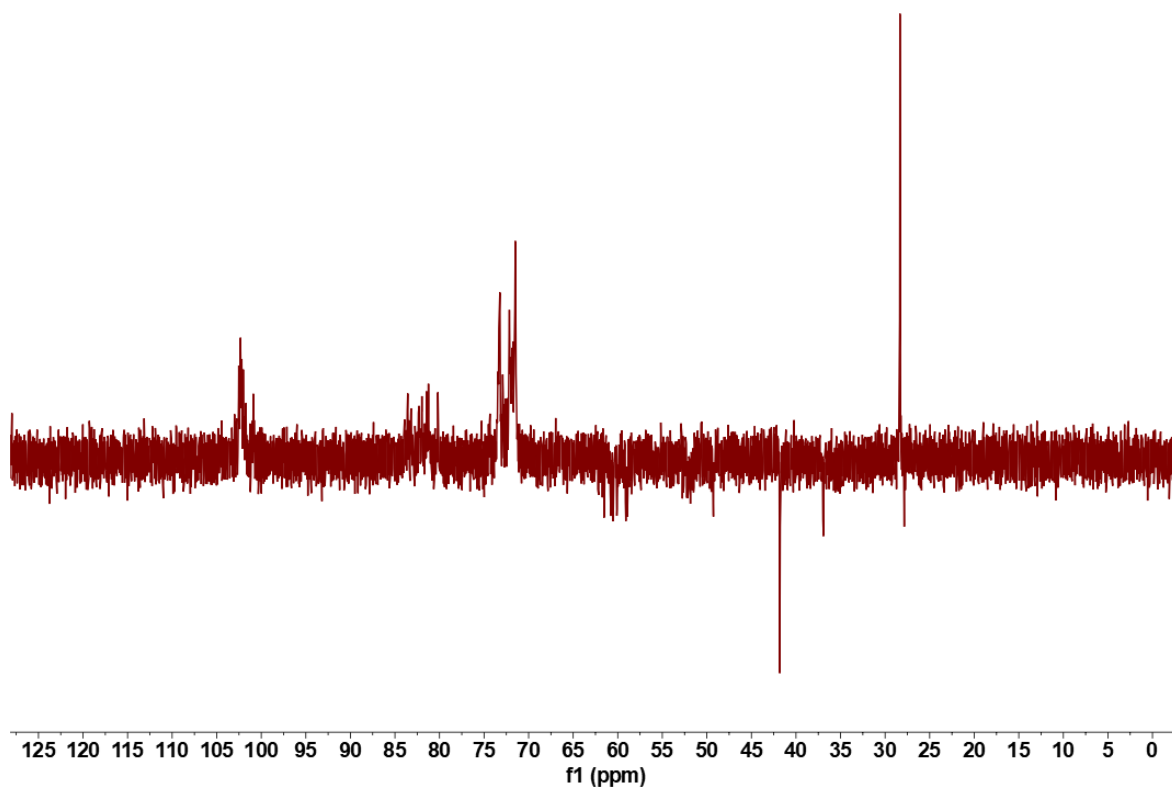
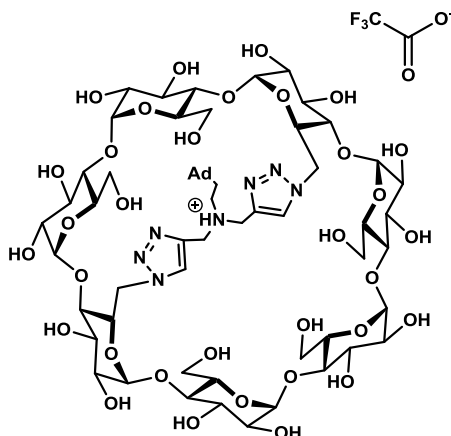


Figure 22: ^{13}C NMR-DEPT 135 (151 MHz, D_2O , 300K) of compound 12

Entirely protonated self-included derivative

6^A, 6^D-Dideoxy-6^A, 6^D-di-triazole-bridged-N-ethyladamantyl-β-cyclodextrin trifluoroacetate (13)

Chemical Formula: $C_{60}H_{94}N_7O_{33}^+$
Exact Mass: 1440.5887

¹H NMR (600 MHz, D₂O, 300K): δ = 8.74 (s, 1H, 1×*H*_{triazA}), 8.37 (s, 1H, 1×*H*_{triazD}), 5.33 (d, ³*J*_{H1-H2} = 6.0 Hz, 2H, 2×H1), 5.16 (m, 2H, 2×H1), 5.13-5.07 (m, 4H, 3×H1, 1×H6), 5.06-4.99 (m, 2H, 2×H6), 4.92 (d, ²*J*_{H6-H6'} = 15.0 Hz, 1H, 1×H6), 4.76 (m, 2H, 2×H6), 4.66 (d, ²*J*_{H6-H6'} = 12.3 Hz, 1H, 1×H6), 4.28 (d, ²*J*_{H6-H6'} = 12.4 Hz, 1H, 1×H6), 4.12 (d, ²*J*_{H6-H6'} = 10.2 Hz, 1H, 1×H6), 4.06-4.00 (m, 2H, 2×H6), 4.00-3.95 (m, 1H, 1×H3), 3.94-3.64 (m, 26H, 6×H2, 6×H3, 7×H5, 3×H6, 4×CHH_{triaz}), 3.64-3.50 (m, 8H, 7×H4, 1×H2), 3.29 (br. m, 1H, 1×N-CHH-CH₂-Ad), 2.94 (br. m, 1H, 1×N-CHH-CH₂-Ad), 2.21 (s, 3H, H_b), 1.91 (br. m, 3H, H_c), 1.72 (br. m, 3H, H_c), 1.26 (br. m, 6H, H_a), 0.89 (br. m, 1H, 1×N-CH₂-CHH-Ad), 0.10 (br. m, 1H, 1×N-CH₂-CHH-Ad).

¹³C NMR (151 MHz, D₂O, 300K): δ = 128.56 (*C*_{triazA}), 124.34 (*C*_{triazD}), 102.74 (2×C1), 102.50 (C1), 102.16 (2×C1), 102.10 (C1), 83.71 (C3), 83.47 (C3), 82.74 (2×C4), 82.45 (2×C4), 81.98 (C4), 81.90 (C2), 81.65 (C4), 74.82 (C5), 73.75-71.42 (19C, 7×C2, 6×C3, 6×C5), 61.45 (C6), 61.24 (C6), 60.55 (C6), 60.46 (C6), 59.77 (2×CH₂_{triaz}), 52.41 (C6), 51.92 (C6), 51.57 (C6), 47.74 (N-CH₂-CH₂-Ad), 42.76 (C_a), 42.10 (N-CH₂-CH₂-Ad), 35.93 (C_c), 27.49 (C_b).

EXPERIMENTAL PART

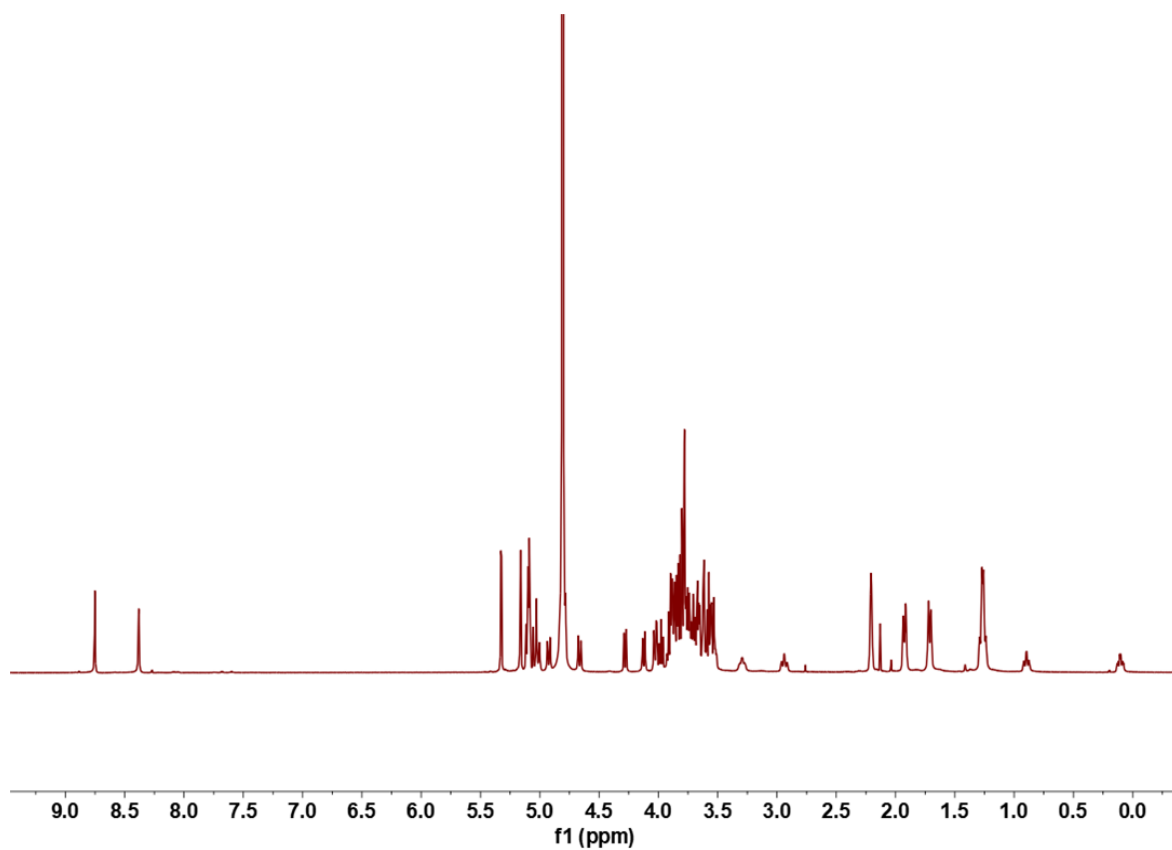


Figure 23: ¹H NMR (600 MHz, D₂O, 300K) of compound 13

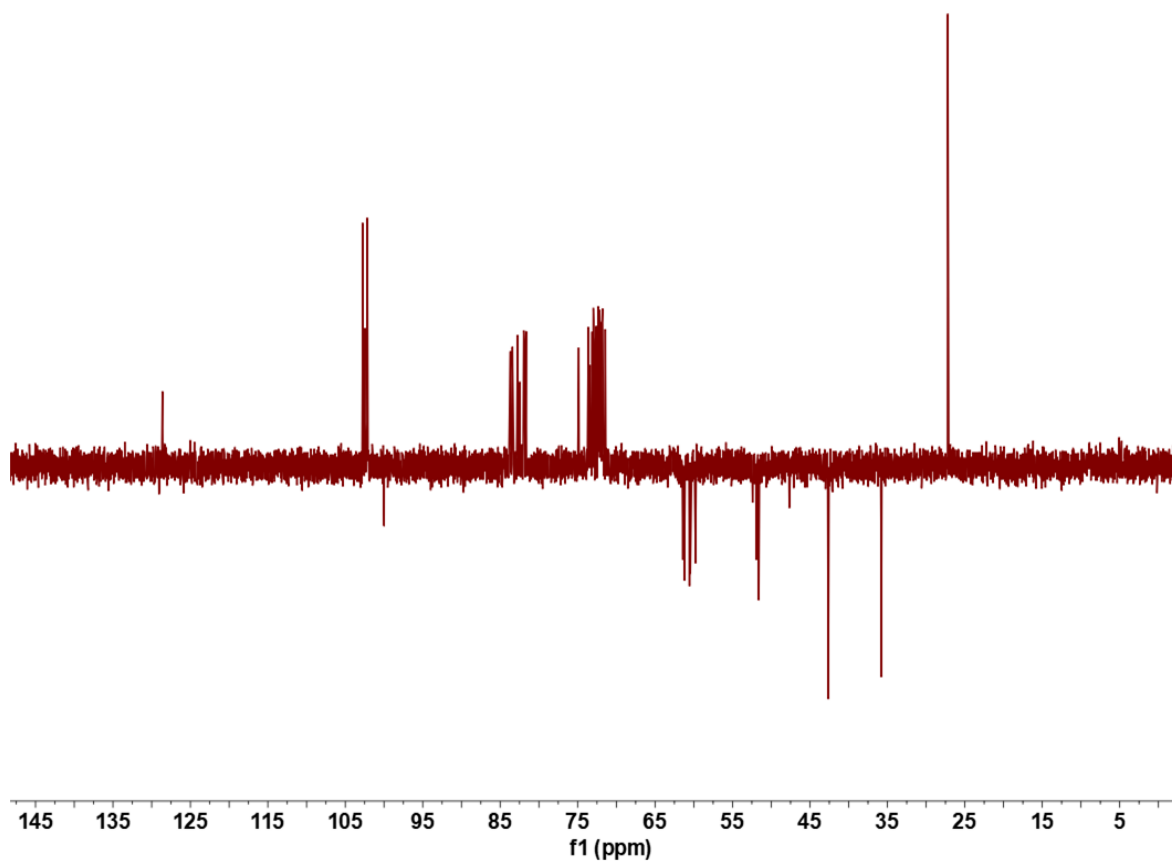
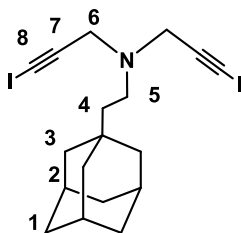


Figure 24: ¹³C NMR-DEPT 135 (151 MHz, D₂O, 300K) of compound 13

N-(2-((3r, 5r, 7r)-Adamantan-1-yl)ethyl)-3-iodo-N-(3-iodoprop-2-yn-1-yl)-prop-2-yn-1-amine (14)



Chemical Formula: $C_{18}H_{23}I_2N$
Exact Mass: 506.9920

The dialkyne product 9 (500 mg, 1.96 mmol, 1eq) was placed 25 mL flame-dried argon-filled flask sealed with a sleeve stopper and 5 mL of distilled THF was added. The solution was cooled to $-78^{\circ}C$ and n-BuLi solution in hexanes (3.2 mL, 7.83 mmol, 4 eq, 2.5 M) was added dropwise. The mixture was stirred at $-78^{\circ}C$ for 30 min, then I_2 (1.98 g, 7.83 mmol, 4 eq) solution in 2 mL of distilled THF was slowly added via syringe. The solution was warmed to room temperature overnight and poured into water, then the aqueous phase was extracted with Et_2O (3×10 mL), and the combined organic layers were washed with brine, dried over $MgSO_4$, filtered and concentrated in vacuo. The residue was purified over silica gel chromatography (cyclohexane/ $EtOAc$ 1:0 then 5:1) to afford desired di-iodo-dialkyne product 14 (694 mg, 70% yield) as the yellow solid.

1H NMR (600 MHz, $CDCl_3$, 300K): δ = 3.57 (s, 4H, 4H-6), 2.50 (m, 2H, 2H-5), 1.95 (s, 3H, 3H-2), 1.73-1.64 (m, 6H, 6H-1), 1.49 (s, 6H, 6H-3), 1.26-1.21 (m, 2H, 2H-4).

^{13}C NMR (151 MHz, $CDCl_3$, 300K): δ = 89.80 (2C, C-7, C-8), 47.34 (C-5), 44.30 (C-6), 42.44 (C-3), 41.56 (C-1), 37.12 (C-4) 31.89 (C-2), 28.64 (Cquat-Ad).

HMRS (ESI): calculated for $[C_{18}H_{23}I_2N+Na]^+$ 529.9812; found 529.9798.

EXPERIMENTAL PART

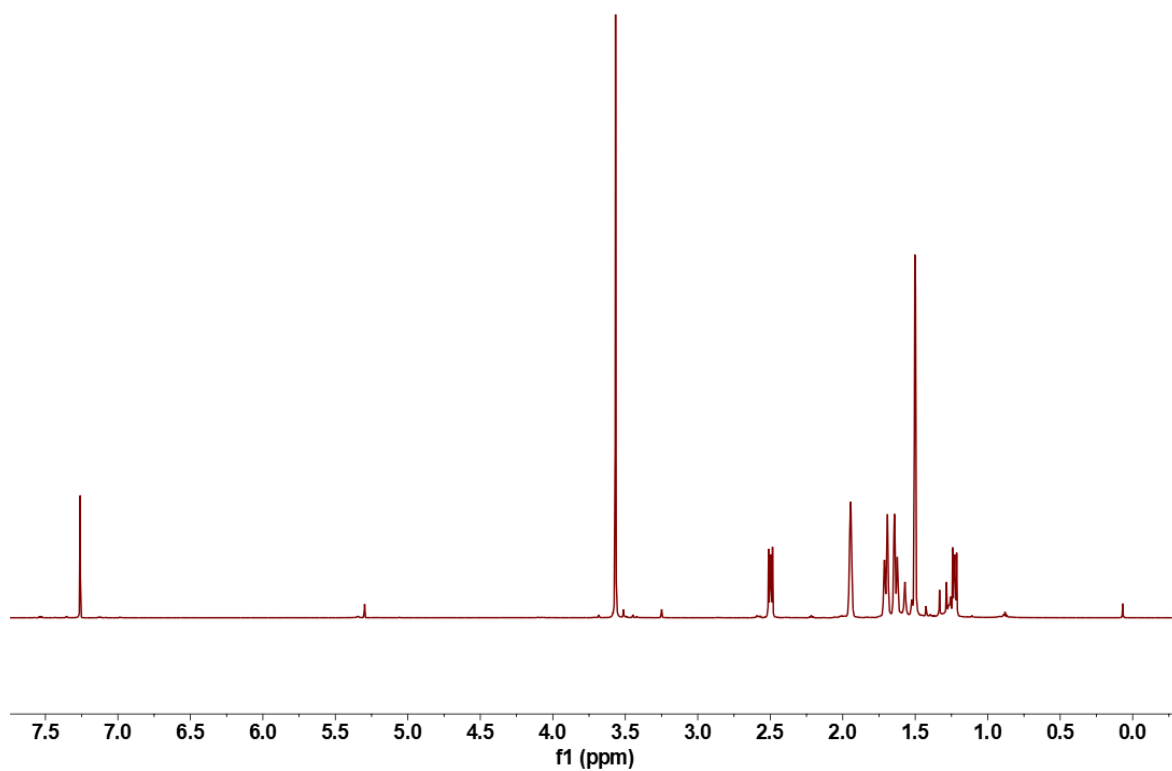


Figure 25: ¹H NMR (600 MHz, CDCl₃, 300K) of compound 14

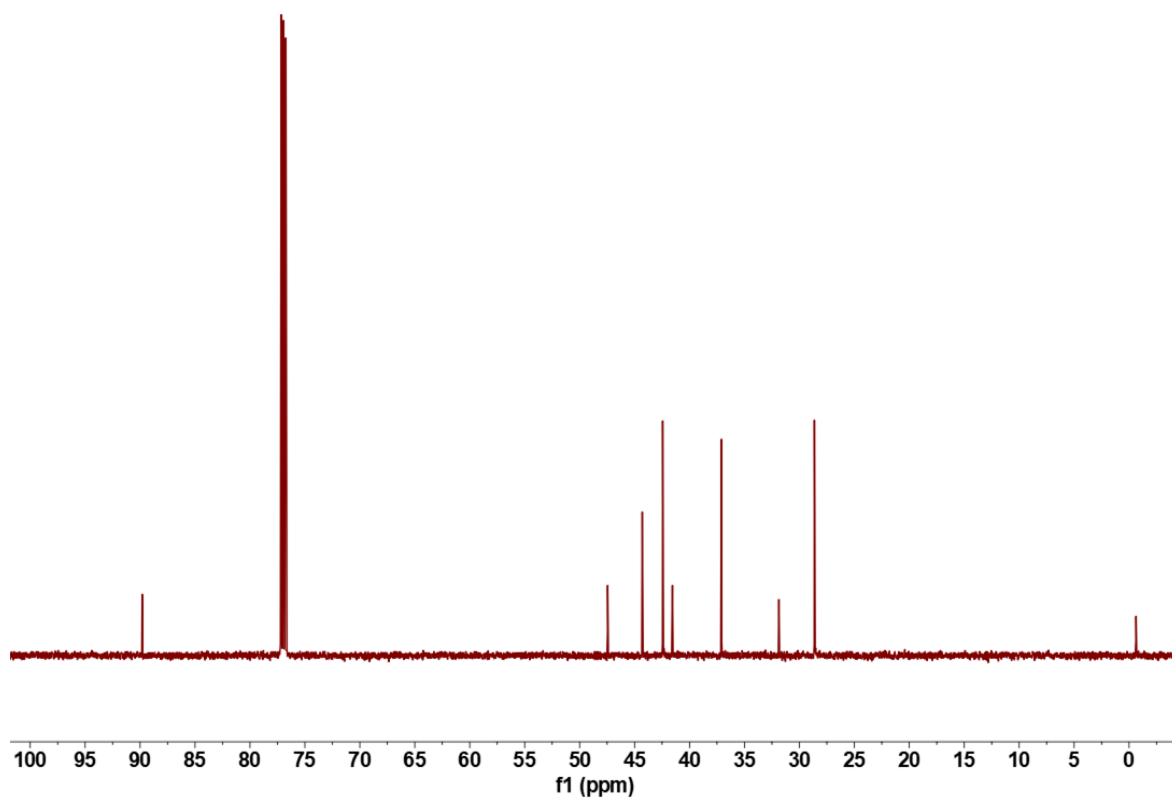
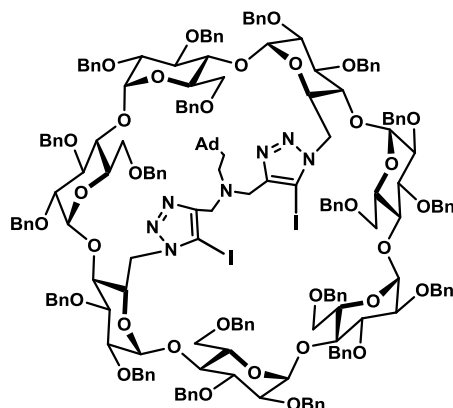


Figure 26: ¹³C NMR (151 MHz, CDCl₃, 300K) of compound 14

**6^A, 6^D-Dideoxy-6^A, 6^D-di-iodotriazole-bridged-N-ethyladamantyl-
2^{A-G}, 3^{A-G}, 6^B, 6^C, 6^E, 6^F, 6^G-nonadeca-O-benzyl-β-cyclodextrin (15)**



Chemical Formula: $C_{193}H_{205}I_2N_7O_{33}$
Exact Mass: 3402.2668

To a solution of product 7 (1 g, 0.345 mmol, 1 eq) in 12 mL DMF followed by di-iodoalkyne product 14 (210 mg, 0.414 mmol, 1.2 eq) and DIPEA (24 μ L, 0.138 mmol, 0.4 eq) was added. A mixture of TBTA (73 mg, 0.138 mmol, 0.4 eq) and $Cu(CH_3CN)_4PF_6$ (52 mg, 0.138 mmol, 0.4 eq) in 1 mL DMF was added. The mixture solution was stirred at 150°C under argon atmosphere for 1 h. Finally, the mixture solution was diluted with diethyl ether (100 mL). The organic solution was washed with 1:1 water/brine solution (2×100 mL), HCl solution (1 M in water, 100 mL), the saturated aqueous solution of $NaHCO_3$ (100 mL), then passed over $MgSO_4$, filtered and concentrated in vacuo. The residue was purified over silica gel chromatography (cyclohexane/EtOAc 7:3) to afford desired diiodotriazole-bridged modified β -cyclodextrin 15 (705 mg, 60% yield) as the yellow foam.

¹H NMR (400 MHz, $CDCl_3$, 300K): δ =7.28-6.81 (m, 95H, 95× H_{Ph}), 5.56 (s, 1H, 1× H_1), 5.29 (d, 2J =7.2 Hz, 1H, 1× CHH_{Ph}), 5.24 (s, 1H, 1× H_1), 5.16 (d, 2J =6.0 Hz, 1H, 1× CHH_{Ph}), 5.08 (s, 1H, 1× H_1), 5.02 (d, 2J =6.0 Hz, 2H, 2× CHH_{Ph}), 4.94 (br. m, 1× H_1 , 1× CHH_{Ph}), 4.82 (s, 1H, 1× H_1), 4.78-4.50 (m, 17H, 2× H_1 , 4× H_6 , 11× CHH_{Ph}), 4.48-4.20 (m, 26H, 1× H_5 , 3× H_6 , 22× CHH_{Ph}), 4.17-3.70 (m, 21H, 7× H_3 , 6× H_4 , 5× H_5 , 3× H_6), 3.64-3.27 (m, 14H, 6× H_2 , 1× H_4 , 1× H_5 , 3× H_6 , 3× CHH_{triaz}), 3.23 (m, 2H, 1× H_2 , 1× H_6), 3.13 (d, 2J =7.2 Hz, 1H, 1× CHH_{triaz}), 2.90 (br. m, 1H, 1× $N-CHH-CH_2-Ad$), 2.47 (br. m, 1H, 1× $N-CHH-CH_2-Ad$), 1.85 (s, 3H, H_b), 1.61 (br. m, 6H, H_c), 1.45 (br. m, 6H, H_a), 1.22-1.13 (m, 2H, 2× $N-CH_2-CHH-Ad$).

¹³C NMR (100 MHz, $CDCl_3$, 300K): δ =129.69-125.13 (97C, 95× $CH-Ar$, 2× C_{triaz}), 99.94 (2× C_1), 99.46 (C1), 99.05 (C1), 98.71 (C1), 98.68 (C1), 98.34 (C1), 82.12 (C4), 81.48 (C4), 81.17-79.98 (11C, 7× C_3 , 4× C_4), 79.71 (C2), 79.54 (C2), 79.24 (C2), 79.14 (C2), 78.93 (C2), 77.85 (2C, 1× C_2 , 1× C_4), 77.25 (C2), 76.24-73.62 (5× CH_2-Ph), 73.45-72.57 (12× CH_2-Ph),

EXPERIMENTAL PART

72.12 (2×CH₂-Ph), 71.80 (2×C5), 71.65 (2×C5), 71.60 (2×C5), 71.44 (C5), 69.50, 69.22, 68.86, 68.72, 68.49, 53.07 (6×C6), 51.37 (N-CH₂-CH₂-Ad), 47.96 (2×CH₂triaz), 44.30 (C6), 42.69 (Ca), 41.99 (N-CH₂-CH₂-Ad), 37.25 (Cc), 28.55 (Cb).

HMRS (ESI): calculated for [C₁₉₃H₂₀₅I₂N₇O₃₃+Na]⁺ 3425.2560; found 3425.2585.

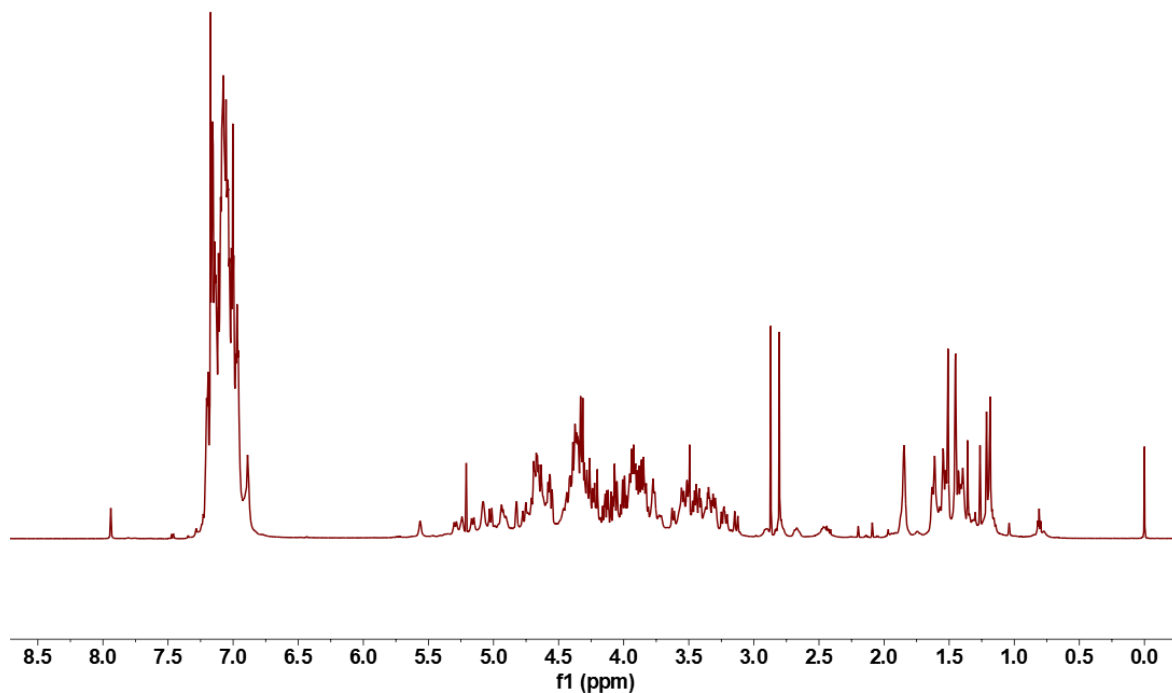


Figure 27: ¹H NMR (400 MHz, CDCl₃, 300K) of compound 15

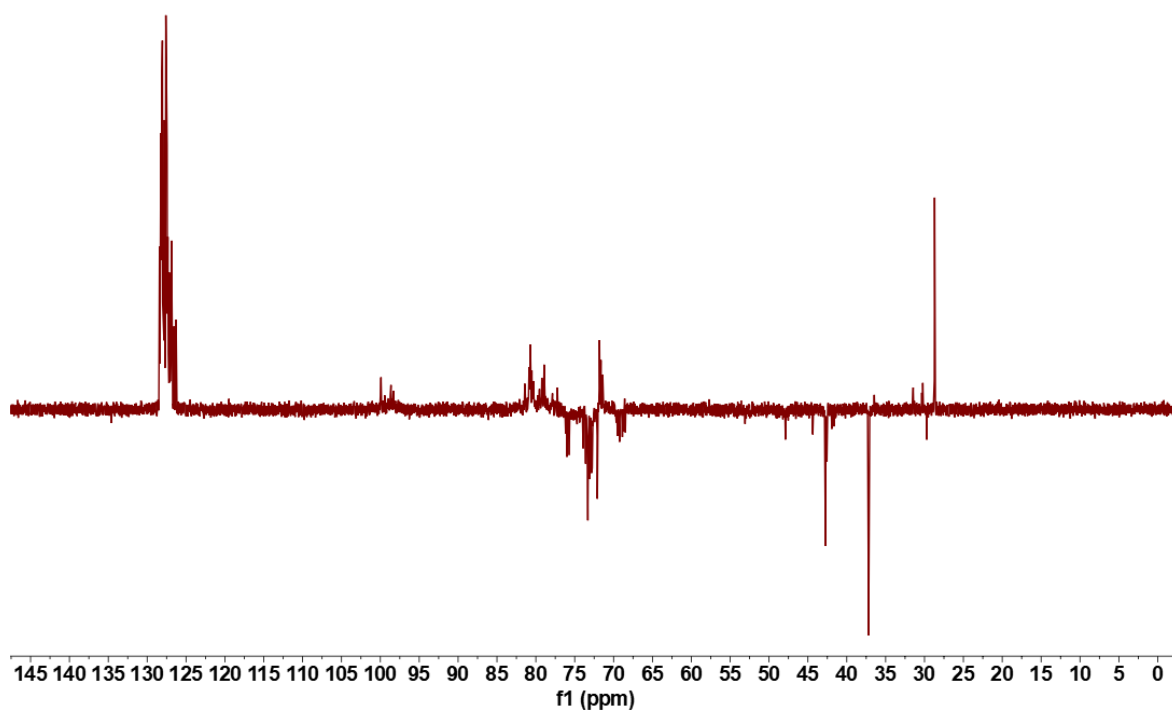
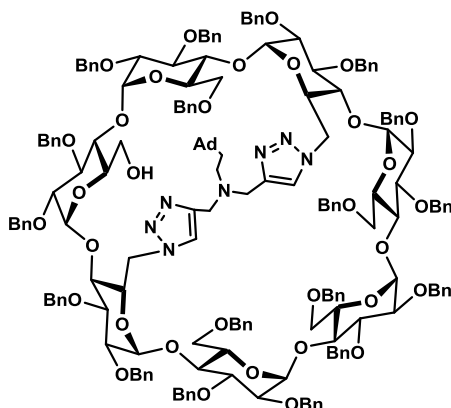


Figure 28: ¹³C NMR-DEPT 135 (100 MHz, CDCl₃, 300K) of compound 15

6^A, 6^C, 6^D-Trideoxy-6^A, 6^D-di-triazole-bridged-N-ethyladamantyl-6^C-hydroxyl-2^{A-G}, 3^{A-G}, 6^B, 6^E, 6^F, 6^G-octadeca-O-benzyl-β-cyclodextrin (16)



Chemical Formula: C₁₈₆H₂₀₁N₇O₃₃
Exact Mass: 3060.4265

To a stirred solution of di-triazole-bridged modified β-cyclodextrin 10 (1.8 g, 0.571 mmol, 1 eq) in toluene (3.8 mL) was added DIBAL-H (1.5 M in toluene, 7.6 mL, 11.418 mmol, 20 eq) was added dropwise at room temperature. The reaction mixture was heated at 60°C and put under nitrogen flux. The reaction mixture was monitored by MS. The reaction mixture was carefully and slowly poured in an ice/water bath (30mL) while stirring frequently. Ethyl acetate (40 mL) and HCl solution (1 M in water, 15 mL) were then added. The mixture was stirred for 3 h and then the aqueous phase was extracted with ethyl acetate (3×40 mL), and the combined organic layers were washed with brine, dried over MgSO₄, filtered and concentrated in vacuo. The residue was purified over silica gel chromatography (cyclohexane/EtOAc 4:1 then 2:1) to afford trideoxy-di-triazole-bridged modified β-cyclodextrin 16 (979 mg, 56% yield) as the white foam.

¹H NMR (400 MHz, CDCl₃, 300K): δ = 7.61 (s, 1H, 1×H_{triazA}), 7.38 (s, 1H, 1×H_{triazD}), 7.37-6.86 (m, 90H, 90×H_{Ph}), 5.49 (d, ³J_{H1-H2} = 4.0 Hz, 1H, 1×H1), 5.35-4.89 (m, 9H, 4×H1, 2×H6, 3×CHHPh), 4.89-4.55 (m, 16H, 2×H1, 2×H5, 12×CHHPh), 4.55-4.11 (m, 27H, 1×H4, 2×H5, 3×H6, 21×CHHPh), 4.11-3.75 (m, 9H, 7×H3, 1×H4, 1×H5), 3.73-3.25 (m, 22H, 7×H2, 5×H4, 2×H5, 7×H6, 1×CHH_{triaz}), 3.24-3.02 (m, 3H, 2×H6, 1×CHH_{triaz}), 2.92-2.76 (m, 2H, 2×CHH_{triaz}), 2.59 (br. m, 1H, 1×N-CHH-CH₂-Ad), 2.39 (br. m, 1H, 1×N-CHH-CH₂-Ad), 1.97 (s, 3H, Hb), 1.81-1.60 (br. m, 7H, Hc, 1×N-CH₂-CHH-Ad), 1.60-1.49 (br. m, 7H, Ha, 1×N-CH₂-CHH-Ad).

¹³C NMR (100 MHz, CDCl₃, 300K): δ = 129.72-125.71 (90C, CH-Ar), 123.28 (2×C_{triaz}), 101.79 (C1), 101.16 (C1), 99.68 (C1), 99.12 (C1), 98.41 (2×C1), 96.54 (C1), 83.09 (C2), 81.98 (C4), 81.80 (C4), 81.46 (C4), 81.29-76.17 (16C, 5×C2, 7×C3, 4×C4), 75.33 (C2), 76.11, 75.74, 75.55, 74.81, 74.55, 73.74 (6×CH₂-Ph), 73.43-72.30 (12×CH₂-Ph), 71.75 (2×C5), 71.57 (C5),

EXPERIMENTAL PART

71.45 (2×C5), 70.17 (C6), 69.99 (2×C5), 69.09 (C6), 67.82 (C6), 67.20 (CH₂triazD), 61.95 (C6), 52.65 (2×C6), 48.62 (N-CH₂-CH₂-Ad), 46.22 (C6), 45.46 (CH₂triazA), 42.47 (Ca), 36.96 (2C, 1×C_C, 1×N-CH₂-CH₂-Ad), 28.84 (Cb).

HMRS (ESI): calculated for [C₁₈₆H₂₀₁N₇O₃₃+Na]⁺ 3083.4158; found 3083.4186.

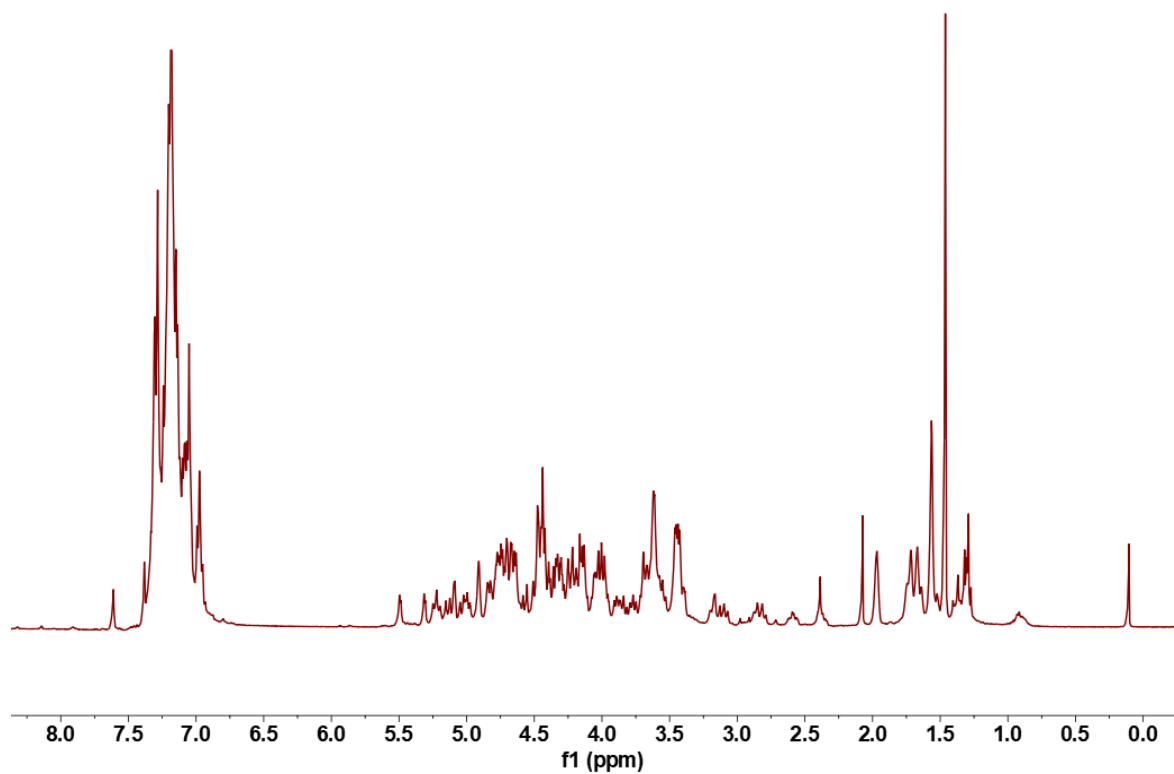


Figure 29: ¹H NMR (400 MHz, CDCl₃, 300K) of compound 16

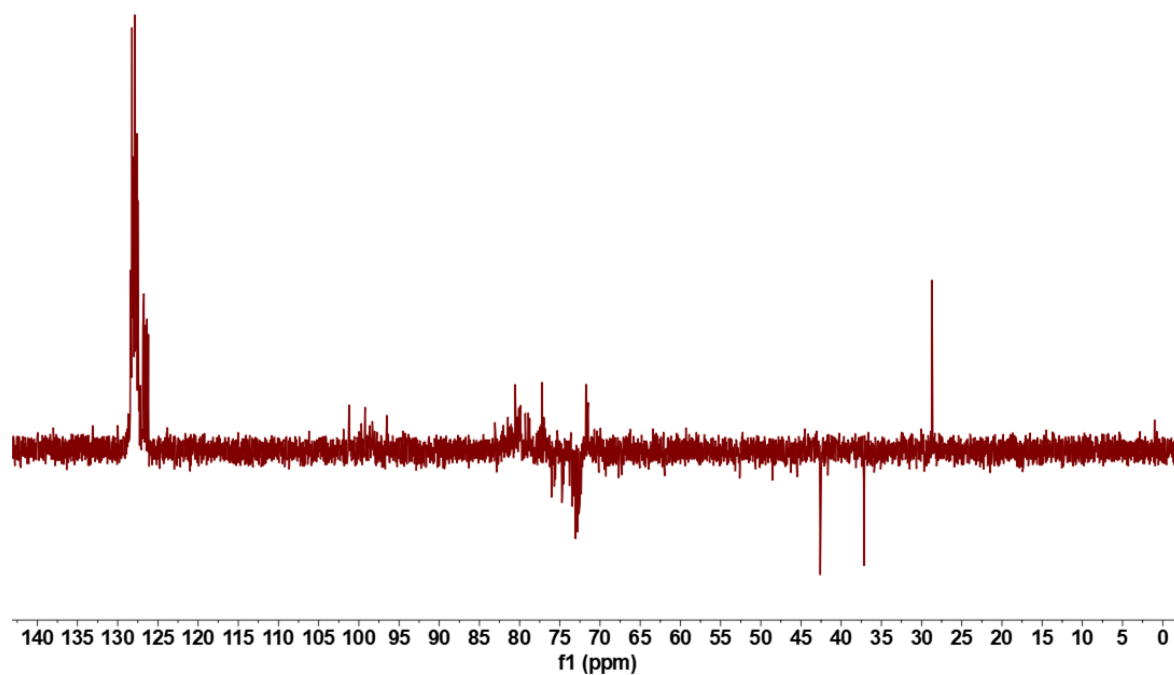
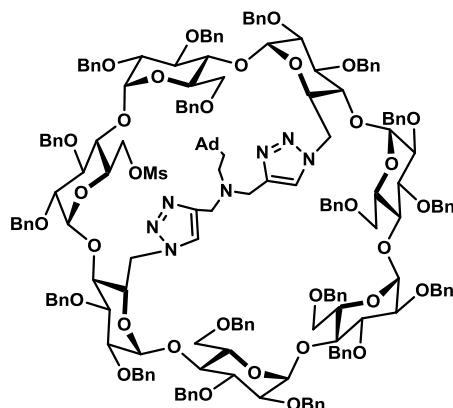


Figure 30: ¹³C NMR-DEPT 135 (100 MHz, CDCl₃, 300K) of compound 16

6^A, 6^C, 6^D-Trideoxy-6^A, 6^D-di-triazole-bridged-N-ethyladamantyl-6^C-methanesulfonyl-2^{A-G}, 3^{A-G}, 6^B, 6^E, 6^F, 6^G-octadeca-O-benzyl-β-cyclodextrin (17)



Chemical Formula: C₁₈₇H₂₀₃N₇O₃₅S
Exact Mass: 3138.4041

To a cooled solution (0°C) of trideoxy-di-triazole-bridged modified β-cyclodextrin 16 (800 mg, 0.261 mmol, 1 eq) in DCM (3.5 mL) followed by triethylamine (146 μL, 1.05 mmol, 4 eq) and mesyl chloride (81.5 μL, 1.05 mmol, 4 eq) sequentially added. The mixture solution was stirred at room temperature under nitrogen atmosphere, and the reaction progress was monitored by TLC (cyclohexane/AcOEt 6:4) after 1 h. Finally, the mixture solution was quenched with H₂O and diluted with DCM (5 mL). The aqueous phase was extracted with DCM (3×10 mL), and the combined organic layers were washed with water, brine, passed over MgSO₄, filtered and concentrated in vacuo. The residue was purified over silica gel chromatography (cyclohexane/EtOAc 4:1) to afford desired product 17 (600 mg, 73% yield) as the white foam.

¹H NMR (400 MHz, CDCl₃, 300K): δ = 7.98 (s, 1H, 1×H_{triazA}), 7.51 (s, 1H, 1×H_{triazD}), 7.47-6.87 (m, 90H, 90×H_{Ph}), 5.47 (s, 1H, 1×H₁), 5.39 (d, ²J = 11.2 Hz, 1H, 1×CHH_{Ph}), 5.29-5.13 (m, 3H, 2×H₁, 1×CHH_{Ph}), 5.11-4.94 (m, 5H, 1×H₁, 2×H₆, 2×CHH_{Ph}), 4.93-4.66 (m, 15H, 3×H₁, 1×H₅, 11×CHH_{Ph}), 4.66-4.32 (m, 19H, 2×H₅, 1×H₆, 16×CHH_{Ph}), 4.32-3.91 (m, 20H, 7×H₃, 2×H₄, 3×H₅, 3×H₆, 5×CHH_{Ph}), 3.91-3.63 (m, 9H, 3×H₄, 1×H₅, 5×H₆), 3.63-3.34 (m, 11H, 7×H₂, 2×H₄, 1×H₆, 1×CHH_{triaz}), 3.18 (br. m, 1H, 1×CHH_{triaz}), 3.09 (d, ²J = 10.4 Hz, 1H, 1×CHH_{triaz}), 2.97 (d, ²J = 11.2 Hz, 1H, 1×CHH_{triaz}), 2.66-2.51 (br. m, 4H, 3×OSO₂CH₂H, 1×N-CHH-CH₂-Ad), 2.30 (br. m, 1H, 1×N-CHH-CH₂-Ad), 1.99 (s, 3H, H_b), 1.79-1.66 (br. m, 7H, 1×N-CH₂-CHH-Ad, H_c), 1.66-1.54 (br. m, 7H, H_a, 1×N-CH₂-CHH-Ad).

¹³C NMR (100 MHz, CDCl₃, 300K): δ = 129.78-124.79 (90C, CH-Ar), 124.25 (2×C_{triaz}), 101.04 (2×C₁), 100.63 (2×C₁), 99.16 (C₁), 98.33 (C₁), 97.80 (C₁), 82.80 (C₄), 82.58 (C₄), 81.35 (C₄), 81.27-80.20 (11C, 7×C₃, 4×C₄), 79.89 (C₂), 79.85 (2×C₂), 79.52 (2C, 1×C₂, 1×C₄),

EXPERIMENTAL PART

79.22 (C2), 77.60 (2×C2), 76.11 (CH₂-Ph), 75.82 (C5), 75.78-75.33 (2×CH₂-Ph), 75.19 (CH₂-Ph), 74.58-74.10 (5×CH₂-Ph), 73.50-72.27 (8×CH₂-Ph), 71.81 (C5), 71.64 (C5), 71.57 (C5), 71.23 (C5), 70.03 (C5), 69.95 (C5), 69.62 (CH₂-Ph), 69.10 (C6), 69.07 (C6), 69.03 (C6), 67.34 (CH₂triaz), 52.94 (C6), 52.87 (C6), 48.82 (N-CH₂-CH₂-Ad), 45.59 (C6), 45.47 (C6), 45.46 (CH₂triaz), 42.56 (Ca), 37.46 (2C, 1×Cc, 1×OSO₂CH₃), 36.05 (N-CH₂-CH₂-Ad), 28.64 (Cb).

HMRS (ESI): calculated for [C₁₈₇H₂₀₃N₇O₃₅S+Na]⁺ 3161.3933; found 3161.3958.

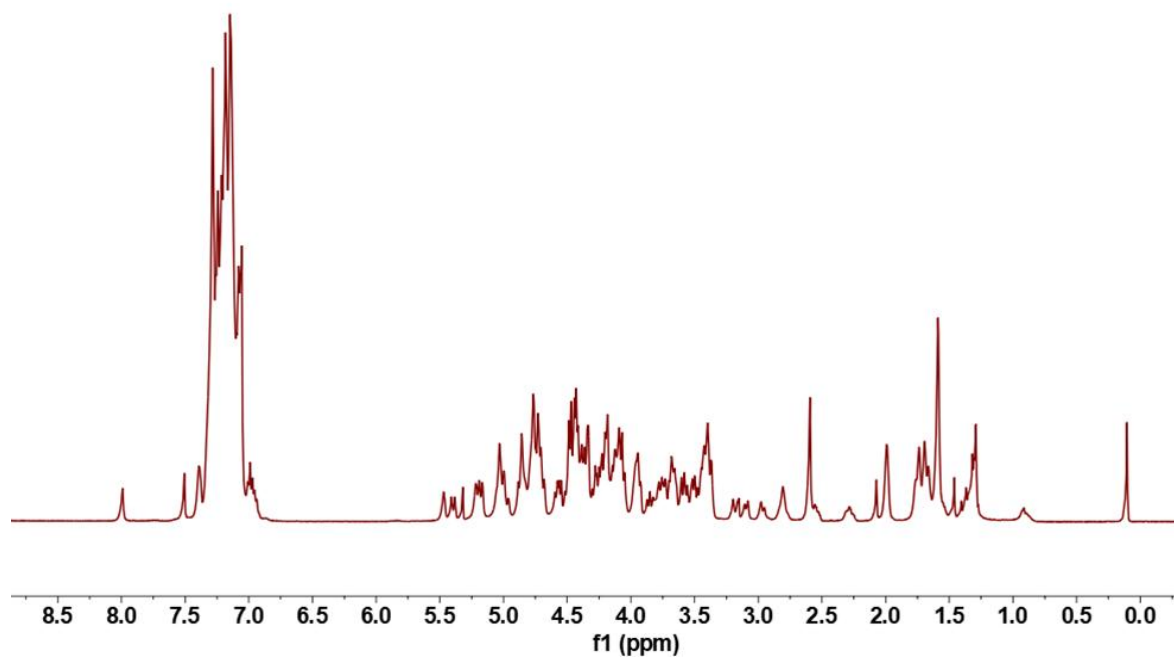


Figure 31: ¹H NMR (400 MHz, CDCl₃, 300K) of compound 17

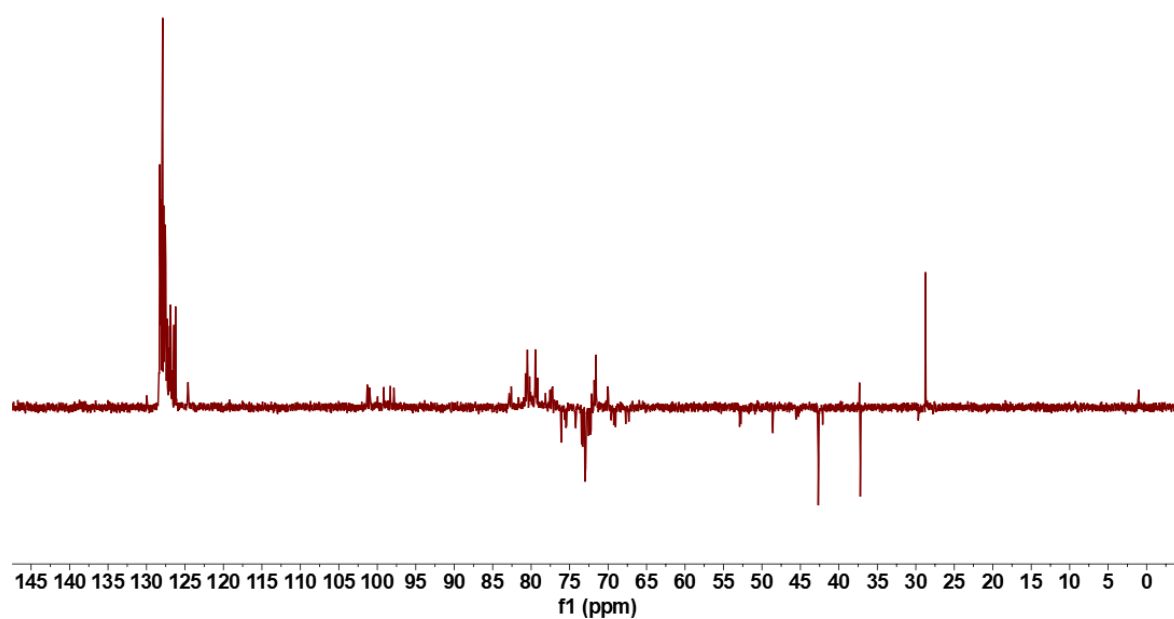
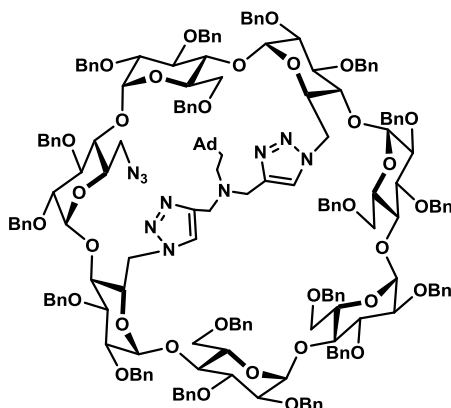


Figure 32: ¹³C NMR-DEPT 135 (100 MHz, CDCl₃, 300K) of compound 17

**6^A, 6^C, 6^D-Trideoxy-6^A, 6^D-di-triazole-bridged-N-ethyladamantyl-6^C-azido-
2^{A-G}, 3^{A-G}, 6^B, 6^E, 6^F, 6^G-octadeca-O-benzyl-β-cyclodextrin (18)**



Chemical Formula: C₁₈₆H₂₀₀N₁₀O₃₂
Exact Mass: 3085.4330

Product 17 (1.5 g, 0.478 mmol, 1 eq) was solubilized in dry DMF (21 mL) under argon atmosphere, sodium azide (250 mg, 3.82 mmol, 8 eq) was added. The mixture solution was stirred at 80°C. The reaction progress was monitored by TLC (cyclohexane/EtOAc 2:1) after 2 h. Water (20 mL) and ethyl acetate (20 mL) were added, and the aqueous phase was extracted with ethyl acetate (3×30 mL), and the combined organic layers were washed with 1:1 water/brine solution, dried over MgSO₄, filtered and concentrated in vacuo. The obtained residue was purified by silica gel chromatography (cyclohexane/EtOAc 3:1) to give product 18 (1.3 g, 87% yield) as the white foam.

¹H NMR (400 MHz, CDCl₃, 300K): δ =8.11 (s, 1H, 1×H_{triazA}), 7.55-6.87 (m, 91H, 1×H_{triazD}, 90×H_{Ph}), 5.45 (s, 1H, 1×H1), 5.32-5.21 (m, 2H, 2×CHHPh), 5.19-4.94 (m, 7H, 3×H1, 2×H6, 2×CHHPh), 4.94-4.59 (m, 16H, 3×H1, 1×H5, 12×CHHPh), 4.59-4.30 (m, 16H, 1×H5, 1×H6, 14×CHHPh), 4.30-4.09 (m, 11H, 2×H3, 1×H4, 1×H5, 1×H6, 6×CHHPh), 4.09-3.82 (m, 10H, 5×H3, 2×H4, 2×H5, 1×H6), 3.82-3.56 (m, 8H, 1×H2, 3×H4, 1×H5, 3×H6), 3.56-3.32 (m, 11H, 6×H2, 1×H4, 1×H5, 3×CHH_{triaz}), 3.23-3.10 (m, 3H, 2×H6, 1×CHH_{triaz}), 3.02 (d, ³J_{H6-H5} =10.4 Hz, 1H, 1×H6), 2.92 (d, ³J_{H6-H5} =10.8 Hz, 1H, 1×H6), 2.73 (br. m, 2H, 2×H6), 2.57 (br. m, 1H, 1×N-CHH-CH₂-Ad), 2.27 (br. m, 1H, 1×N-CHH-CH₂-Ad), 2.01 (s, 3H, H_b), 1.85-1.58 (m, 14H, 2×N-CH₂-CHH-Ad, H_c, H_a).

¹³C NMR (100 MHz, CDCl₃, 300K): δ =130.31-125.36 (90C, CH-Ar), 123.82 (2×C_{triaz}), 101.68, 101.57, 100.06, 99.27, 99.03, 98.56, 96.69 (7×C1), 83.53 (C4), 82.88 (C4), 81.62 (C4), 81.17-79.56 (11C, 7×C3, 4×C4), 79.54 (C2), 79.01 (C2), 78.38 (C2), 77.78 (C2), 77.38 (C2), 77.20 (2×C2), 76.12-72.84 (15×CH₂-Ph), 72.83, 72.66, 72.39 (3×CH₂-Ph), 71.85 (C5), 71.68 (C5), 71.57 (2×C5), 71.28 (C5), 70.81 (C5), 69.61 (C6), 69.60 (C5), 67.37 (C6), 67.30 (C6),

EXPERIMENTAL PART

52.57 (C6), 52.46 (C6), 51.62 (C6), 48.76 (N-CH₂-CH₂-Ad), 44.97 (C6), 44.89 (CH₂triaz), 44.85 (CH₂triaz), 42.59 (Ca), 42.38 (N-CH₂-CH₂-Ad), 37.07 (Cc), 29.05 (Cb).

HMRS (ESI): calculated for [C₁₈₆H₂₀₀N₁₀O₃₂+Na]⁺ 3108.4222; found 3108.4198.

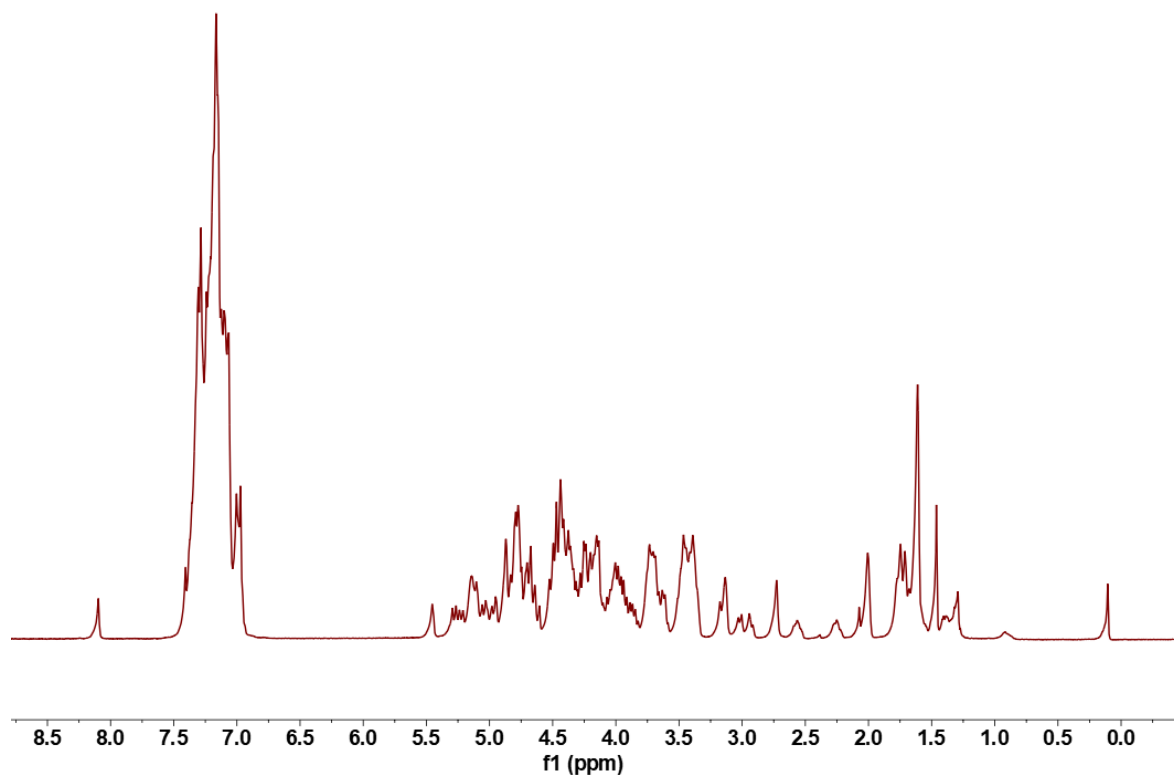


Figure 33: ¹H NMR (400 MHz, CDCl₃, 300K) of compound 18

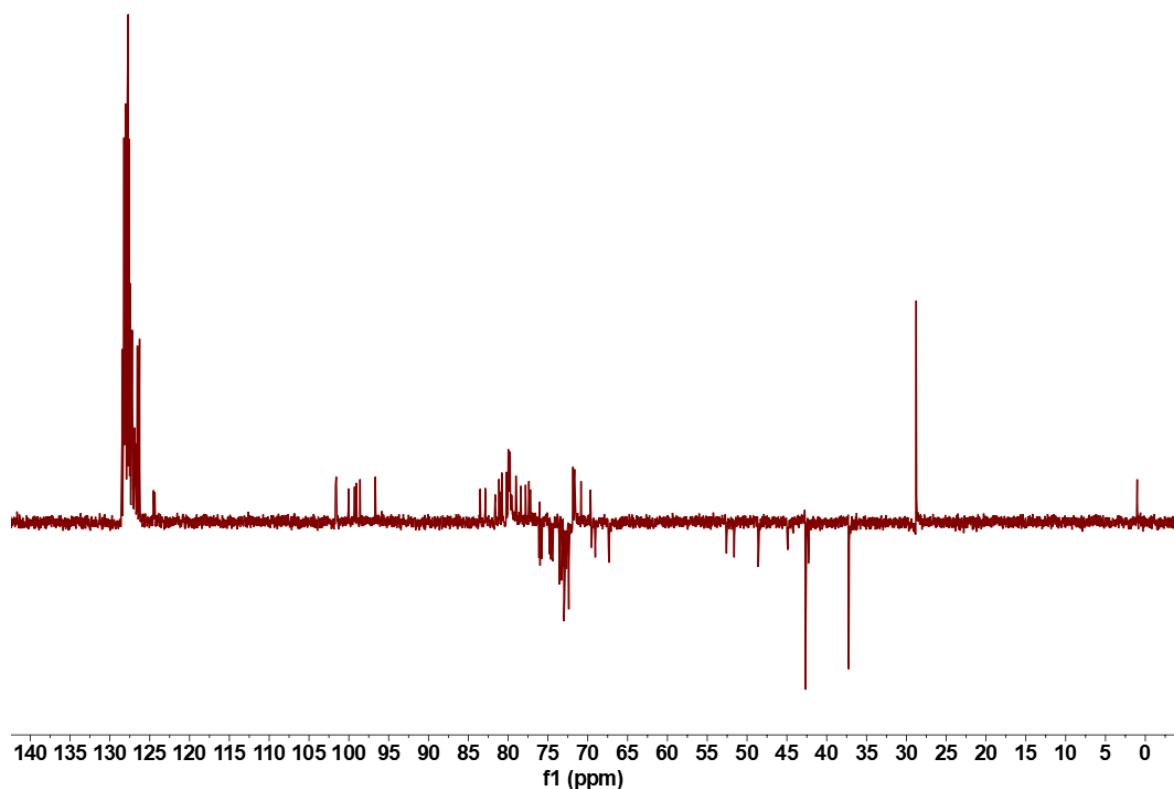
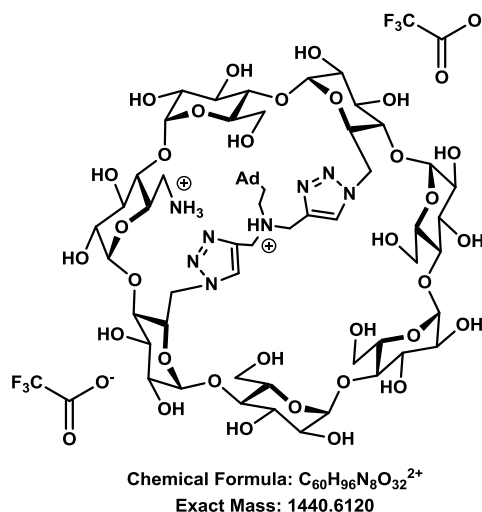


Figure 34: ¹³C NMR-DEPT 135 (100 MHz, CDCl₃, 300K) of compound 18

6^A, 6^C, 6^D-Trideoxy-6^A, 6^D-di-triazole-bridged-N-ethyladamantyl-6^C-ammonio-β-cyclodextrin bis-trifluoroacetate (19)



The perbenzylated product 18 (150 mg, 0.048 mmol, 1 eq) was dissolved in THF/H₂O (3:1, 24 mL). 2, 2, 2-trifluoroacetic acid (30 μL, 0.389 mmol, 8 eq) and Pd/C (129 mg, 1.22 mmol, 25 eq) was added. The mixture was purged 3 times with argon and 3 times with hydrogen. The reaction mixture was monitored by MS, and then the reaction mixture was purged under nitrogen, filtered through a μ-filter (0.2μm-polyester). The organic solvent was evaporated under vacuum and the residue was lyophilized. The crude product was purified by a RediSep Rf Gold C-18 reversed-phase chromatography to afford the desired product 19 as the white amorphous powder (43.7 mg, 62% yield) after freeze drying.

¹H NMR (600 MHz, D₂O, 300K): δ = 8.62-8.25 (br. m, 2H, 2×*H*_{triaz}), 5.30-5.17 (m, 2H, 2×*H*₁), 5.17-5.07 (m, 2H, 1×*H*₁, 1×*H*₆), 5.05-4.86 (m, 5H, 4×*H*₁, 1×*H*₆), 4.83-4.64 (m, 3H, 3×*H*₆), 4.05-3.35 (m, 34H, 7×*H*₂, 7×*H*₃, 6×*H*₄, 7×*H*₅, 7×*H*₆), 3.35-2.86 (m, 9H, 1×*H*₄, 2×*H*₆, 4×*CHH*_{triaz}, 2×*N-CHH-CH*₂-Ad), 2.17 (s, 3H, *H*_b), 1.91 (br. m, 3H, *H*_c), 1.77 (br. m, 3H, *H*_c), 1.72-1.48 (br. m, 8H, *H*_a, 2×*N-CH*₂-*CHH*-Ad).

¹³C NMR (151 MHz, D₂O, 300K): δ = 127.92 (*C*_{triaz}), 126.37 (*C*_{triaz}), 102.51 (*C*₁), 102.26 (2×*C*₁), 101.42 (2×*C*₁), 101.07 (*C*₁), 100.82 (*C*₁), 83.65, 82.37, 82.34, 82.19, 81.82, 80.25 (6×*C*₄), 74.15-70.86 (21*C*, 7×*C*₂, 7×*C*₃, 1×*C*₄, 6×*C*₅), 67.66 (*C*₅), 60.81 (2×*C*₆), 60.64 (2×*C*₆), 59.55 (*CH*₂_{triaz}), 58.92 (*CH*₂_{triaz}), 52.23 (*C*₆), 51.89 (*C*₆), 49.25 (*N-CH*₂-*CH*₂-Ad), 41.88 (*C*_a), 39.46 (*C*₆), 37.99 (*N-CH*₂-*CH*₂-Ad), 36.87 (*C*_c), 28.11 (*C*_b).

HMRS (ESI): calculated for [$C_{60}H_{94}N_8O_{32}+H$]⁺ 1439.6047; found: 1439.6055.

EXPERIMENTAL PART

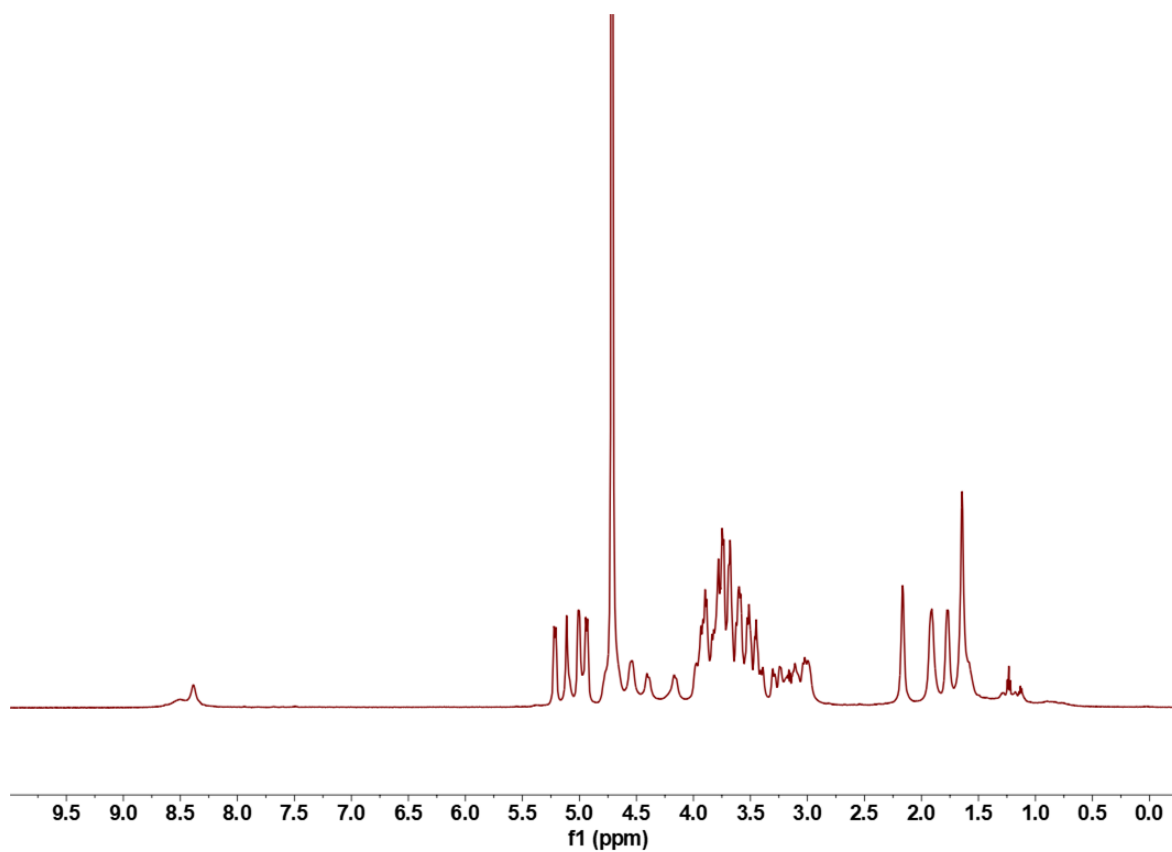


Figure 35: ¹H NMR (600 MHz, D₂O, 300K) of compound 19

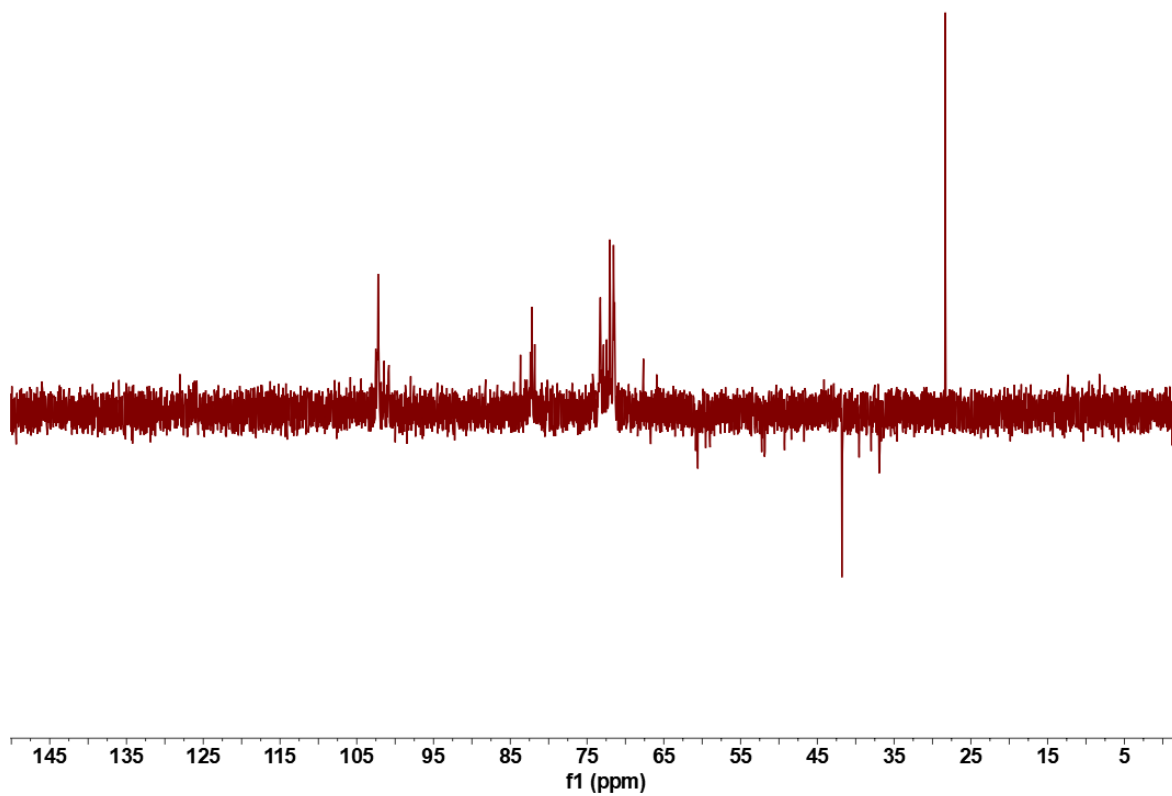
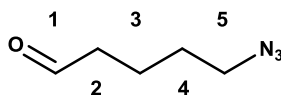


Figure 36: ¹³C NMR-DEPT 135 (151 MHz, D₂O, 300K) of compound 19

5-Azidopentanal (22)

Chemical Formula: $C_5H_9N_3O$
Exact Mass: 127.0746

To a solution of 5-chloropentanal (2 g, 16.59 mmol, 1 eq) and ethylene glycol (4.64 mL, 82.94 mmol, 5 eq) in toluene (65 mL) was added *p*-toluenesulfonic acid monohydrate (*p*-TsOH·H₂O) (0.63 g, 3.32 mmol, 0.2 eq). The resulting solution was heated to reflux for 12 h and the reaction mixture was cooled to room temperature, the volatile was removed under reduced pressure. The reaction mixture was diluted with diethyl ether (75 mL) and water (40 mL). The organic layer was washed with the saturated aqueous solution of NaHCO₃ (2×40 mL), brine solution (2×40 mL), then passed over MgSO₄, filtered and concentrated in vacuo. The obtained residue was purified by silica gel chromatography (cyclohexane/EtOAc 10:1) to give 2-(4-chlorobutyl)-1, 3-dioxolane 20 (2.23 g, 82% yield) as the yellow oil. ¹H NMR (400 MHz, CDCl₃, 300K): δ =4.78 (t, *J* =4.8 Hz, 1H), 3.95-3.70 (m, 4H), 3.46 (t, *J* =6.8 Hz, 2H), 1.82-1.68 (m, 2H), 1.68-1.57 (m, 2H), 1.57-1.42 (m, 2H). ¹³C NMR (100 MHz, CDCl₃, 300K): δ =103.90, 64.75, 44.87, 33.16, 32.45, 21.30.

Product 20 (2.23 g, 13.55 mmol, 1 eq) was solubilized in anhydrous DMSO (8 mL) under argon atmosphere, sodium azide (1.33 g, 20.32 mmol, 1.5 eq) was added. The mixture solution was stirred at 60°C for 24 h. Water (15 mL) and diethyl ether (10 mL) were added, and the aqueous phase was extracted with diethyl ether (3×20 mL), and the combined organic layers were washed with 1:1 water/brine solution (2×40 mL), dried over MgSO₄, filtered and concentrated in vacuo to give the desired 2-(4-azidobutyl)-1, 3-dioxolane 21 (1.99 g, 86% yield) without purification as the colorless oil. ¹H NMR (400 MHz, CDCl₃, 300K): δ =4.84 (t, *J* =5.2 Hz, 1H), 4.00-3.77 (m, 4H), 3.26 (t, *J* =7.2 Hz, 2H), 1.74-1.58 (m, 4H), 1.56-1.42 (m, 2H). ¹³C NMR (100 MHz, CDCl₃, 300K): δ =104.20, 64.87, 51.32, 33.25, 28.72, 21.14.

Product 21 (1.47 g, 8.60 mmol, 1 eq) was dissolved in acetone (24 mL) and water (24 mL) under argon atmosphere, *p*-toluenesulfonic acid (0.82 g, 4.30 mmol, 0.5 eq) was added. The mixture solution was stirred at 60°C for 6 h. The volatile was removed under reduced pressure. Then the reaction mixture was diluted with diethyl ether (80 mL) and the saturated aqueous solution of NaHCO₃ (80 mL). The organic layer was washed with water (40 mL) and brine solution (40 mL), dried over MgSO₄, filtered and concentrated in vacuo.

EXPERIMENTAL PART

The obtained residue was purified by silica gel chromatography (cyclohexane/EtOAc 7:3) to give 5-azidopentanal **22** (0.61 g, 56% yield) as the colorless oil. **¹H NMR** (400 MHz, CDCl₃, 300K): δ =9.72 (t, J =1.6 Hz, 1H, 1H-1), 3.25 (t, J =7.2 Hz, 2H, 2H-2), 2.43 (dt, J =7.2 Hz, J =1.2 Hz, 2H, 2H-3), 1.71-1.52 (m, 4H, 2H-4, 2H-5). **¹³C NMR** (100 MHz, CDCl₃, 300K): δ =201.02 (C-1), 51.11 (C-5), 43.23 (C-2), 28.29 (C-4), 19.24 (C-3). **HMRS (ESI)**: calculated for [C₅H₉N₃O+Na]⁺ 150.0638; found 150.0702.

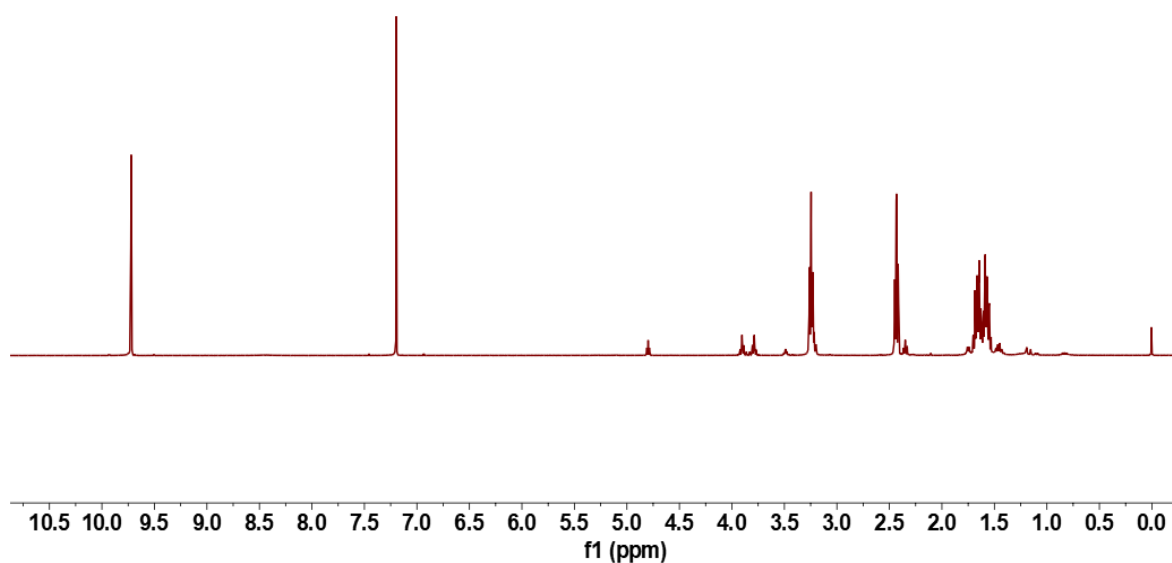


Figure 37: ¹H NMR (400 MHz, CDCl₃, 300K) of compound **22**

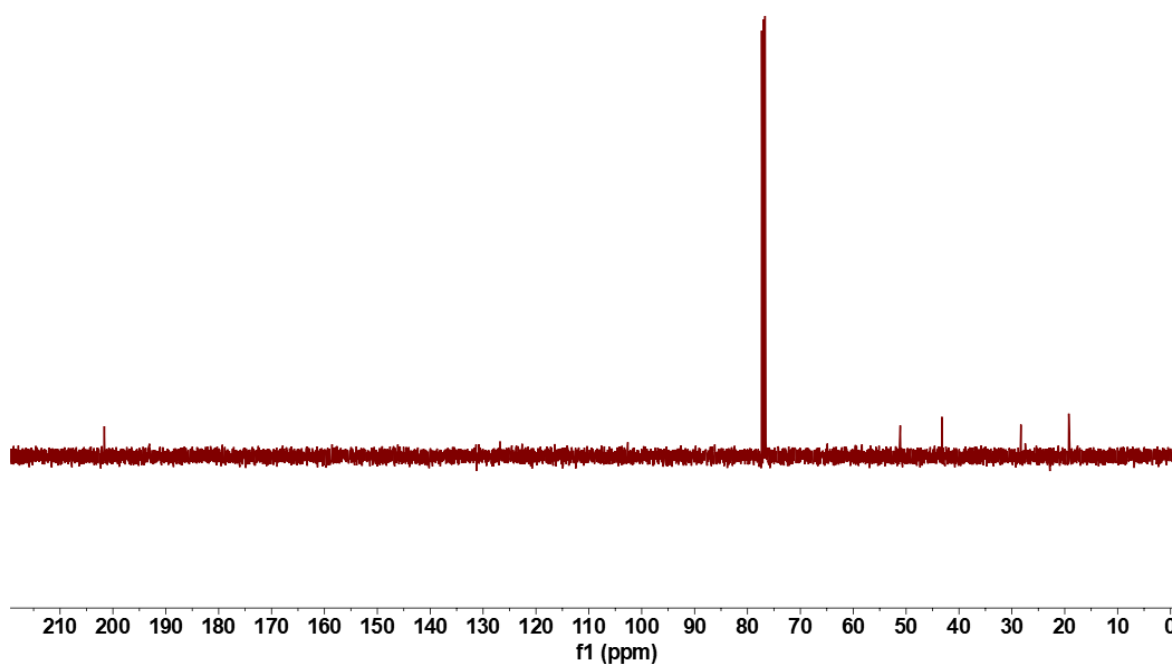
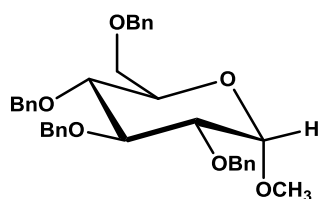


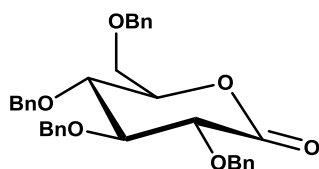
Figure 38: ¹³C NMR (100 MHz, CDCl₃, 300K) of compound **22**

Methyl 2, 3, 4, 6-tetra-O-benzyl- α -D-glucopyranoside (23)

Chemical Formula: $C_{35}H_{38}O_6$
Exact Mass: 554.2668

To a cooled solution (0°C) of methyl α -D-glucopyranoside (5 g, 25.75 mmol, 1 eq) in anhydrous DMF (15 mL) and followed by sodium hydride (6.2 g, 0.155 mmol, 6 eq) and benzyl bromide (18.35 mL, 0.155 mmol, 6 eq) sequentially added. The mixture solution was stirred at room temperature under nitrogen atmosphere, and the reaction progress was monitored by TLC (cyclohexane/EtOAc 4:1) after 8 h. Finally, the mixture solution was quenched with methanol (20 mL) and diluted with ethyl acetate (160 mL). The organic layer was washed with water (2×100 mL), the saturated aqueous solution of $NaHCO_3$ (2×100 mL), brine solution (2×100 mL), then passed over $MgSO_4$, filtered and concentrated in vacuo. The obtained residue was purified by silica gel chromatography (cyclohexane/EtOAc 8:1) to give product 23 (11.1 g, 78% yield).

The structure of the product was confirmed by comparison with the literature [133].

2, 3, 4, 6-Tetra-O-benzyl-D-gluconolactone (25)

Chemical Formula: $C_{34}H_{34}O_6$
Exact Mass: 538.2355

Product 23 (11.1 g, 20.01 mmol, 1 eq) was dissolved in acetic acid (175 mL) and sulfuric acid (50 mL). The resulting solution was heated to reflux for 2 h and the reaction mixture was cooled to room temperature, the white solid was filtered and washed with water (3×75 mL), the solid was dried by pump and gave the desired modified benzyl-D-glucopyranoside 24 (4.82 g, 33% yield) without purification as the white solid.

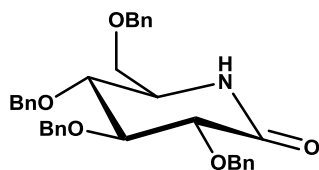
The modified benzyl-D-glucopyranoside 24 (4.82 g, 8.92 mmol, 1 eq) was dissolved in anhydrous DMSO (45 mL), acetic anhydride (16.85 mL, 0.18 mol, 20 eq) was dropwise added, the reaction mixture was stirred at room temperature overnight. The resulting

EXPERIMENTAL PART

solution was diluted with diethyl ether (200 mL) and the organic layer was washed with water (5×100 mL), brine solution (2×100 mL), then passed over MgSO₄, filtered and concentrated in vacuo. The obtained residue was purified by silica gel chromatography to give product 25 (4.32 g, 90% yield) as the colorless oil.

The structure of the product was confirmed by comparison with the literature [15].

2, 3, 4, 6-Tetra-O-benzyl-D-gluconolactam (28)



Chemical Formula: C₃₄H₃₅NO₅
Exact Mass: 537.2515

Product 25 (0.5 g, 0.93 mmol, 1 eq) was dissolved in the saturated methanolic ammonia (7 M, 25 mL). The reaction mixture was stirred at 0°C under nitrogen atmosphere, the reaction progress was monitored by TLC (cyclohexane/EtOAc 5:2) after 3 h and the solvent was removed under reduced pressure. The obtained residue was purified by silica gel chromatography (cyclohexane/EtOAc 1:1) to give product 26 (0.44 g, 86% yield) as the colorless oil.

Product 26 (1.04 g, 1.87 mmol, 1 eq) was dissolved in anhydrous DMSO (8 mL), acetic anhydride (3.54 mL, 37.43 mmol, 20 eq) was dropwise added, the reaction mixture was stirred at room temperature overnight. The resulting solution was diluted with diethyl ether (25 mL) and the organic layer was washed with water (5×10 mL), brine solution (2×10 mL), then passed over MgSO₄, filtered and concentrated in vacuo. The crude compound 27 was dried by the pump and was directly used without purification as the colorless oil (0.73 g, 70% yield).

Product 27 (0.73 g, 1.32 mmol, 1 eq) and sodium cyanoborohydride (0.16 g, 2.64 mmol, 2 eq) was dissolved in dry acetonitrile (13 mL), formic acid (2.95 mL, 78.27 mmol, 59 eq) was dropwise added, the reaction mixture was heated to reflux for 3 h. The resulting solution was cooled to room temperature and quenched with the saturated aqueous solution of NaHCO₃ (15 mL) and stirred for 10 min frequently. The aqueous was extracted with ethyl acetate (30 mL), the organic layer was washed with brine solution (20 mL), then passed over MgSO₄, filtered and concentrated in vacuo. The obtained residue was purified by silica gel chromatography (cyclohexane/EtOAc 2:1) to give product 28 (0.60 g, 85%

yield) as the white solid.

¹H NMR (400 MHz, CDCl₃, 300K): δ =7.51-7.42 (m, 2H), 7.41-7.27 (m, 16H), 7.26-7.19 (m, 2H), 6.01 (s, 1H), 5.21 (d, *J* =10.8 Hz, 1H), 4.88 (dd, *J* =12.0 Hz, *J* =7.2 Hz, 2H), 4.78 (dd, *J* =17.6 Hz, *J* =11.2 Hz, 2H), 4.56-4.46 (m, 3H), 4.03 (d, *J* =7.2 Hz, 1H), 3.94 (t, *J* =8.4 Hz, 1H), 3.67-3.52 (m, 3H), 3.30 (t, *J* =16.8 Hz, *J* =8.3 Hz, 1H).

¹³C NMR (100 MHz, CDCl₃, 300K): δ =170.65, 138.04, 137.86, 137.59, 137.26, 128.55, 128.47, 128.41, 128.36, 128.12, 128.00, 127.87, 127.79, 82.35, 78.80, 74.71, 74.61, 73.35, 70.05, 53.79.

HMRS (ESI): calculated for [C₃₄H₃₅NO₅+Na]⁺ 560.2407; found 560.2387.

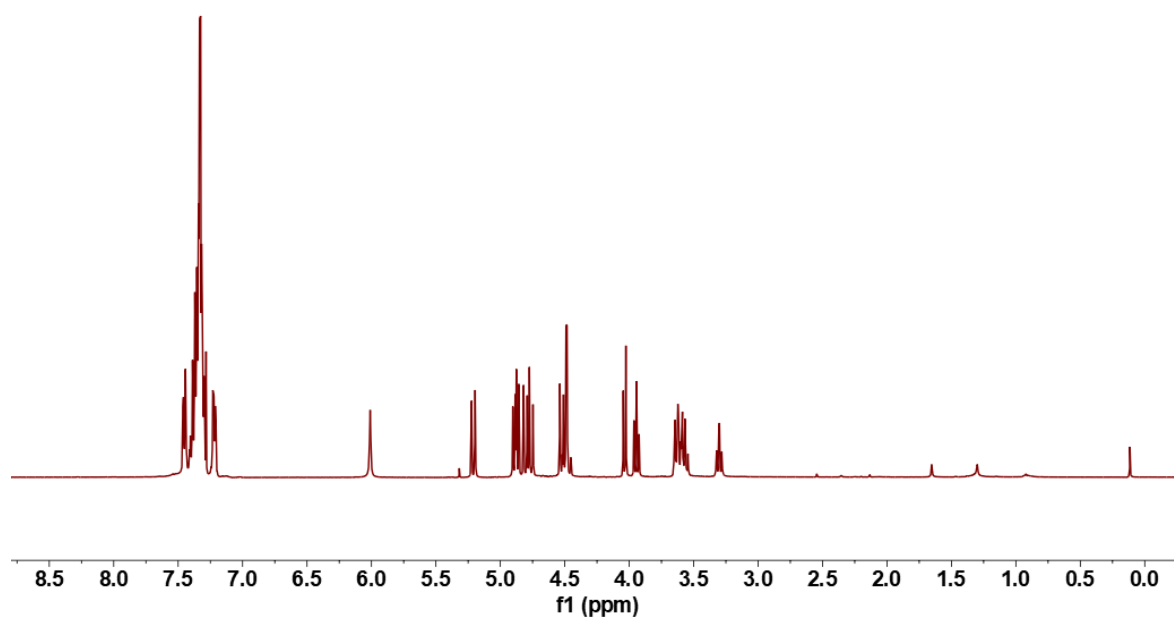


Figure 39: ¹H NMR (400 MHz, CDCl₃, 300K) of compound 28

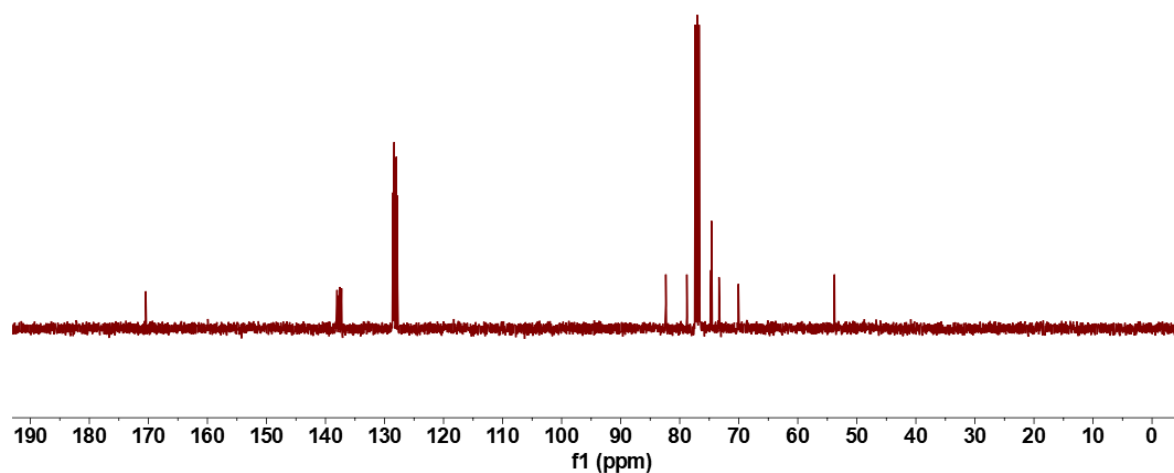
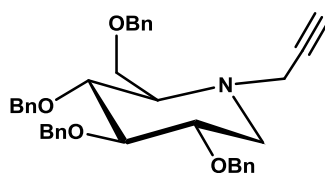


Figure 40: ¹³C NMR (100 MHz, CDCl₃, 300K) of compound 28

EXPERIMENTAL PART

2, 3, 4, 6-Tetra-O-benzyl-N-(3-prop-1-ynyl)-1-deoxynojirimycin (30)



Chemical Formula: $C_{37}H_{39}NO_4$
Exact Mass: 561.2879

To a solution (0°C) of 2, 3, 4, 6-tetra-O-benzyl-D-gluconolactam 28 (302 mg, 0.56 mmol, 1 eq) in anhydrous THF (10 mL) was slowly added Lithium Aluminium Hydride (LAH) (31.97 mg, 0.84 mmol, 1.5 eq). The reaction mixture was heated to reflux under nitrogen atmosphere. The reaction progress was monitored by TLC (cyclohexane/EtOAc 1:1) after 3 h and the reaction mixture was cooled to room temperature and quenched with diethyl ether (15 mL), water (15 mL), and stirred for 15 min continuously. The aqueous solution was filtered and extracted with diethyl ether (15 mL), the organic layer was washed with water (20 mL), brine solution (20 mL), then passed over $MgSO_4$, filtered and concentrated in vacuo. The obtained residue was purified by silica gel chromatography (cyclohexane/EtOAc 2:1) to give modified tetra-O-benzyl-1-deoxynojirimycin 29 (270 mg, 92% yield) as white the solid.

To a solution of 2, 3, 4, 6-tetra-O-benzyl-1-deoxynojirimycin 29 (271 mg, 0.52 mmol, 1 eq) in distilled acetonitrile (9 mL) was added propargyl bromide (80% in toluene, 1.34 mL, 1.04 mmol, 2 eq) and potassium carbonate (143 mg, 1.04 mmol, 2 eq). The reaction mixture was stirred at 90°C for 3 h under argon then cooled at room temperature. The solvent was evaporated under reduced pressure. The obtained residue was purified by silica gel chromatography (cyclohexane/EtOAc 2:1) to give compound 30 (267 mg, 92% yield) as the colorless oil.

1H NMR (400 MHz, $CDCl_3$, 300K): δ = 7.38-7.26 (m, 18H, $18 \times H_{Ph}$), 7.18-7.10 (m, 2H, $2 \times H_{Ph}$), 4.99 (d, J = 9.2 Hz, 1H, $1 \times CHHPh$), 4.89 (d, J = 10.8 Hz, 1H, $1 \times CHHPh$), 4.84 (d, J = 11.2 Hz, 1H, $1 \times CHHPh$), 4.71 (d, J = 11.2 Hz, 1H, $1 \times CHHPh$), 4.68 (d, J = 10.8 Hz, 1H, $1 \times CHHPh$), 4.56 (d, J = 10.8 Hz, 1H, $1 \times CHHPh$), 4.45 (d, J = 12.0 Hz, 1H, $1 \times CHHPh$), 4.38 (d, J = 10.8 Hz, 1H, $1 \times CHHPh$), 3.79-3.70 (m, 3H, $1 \times H_1$, $1 \times H_2$, $1 \times H_6$), 3.66 (t, $J_{H4-H3} = J_{H4-H5} = 9.6$ Hz, 1H, $1 \times H_4$), 3.60 (dd, $J_{H6-H6'} = 11.2$ Hz, $J_{H6-H5} = 2.4$ Hz, 1H, $1 \times H_6$), 3.51 (t, $J_{H3-H2} = J_{H3-H4} = 9.2$ Hz, 1H, $1 \times H_3$), 3.41 (dd, J = 18.0 Hz, J = 2.8 Hz, 1H, $1 \times N-CH_2-C \equiv CH$), 2.98 (dd, $J_{Hax-Heq} = 11.2$ Hz, $J_{Hax-H2} = 4.4$ Hz, 1H, $1 \times N-CHH-C \equiv CH$), 2.56 (t, $J_{Heq-Hax} = J_{Heq-H2} = 11.2$ Hz, 1H, $1 \times N-CHH-C \equiv CH$), 2.46 (m, 1H, $1 \times H_5$), 2.23 (t, $J_{H1-H3} = 2.0$ Hz, 1H, $1 \times H_1$).

^{13}C NMR (100 MHz, CDCl_3 , 300K): δ = 138.93, 138.52, 138.45, 137.65 ($4\times\text{C}_{\text{quat-Ar}}$), 128.44, 128.37, 128.32, 128.30, 127.94, 127.93, 127.81, 127.78, 127.65, 127.51, 127.47, 127.25 ($12\times\text{CH-Ar}$), 87.11 (C3), 78.22 (C2), 78.15 (N- $\text{CH}_2\text{-C}\equiv\text{CH}$), 75.45 ($\text{CH}_2\text{-Ph}$), 75.18 ($\text{CH}_2\text{-Ph}$), 74.08 (2C, $1\times\text{C}_4$, $1\times\text{N-CH}_2\text{-C}\equiv\text{CH}$), 73.59 ($\text{CH}_2\text{-Ph}$), 72.71 ($\text{CH}_2\text{-Ph}$), 64.80 (C6), 62.14 (C5), 54.99 (C1), 42.49 (N- $\text{CH}_2\text{-C}\equiv\text{CH}$).

HMRS (ESI): calculated for $[\text{C}_{37}\text{H}_{39}\text{NO}_4+\text{Na}]^+$ 584.2771; found 584.2800.

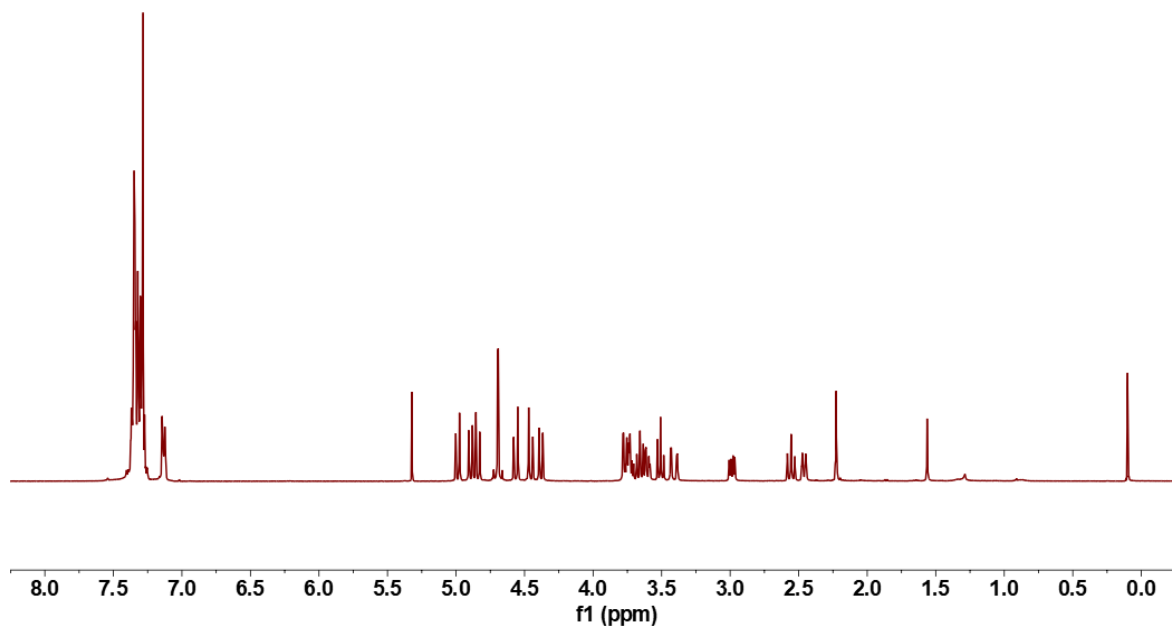


Figure 41: ^1H NMR (400 MHz, CDCl_3 , 300K) of compound 30

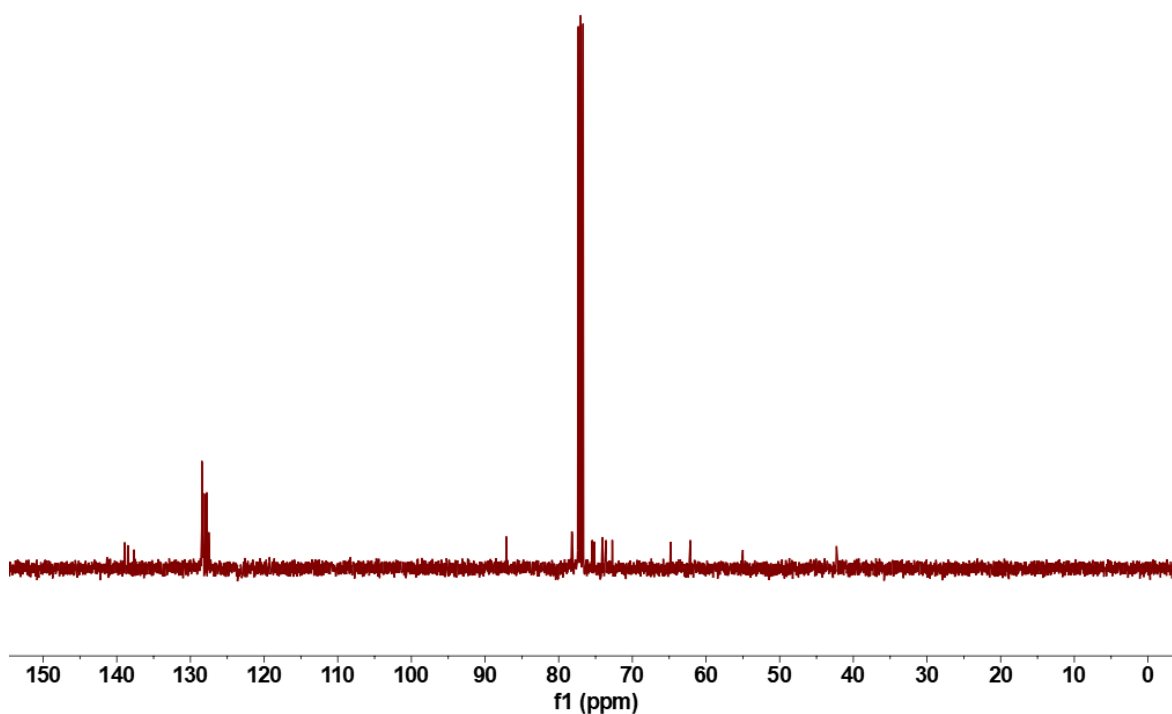
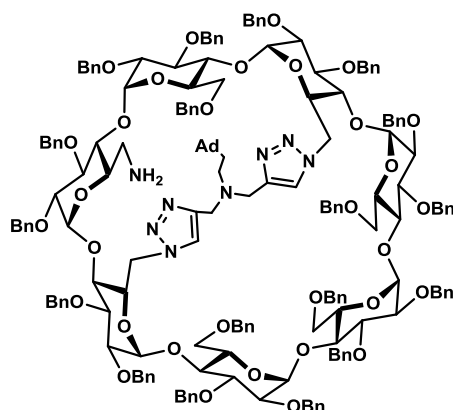


Figure 42: ^{13}C NMR (100 MHz, CDCl_3 , 300K) of compound 30

EXPERIMENTAL PART

6^A, 6^C, 6^D-Trideoxy-6^A, 6^D-di-triazole-bridged-N-ethyladamantyl-6^C-amino-2^{A-G}, 3^{A-G}, 6^B, 6^E, 6^F, 6^G-octadeca-O-benzyl-β-cyclodextrin (31)



Chemical Formula: C₁₈₆H₂₀₂N₈O₃₂
Exact Mass: 3059.4425

The compound 18 (507 mg, 0.16 mmol, 1 eq) was dissolved in distilled THF (4 mL), triphenylphosphine (86.14 mg, 0.33 mmol, 2 eq) was added and distilled water (2 mL) was added when triphenylphosphine dissolved. The reaction mixture was stirred at room temperature overnight under nitrogen atmosphere. The reaction progress was monitored by MS, and the mixture solution was quenched with H₂O and diluted with ethyl acetate (10 mL). The aqueous phase was extracted with ethyl acetate (3×10 mL). The organic layer was passed over MgSO₄, filtered and concentrated in vacuo. The obtained residue was purified by silica gel chromatography (DCM/MeOH 30:1) to give product 31 (476 mg, 95% yield) as the white foam.

¹H NMR (600 MHz, CDCl₃, 300K): δ =8.02 (s, 1H, 1×H_{triazA}), 7.53 (s, 1H, 1×H_{triazD}), 7.53-6.72 (m, 90H, 90×H_{Ph}), 5.48-5.28 (m, 2H, 2×H1), 5.27-4.92 (m, 7H, 1×H1, 2×H6, 4×CHHPh), 4.91-4.55 (m, 20H, 4×H1, 1×H5, 15×CHHPh), 4.53-4.21 (m, 18H, 1×H5, 1×H6, 16×CHHPh), 4.19-3.80 (m, 15H, 7×H3, 2×H4, 3×H5, 2×H6, 1×CHHPh), 3.78-3.33 (m, 21H, 7×H2, 5×H4, 3×H5, 6×H6), 3.18-2.92 (m, 3H, 1×H6, 2×CHH_{triaz}), 2.76 (d, ³J =14.4 Hz, 2H, 2×CHH_{triaz}), 2.66-2.50 (m, 3H, 2×H6, 1×N-CHH-CH₂-Ad), 2.26 (m, 1H, 1×N-CHH-CH₂-Ad), 1.99 (s, 3H, Hb), 1.78-1.40 (m, 14H, Hc, Ha, 2×N-CH₂-CHH-Ad).

¹³C NMR (151 MHz, CDCl₃, 300K): δ =129.64-125.88 (90C, CH-Ar), 124.19 (C_{triazA}), 119.09 (C_{triazD}), 101.54 (C1), 101.40 (C1), 99.81 (C1), 99.47 (C1), 98.73 (2×C1), 96.75 (C1), 83.56 (C4), 82.62 (C4), 81.85-79.29 (11C, 7×C3, 2×C4, 2×C2), 78.79 (C4), 78.28 (C4), 78.21-76.71 (4×C2), 75.64 (2C, 1×C2, 1×C4), 76.11-71.85 (18×CH₂-Ph), 71.87 (C5), 71.75 (2×C5), 71.70 (C5), 71.47 (2×C5), 70.47 (C6), 69.79 (C5), 69.13 (C6), 67.53 (CH₂_{triaz}), 67.25 (CH₂_{triaz}), 52.64 (C6), 52.59 (C6), 48.50 (N-CH₂-CH₂-Ad), 45.22 (C6), 44.82 (C6), 42.59 (2C, 1×C6,

1×Ca), 42.42 (N-CH₂-CH₂-Ad), 37.12 (Cc), 28.68 (Cb).

HMRS (ESI): calculated for [C₁₈₆H₂₀₂N₈O₃₂+H]⁺ 3060.4498; found 3060.4512.

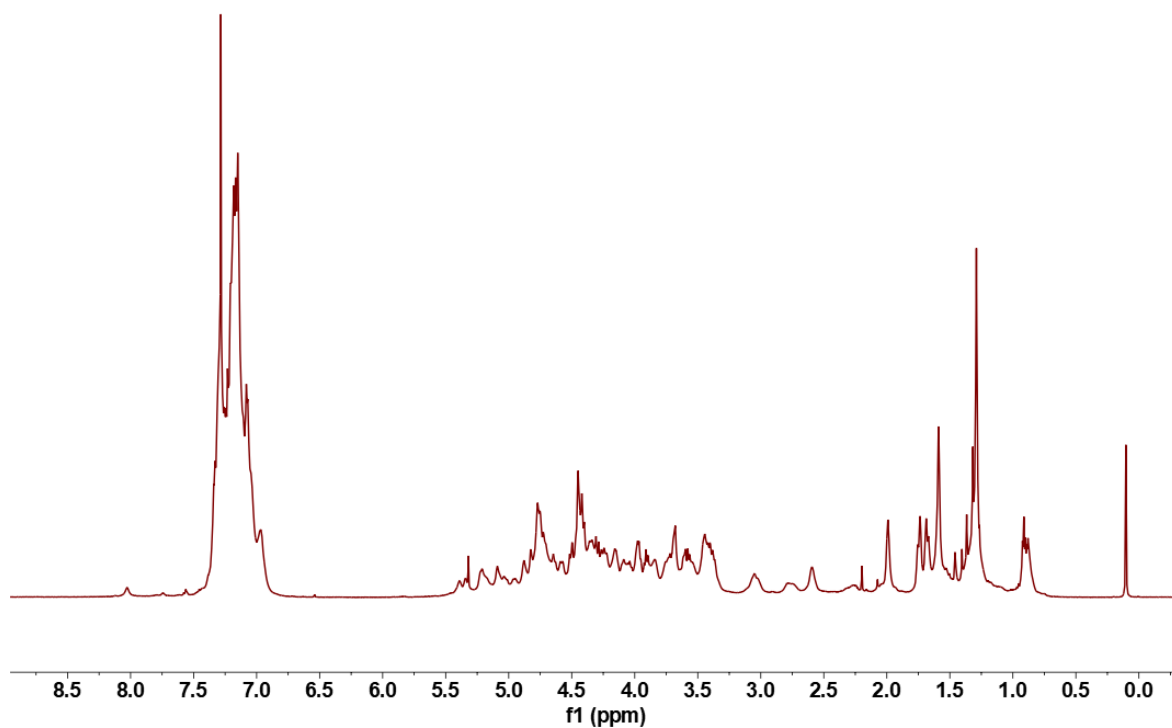


Figure 43: ¹H NMR (600 MHz, CDCl₃, 300K) of compound 31

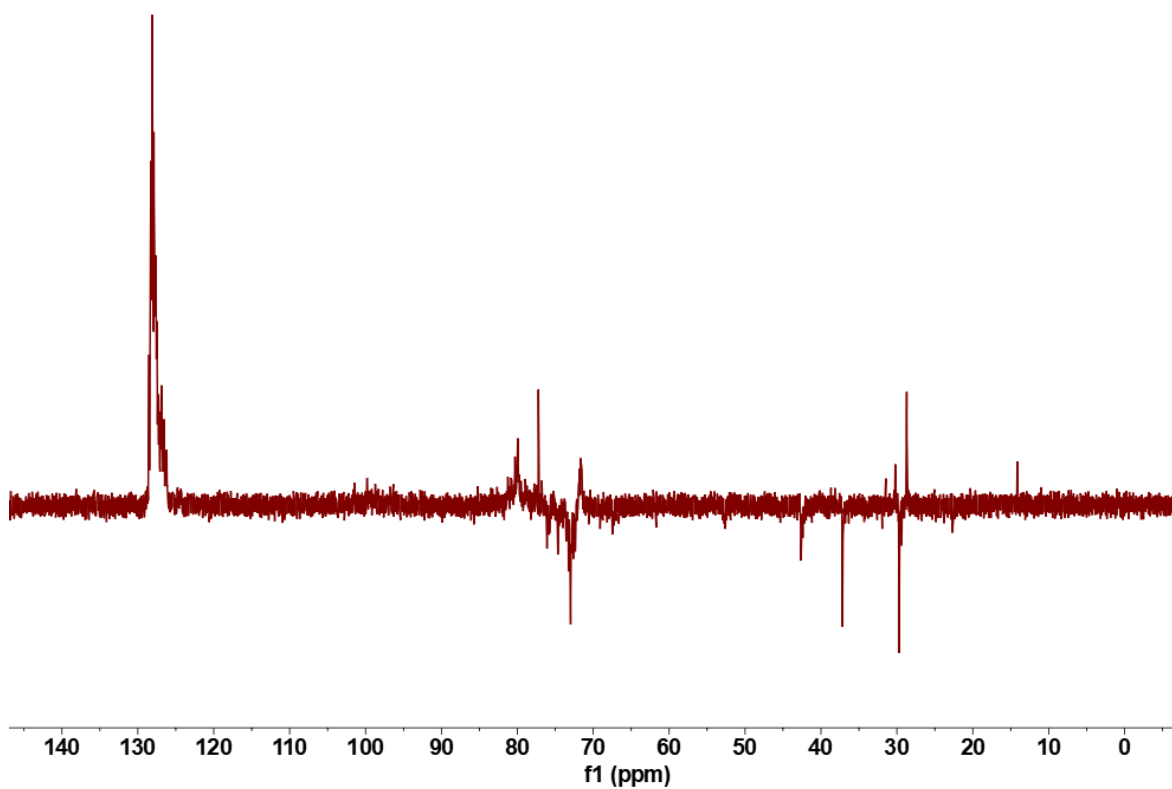
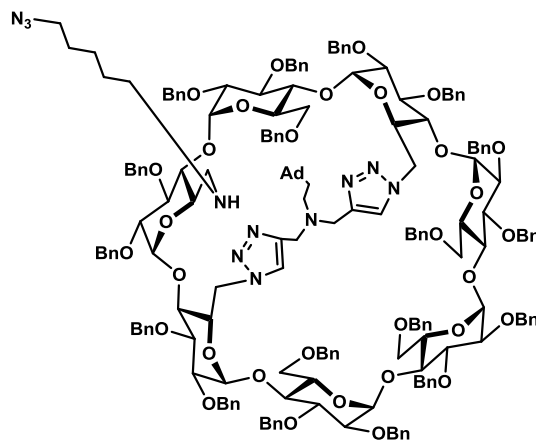


Figure 44: ¹³C NMR-DEPT 135 (151 MHz, CDCl₃, 300K) of compound 31

EXPERIMENTAL PART

6^A, 6^C, 6^D-Trideoxy-6^A, 6^D-di-triazole-bridged-N-ethyladamantyl-6^C-N-5-azidopentyl-2^{A-G}, 3^{A-G}, 6^B, 6^E, 6^F, 6^G-octadeca-O-benzyl-β-cyclodextrin (32)



Chemical Formula: C₁₉₁H₂₁₁N₁₁O₃₂
Exact Mass: 3170.5222

To a solution of modified β-cyclodextrin 31 (334 mg, 0.109 mmol, 1 eq) in dry DCM (5 mL) was added 5-azidopentanal 22 (22.3 mg, 0.175 mmol, 1.6 eq) and the mixture was stirred at room temperature under nitrogen 10 min. Then NaBH(OAc)₃ (64.8 mg, 0.306 mmol, 2.8 eq) was added and the mixture was stirred for 6 h. After quenching the resulting solution with diethyl ether (30 mL), the organic layer was washed with the saturated aqueous solution of NaHCO₃ (2×20 mL), brine (2×20 mL), dried over MgSO₄, filtered and concentrated in vacuo. The residue was purified over silica gel chromatography ((DCM/MeOH 50:1 then 10:1) to afford product 32 (280 mg, 81% yield) as the white foam.

¹H NMR (600 MHz, CDCl₃, 300K): δ = 7.74 (s, 1H, 1×H_{triazA}), 7.59 (s, 1H, 1×H_{triazD}), 7.34-6.94 (m, 90H, 90×H_{Ph}), 5.34 (d, ³J = 12.0 Hz, 1H, 1×CHHPh), 5.27-5.18 (m, 2H, 1×H1, 1×CHHPh), 5.17-5.01 (m, 7H, 3×H1, 1×H6, 3×CHHPh), 4.97 (d, ³J = 15.0 Hz, 1H, 1×H6), 4.89-4.67 (m, 12H, 3×H1, 9×CHHPh), 4.66-4.35 (m, 13H, 2×H5, 11×CHHPh), 4.35-4.08 (m, 15H, 2×H3, 2×H5, 2×H6, 9×CHHPh), 4.08-3.78 (m, 12H, 5×H3, 3×H4, 1×H5, 1×H6, 2×CHHPh), 3.77-3.60 (m, 7H, 2×H4, 2×H5, 3×H6), 3.56-3.45 (m, 5H, 2×H2, 2×H4, 1×H6), 3.45-3.33 (m, 7H, 5×H2, 1×H6, 1×CHH_{triaz}), 3.19 (t, ³J = 4.8 Hz, 2H, 2×NH-CHH-(CH₂)₄-N₃), 3.08 (d, ³J = 13.2 Hz, 1H, 1×CHH_{triaz}), 3.00 (t, ³J = 9.6 Hz, 2H, 2×H6), 2.85-2.72 (m, 3H, 1×H6, 2×CHH_{triaz}), 2.51 (td, ¹J = 12.0 Hz, ²J = 5.4 Hz, 1H, 1×N-CHH-CH₂-Ad), 2.44 (d, ³J = 15.0 Hz, 1H, 1×H6), 2.37 (br. m, 1H, 1×N-CH₂-CHH-Ad), 2.27 (br. m, 1H, 1×N-CH₂-CHH-Ad), 2.15 (td, ¹J = 12.0 Hz, ²J = 5.4 Hz, 1H, 1×N-CHH-CH₂-Ad), 1.96 (s, 3H, H_b), 1.72 (m, 3H, H_c), 1.65 (m, 3H, H_c), 1.58-1.47 (m, 9H, 3×NH-CH₂-(CHH)₄-N₃, H_a), 1.37-1.15 (m, 5H, 5×NH-CH₂-(CHH)₄-N₃).

¹³C NMR (151 MHz, CDCl₃, 300K): δ = 128.81-125.66 (90C, CH-Ar), 124.43 (C_{triazA}), 124.11

(C_{triazD}), 101.24, 100.93, 100.01, 99.44, 99.29, 99.03, 98.27 (7×C1), 82.60 (C4), 82.32 (C4), 82.30 (C4), 81.64 (C4), 81.23 (C4), 80.88 (C3), 80.66 (C3), 80.40 (C3), 80.33-79.82 (5C, 4×C3, 1×C4), 79.65 (C2), 79.43 (C2), 79.12 (C2), 78.86 (C2), 78.14 (C3), 77.83 (C2), 77.45 (C2), 77.26 (C2), 76.25-72.20 (18×CH₂-Ph), 71.80 (C5), 71.64 (2×C5), 71.43 (C5), 71.41 (C5), 71.34 (C5), 71.16 (C5), 69.72 (C6), 69.21 (C6), 67.73 (C6), 67.42 (CH_{2triaz}), 52.98 (C6), 52.69 (C6), 51.38 (NH-CH₂-(CH₂)₄-N₃), 49.87 (NH-CH₂-(CH₂)₄-N₃), 48.83 (C6), 48.37 (N-CH₂-CH₂-Ad), 45.54 (C6), 44.64 (CH_{2triaz}), 42.66 (Ca), 42.41 (N-CH₂-CH₂-Ad), 37.19 (Cc), 29.89 (NH-CH₂-(CH₂)₄-N₃), 28.82(NH-CH₂-(CH₂)₄-N₃), 28.72(Cb), 24.55(NH-CH₂-(CH₂)₄-N₃).

HMRS (ESI): calculated for [C₁₉₁H₂₁₁N₁₁O₃₂+H]⁺ 3171.5294; found 3171.5278.

EXPERIMENTAL PART

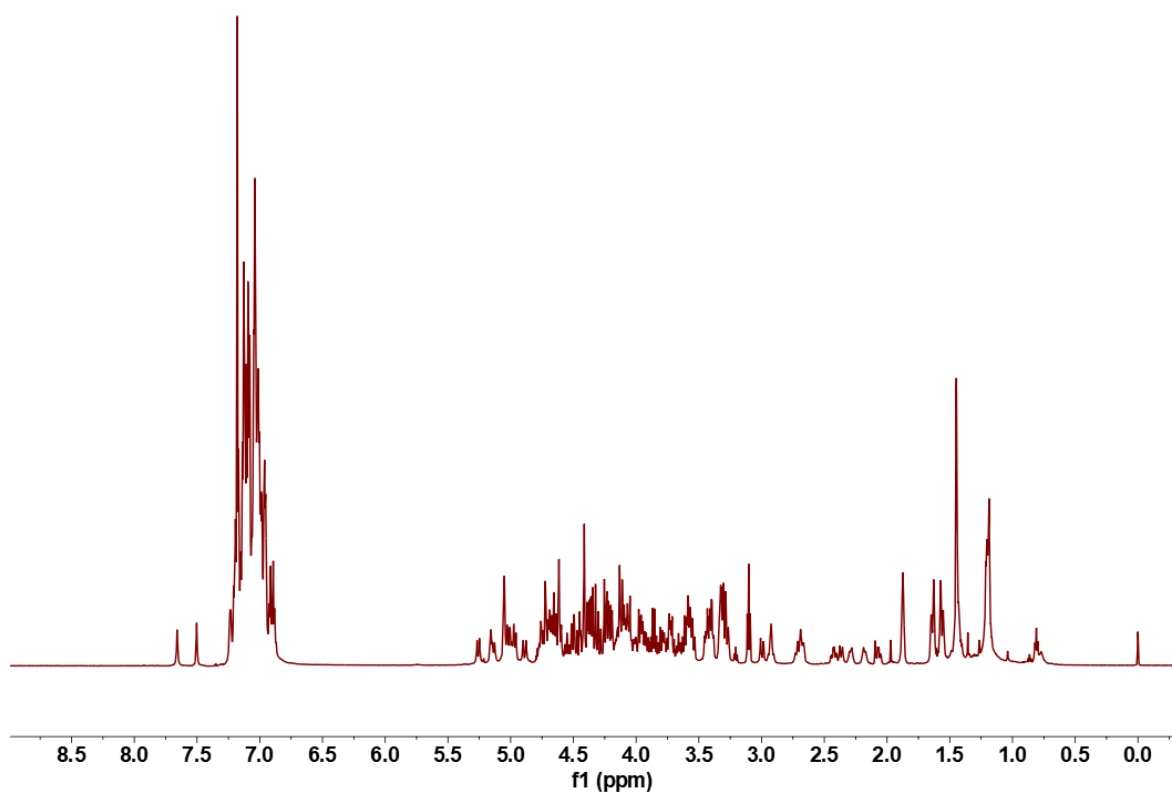


Figure 45: ¹H NMR (600 MHz, CDCl₃, 300K) of compound 32

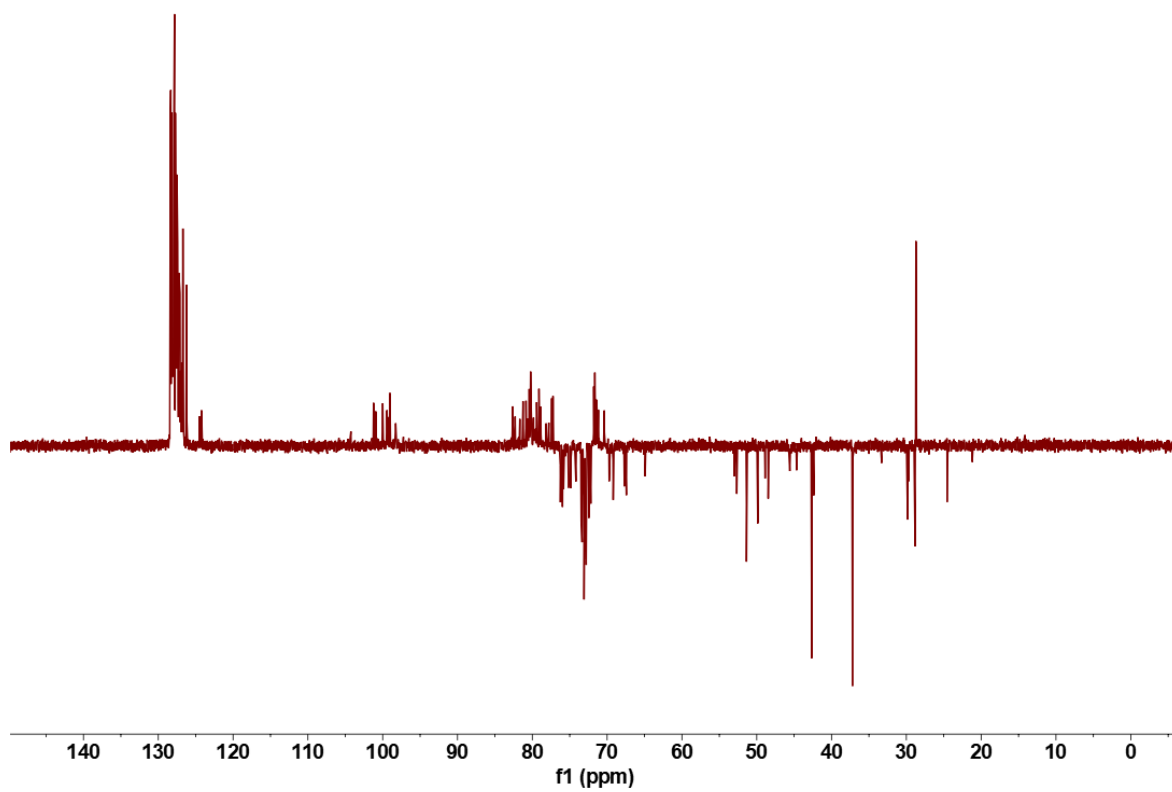
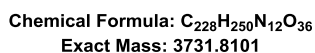
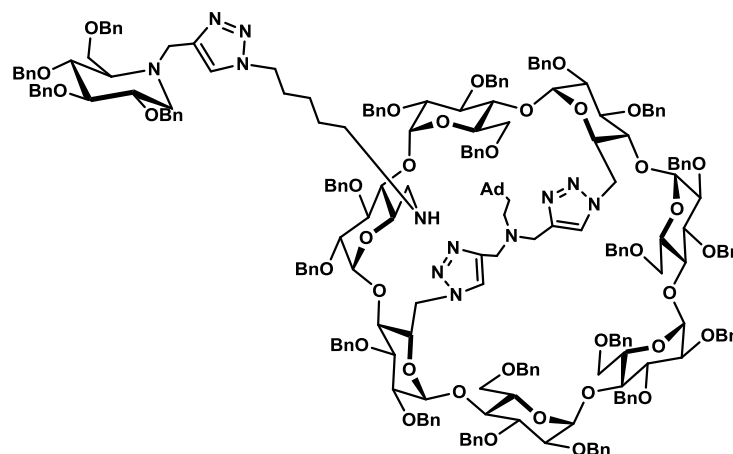


Figure 46: ¹³C NMR-DEPT 135 (151 MHz, CDCl₃, 300K) of compound 32

6^A, 6^C, 6^D-Trideoxy-6^A, 6^D-di-triazole-bridged-N-ethyladamantyl-6^C-N-(pentyltriazole-2, 3, 4, 6-tetra-*O*-benzyl-N-1-deoxynojirimycin)-2^{A-G}, 3^{A-G}, 6^B, 6^E, 6^F, 6^G-octadeca-*O*-benzyl- β -cyclodextrin (33)



To a solution of modified β -cyclodextrin 32 (172 mg, 54.2 μ mol, 1 eq) in dry THF/H₂O (13 mL, 1:1) was added modified benzyl-N-1-deoxynojirimycin 30 (61 mg, 0.108 mmol, 2 eq), CuSO₄•5H₂O (136 mg, 0.54 mmol, 10 eq) and sodium ascorbate (161 mg, 0.81 mmol, 15 eq) was added successively. The mixture was stirred at room temperature under nitrogen overnight. Finally, the mixture solution was diluted with diethyl ether (50 mL). The organic solution was washed with 1:1 water/brine solution (2×30 mL), HCl solution (1 M in water, 30 mL), the saturated aqueous solution of NaHCO₃ (30 mL), then passed over MgSO₄, filtered and concentrated in vacuo. The residue was purified over silica gel chromatography (DCM/MeOH 30:1) to afford desired modified β -cyclodextrin 33 (172 mg, 85% yield) as the yellow foam.

¹H NMR (600 MHz, CDCl₃, 300K): δ = 7.74 (s, 1H, 1×H_{triazA}), 7.62 (s, 1H, 1×H_{triazD}), 7.49-6.80 (m, 111H, 1×H_{sugar-triaz}, 110×H_{Ph}), 5.34 (d, ³J = 13.2 Hz, 1H, 1×CHHPh), 5.29-5.20 (m, 2H, 1×H1, 1×CHHPh), 5.19-4.95 (m, 9H, 3×H1, 2×H6, 4×CHHPh), 4.94-4.61 (m, 19H, 3×H1, 1×H5, 15×CHHPh), 4.60-4.40 (m, 13H, 1×H5, 12×CHHPh), 4.40-4.26 (m, 7H, 1×H6, 6×CHHPh), 4.26-4.08 (m, 11H, 2×H3, 2×H5, 2×H6, 2×NH-(CH₂)₄-CHH-, 3×CHHPh), 4.07-3.90 (m, 9H, 5×H3, 2×H6, 2×CHHPh), 3.89-3.45 (m, 21H, 2×H2, 7×H4, 3×H5, 7×H6, 2×H_{sugar}), 3.44-3.32 (m, 7H, 5×H2, 2×H_{sugar}), 3.16 (dd, ¹J = 4.2 Hz, ²J = 9.6 Hz, 1H, 1×NH-(CHH)₄-CH₂-), 3.02 (br. m, 2H, 2×N_{sugar}-CHH-), 2.97 (dd, ¹J = 4.2 Hz, ²J = 9.6 Hz, 1H, 1×CHH_{triaz}), 2.84-2.71 (m, 3H, 1×CHH_{triaz}, 2×H_{sugar}), 2.59-2.41 (m, 4H, 2×CHH_{triaz}, 1×H_{sugar}, 1×NH-(CHH)₄-CH₂-), 2.40-2.10 (br. m, 5H, 1×H_{sugar}, 2×NH-(CHH)₄-CH₂-, 2×N-CHH-CH₂-Ad),

EXPERIMENTAL PART

1.94 (s, 3H, H_b), 1.77 (br. m, 2H, 2×NH-(CH₂)₄-CH₂-), 1.71 (m, 3H, H_c), 1.63 (m, 3H, H_c), 1.51 (m, 6H, H_a), 1.39-1.18 (m, 4H, 2×N-CH₂-CH₂-Ad, 2×NH-(CH₂)₄-CH₂-).

¹³C NMR (151 MHz, CDCl₃, 300K): δ = 129.44-125.61 (110C, CH-Ar), 124.51 (C_{triazA}), 124.20 (C_{triazD}), 122.63 (C_{sugar-triaz}), 101.25 (C1), 100.87 (C1), 100.06 (C1), 99.46 (C1), 99.07 (2×C1), 98.26 (C1), 87.34 (C_{sugar}), 87.06 (C_{sugar}), 82.58 (C4), 82.60 (C4), 81.68 (C4), 81.27 (C4), 81.23-77.22 (18C, 7×C2, 7×C3, 4×C4), 76.29, 75.95, 75.88, 75.66, 75.48, 75.36, 75.15, 74.76, 74.19, 73.60, 73.53, 73.44, 73.35, 73.08, 73.01, 72.89, 72.84, 72.81, 72.74, 72.61, 72.44, 72.17 (22×CH₂-Ph), 71.76 (C5), 71.67 (2×C5), 71.42 (C5), 71.36 (C5), 71.17 (C5), 70.33 (C5), 70.28 (C6), 69.68 (C6), 67.59 (N_{sugar}-CH₂-), 67.40 (C_{sugar}), 66.19 (C6), 64.79 (C6), 62.70 (C_{sugar}), 62.20 (C_{sugar}), 55.12 (CH₂triaz), 54.62 (NH-(CH₂)₄-CH₂-), 52.92 (C6), 52.72 (C6), 50.12 (NH-(CH₂)₄-CH₂-), 49.73 (N-CH₂-CH₂-Ad), 48.74 (CH₂triaz), 48.44 (NH-(CH₂)₄-CH₂-), 47.15 (C6), 42.64 (2C, 1×Ca, 1×N-CH₂-CH₂-Ad), 42.34 (C_{sugar}), 37.26 (Cc), 30.28 (NH-(CH₂)₄-CH₂-), 29.76 (NH-(CH₂)₄-CH₂-), 28.57 (Cb).

HMRS (ESI): calculated for [C₂₂₈H₂₅₀N₁₂O₃₆+H]⁺ 3732.8173; found 3732.8188.

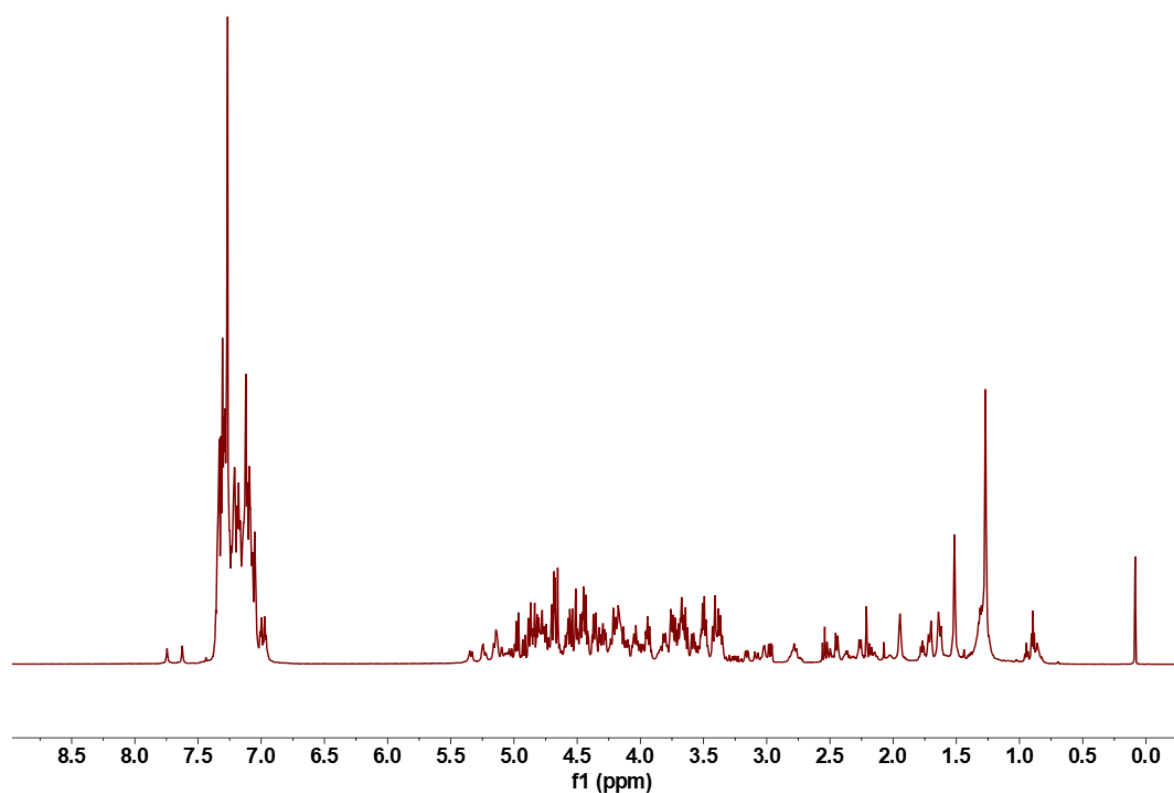


Figure 47: ¹H NMR (600 MHz, CDCl₃, 300K) of compound 33

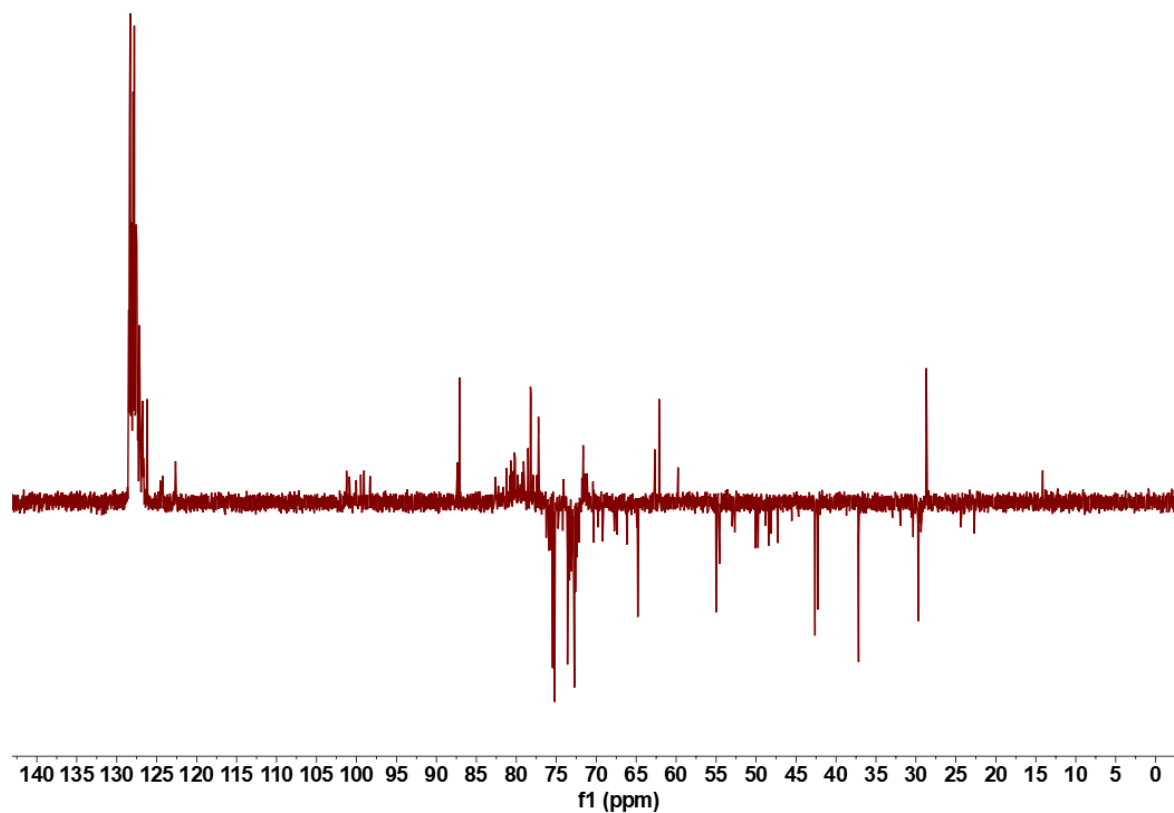
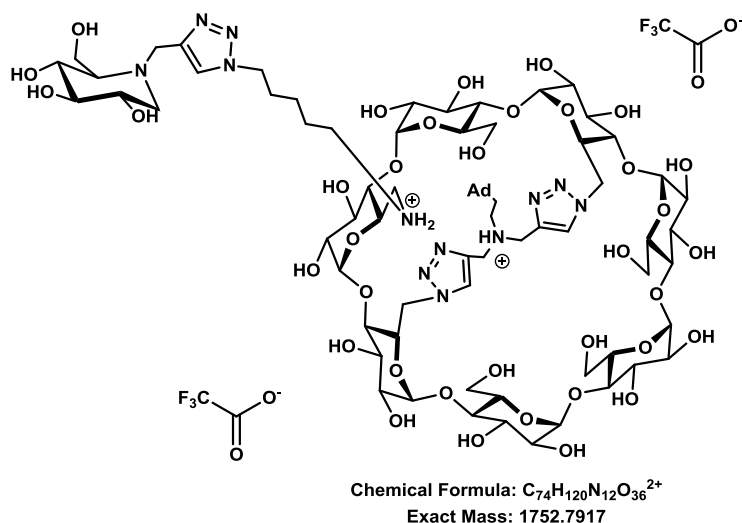


Figure 48: ¹³C NMR-DEPT 135 (151 MHz, CDCl₃, 300K) of compound 33

EXPERIMENTAL PART

6^A, 6^C, 6^D-Trideoxy-6^A, 6^D-di-triazole-bridged-N-ethyladamantyl-6^C-N-(pentyltriazole-2, 3, 4, 6-tetra-N-1-deoxynojirimycin)- β -cyclodextrin bis-trifluoroacetate (34)



The perbenzylated product 33 (237 mg, 0.063 mmol, 1 eq) was dissolved in THF/H₂O (3:1, 16 mL). 2, 2, 2-trifluoroacetic acid (68 μ L, 0.889 mmol, 14 eq) and Pd/C (243 mg, 2.28 mmol, 36 eq) was added. The mixture was purged 3 times with argon and 3 times with hydrogen. The reaction mixture was monitored by MS, and then the reaction mixture was purged under nitrogen, filtered through a μ -filter (0.2 μ m-polyester). The organic solvent was evaporated under vacuum and the residue was lyophilized. The crude product was purified by a RediSep Rf Gold C-18 reversed-phase chromatography to afford the desired product 34 as the white amorphous powder (59.8 mg, 54% yield) after freeze drying.

¹H NMR (600 MHz, D₂O, 300K): δ = 8.71-8.36 (br. m, 2H, 2 \times H_{triaz}), 8.30 (s, 1H, 1 \times H_{sugar-triaz}), 5.27 (d, ³J = 15.6 Hz, 2H, 2 \times H1), 5.16 (s, 1H, 1 \times H1), 5.10-4.93 (m, 4H, 4 \times H1), 4.83-4.57 (m, 7H, 7 \times H6), 4.55-4.41 (m, 2H, 2 \times NH-(CH₂)₄-CHH), 4.29 (d, ²J = 11.4 Hz, 2H, 2 \times H_{sugar}), 4.20 (d, ²J = 11.4 Hz, 2H, 2 \times N_{sugar}-CHH-), 4.14-3.35 (m, 38H, 7 \times H2, 7 \times H3, 7 \times H4, 7 \times H5, 7 \times H6, 3 \times H_{sugar}), 3.34-2.93 (m, 11H, 4 \times CHH_{triaz}, 2 \times N-CHH-CH₂-Ad, 2 \times NH-(CHH)₄-CH₂-, 3 \times H_{sugar}), 2.13 (s, 3H, Hb), 2.06-1.50 (m, 18H, Hc, Ha, 2 \times N-CH₂-CHH-Ad, 4 \times NH-(CHH)₄-CH₂-), 1.39-1.23 (m, 2H, 2 \times NH-(CHH)₄-CH₂-).

¹³C NMR (151 MHz, D₂O, 300K): δ = 128.03 (C_{sugar-triaz}), 127.56 (2 \times C_{triaz}), 102.57 (C1), 102.17 (C1), 102.15 (C1), 102.12 (2 \times C1), 101.27 (2 \times C1), 82.20, 81.97, 76.12, 75.70 (4 \times C4), 74.20-65.31 (26C, 7 \times C2, 7 \times C3, 3 \times C4, 7 \times C5, 2 \times C_{sugar}), 64.89 (C_{sugar}), 61.19 (C6), 60.53 (C6), 59.88 (C_{sugar}), 57.57 (2 \times C6), 54.06 (2C, 1 \times C_{sugar}, 1 \times N_{sugar}-CH₂-), 52.91 (C_{sugar}), 50.37 (NH-(CH₂)₄-CH₂-), 49.24 (N-CH₂-CH₂-Ad), 48.00 (NH-(CH₂)₄-CH₂-), 46.54 (2 \times C6), 45.80 (C6), 45.72 (2 \times CH₂_{triaz}), 41.67 (Ca), 36.84 (2C, 1 \times Cb, 1 \times NH-(CH₂)₄-CH₂-), 36.68

(N-CH₂-CH₂-Ad), 28.73 (Cc), 28.33 (Cb), 24.65 (NH-(CH₂)₄-CH₂-), 22.77 (NH-(CH₂)₄-CH₂-).

HMRS (ESI): calculated for [C₇₄H₁₁₉N₁₂O₃₆+H]⁺ 1751.7844; found: 1751.7896.

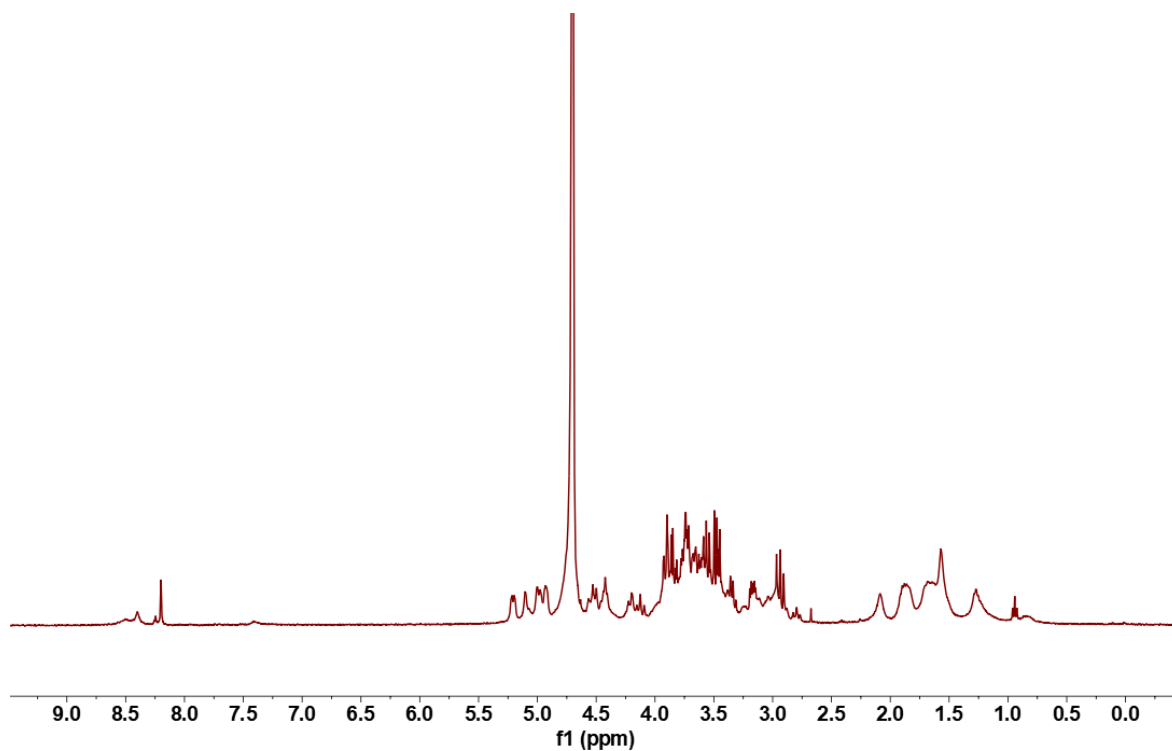


Figure 49: ¹H NMR (600 MHz, D₂O, 300K) of compound 34

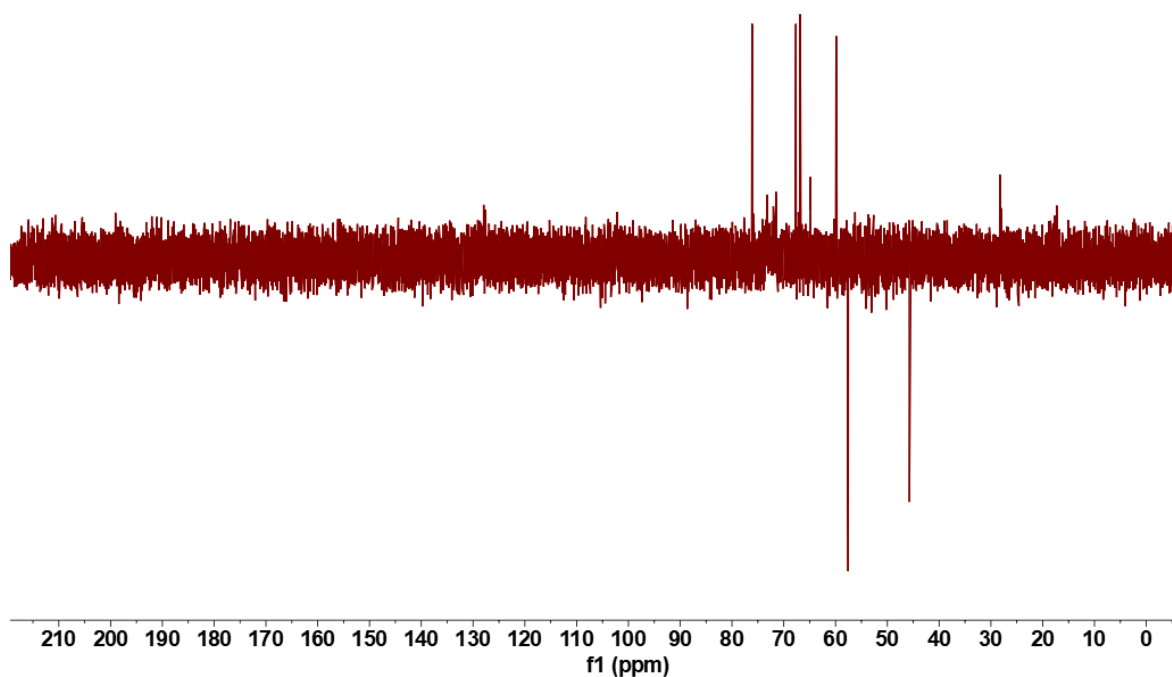
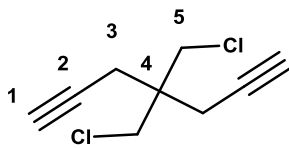


Figure 50: ¹³C NMR-DEPT 135 (151 MHz, D₂O, 300K) of compound 34

EXPERIMENTAL PART

4, 4-Bis (chloromethyl)hepta-1,6-diyne (37)



Chemical Formula: $C_9H_{10}Cl_2$
Exact Mass: 188.0160

Sodium hydride (1.05 g, 26.2 mmol, 2 eq, 60% in oil) was taken in dry THF (27 mL), and the solution was cooled to 0°C. Diethylmalonate (2.10 g, 13.1 mmol, 1 eq) was then added dropwise to the ice-cold solution, and the reaction mixture was allowed to stir for 2h at room temperature. To this solution propargyl bromide (3.90 g, 32.8 mmol, 2.5 eq, 80% in toluene) was added dropwise at 0°C and allowed to reach room temperature with continuous stirring. The stirring was continued for 24 h. THF was removed using a rotary evaporator, 50 mL water was added and the entire solution was extracted with ethyl acetate (3×20 mL). The combined organic layer was then concentrated under reduced pressure. The crude product was then distilled under reduced pressure at 120°C which resulted expected compound diethyl 2, 2-di (prop-2-yn-1-yl)malonate 35 as the colorless liquid with a yield of 75%. 1H NMR (400 MHz, $CDCl_3$, 300K): δ =4.26-4.20 (q, 4H), 3.00 (d, 4H), 2.04 (t, 2H), 1.28 (t, 6H). ^{13}C NMR (100 MHz, $CDCl_3$, 300K): δ =168.56 (2C), 78.49 (2C), 71.56 (2C), 62.09 (2C), 56.28 (1C), 22.52 (2C), 14.00 (2C).

Product 35 (2.32 g, 9.83 mmol, 1 eq) was slowly added to a stirred solution of Lithium aluminium hydride (LAH) (1.19 g, 31.47 mmol, 3.2 eq) in dry THF (45 mL) at -10°C. The temperature was then allowed to come to room temperature and the stirring was continued for 36 h. After NaOH solution (2 M, 1.25 mL) and water (3.8 mL) was added slowly to the reaction mixture at 0°C and stirring for 30 min to quench the unreacted LAH. Once the quenching was over (cease of hydrogen gas evolution) the reaction mixture was filtered, the residue was washed with diethyl ether (2×100 mL). The filtrate was collected and the diethyl ether removed under reduced pressure. The crude product was then distilled at 140°C under high vacuum. The diol modified product 36 was a white crystalline solid with a yield of 55%. The structure of the product was confirmed by comparison with the literature ^[150].

Triphenylphosphine (259 mg, 0.99 mmol, 3 eq) was added into a solution of product 36 (50 mg, 0.33 mmol, 1 eq) in acetonitrile (1.0 mL) and CCl_4 (0.99 ml, 10.2 mmol, 31 eq). Stirring for 5 h at room temperature and refluxing 24 h, the solution was concentrated in

vacuo. The residue was purified over silica gel chromatography (cyclohexane/EtOAc 2:1) to afford desired compound 37 (50 mg, 80% yield) as the yellow solid.

$^1\text{H NMR}$ (400 MHz, CDCl_3 , 300K): δ =3.70 (s, 4H, 4H-5), 2.51 (d, 4H, 4H-3), 2.09 (t, 2H, 2H-1).

$^{13}\text{C NMR}$ (100 MHz, CDCl_3 , 300K): δ =78.76 (2C, 2C-2), 72.18 (2C, 2C-1), 47.21 (2C, 2C-5), 43.20 (2C, 2C-4), 23.26 (2C, 2C-3).

HMRS (ESI): calculated for $[\text{C}_9\text{H}_{10}\text{Cl}_2+\text{Na}]^+$ 211.0052; found 211.0105.

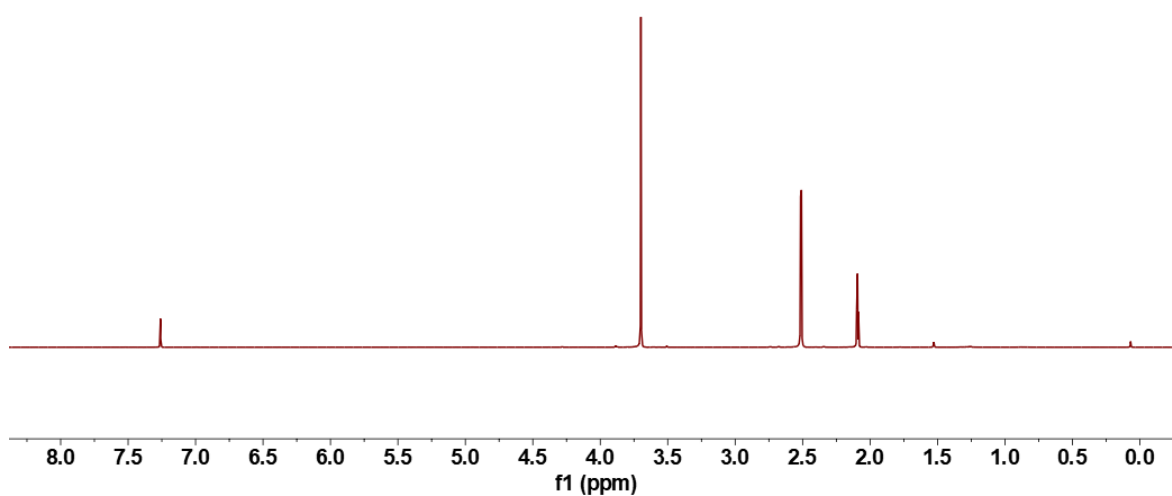


Figure 51: $^1\text{H NMR}$ (400 MHz, CDCl_3 , 300K) of compound 37

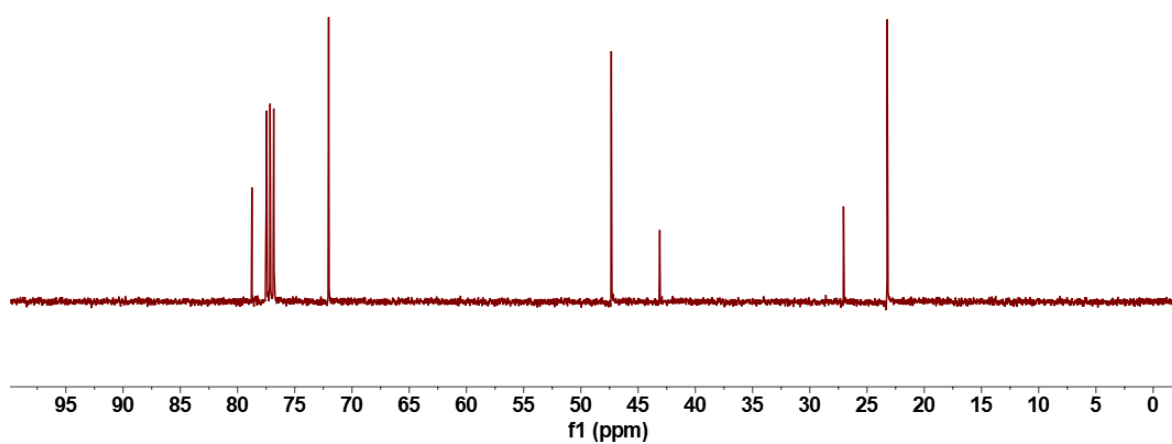
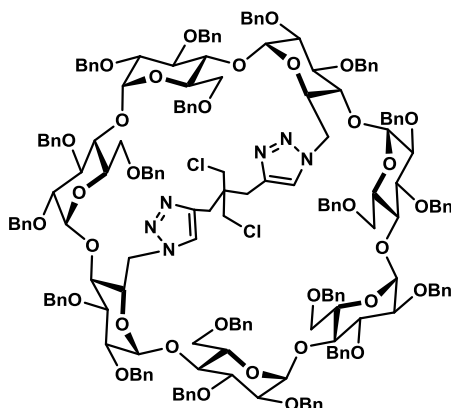


Figure 52: $^{13}\text{C NMR}$ (100 MHz, CDCl_3 , 300K) of compound 37

EXPERIMENTAL PART

**6^A, 6^D-Dideoxy-6^A, 6^D-di-chloride-di-triazole-bridged-
2^{A-G}, 3^{A-G}, 6^B, 6^C, 6^E, 6^F, 6^G-nonadeca-O-benzyl-β-cyclodextrin (38)**



Chemical Formula: C₁₈₄H₁₉₂Cl₂N₆O₃₃
Exact Mass: 3083.2907

To a solution of product 7 (1.2 g, 0.414 mmol, 1 eq) in 12 mL DMF followed by product 37 (78 mg, 0.414 mmol, 1 eq) and DIPEA (29 μL, 0.166 mmol, 0.4 eq) was added. A mixture of TBTA (88 mg, 0.166 mmol, 0.4 eq) and Cu(CH₃CN)₄PF₆ (62 mg, 0.166 mmol, 0.4 eq) in 1 mL DMF was added. The mixture solution was stirred at 150°C under argon atmosphere for 1 h. Finally, the mixture solution was diluted with diethyl ether (100 mL). The organic solution was washed with 1:1 water/brine solution (2×100 mL), HCl solution (1 M in water, 100 mL), the saturated aqueous solution of NaHCO₃ (100 mL), then passed over MgSO₄, filtered and concentrated in vacuo. The residue was purified over silica gel chromatography (cyclohexane/EtOAc 7:3) to afford desired dichloride-ditriazole-bridged modified β-cyclodextrin 38 (664 mg, 35% yield) as the white foam.

¹H NMR (600 MHz, CDCl₃, 300K): δ = 8.00 (s, 1H, 1×H_{triazA}), 7.20 (s, 1H, 1×H_{triazD}), 7.29-6.81 (m, 95H, 95×H_{Ph}), 5.32-5.14 (m, 3H, 2×H1, 1×CHHPh), 5.11-4.90 (m, 7H, 2×H1, 1×H6, 4×CHHPh), 4.85 (d, ³J_{H6-H5} = 9.2 Hz, 1H, 1×H6), 4.79-4.70 (m, 3H, 2×H1, 1×CHHPh), 4.70-4.48 (m, 12H, 1×H1, 1×H5, 10×CHHPh), 4.44-4.03 (m, 25H, 2×H3, 2×H5, 1×H6, 20×CHHPh), 4.03-3.54 (m, 20H, 5×H3, 5×H4, 3×H5, 6×H6, 2×CHHPh), 3.54-3.40 (m, 5H, 2×H2, 2×H4, 1×H5), 3.38-3.26 (m, 5H, 5×H2), 3.25-3.13 (m, 3H, 1×H6, 2×CHH-Cl), 3.06 (d, ²J = 7.6 Hz, 1H, 1×CHH-Cl), 2.99 (d, ³J_{H6-H5} = 7.2 Hz, 1H, 1×H6), 2.92 (d, ³J_{H6-H5} = 7.2 Hz, 1H, 1×H6), 2.82-2.62 (m, 3H, 2×H6, 1×CHH-Cl), 2.50 (d, ²J = 10.0 Hz, 1H, 1×CHH_{triazA}), 2.25 (d, ²J = 10.0 Hz, 1H, 1×CHH_{triazD}), 2.15 (d, ²J = 10.0 Hz, 1H, 1×CHH_{triazA}), 1.91 (d, ²J = 10.0 Hz, 1H, 1×CHH_{triazD}).

¹³C NMR (151 MHz, CDCl₃, 300K): δ = 129.38-125.70 (95C, CH-Ar), 124.60 (C_{triazA}), 123.89 (C_{triazD}), 100.75, 100.57, 100.11, 99.93, 99.46, 98.98, 98.82 (7×C1), 82.20 (C4), 82.10 (C4),

81.52 (C4), 80.99-78.80 (15C, 7×C3, 4×C4, 4×C2), 77.47 (C2), 77.25 (C2), 77.21 (C2), 76.17, 76.00 (2C), 75.80, 75.46, 74.67, 73.98, 73.29, 73.24, 73.14, 73.06, 72.98 (2C), 72.89 (2C), 72.71, 72.57, 72.50, 72.06 (19×CH₂-Ph), 71.81 (2×C5), 71.69 (C5), 71.60 (C5), 71.50 (C5), 71.11 (C5), 70.64 (C5), 69.71 (C6), 69.15 (C6), 68.82 (C6), 67.35 (2×C6), 52.89 (2×C6), 47.43 (2×CH₂-Cl), 27.46 (CH₂triazA), 26.98 (CH₂triazD).

HMRS (ESI): calculated for [C₁₈₄H₁₉₂Cl₂N₆O₃₃+Na]⁺ 3106.2800; found 3106.2809.

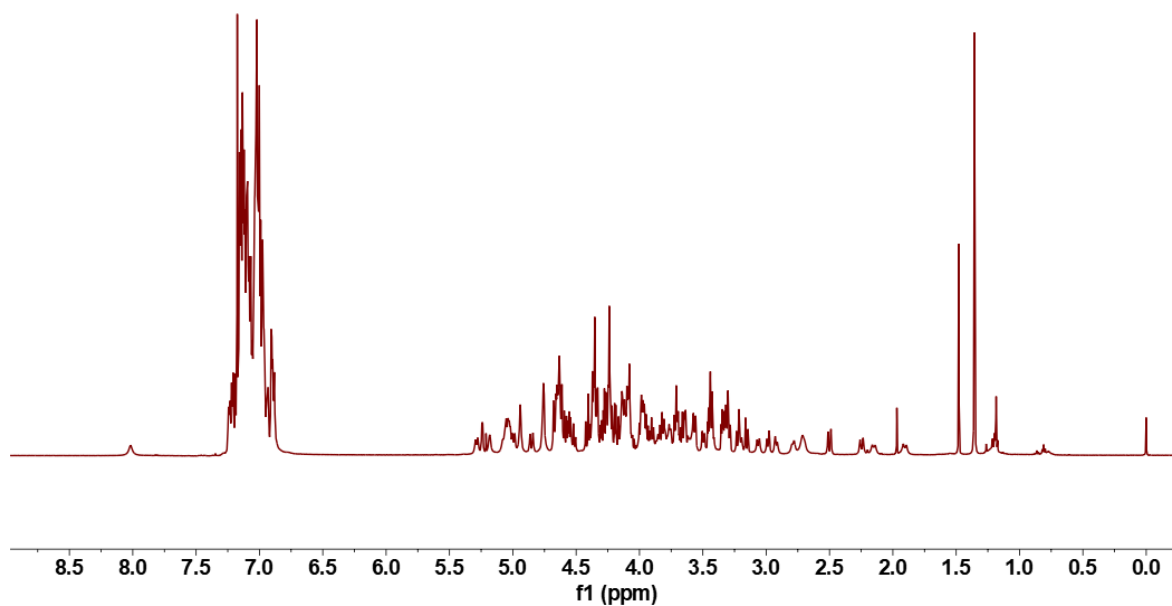


Figure 53: ¹H NMR (600 MHz, CDCl₃, 300K) of compound 38

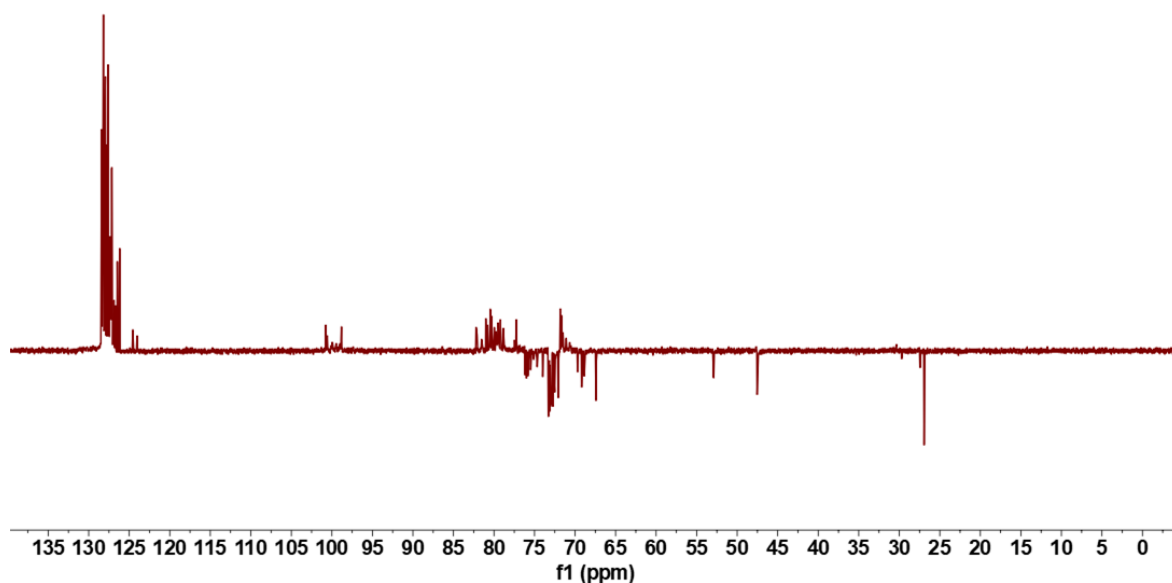
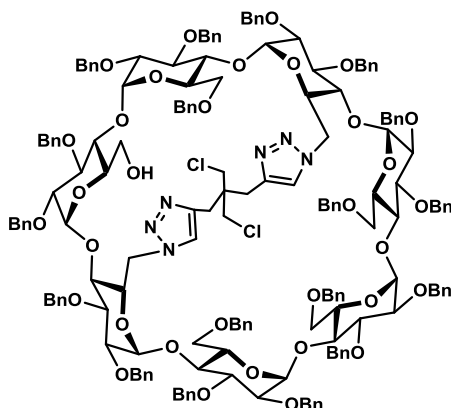


Figure 54: ¹³C NMR-DEPT 135 (151 MHz, CDCl₃, 300K) of compound 38

EXPERIMENTAL PART

**6^A, 6^C, 6^D-Trideoxy-6^A, 6^D-di-chloride-di-triazole-bridged-6^C-hydroxyl-
2^{A-G}, 3^{A-G}, 6^B, 6^E, 6^F, 6^G-octadeca-O-benzyl-β-cyclodextrin (39)**



Chemical Formula: C₁₇₇H₁₈₆Cl₂N₆O₃₃
Exact Mass: 2993.2438

To a stirred solution of product 38 (504 mg, 0.163 mmol, 1 eq) in toluene (1.36 mL) was added DIBAL-H (1.5 M in toluene, 2.7 mL, 4.08 mmol, 25 eq) was added dropwise at room temperature. The reaction mixture was heated at 60°C and put under a nitrogen flux. The reaction mixture was monitored by MS. The reaction mixture was carefully and slowly poured in an ice/water bath (5 mL) while stirring frequently. Ethyl acetate (5 mL) and HCl solution (1 M in water, 5 mL) were then added. The mixture was stirred for 30 min and then the aqueous phase was extracted with ethyl acetate (3×10 mL), and the combined organic layers were washed with brine, dried over MgSO₄, filtered and concentrated in vacuo. The residue was purified over silica gel chromatography (cyclohexane/EtOAc 4:1) to afford trideoxy-dichloride-ditriazole-bridged modified β-cyclodextrin 39 (273 mg, 56% yield) as the white foam.

¹H NMR (600 MHz, CDCl₃, 300K): δ =8.20 (s, 1H, 1×H_{triazA}), 7.32-6.79 (m, 91H, 1×H_{triazD}, 90×H_{Ph}), 5.38 (s, 1H, 1×H1), 5.29 (s, 1H, 1×H1), 5.17-5.03 (m, 4H, 1×H6, 3×CHHPh), 4.94 (s, 1H, 1×H1), 4.88 (br. m, 1H, 1×H6), 4.88-4.58 (m, 12H, 4×H1, 1×H5, 7×CHHPh), 4.57-4.07 (m, 29H, 2×H5, 1×H6, 26×CHHPh), 4.07-3.79 (m, 10H, 7×H3, 2×H5, 1×H6), 3.78-3.68 (m, 3H, 1×H4, 2×H6), 3.67-3.46 (m, 11H, 1×H2, 5×H4, 1×H5, 4×H6), 3.46-3.19 (m, 12H, 6×H2, 1×H4, 1×H5, 4×CHH-Cl), 2.93 (br. m, 1H, 1×H6), 2.82-2.70 (m, 3H, 2×H6, 1×CHH_{triazA}), 2.65 (br. m, 1H, 1×H6), 2.36-2.22 (m, 2H, 1×CHH_{triazA}, 1×CHH_{triazD}), 1.93 (br. m, 1H, 1×CHH_{triazD}).

¹³C NMR (151 MHz, CDCl₃, 300K): δ =129.44-125.77 (90C, CH-Ar), 124.63 (C_{triazA}), 123.81 (C_{triazD}), 101.67, 101.37, 99.21, 98.99, 98.78, 98.65, 96.61 (7×C1), 83.85 (C4), 82.78 (C4), 81.68 (C4), 81.29-78.52 (14C, 7×C3, 4×C4, 3×C2), 77.64 (C2), 77.35 (C2), 77.25 (C2), 76.60 (C2), 76.15-72.24 (18×CH₂-Ph), 71.93 (C5), 71.82 (C5), 71.71 (2×C5), 71.57 (C5), 71.44

(C5), 70.78 (2×C6), 69.68 (C5), 68.97 (C6), 67.38 (C6), 67.13 (C6), 62.14 (CH₂-Cl), 52.92 (C6), 52.35 (C6), 47.56 (CH₂-Cl), 26.79(2C, 1×CH₂triazA, 1×CH₂triazD).

HMRS (ESI): calculated for [C₁₇₇H₁₈₆Cl₂N₆O₃₃+H]⁺ 2994.2511; found 2994.2507.

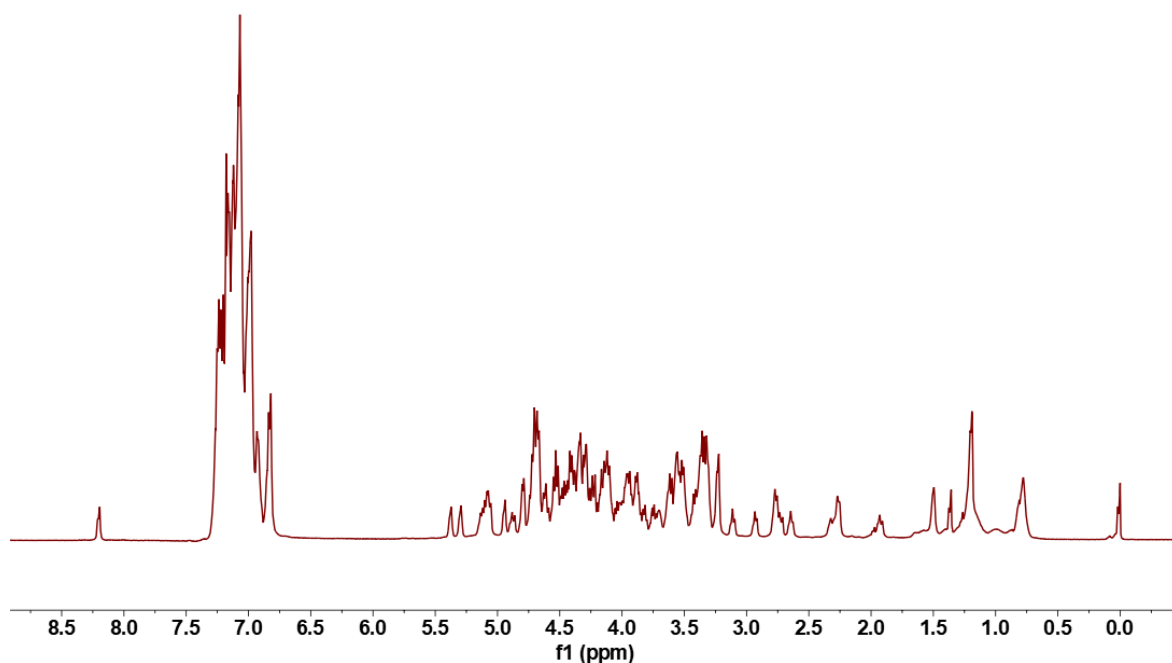


Figure 55: ¹H NMR (600 MHz, CDCl₃, 300K) of compound 39

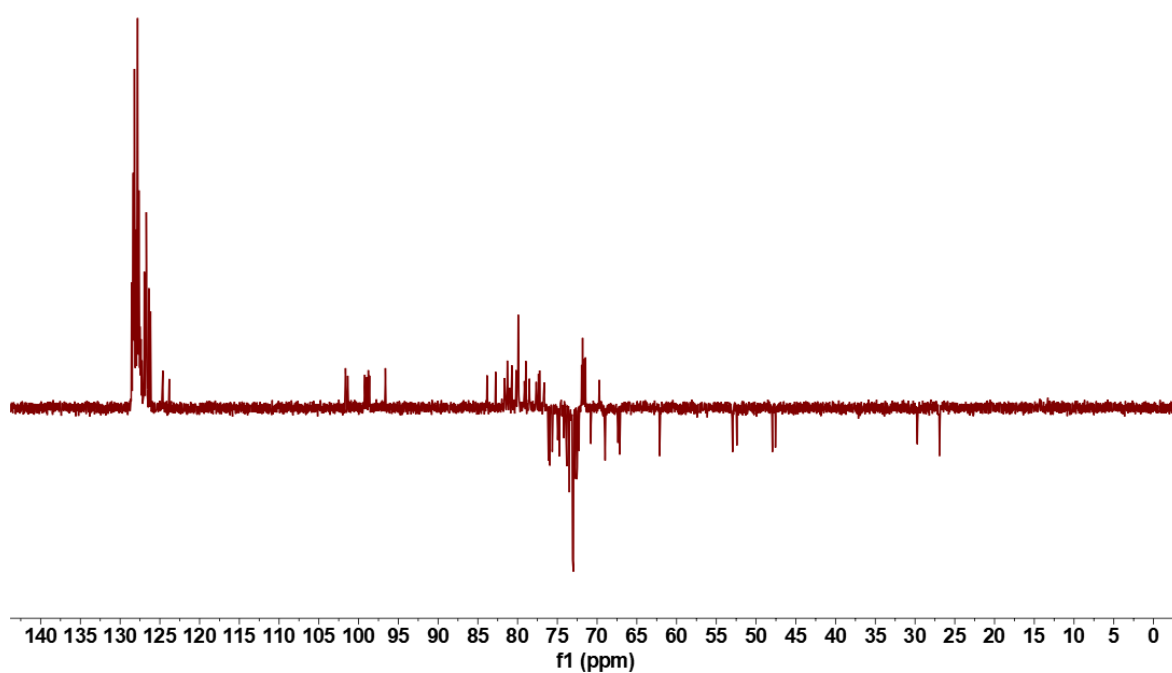


Figure 56: ¹³C NMR-DEPT 135 (151 MHz, CDCl₃, 300K) of compound 39

BIBLIOGRAPHY

BIBLIOGRAPHY

1. Lehn, J. Cryptates: inclusion complexes of macropolycyclic receptor molecules. *Pure and applied Chemistry*, **1978**, *50*, 871-892.
2. Steed, J.W. and J.L. Atwood. *Supramolecular chemistry*. **2013**: John Wiley & Sons.
3. Kumar, D., D. Sharma, G. Singh, M. Singh, and M.S. Rathore. Lipoidal soft hybrid biocarriers of supramolecular construction for drug delivery. *ISRN pharmaceutics*, **2012**, *2012*.
4. James, T.D. Specialty grand challenges in supramolecular chemistry. *Frontiers in chemistry*, **2017**, *5*, 83.
5. Sauvage, J.-P., J. Stoddart, and B. Feringa. 2016 Nobel Prize in Chemistry: conferring molecular machines as engines of creativity. *Current Science*, **2016**, *111*, 1289.
6. Steed, J.W., D.R. Turner, and K. Wallace. *Core concepts in supramolecular chemistry and nanochemistry*. **2007**: John Wiley & Sons.
7. Ariga, K. and T. Kunitake. *Supramolecular chemistry-fundamentals and applications: advanced textbook*. **2006**: Springer Science & Business Media.
8. Lehn, J.-M. *Supramolecular chemistry: receptors, catalysts, and carriers*. *Science*, **1985**, *227*, 849-856.
9. Albrecht, M. *Supramolecular chemistry—general principles and selected examples from anion recognition and metallocsupramolecular chemistry*. *Naturwissenschaften*, **2007**, *94*, 951-966.
10. Blanks, R.F. and J. Prausnitz. Thermodynamics of polymer solubility in polar and nonpolar systems. *Industrial & Engineering Chemistry Fundamentals*, **1964**, *3*, 1-8.
11. Parsegian, V.A. *Van der Waals forces: a handbook for biologists, chemists, engineers, and physicists*. **2005**: Cambridge University Press.
12. Pagni, R. Modern Physical Organic Chemistry (Eric V. Anslyn and Dennis A. Dougherty). *Journal of Chemical Education*, **2006**, *83*, 387.
13. Emsley, J. Very strong hydrogen bonding. *Chemical Society Reviews*, **1980**, *9*, 91-124.
14. Jeffrey, G.A. and G.A. Jeffrey. *An introduction to hydrogen bonding*. Vol. 32. **1997**: Oxford university press New York.
15. Jeffrey, G.A. and W. Saenger. *Hydrogen bonding in biological structures*. **2012**: Springer Science & Business Media.
16. Gao, S., W. House, and W.G. Chapman. NMR/MRI Study of Clathrate Hydrate Mechanisms. *The Journal of Physical Chemistry B*, **2005**, *109*, 19090-19093.
17. Ratkova, E.L., D.S. Palmer, and M.V. Fedorov. Solvation Thermodynamics of Organic Molecules by the Molecular Integral Equation Theory: Approaching Chemical Accuracy. *Chemical Reviews*, **2015**, *115*, 6312-6356.
18. Atwood, J.L. *Comprehensive supramolecular chemistry II*. **2017**: Elsevier.
19. Lehn, J.-M. *Perspectives in Supramolecular Chemistry—From Molecular Recognition*

- towards Molecular Information Processing and Self-Organization. *Angewandte Chemie International Edition in English*, **1990**, *29*, 1304-1319.
20. Yang, L., X. Tan, Z. Wang, and X. Zhang. Supramolecular polymers: Historical development, preparation, characterization, and functions. *Chemical reviews*, **2015**, *115*, 7196-7239.
 21. Brunsveld, L., B.J.B. Folmer, E.W. Meijer, and R.P. Sijbesma. Supramolecular Polymers. *Chemical Reviews*, **2001**, *101*, 4071-4098.
 22. Carothers, W.H. Polymerization. *Chemical Reviews*, **1931**, *8*, 353-426.
 23. De Greef, T.F., M.M. Smulders, M. Wolfs, A.P. Schenning, R.P. Sijbesma, and E. Meijer. Supramolecular polymerization. *Chemical Reviews*, **2009**, *109*, 5687-5754.
 24. de Greef, T.F. and E. Meijer. Materials science: Supramolecular polymers. *Nature*, **2008**, *453*, 171.
 25. Sivakova, S., D.A. Bohnsack, M.E. Mackay, P. Suwanmala, and S.J. Rowan. Utilization of a Combination of Weak Hydrogen-Bonding Interactions and Phase Segregation to Yield Highly Thermosensitive Supramolecular Polymers. *Journal of the American Chemical Society*, **2005**, *127*, 18202-18211.
 26. Martin, R.B. Comparisons of Indefinite Self-Association Models. *Chemical Reviews*, **1996**, *96*, 3043-3064.
 27. Dudowicz, J., K.F. Freed, and J.F. Douglas. Lattice model of equilibrium polymerization. IV. Influence of activation, chemical initiation, chain scission and fusion, and chain stiffness on polymerization and phase separation. *The Journal of Chemical Physics*, **2003**, *119*, 12645-12666.
 28. Kulkarni, C., S. Balasubramanian, and S.J. George. What Molecular Features Govern the Mechanism of Supramolecular Polymerization? *ChemPhysChem*, **2013**, *14*, 661-673.
 29. Chen, C.-C. and E.E. Dormidontova. Ring-Chain Equilibrium in Reversibly Associated Polymer Solutions: Monte Carlo Simulations. *Macromolecules*, **2004**, *37*, 3905-3917.
 30. Hunter, C.A. and H.L. Anderson. What is Cooperativity? *Angewandte Chemie International Edition*, **2009**, *48*, 7488-7499.
 31. Fredy, J.W., A. Méndez-Ardoy, S. Kwangmettatam, D. Bochicchio, B. Matt, M.C.A. Stuart, J. Huskens, N. Katsonis, G.M. Pavan, and T. Kudernac. Molecular photoswitches mediating the strain-driven disassembly of supramolecular tubules. *Proceedings of the National Academy of Sciences*, **2017**, *114*, 11850-11855.
 32. Wang, X., K. Han, J. Li, X. Jia, and C. Li. Pillar[5]arene-neutral guest recognition based supramolecular alternating copolymer containing [c2]daisy chain and bis-pillar[5]arene units. *Polymer Chemistry*, **2013**, *4*, 3998-4003.
 33. Fu, X., R.-R. Gu, Q. Zhang, S.-J. Rao, X.-L. Zheng, D.-H. Qu, and H. Tian. Phototriggered supramolecular polymerization of a [c2]daisy chain rotaxane. *Polymer Chemistry*, **2016**, *7*,

BIBLIOGRAPHY

- 2166-2170.
34. Peterca, M., V. Percec, M.R. Imam, P. Leowanawat, K. Morimitsu, and P.A. Heiney. Molecular Structure of Helical Supramolecular Dendrimers. *Journal of the American Chemical Society*, **2008**, *130*, 14840-14852.
 35. Wang, X., B. Ding, and B. Li. Biomimetic electrospun nanofibrous structures for tissue engineering. *Materials Today*, **2013**, *16*, 229-241.
 36. Daniel, C., F. Makereel, L.M. Herz, F.J.M. Hoeben, P. Jonkheijm, A.P.H.J. Schenning, E.W. Meijer, and C. Silva. Mesoscopic order and the dimensionality of long-range resonance energy transfer in supramolecular semiconductors. *The Journal of Chemical Physics*, **2008**, *129*, 104701.
 37. Lowe, A.B. Stimuli Responsive Water-Soluble and Amphiphilic (Co)polymers. **2001**.
 38. Mendes, A.C., E.T. Baran, R.L. Reis, and H.S. Azevedo. Fabrication of phospholipid-xanthan microcapsules by combining microfluidics with self-assembly. *Acta Biomaterialia*, **2013**, *9*, 6675-6685.
 39. Shchipunov, Y., S. Sarin, I. Kim, and C.-S. Ha. Hydrogels formed through regulated self-organization of gradually charging chitosan in solution of xanthan. *Green Chemistry*, **2010**, *12*, 1187-1195.
 40. Ouchi, H., T. Kizaki, M. Yamato, X. Lin, N. Hoshi, F. Silly, T. Kajitani, T. Fukushima, K.-i. Nakayama, and S. Yagai. Impact of helical organization on the photovoltaic properties of oligothiophene supramolecular polymers. *Chemical Science*, **2018**, *9*, 3638-3643.
 41. Zhang, Q., C.-Y. Shi, D.-H. Qu, Y.-T. Long, B.L. Feringa, and H. Tian. Exploring a naturally tailored small molecule for stretchable, self-healing, and adhesive supramolecular polymers. *Science Advances*, **2018**, *4*, eaat8192.
 42. Bakker, M.H., R.E. Kieltyka, L. Albertazzi, and P.Y.W. Dankers. Modular supramolecular ureidopyrimidinone polymer carriers for intracellular delivery. *RSC Advances*, **2016**, *6*, 110600-110603.
 43. Bouteiller, L. and L. Bouteiller. Assembly via Hydrogen Bonds of Low Molar Mass Compounds into Supramolecular Polymers. **2007**.
 44. Baruah, P.K. and S. Khan. Self-complementary quadruple hydrogen bonding motifs: from design to function. *RSC Advances*, **2013**, *3*, 21202-21217.
 45. Binder, W.H. and R. Zirbs. Supramolecular Polymers and Networks with Hydrogen Bonds in the Main- and Side-Chain. *Advances in Polymer Science*, **2007**, *207*, 1-78.
 46. Dong, R., Y. Zhou, X. Huang, X. Zhu, Y. Lu, and J. Shen. Functional Supramolecular Polymers for Biomedical Applications. *Advanced Materials*, **2015**, *27*, 498-526.
 47. Lehn, J.M. Perspectives in supramolecular chemistry—from molecular recognition towards molecular information processing and self-organization. *Angewandte Chemie*

- International Edition in English*, **1990**, *29*, 1304-1319.
48. Fouquey, C., J.M. Lehn, and A.M. Levelut. Molecular recognition directed self - assembly of supramolecular liquid crystalline polymers from complementary chiral components. *Advanced Materials*, **1990**, *2*, 254-257.
 49. Sijbesma, R.P., F.H. Beijer, L. Brunsveld, B.J. Folmer, J.K. Hirschberg, R.F. Lange, J.K. Lowe, and E. Meijer. Reversible polymers formed from self-complementary monomers using quadruple hydrogen bonding. *Science*, **1997**, *278*, 1601-1604.
 50. Klosterman, J.K., Y. Yamauchi, and M. Fujita. Engineering discrete stacks of aromatic molecules. *Chemical Society Reviews*, **2009**, *38*, 1714-1725.
 51. Lanigan, N. and X. Wang. Supramolecular chemistry of metal complexes in solution. *Chemical Communications*, **2013**, *49*, 8133-8144.
 52. Tanaka, K., G.H. Clever, Y. Takezawa, Y. Yamada, C. Kaul, M. Shionoya, and T. Carell. Programmable self-assembly of metal ions inside artificial DNA duplexes. *Nature Nanotechnology*, **2006**, *1*, 190-194.
 53. Anastassopoulou, J. and T. Theophanides. The Role of Metal Ions in Biological Systems and Medicine. **1995**.
 54. Ribas Gispert, J. Coordination Chemistry. **2008**.
 55. Dong, S., B. Zheng, F. Wang, and F. Huang. Supramolecular Polymers Constructed from Macrocyclic-Based Host-Guest Molecular Recognition Motifs. *Accounts of Chemical Research*, **2014**, *47*, 1982-1994.
 56. Ogoshi, T., T.-a. Yamagishi, and Y. Nakamoto. Pillar-shaped macrocyclic hosts pillar [n] arenes: new key players for supramolecular chemistry. *Chemical reviews*, **2016**, *116*, 7937-8002.
 57. Chi, X., G. Yu, L. Shao, J. Chen, and F. Huang. A Dual-Thermoresponsive Gemini-Type Supra-amphiphilic Macromolecular [3]Pseudorotaxane Based on Pillar[10]arene/Paraquat Cooperative Complexation. *Journal of the American Chemical Society*, **2016**, *138*, 3168-3174.
 58. Hu, C., N. Ma, F. Li, Y. Fang, Y. Liu, L. Zhao, S. Qiao, X. Li, X. Jiang, T. Li, F. Shen, Y. Huang, Q. Luo, and J. Liu. Cucurbit[8]uril-Based Giant Supramolecular Vesicles: Highly Stable, Versatile Carriers for Photoresponsive and Targeted Drug Delivery. *ACS Applied Materials & Interfaces*, **2018**, *10*, 4603-4613.
 59. Kim, H.-J., J. Heo, W.S. Jeon, E. Lee, J. Kim, S. Sakamoto, K. Yamaguchi, and K. Kim. Selective Inclusion of a Hetero-Guest Pair in a Molecular Host: Formation of Stable Charge-Transfer Complexes in Cucurbit[8]uril. *Angewandte Chemie International Edition*, **2001**, *40*, 1526-1529.
 60. Zhu, H., L. Shangguan, B. Shi, G. Yu, and F. Huang. Recent progress in macrocyclic

BIBLIOGRAPHY

- amphiphiles and macrocyclic host-based supra-amphiphiles. *Materials Chemistry Frontiers*, **2018**, *2*, 2152-2174.
61. Qu, D.-H., Q.-C. Wang, Q.-W. Zhang, X. Ma, and H. Tian. Photoresponsive Host-Guest Functional Systems. *Chemical Reviews*, **2015**, *115*, 7543-7588.
 62. Hirao, T., H. Kudo, T. Amimoto, and T. Haino. Sequence-controlled supramolecular terpolymerization directed by specific molecular recognitions. *Nature Communications*, **2017**, *8*, 634.
 63. Hofmeier, H. and U.S. Schubert. Combination of orthogonal supramolecular interactions in polymeric architectures. *Chemical Communications*, **2005**, 2423-2432.
 64. Li, S.-L., T. Xiao, C. Lin, and L. Wang. Advanced supramolecular polymers constructed by orthogonal self-assembly. *Chemical Society Reviews*, **2012**, *41*, 5950-5968.
 65. Dong, S., L. Gao, J. Chen, G. Yu, B. Zheng, and F. Huang. A supramolecular polymer formed by the combination of crown ether-based and charge-transfer molecular recognition. *Polymer Chemistry*, **2013**, *4*, 882-886.
 66. Yan, X., B. Jiang, T.R. Cook, Y. Zhang, J. Li, Y. Yu, F. Huang, H.-B. Yang, and P.J. Stang. Dendronized Organoplatinum(II) Metallacyclic Polymers Constructed by Hierarchical Coordination-Driven Self-Assembly and Hydrogen-Bonding Interfaces. *Journal of the American Chemical Society*, **2013**, *135*, 16813-16816.
 67. Xiao, T., X. Feng, Q. Wang, C. Lin, L. Wang, and Y. Pan. Switchable supramolecular polymers from the orthogonal self-assembly of quadruple hydrogen bonding and benzo-21-crown-7-secondary ammonium salt recognition. *Chemical Communications*, **2013**, *49*, 8329-8331.
 68. Yan, X., T.R. Cook, J.B. Pollock, P. Wei, Y. Zhang, Y. Yu, F. Huang, and P.J. Stang. Responsive Supramolecular Polymer Metallogel Constructed by Orthogonal Coordination-Driven Self-Assembly and Host/Guest Interactions. *Journal of the American Chemical Society*, **2014**, *136*, 4460-4463.
 69. Zhan, J., Q. Li, Q. Hu, Q. Wu, C. Li, H. Qiu, M. Zhang, and S. Yin. A stimuli-responsive orthogonal supramolecular polymer network formed by metal-ligand and host-guest interactions. *Chemical Communications*, **2014**, *50*, 722-724.
 70. Zhan, J., M. Zhang, M. Zhou, B. Liu, D. Chen, Y. Liu, Q. Chen, H. Qiu, and S. Yin. A Multiple-Responsive Self-Healing Supramolecular Polymer Gel Network Based on Multiple Orthogonal Interactions. *Macromolecular Rapid Communications*, **2014**, *35*, 1424-1429.
 71. Gibson, H.W., N. Yamaguchi, and J.W. Jones. Supramolecular pseudorotaxane polymers from complementary pairs of homoditopic molecules. *Journal of the American Chemical Society*, **2003**, *125*, 3522-3533.

72. Bothner-By, A.A., R.L. Stephens, J. Lee, C.D. Warren, and R.W. Jeanloz. Structure determination of a tetrasaccharide: transient nuclear Overhauser effects in the rotating frame. *Journal of the American Chemical Society*, **1984**, *106*, 811-813.
73. Clore, G.M. and A.M. Gronenborn. New methods of structure refinement for macromolecular structure determination by NMR. *Proc Natl Acad Sci U S A*, **1998**, *95*, 5891-5898.
74. Neuhaus, D. and M.P. Williamson. The Nuclear Overhauser Effect in Structural and Conformational Analysis, 2nd Edition. *Proteomics*, **2000**.
75. Matsuba, C.A., S.J. Rettig, and C. Orvig. Main group (IIIA or 13) complexes of benzohydroxamic acid and the crystal structure of tris (benzohydroxamato) indium (III). *Canadian journal of chemistry*, **1988**, *66*, 1809-1813.
76. Haino, T., A. Watanabe, T. Hirao, and T. Ikeda. Supramolecular Polymerization Triggered by Molecular Recognition between Bisporphyrin and Trinitrofluorenone. *Angewandte Chemie International Edition*, **2012**, *51*, 1473-1476.
77. Dhinakaran, M.K., W. Gong, Y. Yin, A. Wajahat, X. Kuang, L. Wang, and G. Ning. Configuration-independent AIE-active supramolecular polymers of cyanostilbene through the photo-stable host-guest interaction of pillar[5]arene. *Polymer Chemistry*, **2017**, *8*, 5295-5302.
78. Claridge, T.D. High-resolution NMR techniques in organic chemistry. Vol. 27. **2016**: Elsevier.
79. Heisel, K.A., J.J. Goto, and V.V. Krishnan. NMR Chromatography: Molecular Diffusion in the Presence of Pulsed Field Gradients in Analytical Chemistry Applications. *American Journal of Analytical Chemistry*, **2012**, *03(06)*, 9.
80. Heisel, K.A., J.J. Goto, and V.V. Krishnan. NMR chromatography: molecular diffusion in the presence of pulsed field gradients in analytical chemistry applications. **2012**.
81. Krell, T., M.E. Guazzaroni, A. Busch, J. Lacal, W. Terán, S. Fillet, H. Silva-Jiménez, and J.L. Ramos. Microcalorimetry as a General Technique to Characterize Ligand Binding: What Needs to be Considered When Analyzing Hydrocarbons. **2010**.
82. Zakharov, P. and F. Scheffold. Advances in dynamic light scattering techniques. *Springer Praxis Books*, **2009**, 433-467.
83. Stetefeld, J., S.A. McKenna, and T.R. Patel. Dynamic light scattering: a practical guide and applications in biomedical sciences. *Biophysical reviews*, **2016**, *8*, 409-427.
84. Liu, Y., Z. Wang, and X. Zhang. Characterization of supramolecular polymers. *Chemical Society Reviews*, **2012**, *41*, 5922-5932.
85. Shibayama, M. Small-angle neutron scattering on polymer gels: phase behavior, inhomogeneities and deformation mechanisms. *Polymer Journal*, **2011**, *43*, 18-34.

BIBLIOGRAPHY

86. Hammouda, B., S. Krueger, and C. Glinka. Small angle neutron scattering at the National Institute of Standards and Technology. *Journal of research of the National Institute of Standards and Technology*, **1993**, *98*, 31.
87. Dragolici, C.A. *Experimental methods in the study of neutron scattering at small angles*. in *AIP Conference Proceedings*. 2014. AIP.
88. Brás, A.R., C.H. Hövelmann, W. Antonius, J. Teixeira, A. Radulescu, J. Allgaier, W. Pyckhout-Hintzen, A. Wischnewski, and D. Richter. Molecular Approach to Supramolecular Polymer Assembly by Small Angle Neutron Scattering. *Macromolecules*, **2013**, *46*, 9446-9454.
89. Saenger, W. Cyclodextrin Inclusion Compounds in Research and Industry. *Angewandte Chemie International Edition in English*, **1980**, *19*, 344-362.
90. Freudenberg, K., G. Blomqvist, L. Ewald, and K. Soff. Hydrolyse und Acetolyse der Stärke und der Schardinger - Dextrine. *Berichte der deutschen chemischen Gesellschaft (A and B Series)*, **1936**, *69*, 1258-1266.
91. French, D., M.L. Levine, J. Pazur, and E. Norberg. Studies on the Schardinger dextrans. The preparation and solubility characteristics of alpha, beta and gamma dextrans. *Journal of the American Chemical Society*, **1949**, *71*, 353-356.
92. Crini, G. Review: A History of Cyclodextrins. *Chemical Reviews*, **2014**, *114*, 10940-10975.
93. Szejtli, J. Past, present and future of cyclodextrin research. *Pure and Applied Chemistry*, **2004**, *76*, 1825-1845.
94. Fourmentin, S., G. Crini, and E. Lichtfouse. *Cyclodextrin Fundamentals, Reactivity and Analysis*. **2018**: Springer.
95. Khan, N.A., & Durakshan, M. Cyclodextrin: an overview. *International Journal of Bioassays*, **2013**, *2(6)*, 858-865.
96. Funasaki, N., S. Ishikawa, and S. Neya. Advances in physical chemistry and pharmaceutical applications of cyclodextrins. *Pure and Applied Chemistry*, **2008**, *80*, 1511-1524.
97. Saenger, W., J. Jacob, K. Gessler, T. Steiner, D. Hoffmann, H. Sanbe, K. Koizumi, S.M. Smith, and T. Takaha. Structures of the Common Cyclodextrins and Their Larger Analogues Beyond the Doughnut. *Chemical Reviews*, **1998**, *98*, 1787-1802.
98. Martin, J., Díaz-Montaña, E. J., & Asuero, A. G. . *Cyclodextrins: Past and Present*. **2018**.
99. Sakurai, M., M. Kitagawa, H. Hoshi, Y. Inoue, and R. Chûjô. A molecular orbital study of cyclodextrin (cyclomalto-oligosaccharide) inclusion complexes. III, dipole moments of cyclodextrins in various types of inclusion complex. *Carbohydrate Research*, **1990**, *198*, 181-191.
100. Rekharsky, M.V. and Y. Inoue. Complexation Thermodynamics of Cyclodextrins. *Chemical Reviews*, **1998**, *98*, 1875-1918.

101. Liu, B.-w., H. Zhou, S.-t. Zhou, and J.-y. Yuan. Macromolecules based on recognition between cyclodextrin and guest molecules: Synthesis, properties and functions. *European Polymer Journal*, **2015**, *65*, 63-81.
102. Carrazana, J., A. Jover, F. Meijide, V.H. Soto, and J. Vázquez Tato. Complexation of Adamantyl Compounds by β -Cyclodextrin and Monoaminoderivatives. *The Journal of Physical Chemistry B*, **2005**, *109*, 9719-9726.
103. Voskuhl, J., M. Waller, S. Bandaru, B.A. Tkachenko, C. Fregonese, B. Wibbeling, P.R. Schreiner, and B.J. Ravoo. Nanodiamonds in sugar rings: an experimental and theoretical investigation of cyclodextrin–nanodiamond inclusion complexes. *Organic & Biomolecular Chemistry*, **2012**, *10*, 4524-4530.
104. Cromwell, W.C., K. Bystrom, and M.R. Eftink. Cyclodextrin-adamantanecarboxylate inclusion complexes: studies of the variation in cavity size. *The Journal of Physical Chemistry*, **1985**, *89*, 326-332.
105. Rong, D. and V.T. D'Souza. A convenient method for functionalization of the 2-position of cyclodextrins. *Tetrahedron Letters*, **1990**, *31*, 4275-4278.
106. Khan, A.R., P. Forgo, K.J. Stine, and V.T. D'Souza. Methods for Selective Modifications of Cyclodextrins. *Chemical Reviews*, **1998**, *98*, 1977-1996.
107. Leggio, C., M. Anselmi, A. Di Nola, L. Galantini, A. Jover, F. Meijide, N.V. Pavel, V.H.S. Tellini, and J.V. Tato. Study on the Structure of Host–Guest Supramolecular Polymers. *Macromolecules*, **2007**, *40*, 5899-5906.
108. Hasegawa, Y., M. Miyauchi, Y. Takashima, H. Yamaguchi, and A. Harada. Supramolecular Polymers Formed from β -Cyclodextrins Dimer Linked by Poly(ethylene glycol) and Guest Dimers. *Macromolecules*, **2005**, *38*, 3724-3730.
109. Takahashi, H., Y. Takashima, H. Yamaguchi, and A. Harada. Selection between Pinching-Type and Supramolecular Polymer-Type Complexes by α -Cyclodextrin– β -Cyclodextrin Hetero-Dimer and Hetero-Cinnamamide Guest Dimers. *The Journal of Organic Chemistry*, **2006**, *71*, 4878-4883.
110. Ohga, K., Y. Takashima, H. Takahashi, Y. Kawaguchi, H. Yamaguchi, and A. Harada. Preparation of Supramolecular Polymers from a Cyclodextrin Dimer and Ditopic Guest Molecules: Control of Structure by Linker Flexibility. *Macromolecules*, **2005**, *38*, 5897-5904.
111. Soto Tellini, V.H., A. Jover, J.C. García, L. Galantini, F. Meijide, and J.V. Tato. Thermodynamics of Formation of Host–Guest Supramolecular Polymers. *Journal of the American Chemical Society*, **2006**, *128*, 5728-5734.
112. Bai, Y., X.-d. Fan, W. Tian, T.-t. Liu, H. Yao, Z. Yang, H.-t. Zhang, and W.-b. Zhang. Morphology transitions of supramolecular hyperbranched polymers induced by double

BIBLIOGRAPHY

- supramolecular driving forces. *Polymer Chemistry*, **2015**, *6*, 732-737.
113. Maciollek, A., Ritter, H., & Beckert, R. Superstructures of fluorescent cyclodextrin via click-reaction. *Beilstein journal of organic chemistry*, **2013**, *9(1)*, 827-831.
114. Deng, W., H. Yamaguchi, Y. Takashima, and A. Harada. A Chemical-Responsive Supramolecular Hydrogel from Modified Cyclodextrins. *Angewandte Chemie International Edition*, **2007**, *46*, 5144-5147.
115. Miyauchi, M., Y. Kawaguchi, and A. Harada. Formation of Supramolecular Polymers Constructed by Cyclodextrins with Cinnamamide. *Journal of Inclusion Phenomena & Macrocyclic Chemistry*, **2004**, *50*, 57-62.
116. Mendes, A.C., E.T. Baran, R.L. Reis, and H.S. Azevedo. Fabrication of phospholipid-xanthan microcapsules by combining microfluidics with self-assembly. *Acta Biomaterialia*, **2013**, *9*, 6675-6685.
117. Wenz, G. Cyclodextrins as Building Blocks for Supramolecular Structures and Functional Units. *Angewandte Chemie International Edition in English*, **1994**, *33*, 803-822.
118. Lecourt, T., A. Herault, A.J. Pearce, M. Sollogoub, and P. SinaÿTriisobutylaluminium and Diisobutylaluminium Hydride as Molecular Scalpels: The Regioselective Stripping of Perbenzylated Sugars and Cyclodextrins. *Chemistry – A European Journal*, **2004**, *10*, 2960-2971.
119. Pearce, A.J. and P. SinaÿDiisobutylaluminum -Promoted Regioselective De-O-benzylation of Perbenzylated Cyclodextrins: A Powerful New Strategy for the Preparation of Selectively Modified Cyclodextrins. *Angewandte Chemie International Edition*, **2000**, *39*, 3610-3612.
120. Bistri, O., P. Sinaÿ J. Jiménez Barbero, and M. Sollogoub. Chemical Clockwise Tridifferentiation of α - and β -Cyclodextrins: Bascule-Bridge or Deoxy-Sugars Strategies. *Chemistry – A European Journal*, **2007**, *13*, 9757-9774.
121. Guieu, S. and M. Sollogoub. Regiospecific Tandem Azide-Reduction/Deprotection To Afford Versatile Amino Alcohol-Functionalized α - and β -Cyclodextrins. *Angewandte Chemie International Edition*, **2008**, *47*, 7060-7063.
122. Guieu, S. and M. Sollogoub. Multiple Homo- and Hetero-functionalizations of α -Cyclodextrin through Oriented Deprotections. *The Journal of Organic Chemistry*, **2008**, *73*, 2819-2828.
123. Zaborova, E., M. Guitet, G. Prencipe, Y. Blériot, M. Ménand, and M. Sollogoub. An "Against the Rules" Double Bank Shot with Diisobutylaluminum Hydride To Allow Triple Functionalization of α -Cyclodextrin. *Angewandte Chemie International Edition*, **2013**, *52*, 639-644.
124. Sato, T., H. Nakamura, Y. Ohno, and T. Endo. Synthesis of

- 1,4-anhydro-2,3,6-tri-O-benzyl- α -D-glucopyranose by cis-ring-closure of a glycosyl chloride. *Carbohydrate Research*, **1990**, *199*, 31-35.
125. Wang, B., F. Guo, J. Ren, G. Ai, B. Aigle, K. Fan, and K. Yang. Identification of Alp1U and Lom6 as epoxy hydrolases and implications for kinamycin and lomaiviticin biosynthesis. *Nature Communications*, **2015**, *6*, 7674.
126. L. May, B., P. Clements, J. Tsanaktsidis, C. J. Easton, and S. F. Lincoln. Square pegs in round holes. Preparation and intramolecular complexation of cubyl substituted β -cyclodextrins† and of an adamantane analogue. *Journal of the Chemical Society, Perkin Transactions 1*, **2000**, 463-469.
127. Tellini, V.H.S., J. Aida, G. Luciano, M. Francisco, and T. José Vázquez. Crystal structure of the supramolecular linear polymer formed by the self-assembly of mono-6-deoxy-6-adamantylamide- β -cyclodextrin. *Acta Crystallographica*, **2010**, *60*, 204-210.
128. Tran, D.N., D. Colesnic, S.A. de Beaumais, G. Pembouong, F. Portier, Á.A. Queijo, J.V. Tato, Y. Zhang, M. Ménand, and L. Bouteiller. Cyclodextrin-adamantane conjugates, self-inclusion and aggregation versus supramolecular polymer formation. *Organic Chemistry Frontiers*, **2014**, *1*, 703-706.
129. Bistri-Aslanoff, O., Y. Blériot, R. Auzely-Velty, and M. Sollogoub. Duplex of capped-cyclodextrins, synthesis and cross-linking behaviour with a biopolymer. *Organic & Biomolecular Chemistry*, **2010**, *8*, 3437-3443.
130. Evenou, P., J. Rossignol, G. Pembouong, A. Gothland, D. Colesnic, R. Barbeyron, S. Rudiuk, A.-G. Marcelin, M. Ménand, D. Baigl, V. Calvez, L. Bouteiller, and M. Sollogoub. Bridging β -Cyclodextrin Prevents Self-Inclusion, Promotes Supramolecular Polymerization, and Promotes Cooperative Interaction with Nucleic Acids. *Angewandte Chemie International Edition*, **2018**, *57*, 7753-7758.
131. Kallemeijn, W.W., M. Witte, T. Wennekes, and J.M.F.G. Aerts. *Advances in Carbohydrate Chemistry and Biochemistry*. **2015**.
132. Theophanides, T. and G.C. Turrell. Infrared study of thermal decomposition of the azide ion. *Spectrochimica Acta Part A: Molecular Spectroscopy*, **1967**, *23*, 1927-1935.
133. Wang, J., Y. Zhao, W. Zhao, P. Wang, and J. Li. Total synthesis of N-butyl-1-deoxynojirimycin. *Journal of Carbohydrate Chemistry*, **2016**, *35*, 445-454.
134. Tran, D.N., D. Colesnic, S. Adam de Beaumais, G. Pembouong, F. Portier, Á.A. Queijo, J. Vázquez Tato, Y. Zhang, M. Ménand, L. Bouteiller, and M. Sollogoub. Cyclodextrin-adamantane conjugates, self-inclusion and aggregation versus supramolecular polymer formation. *Organic Chemistry Frontiers*, **2014**, *1*, 703-706.
135. Valente, A.J.M., R.A. Carvalho, and O. Söderman. Do Cyclodextrins Aggregate in Water?

BIBLIOGRAPHY

- Insights from NMR Experiments. *Langmuir*, **2015**, *31*, 6314-6320.
136. De La Torre, J.G., M.C.L. Martinez, and M.M. Tirado. Dimensions of short, rodlike macromolecules from translational and rotational diffusion coefficients. Study of the gramicidin dimer. *Biopolymers*, **1984**, *23*, 611-615.
137. Pavlov, G.M., E.V. Korneeva, N.A. Smolina, and U.S. Schubert. Hydrodynamic properties of cyclodextrin molecules in dilute solutions. *European Biophysics Journal*, **2010**, *39*, 371-379.
138. Paduano, L., R. Sartorio, V. Vitagliano, and L. Costantino. Diffusion properties of cyclodextrins in aqueous solution at 25°C. *Journal of Solution Chemistry*, **1990**, *19*, 31-39.
139. De Greef, T.F.A., M.M.J. Smulders, M. Wolffs, A.P.H.J. Schenning, R.P. Sijbesma, and E.W. Meijer. Supramolecular Polymerization. *Chemical Reviews*, **2009**, *109*, 5687-5754.
140. Smulders, M.M.J., M.M.L. Nieuwenhuizen, T.F.A. de Greef, P. van der Schoot, A.P.H.J. Schenning, and E.W. Meijer. How to Distinguish Isodesmic from Cooperative Supramolecular Polymerisation. *Chemistry – A European Journal*, **2010**, *16*, 362-367.
141. della Sala, F., S. Neri, S. Maiti, J.L.Y. Chen, and L.J. Prins. Transient self-assembly of molecular nanostructures driven by chemical fuels. *Current Opinion in Biotechnology*, **2017**, *46*, 27-33.
142. Dhiman, S. and S.J. George. Temporally Controlled Supramolecular Polymerization. *Bulletin of the Chemical Society of Japan*, **2018**, *91*, 687-699.
143. Noh, H., S. Myung, M.J. Kim, and S.K. Yang. Stimuli-responsive supramolecular assemblies via self-assembly of adamantane-containing block copolymers. *Polymer*, **2019**, *175*, 65-70.
144. Tang, G., X. Wang, D. Li, Y. Ma, and D. Wu. Fabrication of POSS-embedded supramolecular hyperbranched polymers with multi-responsive morphology transitions. *Polymer Chemistry*, **2018**, *9*, 5377-5384.
145. Qi, M., S. Duan, B. Yu, H. Yao, W. Tian, and F.-J. Xu. PGMA-based supramolecular hyperbranched polycations for gene delivery. *Polymer Chemistry*, **2016**, *7*, 4334-4341.
146. Xiao, S., M. Yang, P. SinaÿY. Blériot, M. Sollogoub, and Y. Zhang. Diisobutylaluminium Hydride (DIBAL-H) Promoted Secondary Rim Regioselective Demethylations of Permethylated β -Cyclodextrin: A Mechanistic Proposal. *European Journal of Organic Chemistry*, **2010**, *2010*, 1510-1516.
147. Hardlei, T. and M. Bols. Unusual hydrogen-bonding differences in stereoisomeric 6-C-alkylated cyclodextrins. *Journal of the Chemical Society, Perkin Transactions 1*, **2002**, 2880-2885.
148. Guitet, M., P. Zhang, F. Marcelo, C. Tugny, J. Jiménez-Barbero, O. Buriez, C. Amatore, V. Mouriès-Mansuy, J.-P. Goddard, L. Fensterbank, Y. Zhang, S. Roland, M. Ménand, and M.

- Sollogoub. NHC-Capped Cyclodextrins (ICyDs): Insulated Metal Complexes, Commutable Multicoordination Sphere, and Cavity-Dependent Catalysis. *Angewandte Chemie International Edition*, **2013**, *52*, 7213-7218.
149. Beeson, T.D. and D.W.C. MacMillan. Enantioselective Organocatalytic α -Fluorination of Aldehydes. *Journal of the American Chemical Society*, **2005**, *127*, 8826-8828.
150. Wilking, M., C. Mück-Lichtenfeld, C.G. Daniliuc, and U. Hennecke. Enantioselective, Desymmetrizing Bromolactonization of Alkynes. *Journal of the American Chemical Society*, **2013**, *135*, 8133-8136.

